

Research Thesis

UNIVERSITY OF SOUTHAMPTON

Faculty of Physical Sciences and Engineering

Electronics and Computer Science

**A MEASUREMENT SYSTEM FOR HAND
REHABILITATION**

By

Nan Hu

Supervised by

Dr. Nick R Harris, Dr. Paul H Chappell

March_2021

UNIVERSITY OF SOUTHAMPTON

ABSTRACT

FACULTY OF PHYSICAL SCIENCES AND ENGINEERING

ELECTRONICS AND COMPUTER SCIENCE

Research Thesis

A MEASUREMENT SYSTEM FOR HAND REHABILITATION

by NAN HU

The emergence of some technological systems and smart devices that realize home-based or tele rehabilitation has exposed alternative delivery forms to promote patients' hand recovery from common physiological conditions. However, due to the motion difficulty of most patients with an impaired hand, extra effort should be made to effectively stimulate their engagement without compromising the clinical outcomes.

The discussion about home-based medical equipment in both the market and academic realms indicates that a good recovery outcome of a home-based rehabilitation device seems to be closely related to the ease of use. The purpose of the research presented in this thesis is to investigate the feasibility of home-based hand rehabilitation with emphasis on ease of use. Towards this target, measurement techniques compatible with the overall aim are explored and selected. The framework of the measuring system is based on a MGC3030 capacitive sensing microcontroller, which allows the noncontact form of measurement of small fingers movements and potentially the thumb. This thesis reports the following parts to improve the stability and accuracy of the targeted measuring techniques:

- A Finite Element Method simulation based on the MGC3030 electrode stack-up design was carried out to guide the practical design of the electrodes. The original simulation model and the modified design with extra ground electrodes placed in between each pair of receive electrodes were compared and analysed.
- Algorithm compensation introduced nonlinear fitted equations to describe the inherent relationship between distance of finger motion and voltage signals. The signals were detected both in the receive electrode underneath the moving finger and the neighbouring ones, in an electrical field generated by an electrode layer stack-up design based on MGC3030 of two fingers' motion (index finger together with the middle finger).

- A validation experiments was conducted to evaluate the prediction model on multi-finger noncontact measuring under laboratory conditions. Twenty-three healthy subjects with normal hand and finger functions participated. An independent near field distance measurement was developed and compared to the output from an optical sensor.

Table of Abbreviation

Abbreviation	Meaning
MGC3030	MGC3030 motion sensor. It uses the principle of quasi-static electrical near field sensing for advanced proximity detection to provide gesture and positional data of a human hand in real time.
FEM	Finite element method.
ADL	Activities of daily living.
EMG	Electromyography.
3D	Three dimensions (three-dimensional).
MGC3X30	Both MGC3030 and MGC3130. They are the same series of motion sensors based on electric near field sensing for gesture and position measurement.
E-field	Electrical field.
Rx	Receive electrode of the MGC3030 three-layer electrode design.
Tx	Transmit electrode of the MGC3030 three-layer electrode design.
GND	Ground electrode of the MGC3030 three-layer electrode design.
I	Index finger.
M	Middle finger.
R	Ring finger.
L	Little finger.
D (D_x)	The distance between the under surface of a finger and the top of the cover layer. D_1 , D_2 , D_3 , D_4 reflect the movement of index, middle, ring and little finger respectively.
V_x	The potential of Rx electrode to ground. V_1 , V_2 , V_3 , V_4 are corresponding to the voltages of the Rx electrodes under the index finger the middle finger, the ring finger and the little finger respectively.
gnd	The smaller ground electrodes placed at the midpoints neighbouring the Rx electrodes pairs in the modified electrode design (Section 3.4).
dV_x/dD_x	The rate of change of the voltage value (V_x) at a certain distance point (D_x).
S_x	The MGC3030 signal detected by the Rx electrode. S_1 , S_2 , S_3 , S_4 are corresponding to the MGC3030 signal detected by the Rx electrode under the index, middle, ring and little finger respectively.
1-F, 2-M...	Participant identification number.
Opt1	Optical sensor1 for index finger.
Opt2	Optical sensor2 for middle finger.
AoI	Angle of incidence.
2D	Two dimensions (two-dimensional).
D_{p1}	The predicted distance value for index finger.

D_{p2}	The predicted distance value for middle finger.
S_{1-i}	The signal change of MGC3030 Signal1 (S_1) for the first step in one sample movement: the index finger extension and then flexion.
S_{1-ii}	The signal change of MGC3030 Signal1 (S_1) for the second step in one sample movement: the middle finger extension and then flexion.
D_{p1-i}	The predicted distance change of the index finger for the first step in one sample movement: the index finger extension and then flexion.
D_{p1-ii}	The predicted distance change of the index finger for the second step in one sample movement: the middle finger extension and then flexion.
D_{p1-iii}	The predicted distance change of the index finger for the third step in one sample movement: both the index finger and the middle finger extension and then flexion.
S_{2-i}	The signal change of MGC3030 Signal2 (S_2) for the first step in one sample movement: the index finger extension and then flexion.
S_{2-ii}	The signal change of MGC3030 Signal2 (S_2) for the second step in one sample movement: the middle finger extension and then flexion.
D_{p2-i}	The predicted distance change of the middle finger for the first step in one sample movement: the index finger extension and then flexion.
D_{p2-ii}	The predicted distance change of the middle finger for the second step in one sample movement: the middle finger extension and then flexion.
D_{p2-iii}	The predicted distance change of the middle finger for the third step in one sample movement: both the index finger and the middle finger extension and then flexion.

Table of Contents

Chapter 1 Introduction	1
1.1 Introduction.....	1
1.2 Research questions and novelty contributions	2
1.3 Report structure.....	3
1.4 List of publications	4
Chapter 2 Literature Review	7
2.1 Background.....	7
2.1.1 Home-based hand rehabilitation	7
2.1.2 Fingers movements: extension and flexion.....	9
2.2 Medical equipment for hand rehabilitation	11
2.2.1 Medical equipment in commercial practice: Exercising, supporting and testing.....	11
2.2.2 Medical equipment in research literature	16
2.3 Tracking the movement	18
2.4 MGC3030 justification	26
2.5 Summary.....	28
Chapter 3 Finite Element Method Modelling of a Customizable Three-Layer Electrode Design.....	29
3.1 Theory of detection: Electrical field (E-field) sensing.....	29
3.2 Simulation model.....	30
3.2.1 Three-layer electrode stack-up design	30
3.2.2 Discussion of fingers movements	31
3.3 Variation of electric field distribution with finger motion.....	32
3.4 Modified electrode layer stack-up design	36
3.5 Comparison and discussion.....	38
3.5.1 Sensitivity	39
3.5.2 Crosstalk	41
3.6 Summary.....	45
Chapter 4 Model Prediction to Sense the Movement of Fingers	47
4.1 Theory of detection: Discussion of the prediction model	48
4.2 Simulated data from COMSOL	50
4.3 Model prediction to sense the movement of fingers	50
4.3.1 Model prediction of one finger's case: $V_x=f(D_x)$	51
4.3.2 Reversed model prediction of one finger's case: $D_x=f(V_x)$	54
4.3.3 Model prediction of two fingers' case: $V_x=f(D_1, D_2)$	56
4.3.4 Reversed model prediction in two fingers' case: $D_x=f(V_1, V_2)$	60

4.4 Discussion.....	64
4.4.1 Further discussion on equation $V_x=f(D_x)$: Influence of parameters on sensitivity.....	64
4.4.2 Further discussion on equation $D_x=f(V_1, V_2)$: Resolution of the target system.....	69
4.5 Summary.....	71
Chapter 5 Experimental Verification Design.....	73
5.1 Discussion of the FEM simulation model.....	73
5.2 Experimental platform design.....	74
5.2.1 System design.....	74
5.2.2 Receptacle design.....	76
5.3 Participants characteristics.....	76
5.4 Experiment process and data acquisition.....	78
5.4.1 Calibration of the optical system.....	78
5.4.2 Testing of combined fingers movements.....	80
5.5 Discussion: Performance of the optical systems.....	81
5.6 Discussion: Evaluation of the MGC3030 system.....	84
5.7 Summary.....	85
Chapter 6 Data Analysis and Experimental Evaluation.....	87
6.1 Crosstalk.....	87
6.2 Nonlinear regression.....	88
6.3 Reduced crosstalk after using the prediction model.....	92
6.4 Discussion:.....	99
6.4.1 Evaluation of the validation results and the MGC3030 system.....	99
6.4.2 Discussion of the prediction models for three/four finger movement.....	100
6.4.3 Potential- uses of electric field sensing in broader applications: Enslaving.....	101
6.4.4 Potential- uses of electric field sensing in broader applications: Tremor.....	101
6.5 Summary.....	103
Chapter 7 Conclusion and Future Work.....	104
7.1 Conclusion.....	104
7.2 Suggestions for future work.....	106
7.3 A personalized receptacle design.....	107
7.3.1 Hand modelling.....	107
7.3.2 Electrodes layer stack-up design.....	108
7.3.3 The design for assembly.....	109
7.3.4 3D printing.....	111
Appendix A: Detailed Settings of Comsol Simulation Model.....	1

Appendix B: Finger Movements Discussion	3
Appendix C: Distance and Corresponding Voltage Values for Original Electrodes Design	5
Appendix D: Distance and Corresponding Voltage Values for Modified Electrodes Design	11
Appendix E: Comparison of Two Electrode Designs within Each Case	17
Appendix F: Variation of Voltage Signal due to the Neighbouring Fingers	27
Appendix G Data from COMSOL Simulation	33
Appendix H: Nonlinear Fitting Results for Equation $V_1=f(D_1)$	35
Appendix I: Nonlinear Fitting Results for Equation $V_2=f(D_2)$	39
Appendix J: Nonlinear Fitting Results for Equation $D_1=f(V_1)$	43
Appendix K: Nonlinear Fitting Results for Equation $D_2=f(V_2)$	47
Appendix L: Improvement of Accuracy using the Prediction Models	51
Appendix M: Participant Questionnaire Sheet.....	65
Appendix N: Participant Information Sheet.....	67
Appendix O: Participant Experiment Record	73
Appendix P: Participant Characteristics	79
Appendix Q: Filtering Issue	83
Appendix R: Experimental Results for Extreme Case 21-F	91
List of References	99

ACKNOWLEDGEMENTS

For the completion of my PhD thesis, first and foremost, I would like to thank my supervisors, Dr. Nick Harris and Dr. Paul Chappell, for their insightful guidance and kind support at all stages of my Ph.D. I learned how to become a scientific researcher from their profound knowledge and serious attitude. And this thesis would not have been possible without their consistent and illuminating instruction.

I would also like to express my heartfelt gratitude to all my colleagues at ECS and many other technicians who have generously provided help and time for my research in the past four years. Their direct and indirect help has benefited me a lot.

Special thanks should go to my friends and my family members for their loving considerations and great confidence in me all through these years. They always share my highs and lows. I feel much grateful and heartily owe my achievement to them.

Finally, I would like to acknowledge the support of the University of Southampton, United Kingdom, the China Scholarship Council, and Xiamen University, China. My heartfelt thanks for a giving me the chance to read for a PhD and supporting me throughout this project.

Chapter 1 Introduction

1.1 Introduction

Technological systems and smart devices that realize home-based or tele-hand rehabilitation have provided an alternative rehabilitation, to encourage hand recovery from some physiological and pathological conditions [1], including: stroke, tremor and Parkinsonism [2]. These investigations are especially important, given the noticeable economic burden on patients and the whole society, as well as the great reliance on healthcare facilities and professionals.

The shared challenge for all home-based devices, however, is to enable people to perform their rehabilitation sessions at home regularly and correctly, without the help from the therapists or carers. People with impaired hand usually suffer from reduced hand or finger functions, which naturally requires more effort from them on both setting and using the rehabilitation device. If a system requires complicated setups and contraptions to be worn, it is unlikely to be a daily rehabilitation choice, for patients' independent usage at home. In addition, a complicated system also makes it difficult for patients to stick to using it. For instance, without continuous supervision from a therapist, they might be unable to correctly comply with the procedures, or even misinterpret the therapy and may potentially lead to injury. In other words, the device should improve the ease of use to improve the efficiency of patients' current practice.

Home-based devices that allow patients to perform regular exercise on their own without continuous involvement of health experts, could assist the rehabilitation process to a large extent and allow significant monetary savings [1]. However, the increasing public health burden associated with chronic stroke-related disease are driving a search for more cost-effective methods for post stroke rehabilitations [3]. A popular rehabilitation device should not increase the cost of health care. Instead, it is supposed to be affordable for patients yet profitable for manufacturers [3].

Therefore, new technological approaches that realize home-based rehabilitation in a user-friendly, low-cost equipment should be investigated. The device should have a minimum set up and operating requirement, for people with impaired hands to use at home easily, without the help of neither the therapist nor their family members. Additionally, targeted stroke therapy systems should provide a cost-effective means for individuals with chronic stroke to maintain movement ability after receiving standard inpatient and outpatient rehabilitation. This is

achieved by both the reduced costs for therapists and public transportations, as well as the low price of the device itself.

1.2 Research questions and novelty contributions

This research investigates the feasibility of home-based hand rehabilitation with emphasis on ease of use. In order to achieve this, it is possible to formulate several research questions:

- What are the key requirements for an easy-to-use finger displacement sensor for the home-based hand rehabilitation, and what is the current state of the art? (Chapter 2)
- What techniques offer the best performance and what level of solution can it give? (Chapter 3, 4)
- How well does the developed technique perform on human subjects? (Chapter 5, 6)

The answers to these research questions will allow a conclusion to be drawn on how well the overall aim of assessing the feasibility of an easy-to-use system for home-based therapy is, using the measurement of finger displacement as an example. The novel contributions of this research are:

- The development of a home-based rehabilitation application for patients with impaired hand and finger functions based on contactless multi-finger movement measurement. The three-dimensional gesture and tracking controller from Microchip, MGC3030, is selected as an input sensor. Approaches using the MGC3030 motion sensor to realize noncontact finger motion detection were explored as mentioned below.

- **Hardware design:** based on the MGC3030 motion sensor. A customizable three-layer electrode and receptacle design for the MGC3030 microcontroller is proposed, to realize the noncontact measurement simultaneously for multi-fingers (index, middle, ring and little).

- **Prediction models:** for compensating the cross impact of multi-finger movement in the electrical field generated from the three-layer MGC3030 electrodes design. A nonlinear model for the movement of two fingers is shown to have uncertainty less than 1mm, over a range of 30mm. This thesis also discusses the prediction model for three-finger and four-finger cases.

- **Validation:** experiments to validate the hardware design and the prediction model. The MGC3030 measuring system was validated under laboratory conditions with 23 healthy participants. An optical measuring system was selected to make an independent comparison of finger movements and shown to have operational disadvantages and unreliable measurements for some participants.

1.3 Report structure

This report is divided into 7 chapters. Chapter 1 highlights the introduction and research questions of this research. Brief description of background is presented in the first section of Chapter 2 to conclude a home-based rehabilitation system addressing ease of use. Further to the discussion of the first section, Chapter 2 reviews medical equipment for hand rehabilitation and sensing technologies that could be used to read finger movements, along with their limitations. A three-dimensional gesture and tracking controller from Microchip, MGC3030, is selected as an input sensor. The working principle and system architecture for this sensor are described in detail in 2.4.

Simulated work related to the design and implementation of the MGC3030 system is described in Chapter 3. In the first section of this chapter, the theory of detection for the designed system is provided. A Finite Element Method (FEM) simulation model in Comsol Multiphysics is described in Section 3.2, with details related to the design of three-layer electrodes and the discussion of potential fingers movement. Quasi-static electric fields generated by two MGC3030 electrodes stack up designs are introduced and analysed in sections 3.3 and 3.4, respectively. Here, the noncontact form of measurement is realized by the variation of electric field, resulted from finger movement. Sensitivity and crosstalk of these two electrode designs on contactless finger motion detection were compared in Section 3.5.

Based on one simulation model reported in Chapter 3, Chapter 4 explores a nonlinear regression model to compensate for the crosstalk of the combined fingers' movement in the quasi-static electrical near field. The theory of detection was discussed in order to derive the form of a prediction model in the first part of this chapter. The Comsol simulated data involved in this nonlinear regression is illustrated in Section 4.2. On the basis of the simulated data, section 4.3 and 4.4 evaluate the mathematic relationship between the fingers' motion (D) and the voltage signals (V) of both the Rx electrodes underneath the moving finger and the neighbouring ones.

An experiment to verify the prediction model on multi-finger noncontact measuring, with human subjects, under laboratory conditions, is presented in Chapter 5. Twenty-three healthy subjects (13 males and 10 females) with normal hand and finger function participated in this study. Chapter 5 details the design of the experimental platform, the characteristics of the participants, the experimental process, and the experimental data obtained.

Further to Chapter 5, Chapter 6 analyses the results from the verification experiments to evaluate the performance of the prediction model and the MGC3030 system. The validation results of preliminary study demonstrate the ability of the proposed system on measuring the movements of fingers. Moreover, it reveals the potential applications of the targeted system on conditions such as enslaving as well as tremor. Finally, Chapter 7 concludes the research work along with a discussion of possible future work.

1.4 List of publications

The main publications of this PhD project are listed in chronological order as follows:

- Conference paper ‘Finger Displacement Sensing: FEM Simulation and Modelling of a Customizable Three-Layer Electrode Design’ is accepted by 2018 IEEE International Instrumentation and Measurement Technology conference. The conference paper mainly includes a finite element method (FEM) simulation based on MGC3030 three-layer electrode design in Comsol, and a nonlinear regression analysis using Matlab. This part of work is introduced in detail in Chapter 3 and Chapter 4.
- An extension of the conference paper is published in IEEE Transactions on Instrumentation and Measurement, titled ‘Finger Displacement Sensing: FEM Simulation and Model Prediction of a Three-Layer Electrode Design’. Based on the customizable three-layer electrodes design for use with a MGC3030 motion sensor IC, a finite element method (FEM) simulation in Comsol Multiphysics, and a nonlinear regression analysis using Matlab were carried out. Four nonlinear equations were introduced to describe the motion of the index and middle fingers in the electrical field generated. Chapter 4 explains the mechanism and performance of this four equation based on the simulated data.
- Paper ‘Experimental Validation of a Contactless Finger Displacement Measurement System Using Electrical Near Field Sensing’ is published in IEEE Transactions on Instrumentation and Measurement. In previous publications, a mathematical model was

developed based on a finite element method (FEM) simulation. This paper validates this model on multi-finger noncontact measuring under laboratory conditions. Twenty-three healthy subjects with normal hand and finger functions participated. The experimental verification design is given in Chapter 5 and the data analysis and experimental evaluation is detailed in Chapter 6.

Chapter 2 Literature Review

2.1 Background

2.1.1 Home-based hand rehabilitation

Home-based therapy is a treatment that takes place in the home of a person rather than in a clinical setting. Conventional occupational or physical therapy mainly involves progressive training exercise executed by hands-on physical therapy or by application of devices. During the treatment, both the patient and the therapist need to participate actively [4]. Demand for more cost-effective treatment is leading to changes in practice that are likely to involve home-based therapy and assistive technologies in addition to the conventional occupational therapy and physiotherapy [5]. Considering the significant financial burden of patients and society, as well as the great dependence on professionals and medical facilities, it can further help people reach their recovery goals with its advantages, including: reduced hospital stay, individualized rehabilitation sessions, time and money savings for both treatment and transportation [6].

Home-based therapy can also enhance conventional physiotherapy and the occupational therapy, to promote continuous functional training in the long run. Following discharge from hospital, it is often impractical for the specialist care centre to provide ongoing therapy for people with chronic stroke at home, which can lead to further deterioration of hand function and a direct impact on an individual's capability to perform essential activities of daily living (ADL) [7]. An important purpose of rehabilitation treatment is to promote the neuroplasticity within the central nervous system, and therefore to ameliorate secondary effects such as muscle weakness and reduced range of motion. The neurological re-organisation or learning occurs in response to experience gained through repetitive training [5]. In this case, the home-based therapy can help to promote the neuroplasticity of patients by the continuous and convenient exercise and functional training given to the patients, which can be conducted by patients at home, either independently or with the help of the physiotherapist.

2.1.1.1 Post stroke hand rehabilitation

Among these home-based treatments, debate of different methods of post stroke hand rehabilitation for a person's ability to perform motor functions has dominated research in recent years [8-18]. As an example, stroke is the most common cause of disability and the second leading cause of death in the world [6]. The annual cost of stroke in the UK is £8.9 billion, which represents 5% of the total money spend in UK National Health Service [19]. In the UK alone, over 110,000 people have a stroke annually and over 300,000 people are living with

disability as a result of a stroke [5]. Approximately 70% of post-stroke patients are left with impaired arm and hand function that is highly likely to last for a lifetime even after they have been discharged from rehabilitation [20, 21]. In addition, because stroke is age-related, the incidence is likely to rise. Prevalence of stroke is also likely to rise due to better survival rates and long-term care [5]. Given the large number of patients who can benefit from a readily available form of treatment, research into home-based hand rehabilitation is particularly important.

2.1.1.2 Tremor detection and Parkinson's disease

Tremor is defined as an involuntary, rhythmic, oscillatory movement of a body part [22]. General tremor characteristics which is widely used for clinical investigations include: body distribution, activation condition, and frequency [22]. Tremor frequency is commonly used in characterizing tremor, and is often categorized as <4, 4 to 8, 8 to 12, and >12 Hz [23]. The frequency of most pathological tremors is 4 to 8 Hz, while primary orthostatic tremor typically has a frequency of 13 to 18 Hz. The central neurogenic component of physiological tremor is 8 to 12 Hz, and rhythmic cortical myoclonus typically has a frequency greater than 8 Hz. For example, one of the initial symptoms of Parkinson's disease is an unilateral limb tremors of 4-6Hz. Parkinson's disease (PD) is a progressive neurodegenerative disorder [24] and commonly affecting elderly people worldwide. It affects around 0.3% of the general population and 1–3% of the population over the age of 65 and its number is going to rise from 8.7 to 9.3 million by 2030 [25]. In order to assess and treat tremor-based diseases, such as Parkinson's disease, precise frequency and amplitude measurement for tremors will be helpful for adjusting medication levels [24]. For dynamic response which is high enough to allow the study of tremor in fingers, up to a frequency of about 20Hz will be required.

The drive for more efficient use of rehabilitation services provides an opportunity to develop rehabilitation therapy that can be used outside hospital and without supervision [5]. There is no consensus on the best provision of home-based hand rehabilitation sessions. However, the disability itself may be a major obstacle to the implementation of these exercise sessions [5]. It could well be that if a system requires complicated setups and contraptions to be worn, it will not be used for a complete course of treatment [1]. For example, body tremors can be measured with wearable sensors [26, 27], but a glove-based physical device is sometimes uncomfortable and requires extra effort such as battery replacement [24]. Another major obstacle to the home-based methods is the implementation without continuous

supervision of therapists. The shared challenge for all home-based devices is to keep people performing their training regularly and correctly, when they are left to do it by themselves. For instance, a device that is not straightforward to set up or configure may cause the patient to deviate from the expected procedures, or even misunderstand the treatment and increase the possibility of injury.

On the contrary, a survey for application of assistive technologies in stroke rehabilitation confirms the easy setting, comfortable use, good value, and suitable for home use as the key factors of any ‘popular’ therapy in clinical practice, which can be widely used outside the healthcare centre [5]. This study also concludes that therapies with the greatest probability of significantly improving upper limb rehabilitation following stroke, should be cost effective and acceptable for use by patients and in health services [5].

Hence, the overall aim of the research presented in this thesis, focuses on the technology for home-based rehabilitation of an impaired hand, addressing ease of setting and use to promote motivation of practice. To achieve this outcome, it is necessary to investigate the measuring techniques that are compatible with this overall aim.

2.1.2 Fingers movements: extension and flexion

2.1.2.1 Finger extension and flexion

To begin with, a typical finger movement was chosen as the exemplar training and assessing exercise. This movement was flexion and extension of the fingers. Declination of finger joint angles is often measured to assess the motor ability by medical professionals, using goniometers or inclinometers [28]. However, the angle measurements fall short of obtaining a complete profile when two or more joints are involved [29]. “Reachable space” is also considered as an effective tool in finger flexibility assessment to describe the range of finger motion in recent times [30, 31]. It refers to the set of all reachable fingertip position. The real-time implementation of this assessment is limited by the complexity for a quantitatively analysing solution, and can be costly in terms of time as well as computational resources.

This research investigates the extension and flexion of fingers as an exemplar movement [32]. It can effectively exercise and strengthen the reduced muscle tone of the impaired hand, which is very common among post-stroke patients [33, 34]. Moreover, it could be applied with simpler mathematical methods and implementation approaches [32], compared to angle measurements techniques [29] or ‘reachable space’ techniques [30, 31]. Therefore,

reducing the execution time and costs. Generally, a good real-time motion capture demands excellent data analysis and algorithms, while a more effective and efficient framework will make the realization of a simpler and more robust algorithm possible and easier. Besides, a system is usually more reliable with less hardware elements [35]. Therefore, an easy movement—extension and flexion of fingers was chosen as the exemplar training exercise here to simplify the system design.

Flexion and extension are necessary for performing daily activities. Patients with a loss of extension of the finger joints commonly have difficulties with the grip formation. The functional range of movements for metacarpophalangeal joint (MCP) is necessary to perform the activities of daily living as defined by the Sollermann test of hand grip function [36]. Generally speaking, the range of motion of the MCP for a healthy subject is 0 ~ 120 degrees. However, patients with deficits in hand motor control usually suffer from loss of range of motion [37], which usually translates into functional disturbance of the hand. Considering the general motor ability of acute stroke patients, 0 ~ 20 mm is the essential measuring range for finger rehabilitation exercise. Taken the recovery process of finger movement ability, this research targets the contactless finger motion detection with 30mm detection range.

2.1.2.2 Movements of fingers

Casual observation suggests that humans rarely move one finger alone when performing functional tasks [38]. When a finger performs its intended movements, the real movements of other fingers may occur [38]. However, a thumb usually has the highest average individuation index [38], which refers to the ability to move without any accompanying motion of the other fingers; and remained most stationary during instructed movements of other fingers [38, 39]. Therefore, a thumb can be considered independent during flexion-extension movements [39].

For this reason, only the index finger, middle finger, ring finger and little finger were considered in this study, as a simple start to explore the movements of fingers. In light of the typical motor ability of an impaired hand and the fine motor function of fingers, a millimeter level accuracy will be preferred to measure the tiny movements of fingers in regular training and testing sessions.

2.2 Medical equipment for hand rehabilitation

Section 2.2 reviews the medical equipment for hand rehabilitation. Here, section 2.2.1 investigates the medical equipment for hand rehabilitation in commercial practice and then, section 2.2.2 compares the devices and systems found in academic research.

2.2.1 Medical equipment in commercial practice: Exercising, supporting and testing

Written sheets of exercise prescribed by the therapist are probably the first assistive approaches for stroke patients' rehabilitation exercising at home. It is a fairly common and low cost approach to hand therapy. However, it lacks guidance and motivation, which are thought to be important for maximising hand movement recovery [40]. With increasing attention to hand rehabilitation from the industry and academic research as well as the healthcare providers, there are some rehabilitation devices available in the market with a variety of appearances, size, price, and functionality.

Fig.2-1 shows a list of the rehabilitation equipment available in the market, ideal for exercises that strengthen weakened or injured hands and fingers. Although they all target exercise, these products are further classified and discussed in Table 2-1, based on the different rehabilitation exercises they focus on.

For example, 'Therapy Putty for Hand Exercise' (Fig. 2-1 a)) is a therapeutic aid that can be squeezed easily and recovers slowly, making it ideal for working on improving flexion ability. Similar products focusing on flexion movement summarized in Table 2-1 include: b) Massage Ball Blue, c) Hand Rehabilitation Exerciser, d) Hand master Plus, e) Graded Pinch Exerciser, f) Cando Latex Free Hand Exercise Web, i) Hand Helper – Standard, j) Cando Digi-Flex Hand/Finger Exerciser, k) Hand & Finger Exercisers, l) Thumb Strengthening Exercise System, n) Strengthening & Toning Hand Grips. This kind of exercise is necessary to regain the grip or pinch ability of an impaired hand. Most of the flexion-targeting device are aimed for whole hand recovery and require little set-up time or effort. Additionally, most of the prices of these products are distributed in the range \$10-\$50.

Apart from this, there are also simple devices presently available on the market for extensor strengthening and conditioning, such as d) Hand master plus, g) Finger and Thumb Flexion Gloves, h) Digi-Extend Finger Exerciser, m) AliMed Antimicrobial Blue Carrot Hand Orthosis Kit. Most devices discussed in Table 2-1 focus on one of the extension or flexion movement. It is worth noting that the product d) hand master plus is able to provide the

combined training for both the extension movement and the flexion movement. Similar to the flexion-targeting device, the majority of these extension-targeting device work for all the five fingers' recovery and cost less than \$50. What is different from the flexion-targeting device is that these extension-targeting devices require additional time to put on before use. Finally, product sets o) E-Z Exer-Board Hand Exercise Kit and p) Table Mounted Finger Ladder are discussed. As a set of products, they are developed for more comprehensive tasks of the whole hand. Although they have little set-up time or effort, their cost is in the range \$100-\$200.



Fig. 2-1 Home-based medical equipment in the market for exercising

Collectively, the majority of the exercising devices tend to be straightforward with simple design, but they ignore the motivation for a home exercise program and emphasize repetition exercise. They generally have the advantage of low cost and convenient use, which contribute to their application in hand rehabilitation training. However, the clinic effect of

devices reported in Table 2-1 to diagnose, treat, cure, or prevent any specific disease or health condition have not been reported.

Table 2-1 Home-based medical equipment for exercising

	Flexion	Extension	Comprehensive exercise
Product	a), b), c), d), e), f), i), j), k), l), n)	d), g), h), m)	o), p)
Finger exercised	Five fingers for most cases, except: One finger: l) Two fingers: e)	Five fingers for most cases, except: Four fingers: g)	Five fingers
Set up	All most no set-up time or effort	Time to wear the device required	All most no set-up time or effort
Price	Less than \$10: n), l) \$10~\$50: a), b), c), d), f), i), k) \$50~\$100: j) \$100~\$200: e)	Less than \$10: g), h) \$10~\$50: d) \$50~\$100: m)	\$100~\$200
Clinical effect	Products are used by patients in hand rehabilitation training. The clinic effect to diagnose, treat, cure, or prevent any specific disease or health condition have not been reported.		

Note: The order a)~p) are consistent with the Fig. 2-1

Apart from the conventional rehabilitation devices presented in Table 2-1, there are FitMi and MusicGlove which provide better motivation and guidance to encourage exercise [40, 41]. FitMi contains two wireless pucks and a therapy app that picks exercises tailored to the stage of recovery. It provides similar training as product o) E-Z Exer-Board Hand Exercise Kit but with interesting feedback forms to motivate users. Additionally, Music Glove works by motivating users to perform appropriate pinching movements according to the musical note that floats down computer screen. It is reported to improve the hand function in 2 weeks. However, it focuses on pinching movements only, and requires noticeable time and effort to carefully put on the glove-like system before usage.

Fig. 2-2 shows hand or finger orthoses that work as mechanical aids to support weak or damaged parts of the hand. The general idea for these products is that stroke patients usually

suffer from a firmly curled hand with strong flexion synergy. Hence, the product listed in Table 2-2 help patients to separate and extend their fingers to prevent pressure concentration.



Fig. 2-2 Home-based medical equipment in the market for mechanical support

Table 2-2 Home-based medical equipment for mechanical support

	Static mechanical support	Mechanical support with movement assist
Product	a), c), d), e), f), g), h)	b)
Finger exercised	One finger: g) Five fingers: a), c), d), e), f), h)	Five fingers
Set up	Time to wear the device required: c), d), e), f), g), h) Noticeable amount of time and effort required to wear the device: a)	Noticeable amount of time and effort required to wear the device
Price	\$10~\$30: g), h) \$30~\$100: a), d), e) \$100~\$200: c) Not available: f)	More than \$500
Clinical effect	Products are aimed for hand rehabilitation purpose. For example, a) is indicated for post-stroke/CVA, finger contractures, neuromuscular, joint weakness and decreased ROM. The clinic effect of these products to diagnose, treat, cure, or prevent any specific disease or health condition have not been reported.	

Note: The order a)~h) are consistent with the Fig. 2-2

For example, product a) Comfy Adjustable Cone Hand is a unique splint worn on the lateral side of the arm of patients. Fingers are positioned around the cone. Finger separators are placed on the cone to separate the fingers. Adjustable hinge at the wrist helps increase wrist

extension. Similar products c), d), e), f), g), h) are also summarized in Table 2-2. Specially, product b) DeRoyal Static-Pro Wrist can aid with both flexion and extension movement. It is achieved with the turn of a knob. The majority of equipment for mechanical support aimed for the whole hand, except for product g) Spring Finger Extension Assist, which is designed for one finger only. Given the purpose of the hand or finger orthoses which help patients separate and extend their fingers, these products usually have more complex mechanical structure than the exercising devices, which will result in higher price as well as more time and effort to set-up. The clinic effect of these products for any specific disease or health condition have not been reported yet.

Fig. 2-3 further provides examples of hand rehabilitation medical equipment that reflect the recovery level of the hand, such as static force and range of movement. Product a), b), c), d), e) measure the force when patient conducts grip or pinch movement while product f), g), h) measure the range of movement, including (hyper-)extension and comprehensive eye hand coordination movement. Similar to the exercising equipment presented in Table 2-1, the use of these products tends to be quite straight-forward and requires little set-up time or effort. The cost of these product, however, is much higher than the exercising equipment, which is mainly distributed in the range \$100-\$400.



Fig. 2-3 Home-based medical equipment in the market to reflect the recovery level of the hand

Table 2-1, 2-2 and 2-3 briefly summarize the home-based medical equipment for hand rehabilitation available in the market, with focuses on the number of fingers aiming at, set-up requirement, price, and clinical effect. Collectively, these products are aimed for hand

rehabilitation purpose and are used by the patients. However, their rehabilitation effect has not been clinically tested and reported yet. Here, devices that do not need to be fastened or attached to the forearm, hand or fingers before usage, are more convenient to use and require less time and effort to set-up. Although, for some supporting equipment presented in Table 2-2, the wearable design scheme is sometimes inevitable, for the exercising or testing devices, the non-wearable implementation will be a better choice, especially for hand rehabilitation devices in home-based application.

Table 2-3 Home-based medical equipment to reflect the recovery level of the hand

	Force measurement	Movement range measurement
Product	a), b), c), d), e)	f), g), h)
Movement measured	Grip & Pinch: a) Grip: b), c), d) Pinch: e)	Hyper- Extension: f) Finger motion (Extension): g) Eye-hand coordination, speed, dexterity: h)
Finger measured	Five fingers in most cases, except: Two fingers: e)	One finger: f), g) Five fingers: h)
Set up	All most no set-up time or effort	
Price	\$100~\$200: a), b), d) \$200~\$300: c) \$300~\$400: e)	Less than \$20: g) \$50~\$100: f) \$200~\$300: h)
Unit	kg/Pound: a), b), e) kg: c), d)	Degree: f) Centimeters: g) Not available: h)

Note: The order a)~h) are consistent with the Fig. 2-3

It is also indicated from the above discussion that, there appears to be a gap between the exercise devices, support devices and test devices. These rehabilitation devices provide their target patients with exercise training, support structure and recovery test, but separately. For a patient with an impaired hand, a series of instruments are needed to realize home hand rehabilitation. Hence, multifunctional rehabilitation devices, which meet the all-round requirements of rehabilitation sessions, including exercise training, support structure and recovery test, will be preferred and worth investigating in home-based application.

2.2.2 Medical equipment in research literature

A search was made in the electronic database of PubMed to collect related literature published from the year 2000 to 2020 with keywords: “device” or “system” with “hand” and

“rehabilitation”. Similar to Section 2.2.1, the academic community has also extensively explored medical devices or systems targeting a smart rehabilitation system, featuring computer based structure [9, 10, 12, 16, 42-47], robot-assisted rehabilitation [7, 48, 49], activities of daily living (ADL) based exercise [7, 45, 49], feedback [44, 45, 47] as well as monitoring function [50], to provide smart exercising sessions for better hand recovery. Reliable testing devices or systems have been investigated to quantify the effects of rehabilitative training and enhance the motivation of patients [15, 16, 42, 45, 50, 51]. For example, the Spatial Augmented Reality System [16] tracks a subject's hand and creates a virtual audio-visual interface for performing rehabilitation-related tasks that involve wrist, elbow, and shoulder movements. It measures range, speed, and smoothness of movements locally and can send real-time photos and data to a clinic for further assessment.

It is observed from the literature review that, few studies have been conducted with a thought of achieving easier and quicker donning of the devices, which is often extremely difficult and very time-consuming for patients with hand impairment [11]. Current systems require an overhead in setting up, such as having to wear a ‘glove’ [52] or a ‘exoskeletons structure’ [53], significant amount of knowledge, and the necessity of other people’s help. There is also a gap between the medical equipment in academic research and in commercial practice, considering the price, size, complexity and knowledge required to use. It indicates a need for low cost and portable device that combines exercise, support, assistance and test function, not only easy to use but also motivates patients in the complete rehabilitation sessions to meet their specific motion goals without having to become experts. It is of greater importance, considering the feasibility for further development in a wider context, such as commercial practice or application in a home-based environment.

Although devices or systems introduced by these articles emphasize one of the different points discussed above (exercising, testing shaping as well as assisting), the majority of them show a clear tendency of the multifunctional design to meet more requirements in a rehabilitation session, with a view to home-based operation [13, 16, 42, 50]. Given their evidence of results presented, these systems are capable of providing their targeted treatment to the particular patients, thus increasing their performance. Notably, unlike in commercial practice, little academic research has been focusing on holding or shaping the impaired hand. A rehabilitation training system (UR System PARKO) conducted trainings by fixing fingers in a hyperextended position and extending the elbow joint while applying resistance load to the

fingertips. It promotes the recovery of motor function, as reflected in the finger extension of the severe plegic hand [8]. Instead, prior studies have queried diverse approaches to assist in particular functional tasks of the hand, such as the common movements of hand function including grip and release patterns [54], controlling the fully extended finger [11], the hand grasp function [13], the spatial finger joint coordination patterns of the functional manual tasks (e.g., power grip and pinch) [14], and hand opening or hand closing functional tasks [17].

Hence, rehabilitation devices that are capable of providing their target patients with multifunctional rehabilitation sessions, including: exercise training, support structure and recovery test, to meet the all-round requirements of the patient, will be preferred in home-based rehabilitation.

2.3 Tracking the movement

Section 2.3 further discusses the sensing technologies as well as sensors used for motion tracking to investigate the feasibility of home-based hand rehabilitation with emphasis on ease of use. In this research, extension and flexion of fingers was chosen as the exemplar training and assessing exercise here to simplify the system design. Taking the typical motor ability of an impaired hand into consideration, the objective system should be capable of detecting small movements of patients' fingers in regular training and testing sessions.

Sensing technologies that could be used to extract information about the improvements of fingers' motor ability mainly include inertial sensor based technology, magnetic sensor based technology, Electromyography (EMG) [55, 56], vision based systems [35], depth based technology [57-60], glove based systems [57, 60-62], robot-aided technology [61] as well as capacitive sensing technology [1, 62, 63]. These technologies are briefly discussed and compared as follows:

- A. **Inertial Sensor Based:** Inertial sensors like accelerometers and gyroscopes have been frequently used in navigation and augmented reality modelling. It is an easy to use and cost-efficient way for full-body human motion detection with high sensitivity and large capture areas. However, this technique requires sensing elements precisely attached, and therefore, is usually applied in glove-based techniques [52] or the 'exoskeleton' [53] design. It is also observed in the inertial sensor that, the position and angle of an inertial sensor cannot be correctly determined due to the fluctuation of offsets and measurement noise, leading to integration drift [61]. The accuracy of these gloves is up

to a few degrees, which makes them not too suitable for precise measurement of hand joint angles [64]. Research over the past 10 years has predominantly focused on validating measurements that the systems produce and classifying users' exercise quality [65].

- B. **Magnetic Sensor Based:** Magnetic sensors have been used for detecting the position of the object in many applications, such as, aerospace and healthcare [64]. Similar to the inertial sensors, the magnetic sensor is usually applied in glove-based techniques [52] or the 'exoskeleton' [53] design as well. Magnetic motion tracking systems have been widely used for tracking user movements in virtual reality because of their size, high sampling rate, lack of occlusion and so on. Nonetheless, magnetic trackers have inherent weaknesses like latency and jitter, more fundamental researches are needed to find solutions to these limitations [61]. Table 2-4 presented the information of the 3D Guidance® product suite, the driveBAY™ electromagnetic tracking systems as an example [61]. It provides real-time unobstructed tracking of miniaturized sensors embedded into medical tools [61]. However, it is also reported from the datasheet that, its accuracy will be degraded if there are interfering electromagnetic noise sources or metal in the operating environment, which have not been identified and minimized [66].
- C. **Electromyography (EMG):** Electromyography is the measurement of surface electric potentials from electrical currents generated in muscles during neuromuscular activities [55]. It has the potential to track the small motion of fingers and has been used for hardware implementation focusing on hand related application like prosthetic hand control, grasp recognition and human computer interaction [55]. This technique is particularly useful when patients cannot move their hands on their own. However, a potential drawback of an EMG-based rehabilitation system is the difficulty to use it. The electrodes have to be placed on precise muscles at specific locations, which require the instruction and supervision of therapists [56]. Besides, during detection, the EMG signals will be affected by both the internal and the external factors with different types of noise. Extra calibration effort should be made to compensate for it. One of the main problems of existing EMG technology is the high cost of commercial devices [2-8]. The price of commercial EMG devices can be up to thousands of dollars, as shown in Table 2-4.

- D. Vision based system (2-D motion tracking): 2-D motion tracking vision based system is concerned with human movement in an image plane [61]. In vision based systems, cameras are typically used to obtain the targeted image or video, and complicated geometrical modelling processing with statistical algorithms, decision theory and techniques are then used to extract desired features. Thus, it involves execution of complex algorithms and a large number of computations, demanding huge processing capability in a quick response time and making the technique inconvenient for embedded applications in a portable home-based device [35]. Moreover, the vision-based system is easily affected by ambient light conditions and cluttered backgrounds, robust algorithms are required to counter these influences [57, 60].
- E. Depth based technology (3-D motion tracking): 2-D motion tracking have natural restrictions, due to their viewing angle [61]. In the depth-based technology, it is advantageous as 3D information about the hand is provided. Kinect is a series of motion sensing input devices from Microsoft built to revolutionize the way people play games and experience entertainment [59]. It is also a popular option for body motion measurement research. The main disadvantage of this technology, however, is the low resolution provided by the Kinect sensor. For example, due to the low-resolution of the Kinect depth map, typically, only 640×480 . Although it works well to track a large object (e.g. the human body), it is difficult to detect and segment a small object (e.g. a human hand). In a typical application, the segmentation of the hand occupies a very small portion of the image and will usually be inaccurately represented in the recognition step, thus may significantly affect the calibration and calibration process [60]. Many of these research techniques are focusing on a relative big motion detection [67, 68] and are costly [69, 70], which fail at accurate hand movement detection for home-based usage.
- F. Optical sensing technology: Optical sensing is also a noncontact measurement [71], which can be realized without any sensing devices attached on the limbs. But, there are potential issues as: it tends to be easily affected by ambient conditions; multiple optical sensors will be required when measuring the movements of multiple fingers. Here, multiple sensors for a human hand might cause occlusions when placing the sensors, and requires significant calibration work. The optical sensing technology can be realized by different technologies. The laser-based optical sensing, such as time of

flight and 3D laser scanning, are relatively expensive. Although featured with a high precision, their usefulness is limited [48, 49]. On the contrary, the price of LED-based optical sensing devices, such as an IR-LED distance measuring unit from Sharp [21] is much lower. However, this distance measuring technique tends to be effected by the variety of the reflectivity of the object, the environmental temperature and the operating duration.

- G. Capacitive sensor: Capacitive sensors work by detecting small changes in capacitance due to the presence of an object in the electric field generated by the electrodes of a capacitor, and providing corresponding digital output [62]. A basic capacitive sensor consists of receiver and transmitter electrodes made of metal or conducting traces with a dielectric medium separating them. The transmitter of the sensor is connected to an excitation source and generates an electric field between the electrode surfaces. The electric field changes when an object (e.g. hand) is introduced in the field causing a change in capacitance [63]. However, the capacitive based sensor, such as MGC3030 [72] and the HOVER board [73], provides gesture recognition/proximity recognition only from the variation in field strength. Research should be conducted to explore the distance measurement.

Table 2-4 Sensing technologies

	Price	Set-up	Range of movement	Accuracy	Limitations	Clinical effect
Inertial measurement unit technologies	\$70~\$1350 [65]	Usually applied in glove-based [52] or the ‘exoskeleton’ [53] design.	Often used for gesture recognition [64], or even full body motion reconstruction [74].	About 35 mm average position estimation error reported [74].	<ul style="list-style-type: none"> • Sensing elements precisely attached required. • The issues of integration drift. 	Few user evaluation studies and no clinical trials in this field to date [65]
Magnetic technology	driveBAY™ [66]: \$1500~\$3000	Usually applied in glove-based [52] or the ‘exoskeleton’ [53] techniques.	driveBAY™ [66] 1.5~3m	driveBAY™ [66] Static Accuracy Position 7.6mm RMS at 1.52m range; 15mm RMS at 3.05m range	<ul style="list-style-type: none"> • Inherent weaknesses like latency and jitter. 	driveBAY™ [66]: Class I Medical Device with Type B Applied Part (Sensors), EN60601-1 Compliant.
Electromyography based technology	<ul style="list-style-type: none"> • Delsys Trigno \$ 20,000 [75] • Cometa \$15,000 [75] 	The electrodes have to be placed on precise muscles at specific locations [56].	Full body motion	Recognition accuracy: 68 ~ 99.8% Capture efficiency: 50 to 80% [76]	<ul style="list-style-type: none"> • Difficulty in placing the electrode on precise muscles; • Requiring the supervision of therapists 	Positive reports were obtained through research-oriented clinical trial studies [77]

Visual/Depth based technology	<ul style="list-style-type: none"> • Microsoft Kinect \$123 [78] • LEAP Motion \$70 [52, 79] 	<p>Noticeable amount of time and effort for set-up and calibration.</p> <p>For example, it takes at least 20 minutes before using the Kinect v2 [80].</p>	<p>Microsoft Kinect: Microsoft recommends a range of 1.2–3.5 m between the Kinect and the user [80].</p>	<ul style="list-style-type: none"> • The Kinect v1: a standard deviation of 15 mm in its depth accuracy; • Kinect v2: a depth accuracy of 2mm-4mm [80]. 	<ul style="list-style-type: none"> • Relatively low resolution; • Easily affected by ambient light conditions and cluttered backgrounds; • A large overhead in signal processing; • Costly and bulky 	<p>Positively assessed by academic research in medical applications, including:</p> <ul style="list-style-type: none"> • Kinect: Upper/lower limb rehabilitation, balance training/monitoring, and motion exercises [78]. • LEAP Motion: Upper limb rehabilitation from stroke, cerebral palsy and other injury [81-84].
Optical based technology	<ul style="list-style-type: none"> • Laser-based: >= \$2000; • Sharp LED sensor [21]: \$12.5 	<ul style="list-style-type: none"> • Significant setting-up and calibration work required; • Multiple optical sensors required for measuring multiple fingers. 	<ul style="list-style-type: none"> • Laser-based [85]: 60-80mm • Sharp LED sensor [21]: 0-300mm 	<ul style="list-style-type: none"> • Laser-based [85]: 0.25 μm • Sharp LED sensor [21]: Not applicable. 	<ul style="list-style-type: none"> • Multiple sensors required for multiple fingers, which might cause occlusions; • Easily affected by ambient conditions 	<p>Not much clinically specific application to date.</p>

Capacitive sensing-based technology	<ul style="list-style-type: none"> • MGC3030 [72]: \$139.00 /\$5.5 [86] • HOVER board \$41.5 [73] 	Capable of noncontact measurement and requires little setting-up effort.	MGC3030 [72]: Best detection range is 0 – 100mm for general applications [72] HOVER board: 13cm hand gesture detection [73]	Recognizable hand gestures, including swipe up, down, left and right; Electrodes for touch sensitive inputs only.	<ul style="list-style-type: none"> • MGC3030: Aimed for gesture/proximity recognition only • HOVER board: Not accommodate for a good range of hand gestures; electrodes for touch sensitive input only 	MGC3030 [72]: E.G. Stroke rehabilitation for motor impairment [1, 73, 87]; The application for hand rehabilitation [88].
-------------------------------------	---	--	--	---	--	--

Note:

1. For Electromyography (EMG) based technology: Recognition accuracy is defined as the ability to correctly classify the action by EMG signal decoding; EMG capture efficiency is defined by the ability to accurately capture the EMG signals with respect to a standard electromyogram [76].
2. Cost of Microsoft Kinect depends on the number of sensors. For example, a 3D scanner system which was arranged with four Kinect devices, so the total cost for the Kinect will be approximately \$492 [80].
3. There is conflicting information about the range and accuracy of the Kinect v1 and v2. The table shows some typical data.
4. Cost of Laser-based sensing technique depends on the specific requirements of device, so only a rough estimate is given in this table.
5. For MGC3030 motion sensor, \$139.00 is the cost of the whole development kit, while for a sole chip, the cost is \$5.5.

From the previous discussion of the sensing technology, glove based (or exoskeleton [53]) design is a prevailing approach used in hand rehabilitation sensing techniques such as inertial sensor, magnetic sensor, electromyography-based sensor, as reported in Table 2-4. These glove-based systems were usually of relatively high accuracy and reliability, however, at the expense of the complex model design, as well as the donning and setting effort. Generally, these instruments cannot be used by patients without the help of professionals. Additionally, the glove-based structure might obstruct natural finger movement. These issues are especially inconvenient for home-based usage of patients with an impaired hand [57, 60, 62], and are contrary to a preferred home-based hand rehabilitation approaches advocated in Section 2.1. Therefore, the non-contact detection method is a primary feature of the target measuring system. From Table 4-2, the visual/depth-based technology, the optical based technology and the capacitive based technology are capable of finger motion measurement without a sensing element attached.

The capacitive sensors are adopted in this research to precisely measure the extension and flexion of fingers. This technology has a user-friendly donning, setting, and using requirement, and provides the possibility of widely usage outside the healthcare center. Optical sensing is also a noncontact measurement [16] but has potential issues as: influence of ambient conditions; multiple optical sensors required for multiple fingers. The visual/depth-based systems works well to track a large object (e.g. the human body) in a noncontact form, while it is difficult to detect and segment a small object (e.g. a human hand). In contrast, the sensitivity of the capacitive sensing decreases quickly when the distance between the sensor and human body increases [63], making it particularly sensitive to the small and easy movements, like the movement of fingers. Further to this, unlike vision-based systems, the capacitive sensors will not be affected by ambient light conditions or cluttered backgrounds; and therefore, can work without a large overhead in signal processing.

Based on the capacitive sensing technology, the specification of the targeted measuring system includes:

- a noncontact form of measurement for fingers
- a millimetre level accuracy within the normal range of motion of the finger
- 30mm measuring range considering the general motor ability of stroke patients and the recovery process.

- a sampling rate of more than 20Hz to provide the potential for a contactless study of tremor in fingers.

An optical method is also adopted in this research as a comparing technique for the capacitive sensing technique in real-time contactless measurement. This was accomplished using an optical sensor system which works as a flexible contactless ‘ruler’ to measure the finger movements.

2.4 MGC3030 justification

The aim of the research is to develop an easy-to-use device for home-based hand rehabilitation. Towards this target, measurement techniques consistent with the overall aim are explored and discussed in previous sections. The glove-based techniques [52], the ‘exoskeleton’ [53] and Electromyography (EMG) [55] have been proposed to support hand rehabilitation, and are particularly useful when patients cannot move their hands on their own. However, these techniques require sensing elements precisely attached and have an overhead in setting up, which results in the necessity of other people’s help. To reduce these overheads to a minimum and improve the ease of use, the capacitive sensing technology was chosen for contactless finger motion detection in this study.

Limitations of this adoption, however, is that, current capacitive based sensors, such as MGC3030 [72] and the HOVER board [73], only provide gesture recognition/proximity recognition, instead of precise distance measurement. Here, the electrodes of HOVER board [73] provides touch sensitive input only, which limits its extending application in distance detection. The MGC3030 motion sensor is a low cost (4 GBP) and reliable off-the-shelf option, given the economic reasons and time restrictions [1, 73]. Therefore, the MGC3030 motion sensor is selected as an input sensor.

In this research, techniques compatible with the MGC3030 sensing technology for the non-contact multi-finger distance measurement for home-based hand rehabilitation purpose will be explored. To the best of our knowledge, this is the first time that the MGC3030 sensing technology have been applied for multi-finger movement measurement. The choice of this technology can be justified with reference to the specifications of the targeted measuring system concluded in Section 2.4:

The MGC3030 motion sensor uses the principle of electrical near field sensing for advanced proximity detection to provide gesture and positional data of a human hand in real

time [72]. Based on the quasi-static electrical field sensing, the MGC3030 motion sensor is capable of measuring the movements of fingers without attaching sensing elements to the limbs. Characterized by the user-friendly setting and donning requirements, this measuring system is easy for patients to use at home, without the assistance from either therapists or carers [32].

By applying a sinusoidal voltage, the MGC3030 motion sensor generates a quasi-static electrical near field and propagates three-dimensionally [72]. When fingers move towards the sensor, they will decrease the electrical field locally [72]. Therefore, the fingers' motion can be measured by the electrical field variations. Due to the quasi-static electrical sensing mechanism of the MGC3030, its sensitivity is inversely proportional to its distance from the human body and has no ambient influences (such as light, sound and radio interference) [72]. Hence, it is particularly sensitive for small distance applications, which is capable of providing a millimeter level accuracy within the normal range of motion of the finger.

Moreover, the MGC3030 chip provides proximity detection with 0 – 150 mm detecting range. Driven by 100 kHz sinusoidal signals, this adoption works with 44 kHz-115 kHz carrier frequency. Therefore, the measuring range of 0~30mm and sampling rate of more than 20Hz can be satisfied as well. A notable advantage of the GestIC chip is that, it does not require host processing and eliminates the need to be constantly bridged through a computer. This means the future integration into a home-based smart rehabilitation system is more plausible [73]. Collectively, MGC3030 sensor is a suitable option with preferred features to achieve the objectives of this project.

The entire MGC3X30 system (both MGC3030 and MGC3130) is composed of three blocks as presented in Fig. 2-5 [72]. The MGC3030 controller consists of analogue front end that transmits signals to generate E-field and conditions the signals received from Rx electrodes, signal processing unit that performs digital signal processing tasks, and communication interface that sends the processed digital data to the application host. GESTIC Library is an embedded library that provides concurrent and continuous position tracking and gesture recognition. External electrodes include a transmit electrode and maximum of five receive electrodes for optimal E-field distribution and detection of E-field variations.

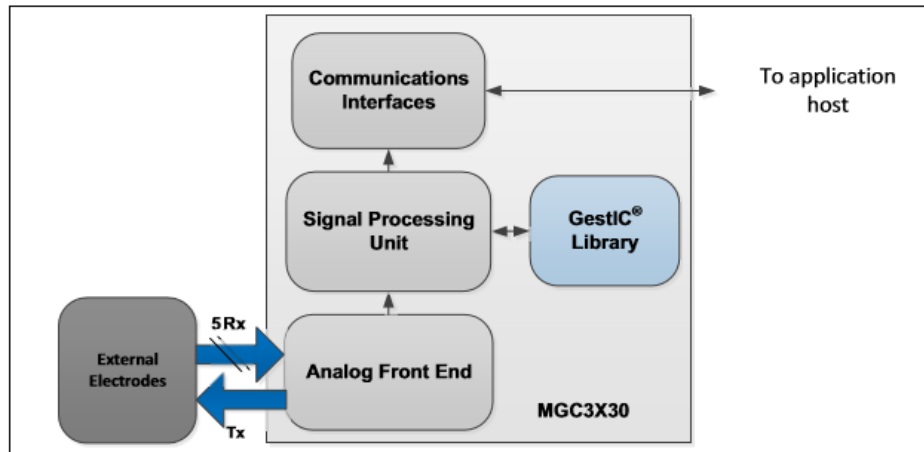


Fig. 2-5 MGC3X30 controller system architecture [72]

2.5 Summary

The aim of the research focuses on the technology for the rehabilitation of an impaired hand, investigating the feasibility of home-based approaches, addressing ease of setting and use to promote motivation of practice. Chapter 2 investigates the measuring techniques that are compatible with this overall aim. The extension and flexion of fingers are chosen as an exemplar training and assessing movement in this research. The MGC3030 motion sensor was chosen for contactless finger motion detection in this study.

Chapter 3 Finite Element Method Modelling of a Customizable Three-Layer Electrode Design

The design process of the GestIC MGC3030 module includes electrode design and simulation, module integration, and module parameterization [89]. In accordance with this, Chapter 3 carries out a Finite Element Method (FEM) simulation derived from the MGC3030 electrode stack-up design in Comsol Multiphysics to guide the practical design of the electrodes [89].

3.1 Theory of detection: Electrical field (E-field) sensing

The MGC3030 motion sensor utilizes an electrical field (E-field) for advanced proximity sensing. An E-field is generated and propagates three-dimensionally around the three-layer electrodes carrying the electrical charge. Applying direct voltages (DC) to an electrode results in a constant electric field while applying alternating voltages (AC) makes the charges and the field vary over time. When applying sinusoidal voltage to electrodes with a wavelength much larger than the electrodes, the magnetic component is practically zero and no wave propagation takes place. This will result in quasi-static electrical near field that can be used to sense conductive objects, such as the human body [72].

Microchip's GestIC uses transmit frequencies around 100 KHz, whose wavelength will be much larger than the electrode geometry. Receive electrodes (Rx) are used to detect the E-field variations at different positions to measure the origin of the electric field distortion. When a person's hand or fingers intrudes into the electrical field, the field lines are drawn to the hand, and then shunted to the ground due to the conductivity of the human body. Therefore, the three dimensional electric field decreases locally. This minuscule change then causes a compression of the equipotential lines and shifts the Rx signal levels to a lower potential [72]. Fig. 3-1 show the influence of an earth-grounded body to the electric field.

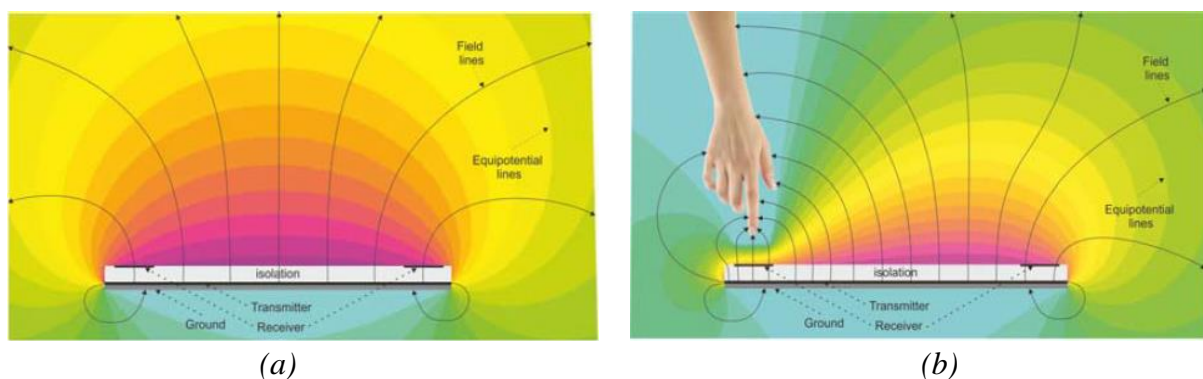
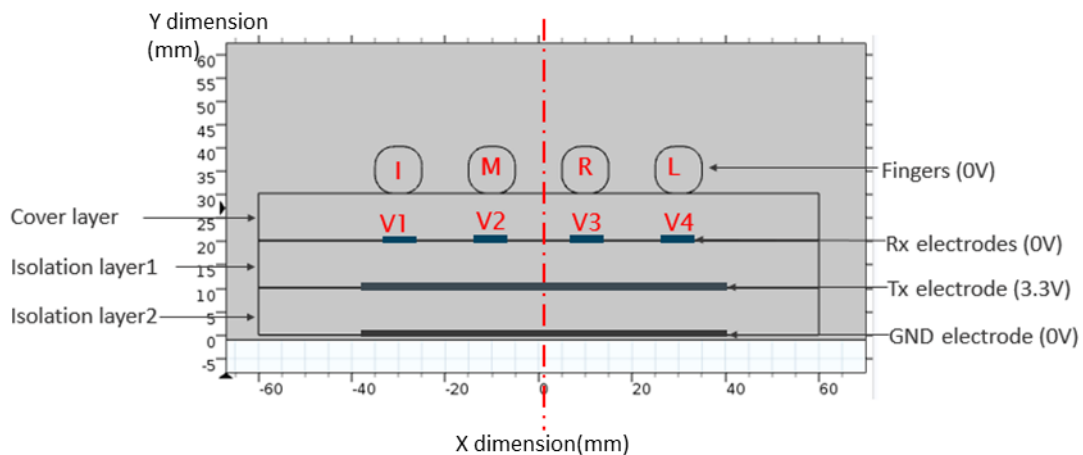


Fig. 3-1 Equipotential lines of E-field: (a) Undistorted E-field, (b) Distorted E-field [72]

3.2 Simulation model

3.2.1 Three-layer electrode stack-up design

The Comsol simulation model, as presented in Fig.3-2 (a), is an implementation for this research. It is derived from the MGC3030 electrode stack-up design, and consists of four receive electrodes (Rx), a transmit electrode (Tx), a ground electrode (GND), a cover layer and two isolation layers, and [1, 89]. This two-dimensional simulation model is customizable by changing the settings of components for broader application. An exemplar receptacle model is also shown in Fig. 3-2. The four fingers of the human hand are modelled as conductive cylinders placed on the top layer. The hand is pronated with the fingers extended and the thumb adducted so that the hand adopts a horizontal posture. Each finger can be extended from the flat posture but not into hyperextension. Between the top layer and isolation layer1, four Rx electrodes are placed underneath four fingers accordingly. Here, the potential of Rx electrode to ground can reflect the finger motion. The Tx electrode and the GND electrode are inserted between isolation layer1 / isolation layer2, and isolation layer2 / bottom layer respectively.



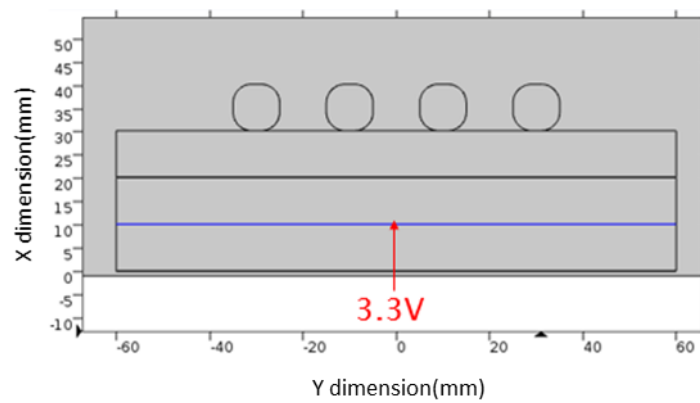
(a)



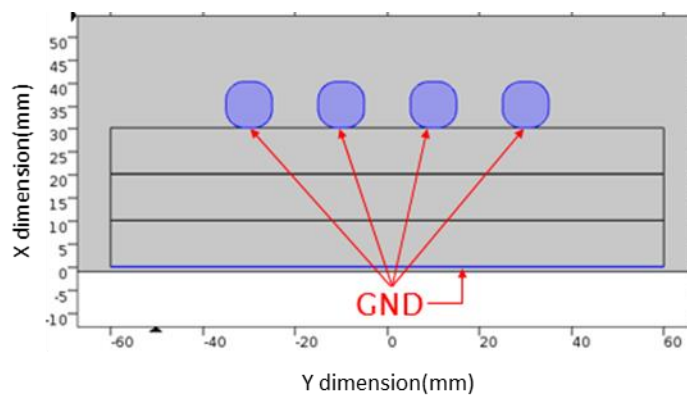
(b)

Fig. 3-2 Electrode stack-up design (I: index; M: middle; R: ring; L: little): (a) Simulation model, (b) Experimental hand receptacle

In the Comsol simulation package, all the electrodes are set to use the default material ‘copper’, while the ‘Acrylic plastic’ is chosen as the material of the isolation layers with necessary parameter settings (relative permittivity and density). To simplify the simulation model of a human finger without losing its important electrical physical characteristics, ‘water’ was chosen to represent the soft and hard tissues of a finger. Fig. 3-3 shows the electrical terminal settings of the simulation model. Here, 3.3 V A.C is applied to Tx electrode, whereas both the GND electrode and the fingers are set to the ground potential. Detailed material settings in the simulation model are shown in Appendix A.



(a)



(b)

Fig. 3-3 Terminal settings: (a) 3.3V, (b) GND

3.2.2 Discussion of fingers movements

As proposed in Section 2.1.2, the combined movement--extension and flexion--of the index finger, middle finger, ring finger and little finger were considered in this study, targeting the contactless finger motion measurement with a millimeter level accuracy. Concerning different combinations of fingers’ movement, in total, there are fifteen possible combinations

of finger movement. However, considering the symmetrical structure of the simulation model, not all the cases have to be explored.

As presented in Table 3-1, there are four possible cases if one finger moves. Considering the symmetrical structure, case 1-2 (Little finger) and case 2-2 (Ring finger) will end up with similar outcomes from the case 1 (Index finger) and case 2 (Middle finger) respectively. Hence, only two cases should be explored to study one finger's situation. Similarly, there will be: six cases (case 3 & case 3-2, case 4 & case 4-2, case 5 and case 6) if two fingers move together; and four cases (case 7 & case 7-2, case 8 and case 8-2) if three fingers move together. Concerning the symmetrical simulation model, only four possible combination should be explored to study two fingers' situation; and only two possible combination should be explored to study three fingers' situation. Particularly, there is a sole case if all four fingers move together.

Table 3-1 Finger movement combinations

Category	Finger Combinations					Symmetrical Finger Combinations				
	Case	I	M	R	L	Case	I	M	R	L
One finger moves	1	1	0	0	0	1-2	0	0	0	1
	2	0	1	0	0	2-2	0	0	1	0
	3	1	1	0	0	3-2	0	0	1	1
Two fingers move	4	1	0	1	0	4-2	0	1	0	1
	5	1	0	0	1					
	6	0	1	1	0					
	7	1	1	1	0	7-2	0	1	1	1
Three fingers move	8	1	1	0	1	8-2	1	0	1	1
	9	1	1	1	1					
Four fingers move	9	1	1	1	1					

Note: 1) A '1' indicates movement and a '0' no movement. 2) I: index; M: middle; R: ring; L: little.

The case of two fingers will be further explained and studied in Section 4.2. A discussion with more details for all the possible cases can be found in Appendix B: Finger Movements Discussion.

3.3 Variation of electric field distribution with finger motion

Case 2(0100) and case 2-2 (0010) are chosen as the exemplar finger motion to show the influence of an earth-grounded body to the electric field distribution, as shown in Fig 3-4. Underneath each finger, four Rx electrodes are used to detect the electric field distortion from the varying signals received. A variable 'D', which is the distance between the under surface of a finger and the top of the cover layer, was used to represent the approaching and departure

of the moving finger, as shown in Fig. 3-4 as the red vertical lines below the middle and ring fingers. In other words, it is a height parameter to record the changes in the vertical coordinate.

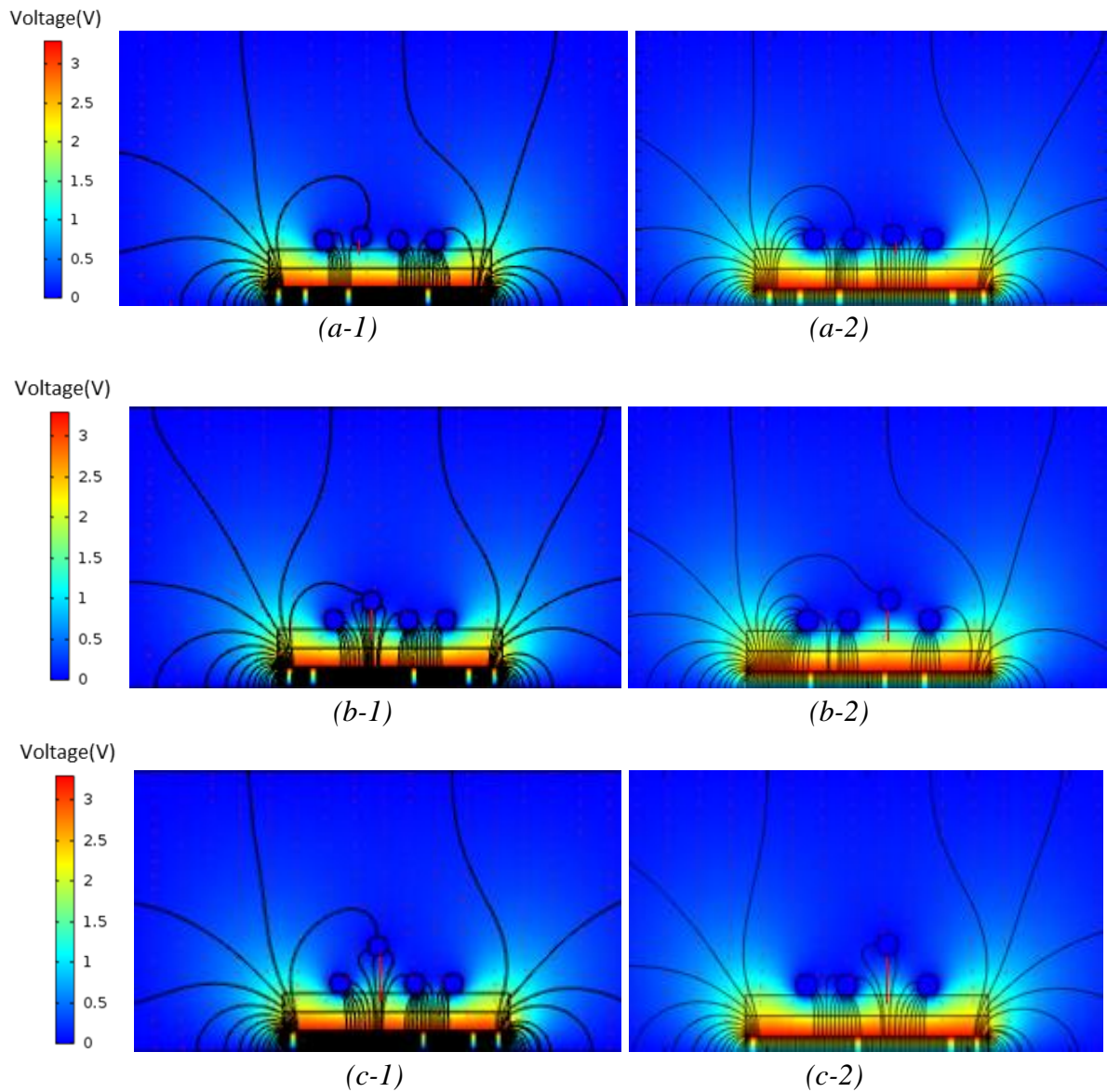


Fig. 3-4 Simulation model when finger moves (case2:0100, case 2-2: 0010) ((a-1) case2 distance = 2mm, (a-2) case2-2 distance = 2mm; (b-1) case 2 distance = 10mm, (b-2) case2-2 distance = 10mm; (c-1) case2 distance = 20mm, (c-2) case 2-2 distance = 20mm)

Ten values of the height parameter ‘D’ were selected to repeat the simulation of each case. The heights are 0mm, 2mm, 4mm, 6mm, 8mm, 10mm, 15mm, 20mm, 25mm and 30mm. The voltages of electrodes corresponding to the varied distance were calculated in Comsol using point evaluation, as presented in Fig. 3-5. The plots in Fig. 3-4 and 3-5 show similarity that implies a symmetrical pattern of voltages of the entire electrode stack-up structure. This relationship of electrodes behaviour is in line with the symmetrical structure proposed at the

start of the 3.2, when the fingers' motion was discussed. Moreover, the voltage distance characteristics of the four Rx electrode channels all show a trend of rapid growth first and then slowly approaching a constant value, although the increase amplitude is different. In other words, as the moving distance becomes larger, the finger will eventually be so far away from the electrodes that no movement will be detected. Therefore, the voltage will approach a constant value, which is the same as when there is no finger interference in the entire space. This is also in agreement with the quasi-static electrical near field mechanism of the capacitive sensor MGC3030, where the better resolution will be obtained at smaller movements.

Table 3-2 and Table 3-3 presented the voltages values calculated in Comsol, corresponding to the moving finger at each distance point, for case 2 and case 2-2 respectively. Here, sensitivity refers to the voltage increase of the electrode under a moving finger, when the finger moves by one millimetre. For case 2, as the middle finger moves away from the model surface, the voltages of the Rx electrode under the middle finger (V_2) present a most significant increase from 1.83788 to 2.25820V, as the input signal to reflect this motion. The voltages of the Rx electrodes under the index finger (V_1) and the ring finger (V_3) increase accordingly, in a similar pattern but with different initial values. The MGC signal of the little finger, however, is hardly affected by the movement of the middle finger, as shown in the V_4 column in Table 3-2. Similarly, in Table 3-3, the voltages of the Rx electrodes under the moving finger (V_3) and the neighbouring fingers (V_2, V_4) increase accordingly when the ring finger moves away from the model surface, while the MGC signal of the non-adjacent one (V_1) remains almost unchanged. Raw data for all possible cases have been calculated and presented in Appendix C.

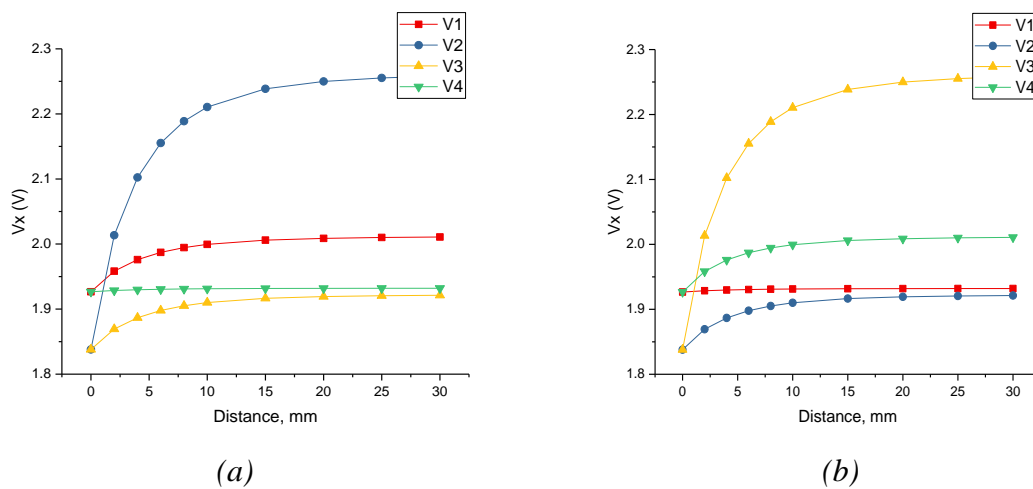


Fig. 3-5 Relationship between distance and voltage: (a) case2 (0100), (b) case2-2(0010)

Table 3-2 Case 2: Voltages values corresponding to the movement of the middle finger

Distance (mm)	V ₁ (V)	V ₂ (V)	Sensitivity- V ₂ (V/mm)	V ₃ (V)	V ₄ (V)
0	1.92663	1.83788		1.83788	1.92663
2	1.95838	2.01354	0.08783	1.86931	1.92865
4	1.97601	2.10229	0.04438	1.88677	1.92978
6	1.98718	2.15526	0.02649	1.89784	1.93050
8	1.99455	2.18877	0.01675	1.90515	1.93097
10	1.99949	2.21058	0.01091	1.91005	1.93128
15	2.00602	2.23859	0.00560	1.91653	1.93169
20	2.00875	2.24994	0.00227	1.91923	1.93185
25	2.01009	2.25528	0.00107	1.92051	1.93194
30	2.01086	2.25820	0.00058	1.92122	1.93199
Average			0.02176		

Calculation Example:

$$\text{Sensitivity- } V_{2-2\text{mm}} = (V_{2-2\text{mm}} - V_{2-0\text{mm}}) \div (2-0) = (2.01354-1.83788) \div (2-0) = 0.08783 \text{ V/mm}$$

$$\text{Average-Sensitivity- } V_2 = \text{SUM (Sensitivity- } V_2) \div 9 = (0.08783+0.04438+\dots+0.00058) \div 9 = 0.02176 \text{ V/mm}$$

It can be observed in Table 3-2 and Table 3-3 that, when a finger moves, the voltage of the electrodes under the other fingers varies simultaneously, especially the neighbouring ones. The MGC signal of the non-adjacent ones will hardly be affected by the movement of a moving finger. This result is in accordance with the quasi-static electrical near field theory, and indicates a ‘crosstalk’ generated in this simulation model where there are signal changes due to an electrical field leakage from a neighbouring moving finger. In the following chapters, the crosstalk will be further investigated.

Table 3-3 Case 2-2: Voltages values corresponding to the movement of the ring finger

Distance (mm)	V ₁ (V)	V ₂ (V)	V ₃ (V)	Sensitivity- V ₃ (V/mm)	V ₄ (V)
0	1.92663	1.83788	1.83788		1.92663
2	1.92866	1.86931	2.01354	0.08783	1.95838
4	1.92978	1.88677	2.10229	0.04438	1.97601
6	1.93050	1.89784	2.15526	0.02649	1.98718
8	1.93097	1.90515	2.18877	0.01675	1.99455
10	1.93128	1.91005	2.21058	0.01091	1.99949
15	1.93169	1.91653	2.23859	0.00560	2.00602
20	1.93186	1.91923	2.24994	0.00227	2.00875
25	1.93194	1.92052	2.25528	0.00107	2.01008
30	1.93199	1.92122	2.25820	0.00058	2.01085
Average				0.02176	

Calculation Example:

$$\text{Sensitivity- } V_{3-2\text{mm}} = [V_{3-2\text{mm}} - V_{3-0\text{mm}}] \div (2\text{mm}-0\text{mm}) = (2.01354-1.83788) \div (2-0) = 0.08783 \text{ V/mm}$$

$$\text{Average- Sensitivity- } V_3 = \text{SUM (Sensitivity- } V_3) \div 9 = (0.08783+0.04438+\dots+0.00058) \div 9 = 0.02176 \text{ V/mm}$$

3.4 Modified electrode layer stack-up design

In this section, a different electrode layer stack-up design is explored in Comsol to optimize the performance on reducing crosstalk. Three extra ground electrodes were placed at the midpoints of the neighbouring Rx electrodes pairs. The main ground electrode is denoted as GND electrode, while the smaller ground electrodes, placed in between each pair of Rx electrodes, are denoted as ‘gnd’, as presented in Fig 3-6. In the Comsol simulation model, 3.3 V A.C is applied to Tx electrode, whereas both the GND electrode and the added gnd electrodes are connected to the ground potential.

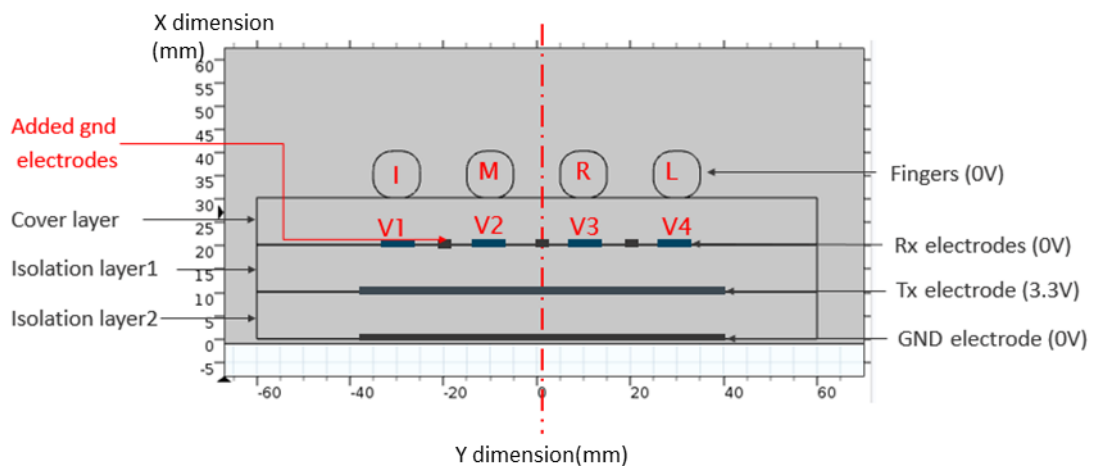


Fig. 3-6 Comsol simulation model with added gnd electrodes (I: index; M: middle; R: ring; L: little)

Fig. 3-7 shows the electric field distribution of the modified simulation model with added gnd electrodes when the middle (case 2 (0100)) or ring finger (case 2-2 (0010)) moves 2mm, 10mm and 20mm away from the upper surface of the cover layer.

Analogous to the previous electrode design, when a finger moves away from the Rx electrodes, the corresponding voltages increase to reflect this process. This relationship of modified simulation model in case 2 and case 2-2 were also recorded, as presented in Fig. 3-8. Comparing Fig. 3-8(a) and Fig. 3-8(b), the similarity implies a symmetrical relationship of electrodes, which is in accordance with the symmetrical structure discussed in the modified electrode stack-up design summarized in Fig. 3-6. When a finger moves, the voltages of the Rx electrode under the moving finger present a most significant increase, as shown as V₂ in Fig. 3-8(a), and V₃ in Fig. 3-8(b). Additionally, the voltage of the neighbouring electrodes under the other fingers varies simultaneously during this motion (such as V₁ and V₃ in Fig. 3-8(a), and V₂ and V₄ in Fig. 3-8(b)), while the MGC signal of the non-adjacent ones will hardly be affected by the movement of a moving finger (such as V₄ in Fig. 3-8(a), and V₁ in Fig. 3-8(b)).

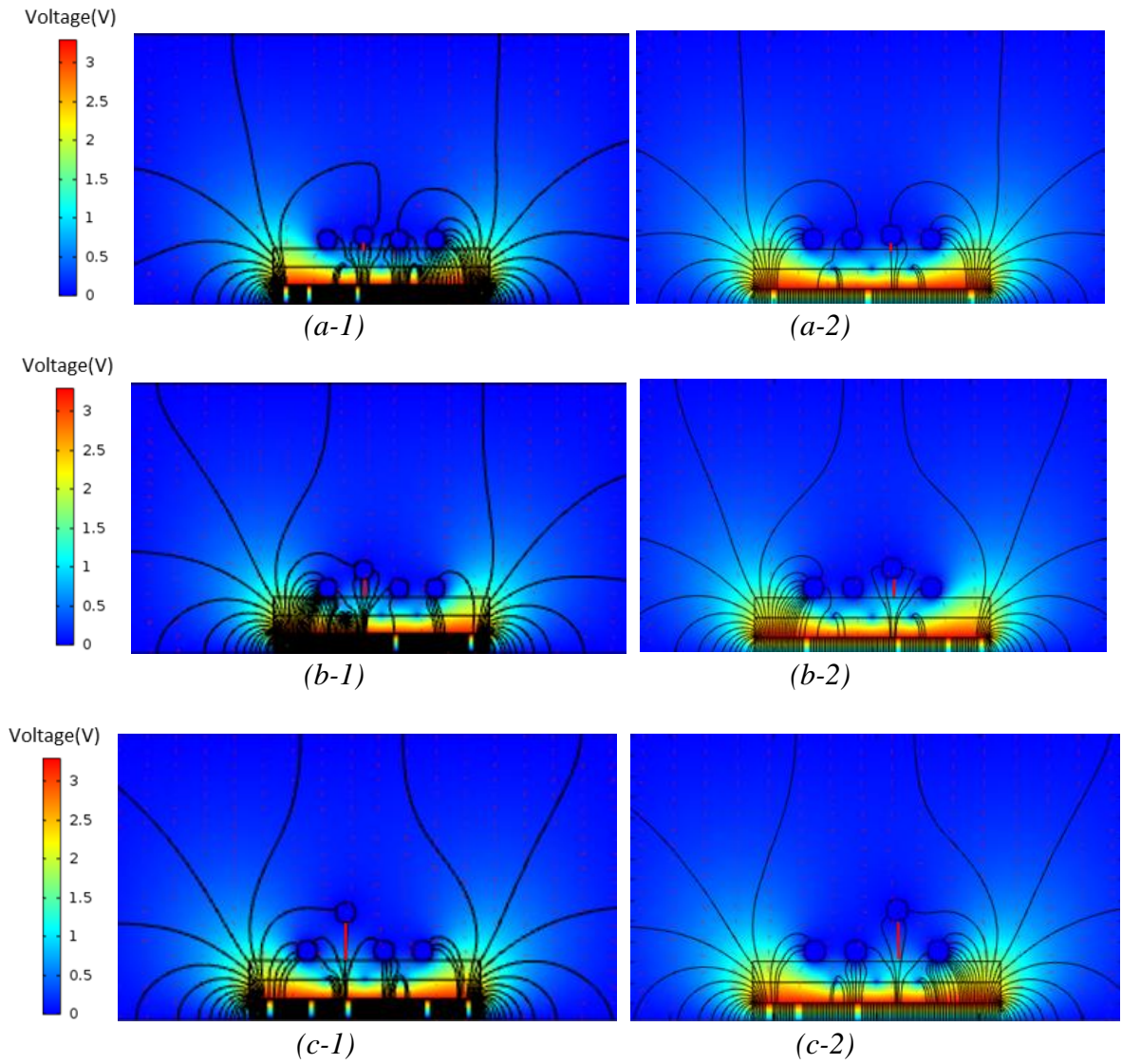


Fig. 3-7 Simulation model with add gnd electrodes (case2: 0100, case 2-2: 0010) ((a-1) case2 distance = 2mm, (a-2) case2-2 distance = 2mm; (b-1) case 2 distance = 10mm, (b-2) case2-2 distance = 10mm; (c-1) case2 distance = 20mm, (c-2) case 2-2 distance = 20mm)

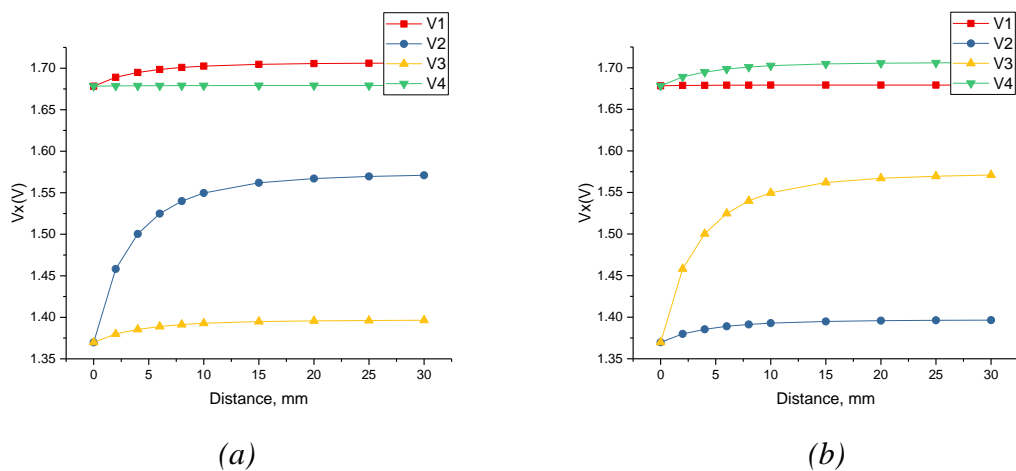


Fig. 3-8 Relationship between distance of the fingers and the voltage of electrodes in modified simulation model: (a) case2 (0100), (b) case2-2(0010)

Detailed voltages values corresponding to the moving finger for the modified electrode stack-up design in case 2 and case 2-2 are presented in Table 3-4 and Table 3-5 respectively. Here, sensitivity of the electrode under a moving finger when the finger moves by one millimetre, is also calculated. Similarly, a ‘crosstalk’ was observed when the signal changes due to the neighbouring moving finger. Data for all possible cases in the modified electrode design have been calculated and are shown in the Appendix D.

Table 3-4 Case2: Voltages values corresponding to the movement of the middle finger

Distance (mm)	V ₁ (V)	V ₂ (V)	Sensitivity- V ₂ (V/mm)	V ₃ (V)	V ₄ (V)
0	1.67836	1.36984		1.36981	1.67834
2	1.68901	1.45823	0.04419	1.37991	1.67867
4	1.69482	1.50045	0.02111	1.38547	1.67886
6	1.69849	1.52482	0.01219	1.38897	1.67900
8	1.70089	1.53993	0.00755	1.39127	1.67905
10	1.70250	1.54967	0.00487	1.39283	1.67909
15	1.70463	1.56206	0.00248	1.39489	1.67915
20	1.70553	1.56714	0.00102	1.39577	1.67916
25	1.70599	1.56963	0.00050	1.39619	1.67914
30	1.70627	1.57106	0.00029	1.39644	1.67914
average			0.01047		

Calculation Example:

$$\text{Sensitivity- } V_{2-2\text{mm}} = (V_{2-2\text{mm}} - V_{2-0\text{mm}}) \div (2-0) = (1.45823-1.36984) \div (2-0) = 0.04419 \text{ V/mm}$$

$$\text{Average-Sensitivity- } V_2 = \text{SUM (Sensitivity- } V_2) \div 9 = (0.04419+0.02111+\dots+0.00029) \div 9=0.01047 \text{ V/mm}$$

Table 3-5 Case 2-2: Voltages values corresponding to the movement of the ring finger

Distance (mm)	V ₁ (V)	V ₂ (V)	V ₃ (V)	Sensitivity- V ₃ (V/mm)	V ₄ (V)
0	1.67836	1.36984	1.36981		1.67834
2	1.67869	1.37996	1.45821	0.04420	1.68900
4	1.67889	1.38549	1.50041	0.02110	1.69479
6	1.67901	1.38901	1.52479	0.01219	1.69845
8	1.67908	1.39131	1.53989	0.00755	1.70086
10	1.67913	1.39287	1.54963	0.00487	1.70249
15	1.67917	1.39491	1.56199	0.00247	1.70460
20	1.67918	1.39579	1.56707	0.00102	1.70549
25	1.67918	1.39625	1.56957	0.00050	1.70595
30	1.67918	1.39650	1.57100	0.00029	1.70623
Average				0.01046	

Calculation Example:

$$\text{Sensitivity- } V_{3-2\text{mm}} = [V_{3-2\text{mm}} - V_{3-0\text{mm}}] \div (2\text{mm}-0\text{mm}) = (1.45821-1.36981) \div (2-0) = 0.04420\text{V/mm}$$

$$\text{Average- Sensitivity- } V_3 = \text{SUM (Sensitivity- } V_3) \div 9 = (0.04420+0.02110+\dots+0.00029) \div 9=0.01046 \text{ V/mm}$$

3.5 Comparison and discussion

This research investigates a noncontact form of finger movement measurement with a millimeter level accuracy within 30mm measuring range. Therefore, in Chapter 3, the height

parameter ‘D’ was set to the values of 0mm, 2mm, 4mm, 6mm, 8mm, 10mm, 15mm, 20mm, 25mm and 30mm to explore the entire measuring range (30mm) in the simulation of each case. Considering the millimetre level accuracy over 30mm’s range, ideally, the noise-signal ratio should be no more than 3.3%. Currently, the simulation model only gives the simulated value of voltage signal without data fitting scheme. Therefore, here only discuss the sensitivity and crosstalk of the two electrode design models for comparison purpose.

Comparing Table 3-2 with Table 3-4 and Table 3-3 with Table 3-5, reveals a decrease in the voltages at all the electrodes in the modified electrode design and also the sensitivity and crosstalk. In order to assess the advantages and disadvantages of the added gnd electrodes, a comparison of the two electrode designs was conducted.

3.5.1 Sensitivity

The example calculation process for comparison between electrode design with or without gnd electrodes added in case 2 is illustrated in Table 3-6. The crosstalk and sensitivity data of original model here are consistent with the data highlighted in light orange in the Table 3-2. Likewise, these of the modified model are in accordance with the data highlighted in light gold in the Table 3-4. The details of each case in similar calculation steps are given in Appendix E. In Table 3-6, the percentage change is calculated using the sensitivity with added gnd electrodes divided by that without gnd electrodes. An average percentage of each finger is calculated, as presented in the last row ‘average1’.

Table 3-6 Comparison of sensitivity between electrode designs with or without gnd added in case 2

Distance (mm)	Sensitivity- V_2		Percentage
	Original (V/mm)	Modified (V/mm)	
0			
2	0.08783	0.04419	50.313%
4	0.04438	0.02111	47.573%
6	0.02649	0.01219	46.013%
8	0.01675	0.00755	45.093%
10	0.01091	0.00487	44.669%
15	0.00560	0.00248	44.224%
20	0.00227	0.00102	44.782%
25	0.00107	0.00050	46.629%
30	0.00058	0.00029	48.885%
average1	0.02176	0.01047	46.465%

Calculation Example:

$$\text{Percentage- } V_{2-2\text{mm}} = \text{Modified- } V_{2-2\text{mm}} \div \text{Original- } V_{2-2\text{mm}} = 0.04419 \div 0.08783 = 50.313\%$$

$$\text{average1-Percentage- } V_2 = \text{SUM(Percentage- } V_2) \div 9 = (50.313\% + 47.573\% + \dots + 48.885\%) \div 9 = 46.465\%$$

An overall comparison of the average sensitivity and percentage within each case is summarized in Table 3-7. In Table 3-6, the average sensitivity of original design, average sensitivity of modified design and average percentage are highlighted in orange, golden and light blue respectively. They represent detailed impact of the added ‘gnd’ electrodes in case 2, which are also highlighted accordingly in Table 3-7.

The data of other 14 cases are also presented in Table 3-7. The ‘Percentage’s in all the cases are less than one, which suggest the added ‘gnd’ will reduce the sensitivity of the measuring system. Taking all the combination of movement into consideration, for each finger, the average sensitivity in both designs as well as their percentage are easily calculated, as shown in row ‘average2’. These ‘average2- Sensitivity’ indicate the average increase of the voltage signal when moving per unit for each finger. Based on the ‘average2- Percentage’, the reduction of sensitivity for each finger could then be calculated, as shown in the row ‘reduction’.

Finally, considering all the fingers, the average sensitivity in original electrode design is 0.03513 V/mm while that in the modified electrode design is 0.01986 V/mm, as presented in row ‘average3’. By adding ‘gnd’ electrodes, there will be a reduction of 43.8% on average in the sensitivity.

Table 3-7 Overall comparison of the sensitivity percentage within each case

Case	Sensitivity-V ₁			Sensitivity-V ₂		
	Original	Modified	Percentage	Original	Modified	Percentage
1	0.02928	0.02167	74.542%			
1_2						
2				0.02176	0.01047	46.465%
2_2						
3	0.04066	0.02601	61.500%	0.03424	0.01590	45.871%
3_2						
4	0.02971	0.02175	73.555%			
4_2				0.02228	0.01059	45.770%
5	0.02931	0.02168	74.434%			
6				0.03183	0.01375	40.357%
7	0.04319	0.02663	57.867%	0.04556	0.01949	41.392%
7_2				0.03472	0.01461	39.282%
8	0.04076	0.02602	61.343%	0.03478	0.01602	45.523%
8_2	0.02986	0.02178	72.816%			
9	0.04392	0.02681	56.787%	0.04868	0.02040	40.301%
average2	0.03584	0.02404	67.092%	0.03423	0.01515	44.266%
reduction			32.908%			55.734%

Case	Sensitivity- V ₃			Sensitivity- V ₄		
	Original	Modified	Percentage	Original	Modified	Percentage
1						
1_2				0.02928	0.02167	74.531%
2						
2_2	0.02176	0.01046	46.470%			
3						
3_2	0.03424	0.01590	45.870%	0.04066	0.02600	61.497%
4	0.02228	0.01059	45.749%			
4_2				0.02971	0.02175	73.552%
5	0.02931	0.02167	74.411%			
6	0.03183	0.01375	40.362%			
7	0.03472	0.01460	39.270%			
7_2	0.04556	0.01949	41.396%	0.04319	0.02663	57.862%
8				0.02986	0.02178	72.810%
8_2	0.03478	0.01603	45.543%	0.04076	0.02602	61.352%
9	0.04868	0.02040	40.297%	0.04392	0.02681	56.781%
average2	0.03368	0.01588	47.134%	0.03677	0.02438	66.308%
reduction			52.866%			33.692%
average3	Sensitivity (original): 0.03513 V/mm; Sensitivity (modified): 0.01986 V/mm					
	Reduction: 43.800%					

Calculation Example:

average2- Sensitivity_{original}-V₁= SUM (Sensitivity_{original}-V₁) ÷8= (0.02928+0.04066+...+0.04392) ÷8=0.03584 V/mm

average2- Sensitivity_{modified}-V₁= SUM (Sensitivity_{modified}-V₁) ÷8= (0.02167+0.02601+...+0.02681) ÷8=0.02404 V/mm

average2- Percentage- V₁= SUM (Percentage- V₁) ÷8= (74.542%+61.500%+...+56.787%) ÷8=67.092%

reduction- Percentage- V₁= 1- (average2- Percentage- V₁)=1- 67.092%= 32.908%

average3- Sensitivity_{original}=(average2- Sensitivity_{original}- V₁+ average2- Sensitivity_{original}- V₂+ average2- Sensitivity_{original}- V₃+ average2- Sensitivity_{original}- V₄)/4=(0.03584+0.03423+0.03368+0.03677)÷4=0.03513 V/mm

average3- Sensitivity_{modified}=(average2- Sensitivity_{modified}- V₁+ average2- Sensitivity_{modified}- V₂+ average2- Sensitivity_{modified}- V₃+ average2- Sensitivity_{modified}- V₄)/4=(0.02404+0.01515+0.01588+0.02438)÷4 =0.01986 V/mm

average3- Reduction=(average2- Reduction - V₁+ average2- Reduction - V₂+ average2- Reduction - V₃+ average2- Reduction - V₄)/4 =(32.908%+55.734%+52.866%+33.692%)=43.800%

3.5.2 Crosstalk

In section 3.3 and 3.4, crosstalk was observed in both the original simulation model and the modified simulation model, where the voltage of the electrodes under the other fingers, especially the neighbouring ones, varies simultaneously when a finger moves. From Table 3-2 and Table 3-4, when middle finger moves (case 2), there are noticeable signal changes in V₁ and V₃, which are under the index and middle finger respectively. Whereas, the variation of V₄ under little finger stays negligible during the whole process. Similarly, Table 3-3 and Table 3-5 document the voltage signals when ring finger moves (case 2-2), where V₂ and V₄ under the neighbouring fingers were impacted to a much larger extent compared with V₁. Collectively,

only the cross influence in the neighbouring fingers were explored here to compare the crosstalk of two electrode designs.

On the basis of the symmetrical structure of the simulation model introduced in Section 3.2, Table 3-1 discussed the possible combination of finger movements. For example, case 1, when index finger moves, and case 1-2, when little finger moves are symmetrical, and so do case 2, when middle finger moves, and case 2-2, when ring finger moves. Further to this, the simulation results of both the original model in Section 3.3 and the modified one in Section 3.4 are in the similar symmetrical pattern. This means, the behaviour of the ring finger or the little finger can be view as equivalent to the behaviour of the middle finger or the index finger in the simulation models for the most part. Therefore, there are two situations: the variation of V_1 due to the movement of middle finger and the variation of V_2 resulted from the movement of index or ring finger. The groups of neighbouring fingers in these two situations are summarized as follows:

Table 3-8 Groups of neighbouring fingers discussed in two situations

	Situation 1: the variation of V_1 (under index finger) due to middle finger	Situation 2: the variation of V_2 (under middle finger) due to index finger due to ring finger	
	Original Model	Detailed in Table F-1	Detailed in Table F-2
Modified Model	Detailed in Table F-4	Detailed in Table F-5	Detailed in Table F-6

Data for these groups of neighbouring fingers were generated to explore the crosstalk in both electrode designs, detailed in Appendix F. Here, the crosstalk is represented by ‘Variation of V_x ’. For instance, Table 3-9 presents the 'index-middle map to show the variation of V_1 due to the movement of middle finger in the original simulation model. Here, the index finger moves from 0 mm to 30 mm, and at each height, the middle finger ranges over the 10 heights as well. At the right of Table 3-9, ‘ Δ ’ shows the variation of V_1 when index finger is fixed at certain height while middle finger moves.

Table 3-9 Variation of V_1 due to the movement of middle finger in original electrode design

V_1 (V)	D_2 (mm)										Variation of V_1		
	0	2	4	6	8	10	15	20	25	30	Δ (V)	average (V)	
0	1.92663	1.95838	1.97601	1.98718	1.99455	1.99949	2.00602	2.00875	2.01009	2.01086	0.08423	1.98780	
2	2.13640	2.17922	2.20363	2.21941	2.22997	2.23711	2.24655	2.25041	2.25222	2.25323	0.11682	2.22082	
4	2.24931	2.29939	2.32854	2.34777	2.36085	2.36980	2.38170	2.38650	2.38867	2.38983	0.14052	2.35024	
6	2.32195	2.37729	2.41014	2.43225	2.44759	2.45824	2.47263	2.47843	2.48095	2.48225	0.16030	2.43617	
D_1 (mm)	8	2.37217	2.43140	2.46716	2.49171	2.50909	2.52141	2.53843	2.54535	2.54832	2.54978	0.17761	2.49748
10	2.40833	2.47045	2.50848	2.53504	2.55424	2.56814	2.58792	2.59616	2.59966	2.60131	0.19298	2.54297	
15	2.46376	2.53010	2.57162	2.60160	2.62418	2.64135	2.66794	2.68024	2.68564	2.68807	0.22431	2.61545	
20	2.49327	2.56144	2.60451	2.63613	2.66053	2.67970	2.71158	2.72834	2.73648	2.74024	0.24697	2.65522	
25	2.51061	2.57953	2.62320	2.65549	2.68071	2.70085	2.73587	2.75622	2.76744	2.77315	0.26254	2.67831	
30	2.52163	2.59084	2.63470	2.66721	2.69273	2.71328	2.74981	2.77237	2.78612	2.79404	0.27241	2.69227	
average4											0.18787	2.46767	

Note: Voltage signal when index finger is at x mm while middle finger is at y mm is noted as $V_{1-x,y}$.

Calculation Example:

$$\text{Variation of } V_1 - \Delta - \text{index}_{0\text{mm}} = V_{1-0,30} - V_{1-0,0} = 2.01086 - 1.92663 = 0.08423 \text{ V}$$

$$\text{Variation of } V_1 - \text{average- index}_{0\text{mm}} = \text{SUM}(V_{1-0,0} + V_{1-0,2} + \dots + V_{1-0,30}) \div 10 = (1.92663 + 1.95838 + \dots + 2.01086) \div 10 = 1.98780 \text{ V}$$

$$\text{average4- Variation of } V_1 - \Delta = \text{SUM}(\text{Variation of } V_1 - \Delta - \text{index}_{0\text{mm}} + \dots + \text{Variation of } V_1 - \Delta - \text{index}_{30\text{mm}}) \div 10 = (0.08423 + \dots + 0.27241) \div 10 = 0.18787 \text{ V}$$

$$\text{average4- Variation of } V_1 - \text{average} = \text{SUM}(\text{Variation of } V_1 - \text{average} - \text{index}_{0\text{mm}} + \dots + \text{Variation of } V_1 - \text{average} - \text{index}_{30\text{mm}}) \div 10 = (1.98780 + \dots + 2.69227) \div 10 = 2.46767 \text{ V}$$

The average ‘ Δ ’ highlighted in light green in Table 3-9 presents the average variation of V_1 due to the movement of middle finger in original electrode design, in the row ‘average4’. It is also highlighted in Table 3-10. With the average variation of $V_x(x=1,2)$ of situation 1 and situation 2 in both electrode designs compared, Table 3-10 discusses the variation of voltage signal due to the movement of a neighbouring finger in general.

Table 3-10 Variation of voltage signal due to the neighbouring crosstalk

	Variation of V_1		Variation of V_2			
	due to middle finger		due to index finger		due to ring finger	
	Δ (V)	average (V)	Δ (V)	average (V)	Δ (V)	average (V)
Original	0.18787	2.46767	0.22107	2.29342	0.17082	2.26799
Modified	0.06999	2.03154	0.09761	1.58295	0.05569	1.55913
Percentage	37.253%		44.155%		32.601%	
Reduction	62.747%		55.845%		67.399%	
average5	Variation of voltage due to crosstalk (V/mm): <ul style="list-style-type: none"> • Original: 0.19191(Index finger: 0.18787 , Middle finger: 0.19594) • Modified: 0.07332 (Index finger: 0.06999, Middle finger: 0.07665) Overall reduction: 62.185% (Index finger: 62.747%, Middle finger: 61.622%)					

Calculation Example:

Percentage- Variation of V_1 - due to middle finger= Modified- Variation of V_1 - due to middle finger \div original- Variation of V_1 - due to middle finger=0.06999 \div 0.18787=37.253%

Reduction- Variation of V_1 - due to middle finger= 1- Percentage-Variation of V_1 -due to middle finger =1-37.253%=62.747%

As presented in row ‘average5’, the average variation of voltage signal due to crosstalk in original electrode design is 0.19191 V while the variation of voltage signal in the modified electrode design is 0.07332 V. By adding extra ‘gnd’ electrodes, the overall crosstalk due to the neighbouring fingers is reduced by approximately 62%. It is illustrated in Section 3.5.1 that, there will be a reduction of 43.8% on average in the sensitivity of finger motion detection with added ‘gnd’ electrodes in the modified electrode design. Comparing the reduction of sensitivity with that of crosstalk, it can be derived that, by adding extra ‘gnd’ electrodes, there is always more reduction in the crosstalk which is advantageous than in the sensitivity.

3.6 Summary

Chapter 3 presents a Finite Element Method (FEM) simulation based on the MGC3030 electrode stack-up design in Comsol Multiphysics. Crosstalk was observed in the original simulation model when a finger moves, where the voltage of the electrodes under the other fingers, especially the neighbouring ones, varies simultaneously. A modified simulation model was proposed to optimize the performance on reducing the crosstalk. By adding extra gnd electrodes, in the modified electrode design, there is a decrease in the voltages, the sensitivity and the crosstalk at all of the electrodes.

Considering all the fingers, the average sensitivity in original electrode design is 0.03513 V/mm while that in the modified electrode design is 0.01986 V/mm. The average variation of voltage signal due to crosstalk in original electrode design is 0.19191 V while it is 0.07332 V in the modified electrode design. By adding 'gnd' electrodes, there will be a reduction of 43.8% on average in the sensitivity, whereas the overall crosstalk due to the neighbouring fingers is reduced by approximately 62%. In general, added gnd electrodes results in a much greater reduction in the crosstalk, which is advantageous compared to the sensitivity.

To conclude, the modified electrodes design can potentially help to reduce the crosstalk of the simulation model, as long as the signal is still big enough. However, it still requires further exploring on the 'crosstalk' issue of the MGC3030 measuring technique, to guide the practical design of the MGC3030 system for fine motor control rehabilitation.

Chapter 4 Model Prediction to Sense the Movement of Fingers

Chapter 3 carried out a finite element method simulation derived from the MGC3030 electrode stack-up design, which shows that the finger movements can be reflected by the voltage signals detected from the Rx electrode. However, the mathematical relationship between the voltage signals and finger's movement is not simple or linear. A 'crosstalk' is also observed in the simulation, which refers to the signal changes due to an electrical field leakage from a neighboring moving finger.

Further to this, Chapter 4 investigates the method of fitting simple functional forms to the voltage-position relationship and analyses the crosstalk to improve the performance of finger motion detection. A general approach to analyze the relationship between two physical quantities is mapping these two physical variables to establish a simple correspondence. However, to validate the quasi-static electrical measuring theory, investigation for the underlying mechanism is required, and is discussed in Section 4.1.

Based on the original Comsol simulation model demonstrated in Chapter 3, Chapter 4 conducts a nonlinear regression in Matlab. The mathematic relationships between the fingers' motion and the voltage signals of the Rx electrodes are proposed in Section 4.3. Except for the validation purpose, these formulas also have advantages over mapping in its simplicity for implementing on a low-cost microchip. The interaction between the index finger and middle finger are picked as the simplest combination to explore the cross impact of finger movement in the electrical field generated by the three-layer electrode stack-up. To be more precise, key points in this chapter can be summarized as follows:

- Section 4.3.1: Model prediction, exploring the case of one finger only when a distance that represents the finger motion (D_x) is the input to determine the voltage at the corresponding Rx electrode (V_x), namely $V_x=f(D_x)$.
- Section 4.3.2: Reversed model prediction in single finger case when the voltage value of a Rx electrode (V_x) is the input to determine the distance to present the corresponding finger motion (D_x), namely $D_x=f(V_x)$.
- Section 4.3.3: Model prediction in the case for two fingers when distance values of both fingers are the input, to determine the voltage at an Rx electrode (V_x), namely $V_x=f(D_1, D_2)$.

- Section 4.3.4: Reversed model prediction in case for two finger when voltage values of both Rx electrodes (V_x) are the input to determine the distance to present a finger motion (D_x), namely $D_x=f(V_1, V_2)$.

The one-finger models reveal the form of the relationship between finger movement and signals detected by Rx electrodes, as discussed in Section 4.3.1 and 4.3.2. On the basis of one-finger's case, crosstalk, which refers to the signal changes due to an electrical field leakage from a neighboring moving finger, can be compensated by the two-fingers models, as presented in Section 4.3.3 and 4.3.4. In two-fingers models, the other finger's movement is also considered as an input to determine the finger motion, and therefore, it will provide better accuracy.

4.1 Theory of detection: Discussion of the prediction model

The MGC3030 motion sensor is based on the quasi-static electrical near field theory for advanced proximity sensing. As shown in Fig. 4-1 (a), by applying 100 KHz sinusoidal voltage to the MGC3030 electrode stack-up, a quasi-static electrical near field (direction: Tx to GND) is produced and propagates three-dimensionally around the surface carrying the electrical charge. Underneath each finger, four Rx electrodes are used to detect the E-field variations from the varying signals received [72]. There is a constant field strength E^0 at each of the receive electrodes, generated by the MGC3030 electrode stack-up, as shown in Fig. 4-1 (a). When conductive objects, such as a person's hand or fingers, intrude the electrical field, some of the field lines are drawn to the hand instead of shunted to the ground [72], as presented in Fig. 4-1 (b). A new three-dimensional electric field (direction: Tx to finger) is introduced, whose field strength at Rx is E' . Therefore, the electrical field now is a superposition of both fields, whose field strength E can be described as follow:

$$\vec{E} = \vec{E}^0 + \vec{E}' \quad (4-1)$$

Since there is an obtuse angle between E^0 and E' , and $E^0 > E'$ in the current electrode stack-up design, this minuscule change then shifts the Receive electrodes (Rx) signal levels to a lower potential [72]. A variable ' D_x ($x=1,2,3,4$)', which is the distance between the under surface of a finger and the top of the cover layer, was used to represent the approaching and departure of the fingers in the vertical coordinate, as shown in Fig. 4-1 (b) as the red vertical lines below the fingers. The relationship between field strength E and electric potential difference V in a uniform electric field is:

$$E = V/D \quad (4-2)$$

This equation can also be used in non-uniform field for qualitative analysis. Since the potential difference of the electrodes stack-up is 3.3V, the voltages of the Rx electrodes (V_x : V_1, V_2, V_3, V_4) can be used as the input signal to reflect the finger motion. Here, the variable D is made up of two parts:

$$D = D_x + d_0 \quad (4-3)$$

' d_0 ' represents the thickness of the top layer in between fingers and Rx electrodes. If the edge effect and the complex shape of hand are ignored, the relationship between the voltages of electrodes (V_x), corresponding to the varied distance (D_x), should share a similar trend with the following rule based on (4-1), (4-2) and (4-3):

$$V_x = V^0 - a/(D_x + d_0) \quad (4-4)$$

Including factors like edge effect, the complex shape of hand and the cross-impact of fingers' movement into consideration, further steps to evaluate this hypothesis were carried out with the help of Comsol and Matlab.

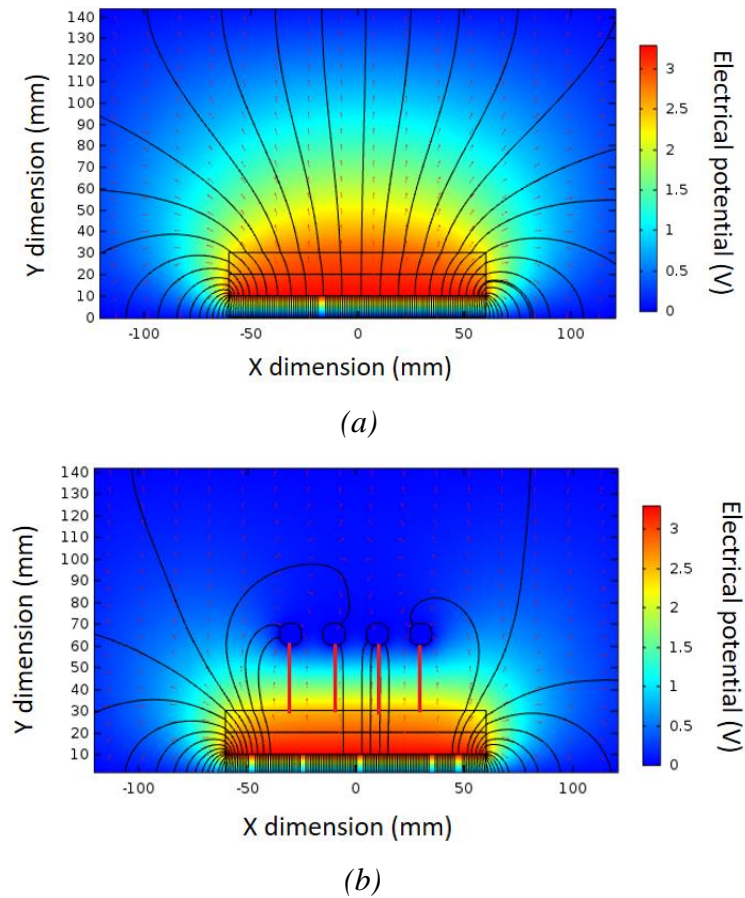


Fig. 4-1 Equipotential lines of simulation model: (a) Electrode stack up without fingers, (b) $D_1, D_2, D_3, D_4 = 30$ mm

4.2 Simulated data from COMSOL

Further to the discussion in Section 2.1.2 and Section 3.2.2, this study explores different combinations of fingers' extension and flexion movements. Concerning the symmetrical simulation model, there are four possible combination if two fingers move together: ① index & middle (or the symmetric equivalent is little & ring); ② index & ring (or little & middle); ③ middle & ring; ④ index & little [88]. Typically, only adjacent fingers were similar in the flexion and extension phases during cycles of individuated movements (combination① and combination③) [39]. Hence, the interaction between the index finger and middle finger are picked, as a simpler option with less neighbouring effects than the middle finger and ring finger, to explore the cross-impact of finger movement here, to explore the cross-impact of finger movement in the electrical field generated by the three-layer electrode stack-up.

An index-middle map of 196 data points in total were simulated (14*14=196 combinations) using point evaluation in Comsol. The positions of the index finger over 14 heights (D_1 ranging from 0mm, 0.5mm, 1mm, 1.5mm, 2mm, 3mm, 4mm, 6mm, 8mm, 10mm, 15mm, 20mm, 25mm to 30mm) were explored, while the middle finger is also at each one of these points. For each data point, values of voltage signals (V_x : $x=1,2,3,4$) were read, as illustrated in the template shown in Fig. 4-2. A detailed index-middle map is shown in Appendix G.

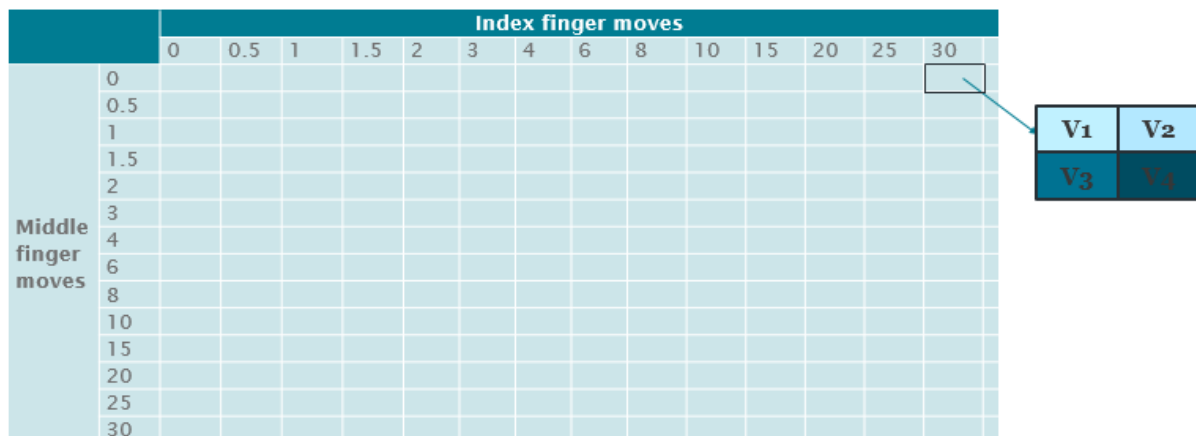


Fig. 4-2 Simulated data of index-middle map (mm)

4.3 Model prediction to sense the movement of fingers

Based on the simulated result, the mathematic relationship between the fingers' motion (D_1 , D_2) and the voltage signals (V_1 , V_2) was explored to improve the performance of finger motion detection. Primary data analysis started with the one finger case in Excel, where the

plot of a distance representing the finger motion versus the voltage value of the corresponding Rx electrode presents a clear nonlinear relation [88]. The exponential, polynomial, fractional and rational relations were then explored in Excel by comparing the R-squared value of each fitted function. The data show a very good fit to an inverse proportional function, which is in a similar form to equation (4-4) and therefore supports the hypothesis proposed in section 4.1.

Further to this, a nonlinear regression in Matlab was investigated for detailed statistic criteria and for plotting a two-dimensional surface. The standard Matlab function block ‘fitnlm’ was used to investigate the parametric nonlinear models, which represents the relationships between the distance of fingers’ movements (D1, D2) and the voltage signals (V1, V2), in the form of the proposed hypothesis. The ‘fitnlm’ function adapts the prediction models to the experimental results (D_x, V_x), and returns the nonlinear model with values of the fitted parameters that gives a least-square fit of the response to the data [90]. Starting from pre-setting parameters b₁, b₂ and b₃, the regression process attempts to find the fitted parameters which minimize the mean squared differences with the ‘fitnlm’ function [91]. Therefore, the regression process will be influenced by the setting of initials parameters. However, this limitation has been eliminated by reasonable setting of initial parameters corresponding to each prediction model and will not influence the results discussed in this thesis.

4.3.1 Model prediction of one finger’s case: $V_x=f(D_x)$

Model prediction in one finger’s case, namely $V_x=f(D_x)$ were found to fit an inverse proportional function relation, as shown in equation (4-5), where b₁, b₂ and b₃ are parameters:

$$V_x = b_1 - b_2/(D_x + b_3) \quad (4-5)$$

Table 4-1 gives the curve fitting results of equation (4-5) that defines the voltage value of the electrode under a moving finger (V_x) by distance of the finger away from the surface (D_x). For $V_1 =f(D_1)$, there are 14 groups of b₁, b₂ and b₃ when the index finger moves, in accordance with 14 heights of the middle finger away from the surface (D₂=0mm, 0.5mm, 1mm, 1.5mm, 2mm, 3mm, 4mm, 6mm, 8mm, 10mm, 15mm, 20mm, 25mm, 30mm). Predicted values of V₁ can be calculated with equation (4-5) together with the parameters b₁, b₂, and b₃. R-squared values of these regression processes are presented in Table 4-1, as a statistical measure of data fitting effect. It represents the proportion of the variance for a dependent variable that is explained by independent variables. For better consistency of evaluating the

fitting process for both the simulation and experiment with different motion range, the R-squared is selected and reported in this thesis.

Table 4-1 Parameters of nonlinear curve fitting equation

Parameters in $V_1=f(D_1)$					Parameters in $V_2=f(D_2)$				
D_2	b_1	b_2	b_3	R-Squared	D_1	b_1	b_2	b_3	R-Squared
0	2.6185	3.1156	4.4941	1	0	2.3165	1.5321	3.1579	0.998
0.5	2.6427	3.1901	4.5105	1	0.5	2.3398	1.5812	3.1793	0.998
1	2.663	3.256	4.5265	1	1	2.3596	1.6247	3.199	0.998
1.5	2.6807	3.317	4.5432	1	1.5	2.3769	1.6648	3.2181	0.998
2	2.6964	3.3746	4.5607	1	2	2.3924	1.7027	3.2372	0.998
3	2.7239	3.4852	4.6001	1	3	2.4193	1.7746	3.2766	0.998
4	2.7474	3.5931	4.6453	1	4	2.4425	1.8439	3.3189	0.998
6	2.7866	3.8092	4.753	1	6	2.4811	1.9805	3.4129	0.998
8	2.8185	4.0284	4.8793	1	8	2.5126	2.1171	3.5181	0.998
10	2.845	4.2478	5.0174	1	10	2.5391	2.2534	3.6308	0.998
15	2.8938	4.759	5.3651	1	15	2.589	2.5776	3.9174	0.998
20	2.9243	5.1586	5.6512	1	20	2.622	2.8485	4.1674	0.998
25	2.9421	5.4224	5.844	1	25	2.6432	3.0469	4.3531	0.999
30	2.9517	5.5719	5.954	1	30	2.6562	3.1751	4.4732	1
Average	2.7810	4.0235	4.9532	1	Average	2.4779	2.1231	3.5757	0.998
Start1= [$b_1=2.2, b_2=2.5, b_3=2$];					Start2= [$sb_{11}=2.2, sb_{12}=4.0, sb_{13}=5.0$];				
Number of observations: 14, Error degrees of freedom: 11.					Number of observations: 14, Error degrees of freedom: 11.				

Similarly, parameters for the fourteen opposite situations when the middle finger moves while the index finger is at some height away from the surface ($D_1=0\text{mm}, 0.5\text{mm}, 1\text{mm}, 1.5\text{mm}, 2\text{mm}, 3\text{mm}, 4\text{mm}, 6\text{mm}, 8\text{mm}, 10\text{mm}, 15\text{mm}, 20\text{mm}, 25\text{mm}, 30\text{mm}$) were also listed in Table 4-1. Therefore, the predicted values of V_2 in each situation can also be calculated.

Fig. 4-3 compared the real voltage values (blue ‘*’) from Comsol simulation, and the predicted values (red ‘□’) determined by the regression model from Matlab. Fig. 4-3 (a) are an exemplar fitted curves for $V_1=f(D_1)$ when index finger moves (D_1 ranging from 0mm, 0.5mm, 1mm, 1.5mm, 2mm,3mm, 4mm, 6mm, 8mm, 10mm, 15mm, 20mm, 25mm,to 30mm) while middle finger is fixed to 0mm ($D_2=0\text{mm}$). Similar to Fig. 4-3 (a), Fig. 4-3 (b) are the regression fitting curves for $V_2=f(D_2)$ when middle finger moves while the index finger is fixed ($D_1=0\text{mm}$). The entire 14 curve fitted plots of V_1 and V_2 are shown in Appendix H and Appendix I respectively.

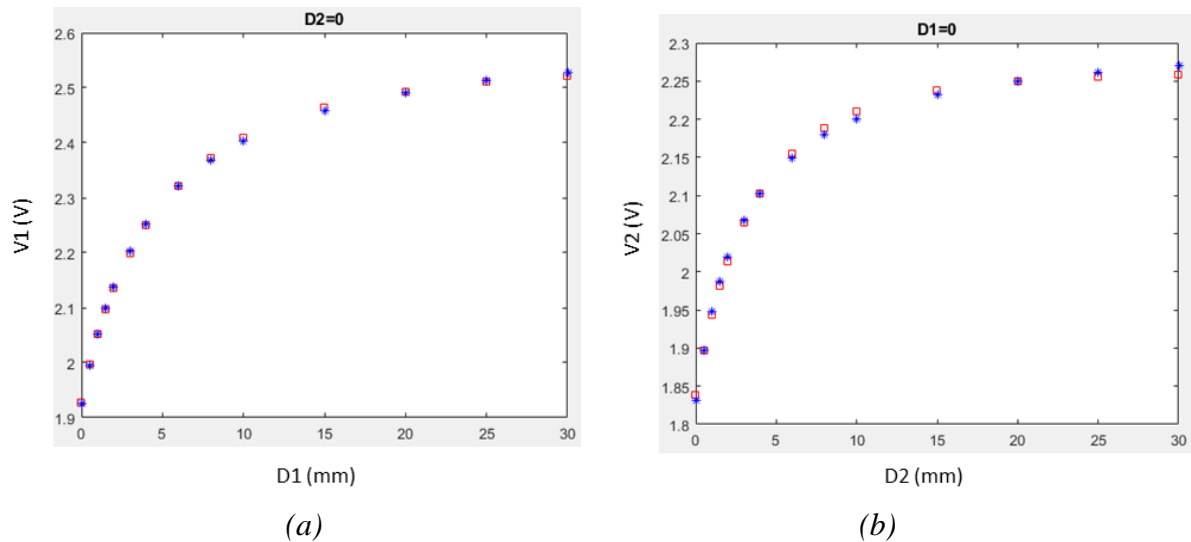


Fig. 4-3 Exemplar fitted curves: (a) $V_1=f(D_1)$, (b) $V_2=f(D_2)$

Comparing the fitted equation with Fig. 4-3, the physical meaning of the three parameters in the equation can be explained:

- ‘ b_1 ’ is the voltage value when a finger is at a large distance and the effect of this finger can be neglected.
- ‘ b_2 ’ can be regarded as a sensitivity factor. It reflects the magnitude of an intruding finger to the signal read from the specified Rx electrode.
- ‘ b_3 ’ is the offset value associated with the original distance of the finger to the electrode. It is possibly resulted from the thickness of the top layer in between fingers and Rx electrodes.

Apart from the original 196 points, extra points were also simulated to test the fitted equation (4-5) $V_x = f(D_x)$, as shown in Table 4-2. There is one testing point in each of the 14 situations where D_2 increases from 0mm, 0.5mm, 1mm, 1.5mm, 2mm, 3mm, 4mm, 6mm, 8mm, 10mm, 15mm, 20mm, 25mm, to 30mm. Distance value (D_1) of these testing points were randomly generated, using the ‘RANDBETWEEN()’ function in Excel. The ‘Difference of V_1 determined by $f(D_1)$ ’ is described as the difference between the real values and the predicted values, as shown in the last column. In the same way, the testing result of the fitted equation defining V_2 with D_2 is also presented. By comparing their average difference calculated, both of the regression models showed very good performance as a prediction model for the case of only one finger, while $f(D_1)$ seems to work better.

Table 4-2 Testing points of nonlinear curve fitting equation $V_x=f(D_x)$

$V_1=f(D_1)$					$V_2=f(D_2)$				
D_2	D_1	Real value of V_1	Predicted value of V_1	Difference of V_1 by $f(D_1)$	D_1	D_2	Real value of V_2	Predicted value of V_2	Difference of V_2 by $f(D_2)$
0	12	2.4351	2.4296	0.0055	0	1.5	1.9817	1.9875	0.0058
0.5	1	2.0638	2.0638	0	0.5	25	2.2767	2.2837	0.0070
1	17	2.5162	2.5117	0.0045	1	5	2.1647	2.1615	0.0032
1.5	22	2.5561	2.5557	0.0004	1.5	2.5	2.0802	2.0858	0.0056
2	29	2.589	2.5959	0.0069	2	15	2.3066	2.299	0.0076
3	12	2.5211	2.514	0.0071	3	8	2.2728	2.262	0.0108
4	0.5	2.0509	2.0491	0.0018	4	20	2.3636	2.3634	0.0002
6	24	2.6524	2.6541	0.0017	6	0	1.9085	1.9008	0.0077
8	19	2.6549	2.6498	0.0051	8	30	2.4336	2.4495	0.0159
10	10	2.5681	2.5621	0.006	10	1.5	2.0937	2.0999	0.0062
15	6	2.4726	2.4751	0.0025	15	6	2.3321	2.329	0.0031
20	5	2.4364	2.44	0.0036	20	3	2.2197	2.2246	0.0049
25	30	2.7861	2.7908	0.0047	25	4	2.2754	2.2785	0.0031
30	0	2.0109	2.0159	0.0050	30	8	2.4051	2.4016	0.0035
Average				0.0039	Average				0.0060

Collectively, from the R-squared values in Table 4-1, the distance from finger motion and the voltage signals of Rx electrodes fits well with equation (4-5), which indicates an inverse proportional function relationship featured with three parameters, b_1 , b_2 and b_3 [92]. Moreover, the predicted values of both V_1 and V_2 are very close to their real voltage values in Fig. 4-3. It agrees with the ‘Difference of V_1 determined by $f(D_1)$ ’ and Difference of V_2 determined by $f(D_2)$ ’ proposed in Table 4-2, and therefore supports the equation (4-5) as well.

4.3.2 Reversed model prediction of one finger’s case: $D_x=f(V_x)$

It can be seen from the derivation of equation (4-5) and Fig. 4-3 that, formula (4-5) increases monotonously and satisfies the condition for a function to have an inverse. Therefore, a reversed model prediction was proposed based on the relationship of a function and its inverse function. The reversed model prediction in one finger’s case when the voltage value of a Rx electrode is the input to determine the distance relating to the corresponding finger motion, namely $D_x=f(V_x)$ was given, as equation (4-6):

$$D_x = -b_3 + b_2/(b_1 - V_x) \quad (4-6)$$

Since the original function (4-5) is convergent, the inverse function (4-6) here is divergent. Table 4-3 gives the curve fitting results b_1 , b_2 and b_3 of equation (4-6) to define the distance of the finger away from the surface (D_x) by the voltage of the electrode under a moving finger (V_x). With the particular b_1 , b_2 and b_3 in one of the fourteen situations as well as the

equation (4-6), predicted voltage values of D_1 and D_2 could be calculated respectively, when V_1 or V_2 is provided as the input.

Table 4-3 Parameters of nonlinear curve fitting equation $D_x=f(V_x)$

Parameters in $D_1=f(V_1)$					Parameters in $D_2=f(V_2)$				
D_2	b_1	b_2	b_3	R-Squared	D_1	b_1	b_2	b_3	R-Squared
0	2.5968	2.4744	3.3751	0.999	0	2.2827	0.72063	0.66603	0.993
0.5	2.6197	2.5106	3.348	0.999	0.5	2.3048	0.73722	0.65298	0.993
1	2.6388	2.5411	3.3236	0.999	1	2.3234	0.75131	0.6404	0.992
1.5	2.6554	2.5685	3.3024	0.999	1.5	2.3397	0.764	0.62898	0.992
2	2.6701	2.5947	3.2849	0.999	2	2.3541	0.77602	0.61939	0.992
3	2.6956	2.6463	3.2601	0.999	3	2.3793	0.79976	0.60716	0.991
4	2.7174	2.7004	3.2498	0.998	4	2.4008	0.82497	0.60615	0.991
6	2.7539	2.8251	3.2737	0.998	6	2.4368	0.88336	0.63819	0.99
8	2.784	2.9777	3.3555	0.998	8	2.4665	0.95721	0.7208	0.99
10	2.8098	3.1599	3.4908	0.998	10	2.492	1.0479	0.85078	0.99
15	2.8617	3.7198	4.0065	0.998	15	2.5429	1.3439	1.3428	0.991
20	2.9	4.3342	4.6261	0.999	20	2.5809	1.7005	1.9561	0.994
25	2.9265	4.8702	5.1747	0.999	25	2.6086	2.0498	2.5431	0.996
30	2.943	5.246	5.558	1	30	2.6276	2.3324	3.004	0.998
Average	2.7552	3.2264	3.7592	0.999	Average	2.4386	1.1206	1.1055	0.992
beta1= [4, 3, 3, 6]; Number of observations: 14, Error degrees of freedom: 11.					beta1= [4, 3, 3, 6]; Number of observations: 14, Error degrees of freedom: 11.				

Fig. 4-4 compared the real voltage values (blue ‘*’) and the predicted values (red ‘□’). Fig. 4-4 (a) is the exemplar fitted curves for $D_1=f(V_1)$ when index finger moves, while the middle finger is fixed at 0mm ($D_2=0$ mm). Likewise, Fig. 4-4 (b) is the regression fitting curves for $D_2=f(V_2)$ when middle finger moves and index finger is fixed ($D_1=0$ mm). The entire 14 curve fitted plots for D_1 and D_2 are shown in Appendix J and Appendix K respectively.

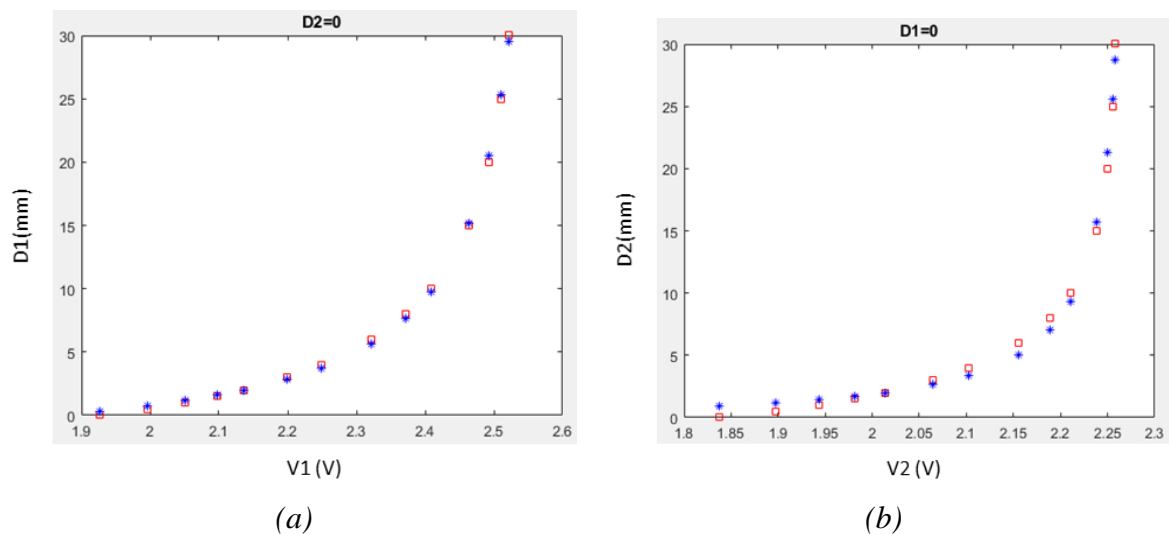


Fig. 4-4 Exemplar fitted curves for $D_x=f(V_x)$

Table 4-4 Testing points of nonlinear curve fitting equation $D_x=f(V_x)$

$D_1=f(V_1)$					$D_2=f(V_2)$				
D_2	Real value of D_1	V_1	Predicted value of D_1	Difference of D_1 by $f(V_1)$	D_1	Real value of D_2	V_2	Predicted value of D_2	Difference of D_2 by $f(V_2)$
0	12	2.4351	11.9237	0.0763	0	1.5	1.9817	1.7281	0.2281
0.5	1	2.0638	1.1684	0.1684	0.5	25	2.2767	25.5870	0.5870
1	17	2.5162	17.4032	0.4032	1	5	2.1647	4.0929	0.9071
1.5	22	2.5561	22.5718	0.5718	1.5	2.5	2.0802	2.3156	0.1844
2	29	2.589	28.7086	0.2914	2	15	2.3066	15.7077	0.7077
3	12	2.5211	11.9024	0.0976	3	8	2.2728	6.9035	1.0965
4	0.5	2.0509	0.8015	0.3015	4	20	2.3636	21.5492	1.5492
6	24	2.6524	24.5669	0.5669	6	0	1.9085	1.0338	1.0338
8	19	2.6549	19.7131	0.7131	8	30	2.4336	28.3478	1.6522
10	10	2.5681	9.5817	0.4183	10	1.5	2.0937	1.7805	0.2805
15	6	2.4726	5.5534	0.4466	15	6	2.3321	5.0331	0.9669
20	5	2.4364	4.7238	0.2762	20	3	2.2197	2.7520	0.2480
25	30	2.7861	29.5045	0.4955	25	4	2.2754	3.6082	0.3918
30	0	2.0109	0.0700	0.0700	30	8	2.4051	7.4800	0.5200
Average				0.3498	Average				0.7395

Table 4-4 presents the testing result of the regression model (4-6). For better consistency, the randomly generated testing points of the 14 situations are same with the points in Table 4-2. By comparing their average difference, both of the models perform well as the reverse prediction model in one finger's case. The function $f(V_1)$ is better than $f(V_2)$ as it has a smaller average difference which seems to be in accordance with the results of the original 196 points discussed in Table 4-3 and Fig. 4-4. Additionally, it is consistent with the performance of the prediction models discussed in 4.3.1.

In summary, the R-squared values in Table 4-3 indicate that the distance from finger motion and the voltage signals of Rx electrodes fits well with equation (4-6). Also, the predicted values of both D_1 and D_2 are very close to their real values in Fig. 4-4 (a) and Fig. 4-4 (b) respectively. It therefore agrees with the 'Difference of D_x determined by $f(V_1)$ ' proposed in Table 4-4 and equation (4-6) as well.

4.3.3 Model prediction of two fingers' case: $V_x=f(D_1, D_2)$

Further to the model predictions of one finger's case discussed in 4.3.1, $V_x=f(D_1, D_2)$ fits all the 196 simulation data to a model prediction when distance values of both fingers are the inputs to determine the voltage value of a specified Rx electrode. It is the superimposed form of $V_1=f(D_1)$ and $V_2=f(D_2)$. Here, the inherent relationship was found to fit the equation (4-7):

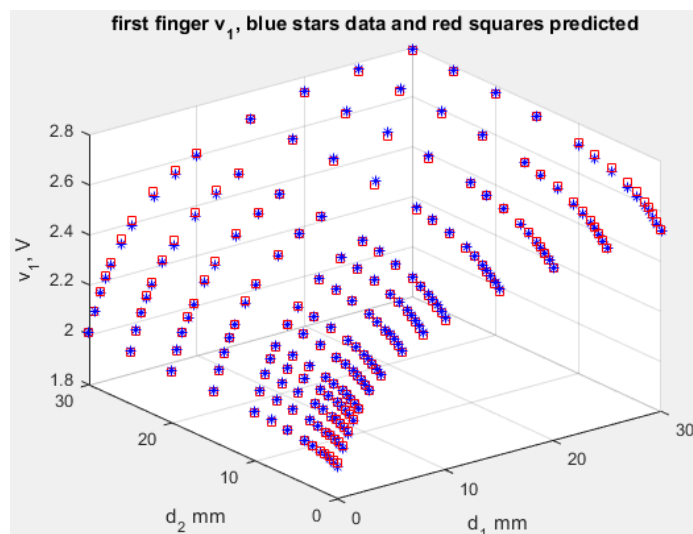
$$V_x = [b_1 - b_2/(D_1 + b_3)] [b_4 - b_5/(D_2 + b_6)] + b_7 \quad (4-7)$$

Table 4-5 also gives the curve fitting results of defining V_x in terms of D_1 and D_2 . With the listed parameters $b_1, b_2, b_3, b_4, b_5, b_6$ and b_7 , as well as the equation (4-7), the predicted voltage values of both V_1 and V_2 could be defined.

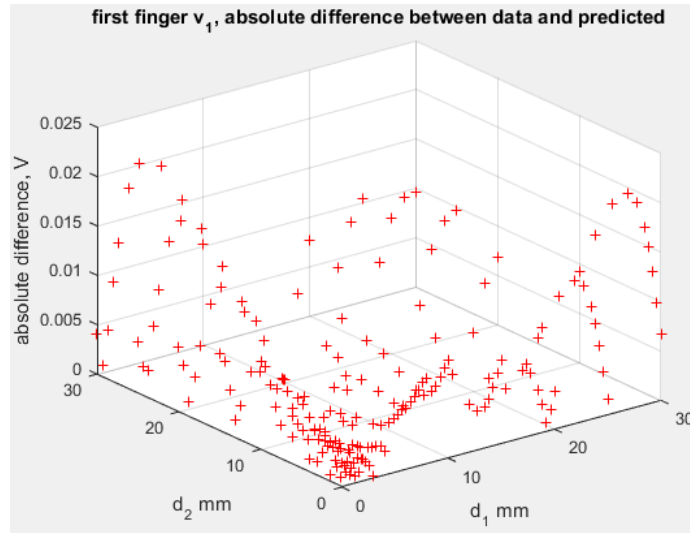
Table 4-5 Parameters of nonlinear curve fitting equation $V_x = f(D_1, D_2)$

		b_1	b_2	b_3	b_4	b_5	b_6	b_7
$V_1=f(D_1, D_2)$	Value	1.1499	4.4925	5.0017	1.0574	1.6931	5.6811	1.7526
	pValue	2.1522e-130	1.8199e-195	7.9816e-162	6.5522e-168	8.1996e-52	2.7537e-60	8.948e-169
	Details	Number of observations: 196, Error degrees of freedom: 190 Root Mean Squared Error: 0.00753, R-Squared: 0.999, P-value = 4.16e-282 Mean absolute difference =0.0058465						
$V_2=f(D_1, D_2)$	Value	0.99241	2.5824	7.1772	1.0413	2.7174	3.6369	1.6646
	pValue	1.0105e-104	2.5877e-67	5.3499e-53	2.1363e-94	8.4559e-84	2.0208e-125	7.8384e-157
	Details	Number of observations: 196, Error degrees of freedom: 190 Root Mean Squared Error: 0.00941, R-Squared: 0.997, P-value = 5.66e-243 Mean absolute difference = 0.0074993						

Fig. 4-5 (a) compared the real voltage values (blue ‘*’) from Comsol simulation, and the predicted values (red ‘□’) determined by the regression model from Matlab. Further to this, plot (b) shows the absolute difference between the real values and the predicted values of V_1 in the 196 data points.



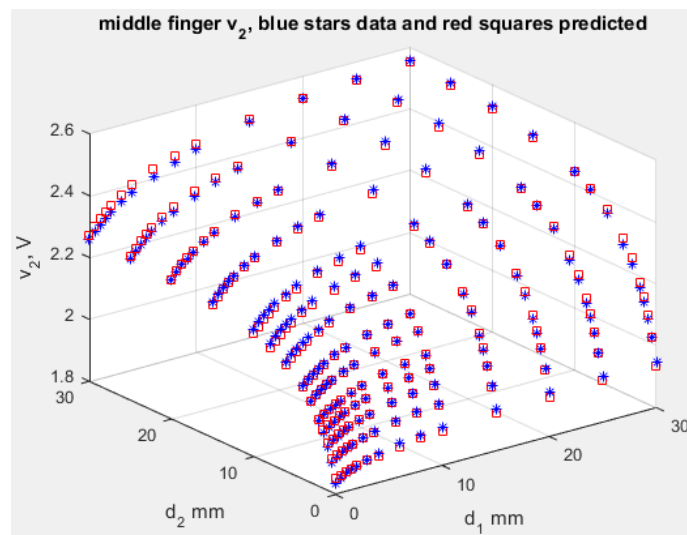
(a)



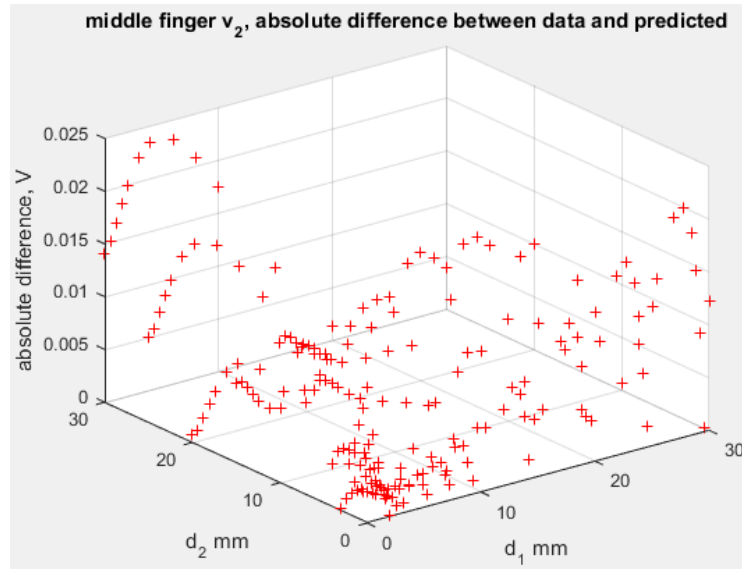
(b)

Fig. 4-5 Fitted curves for $V_1=f(D_1, D_2)$

Similarly, Fig. 4-6 (a) and (b) are the regression fitting curves for $V_2=f(D_1, D_2)$ when index finger and middle finger move to the entire 196 curve fitted points (D_1 and D_2 ranging from 0mm, 0.5mm, 1mm, 1.5mm, 2mm, 3mm, 4mm, 6mm, 8mm, 10mm, 15mm, 20mm, 25mm, to 30mm). In view of the low difference demonstrated by Fig. 4-5 and Fig. 4-6, both regression models work well as a prediction model for the two finger's case. It also agrees with the curve fitting results in Table 4-5.



(a)



(b)

Fig. 4-6 Fitted curves for $V_2=f(D_1, D_2)$

Apart from the points used to conduct the regressions, ten randomly generated testing points were also simulated to test the regression model (4-7). Table 4-6 presents the testing result of the fitted equation defining V_x with both D_1 and D_2 . By comparing their average difference calculated, both of the models perform well as the prediction models of one finger's case. Here, $V_1=f(D_1, D_2)$ seems to be better compared to $V_2=f(D_1, D_2)$, which agrees with the performance of the prediction models discussed in 4.3 and 4.4.

Table 4-6 Testing points of nonlinear curve fitting equation $V_x=f(D_1, D_2)$

D ₁	D ₂	V ₁ =f(D ₁ , D ₂)			V ₂ =f(D ₁ , D ₂)		
		Real value of V ₁	Predicted value of V ₁	Difference of V ₁ by f(D ₁ , D ₂)	Real value of V ₂	Predicted value of V ₂	Difference of V ₂ by f(D ₁ , D ₂)
4	10.5	2.3716	2.3727	0.0011	2.3218	2.3111	0.0107
28	0.5	2.5394	2.5469	0.0075	2.0185	2.0179	0.0006
12.5	21.5	2.6459	2.6415	0.0044	2.4704	2.4683	0.0021
24.5	20	2.7541	2.7418	0.0123	2.5207	2.5084	0.0123
13.5	9	2.6167	2.6072	0.0095	2.3932	2.3814	0.0118
14	4.5	2.5704	2.5666	0.0038	2.2781	2.2803	0.0022
7	25.5	2.5172	2.5306	0.0134	2.418	2.4328	0.0148
16.5	12	2.6692	2.6575	0.0117	2.4456	2.4309	0.0147
8.5	28.5	2.5636	2.5762	0.0126	2.4388	2.4565	0.0177
8	8.5	2.5126	2.5071	0.0055	2.3483	2.3367	0.0116
Average				0.0082			0.0099

In summary, based on the R-squared values in Table 4-5, the relationship between the distance from the finger motion and the voltage signals of Rx electrodes fits well with equation (4-7). Both V_1 and V_2 are very close to their real values in Fig. 4-5 and Fig. 4-6 respectively.

The ‘Difference of V_1 determined by $f(D_1, D_2)$ ’ and ‘Difference of V_2 determined by $f(D_1, D_2)$ ’ proposed in Table 4-6 approve of the equation (4-7) as well.

4.3.4 Reversed model prediction in two fingers’ case: $D_x=f(V_1, V_2)$

This section introduces the reversed model prediction to define the distance of a finger motion (D_x , $x=1, 2$) with combined voltage values of both Rx electrodes (both V_1 and V_2). According to simple mathematical operations, equation (4-7) is monotonic in both variables (D_1 and D_2), and satisfies the condition that the function has an inverse function. Therefore, the reversed model prediction for two fingers’ case could be proposed, based on the previous sections. However, since the relative complicated form of equation (4-7), the equation (4-8) is unable to be obtained simply by the relationship of a function and its inverse function.

As stated in section 4.3.3, model prediction of two finger’s case ($V_x=f(D_1, D_2)$) is the superimposed form of the model prediction for the index finger and middle finger’s case ($V_x=f(D_x)$, $x=1,2$). Therefore, the investigation of the reversed model prediction in two fingers’ case $D_x=f(V_1, V_2)$ was started with a similar superimposed form of the one finger’s case: $D_x=f(V_x)$. However, since the function $D_x=f(V_x)$ is divergent, it will face the problem of zero crossing. With different fitted parameters for the index finger and the middle finger, their zero crossing values could be different, and therefore, are complicated to work on directly.

A mathematically transformed superposition form for $D_1=f(V_1)$ and $D_2=f(V_2)$ is investigated in Matlab. Based in the 196 simulated points, equation (4-8), which determines the distance of a finger’s motion with combined voltage values of both Rx electrodes, is proposed as follows:

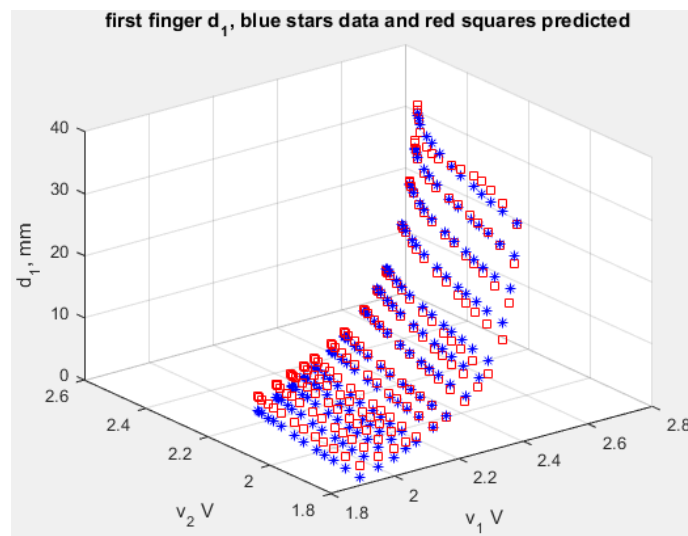
$$D_x = b_3 / [(1 - b_1 * V_1) * (1 - b_2 * V_2) + b_4] \quad (4-8)$$

Table 4-7 gives the curve fitting results of the equation (4-8). Likewise, the predicted voltage values of both D_1 and D_2 can be calculated with the curve fitting results of the equation (4-8). Specially, $D_2=f(V_1, V_2)$ has better R-Squared value comparing with $D_1=f(V_1, V_2)$. This is not the same as the situation of several other models presented in this chapter, and is potentially resulted from the approximate effect caused by the mathematical transformation when obtaining equation (4-8).

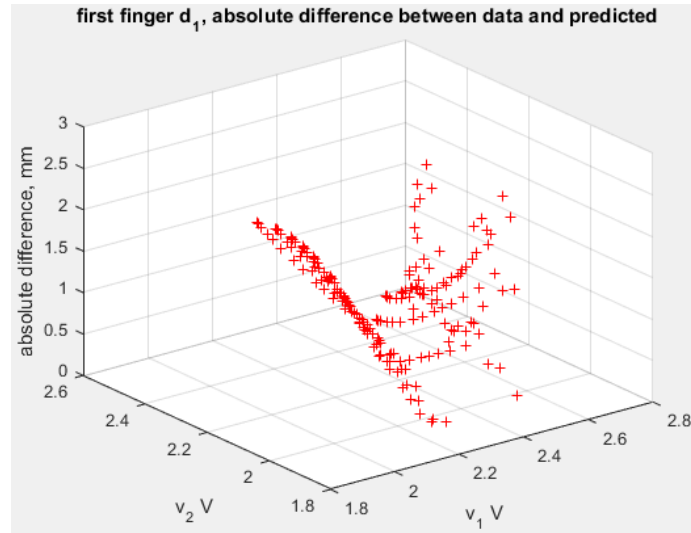
Table 4-7 Parameters of nonlinear curve fitting equation $D_x=f(V_1, V_2)$

	$D_1=f(V_1, V_2)$				$D_2=f(V_1, V_2)$			
Parameters	b_1	b_2	b_3	b_4	b_1	b_2	b_3	b_4
Estimate	0.47233	0.2885	0.24196	0.091752	0.22809	0.60244	0.18859	0.2019
pValue	3.5643e-180	1.2853e-155	2.8516e-64	3.0539e-36	4.2731e-198	1.7529e-197	2.699e-92	4.705e-79
Mathematic details	Root Mean Squared Error: 1.23, R-Squared: 0.983, P-value = 3.09e-196, Mean absolute difference = 1.03684.				Root Mean Squared Error: 0.97, R-Squared: 0.99, P-value = 2.74e-216, Mean absolute difference = 0.8318.			
	Number of observations: 196, Error degrees of freedom: 192.							

Fig. 4-7 (a) compared the real voltage values (blue ‘*’) from Comsol simulation, and the predicted values (red ‘□’) determined by the model from Matlab. Since the other finger’s movement is also considered as an input here, the crosstalk in two fingers’ case can be eliminated. Further to this, Fig. 4-7 (b) presents the absolute difference between the real values of the 196 data points and the predicted values from regression model. Due to the fractional form of equation (4-8), there will be a problem of zero crossing in the calculation of distance, that is, when the value of the denominator is approaching 0, the prediction of distance is prone to a larger error, which can be observed in Fig.4-7 (b). This problem mainly occurs when measuring very small distance, and only occupies a small part of the whole measurement range.



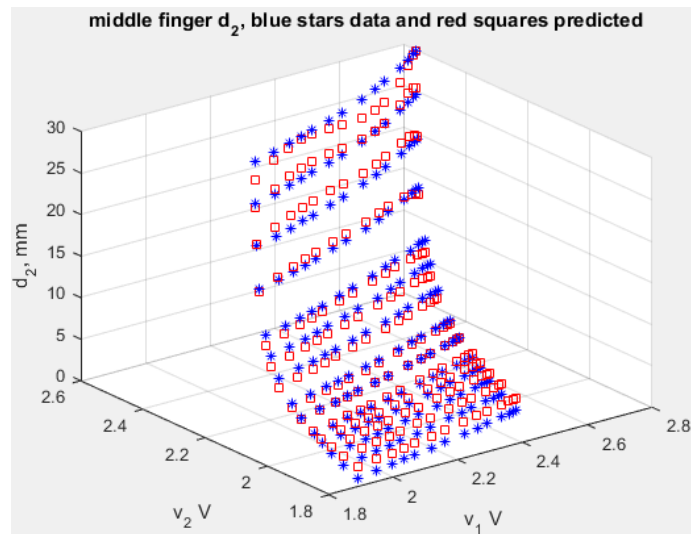
(a)



(b)

Fig. 4-7 Fitted curves for $D_1=f(V_1, V_2)$

Fig. 4-8 (a) and (b) are the regression fitting curves for $D_2=f(V_1, V_2)$ when index and middle finger move to the 196 curve fitted points (D_1 and D_2 ranging from 0mm, 0.5mm, 1mm, 1.5mm, 2mm, 3mm, 4mm, 6mm, 8mm, 10mm, 15mm, 20mm, 25mm, to 30mm).



(a)

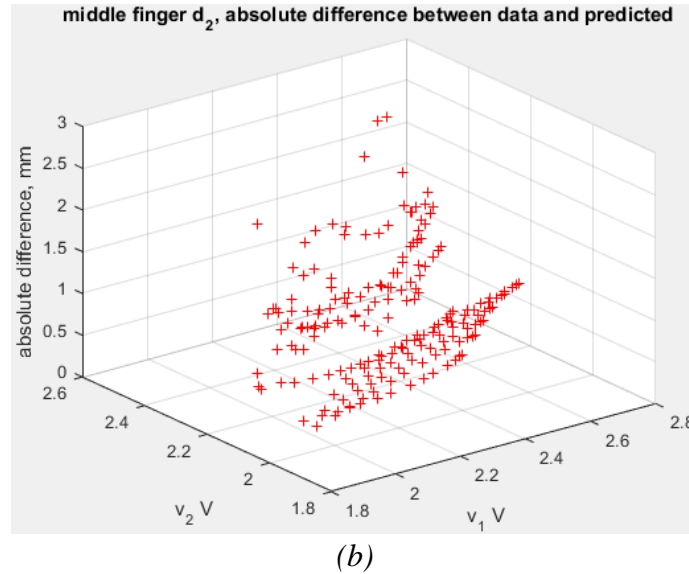


Fig. 4-8 Fitted curves for $D_2=f(V_1, V_2)$

In addition to the points used to conduct the regressions, testing points were simulated to test the regression model (4-8) as well. Table 4-8 presents the testing result of the fitted equation defining D_1 or D_2 with V_1 and V_2 . The 10 randomly generated testing points are same as those shown in Table 4-6. In view of the low average difference, both regression models work well in general, as a prediction model for two finger's case. Just as the performance of the prediction models discussed in 4.3.1, 4.3.2 and 4.3.3, $D_1=f(V_1, V_2)$ works better compared to $D_2=f(V_1, V_2)$.

Table 4-8 Testing points of nonlinear curve fitting equation $D_1=f(V_1, V_2)$ and $D_2=f(V_1, V_2)$

V_1	V_2	$D_1=f(V_1, V_2)$			$D_2=f(V_1, V_2)$		
		Real value of D_1	Predicted value of D_1	Difference of D_1 by $f(V_1, V_2)$	Real value of D_2	Predicted value of D_2	Difference of D_2 by $f(V_1, V_2)$
2.3716	2.3218	4	4.646	0.646	10.5	10.0046	0.4954
2.5394	2.0185	28	28.5982	0.5982	0.5	1.699	1.199
2.6459	2.4704	12.5	12.0916	0.4084	21.5	22.7171	1.2171
2.7541	2.5207	24.5	24.9584	0.4584	20	20.7599	0.7599
2.6167	2.3932	13.5	12.9268	0.5732	9	7.9239	1.0761
2.5704	2.2781	14	13.1654	0.8346	4.5	3.9435	0.5565
2.5172	2.418	7	6.9895	0.0105	25.5	25.4436	0.0564
2.6692	2.4456	16.5	16.1486	0.3514	12	11.2651	0.7349
2.5636	2.4388	8.5	8.2705	0.2295	28.5	26.7817	1.7183
2.5126	2.3483	8	7.6767	0.3233	8.5	7.5865	0.9135
Average				0.4434			0.87271

In brief, the distance from finger motion and the voltage signals of Rx electrodes in two fingers' case fits well with equation (4-8). Here, the predicted values of both D_1 and D_2 are

very close to their real values, as presented in Fig. 4-7 and Fig. 4-8 respectively, and are in consistency with the ‘Difference of D_1 determined by $f(V_1, V_2)$ ’ and ‘Difference of D_2 determined by $f(V_1, V_2)$ ’, proposed in Table 4-8.

4.4 Discussion

In this chapter, four nonlinear equations were introduced to describe finger motion (index & middle finger) in an electrical field generated by MGC3030 electrode layer stack-up design. As summarized in Fig. 4-9, these prediction equations mathematically describe the inherent relationship between distance of finger motion (D_x) and the voltage signals of the Rx electrodes (V_x). Given the evidence from the analysis of simulated data, like p-values and R-squared values, as well as the results from the testing points, these fitted equations work well in all cases.

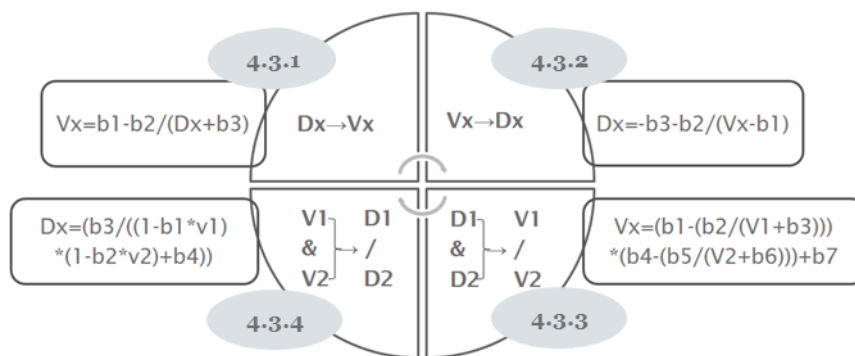


Fig. 4-9 Prediction models discussed

Although only the combined movement of index & middle fingers was investigated, the underlying research approach can be applied to middle & ring fingers’ or ring & little fingers’ combinations as well. It was also observed from the simulation results that, the impact of a finger’s movement to the signals read from Rx electrodes underneath non-neighbouring fingers is negligible in the measuring range. Hence, the more finger’s case can be converted into the two neighbouring fingers’ problem as addressed in this section.

4.4.1 Further discussion on equation $V_x = f(D_x)$: Influence of parameters on sensitivity

As presented in section 4.3.1, equation (4-5) describes the voltage values of a specified Rx electrode due to the distance change of a moving finger. The parameters of equation (4-5) ---- b_1 , b_2 and b_3 are all positive. Based on the simulation of the electrode designs with and without adding the ‘gnd’ electrode in Chapter 3, the voltage value (V_x) and the corresponding distance value (D_x) were fitted into the equation (4-5). Table 4-9 gives the curve fitting results of both electrode designs for case 1, case 1-2, case 2 and case 2-2 respectively.

$$V_x = b_1 - b_2/(D_x + b_3) \quad (4-5)$$

From parameters reported in Table 4-9, b_3 is always greater than b_2 , and therefore b_2/b_3 will be less than 1 in all the cases. The value of b_1 will be greater than b_2/b_3 . Hence, it can be obtained from equation (4-5) with simple mathematical derivation that, the voltage of the Rx electrode under the moving finger (V_x) will always have a positive value. When a finger moves away from the electrodes (D_x increases), the voltage will increase to reflect this movement, while when a finger flexes towards the electrodes (D_x decreases), the voltage will also decrease. Particularly, the voltage (V_x) will reach the value of b_1 , if a finger moves far away from the electrodes (D_x approaches infinity).

Table 4-9 Parameters of nonlinear curve fitting

Original electrode design						
	b_{1o}	b_{2o}	b_{3o}	R-squared	V_0 (V)	dV_0/dD_0 (V/mm)
case 1	2.6171	3.0776	4.4461	1	1.92	0.156
case 1-2	2.6171	3.0775	4.4460	1	1.92	0.156
case 2	2.3126	1.453	3.0407	0.997	1.83	0.157
case 2-2	2.3126	1.453	3.0407	0.997	1.83	0.157
Modified electrode design						
	b_{1m}	b_{2m}	b_{3m}	R-squared	V_0 (V)	dV_0/dD_0 (V/mm)
case 1	2.189	2.2629	4.4243	1	1.68	0.116
case 1-2	2.1889	2.2625	4.4238	1	1.68	0.116
case 2	1.5948	0.6307	2.7871	0.997	1.37	0.081
case 2-2	1.5948	0.6302	2.7857	0.997	1.37	0.081

Note: 1) Case 1 (1000): index finger moves; 2) Case 1-2 (0001): little finger moves; 3) Case 2 (0100): middle finger moves; 4) Case 2-2 (0010): ring finger moves.

Comparing the parameters of nonlinear curve fitting in case 1 with case 1-2, case 2 with case 2-2 in both electrode design, similar fitted parameters were observed. This similarity is in accordance with the symmetrical structure in the electrode designs discussed in Chapter 3, where case 1-2 and case 2-2 can be regarded as the symmetrical cases of case 1 and case 2 respectively in both electrode designs. Based on equation (4-5), the voltage values (V_0) when a finger is just placed on the electrode can be calculated ($D_x=0$) using following equation:

$$V_0 = b_1 - b_2/b_3 \quad (4-9)$$

As presented in Table 4-9, the voltage values for original electrode design for case 1 and case 1-2 are both 1.92V, and for the modified electrode design, the added 'gnd' electrode will reduce

the voltage value to 1.68V. For case 2 and case 2-2, the voltage values for original electrode design are lower, both 1.83V. A larger decrease in the voltage values for the modified electrode design are observed in case 2 and case 2-2. For the modified electrode design, the voltage value is reduced to 1.37 V. It is mainly because the position of the middle finger and the ring finger are more exposed to the electrical field generated by the added ‘gnd’ electrodes (zero potential).

From Chapter 3, the average sensitivity in the original electrode design is 0.03513 V/mm while that in the modified electrode design is 0.01986 V/mm. Here, sensitivity refers to the change in the voltage value of the Rx electrode under a moving finger, when the finger moves by one millimetre. The derivative of the equation (4-5) for distance can also be used to explore the sensitivity, which, similarly to previous investigation in Section 3.5.1, represents the voltage increase or decrease of an electrode, when the corresponding finger moves by one millimetre. In other words, the dV_x/dD_x could be used to describe the rate of change of the voltage value (V_x) at a certain distance point (D_x). The derivative of the equation (4-5) could be obtained by simple mathematical calculations, as given in equation (4-10). Particularly, the sensitivity (dV_x/dD_x) will be decreased to zero when D_x approaches infinity. It refers to the case when a finger moves far away from the electrodes (D_x approaches infinity), it has little influence on the electrical field generated by the MGC3030 electrodes.

$$\frac{dV_x}{dD_x} = b_2/(D_x + b_3)^2 \quad (4-10)$$

Similar to the discussion on equation (4-9), when a finger is just placed on the electrode ($D_x=0$), the sensitivity of the MGC3030 electrode design (dV_x/dD_x) can be calculated using following equation:

$$\frac{dV_0}{dD_0} = b_2/(b_3)^2 \quad (4-11)$$

As presented in Table 4-9, for original electrode design, the sensitivity of the electrode design (dV_x/dD_x) for case 1 and case 1-2 is 0.156 V/mm, and for the modified electrode design, the added ‘gnd’ electrode will reduce the sensitivity to 0.116 V/mm. For case 2 and case 2-2, the sensitivity for original electrode design are both 0.157 V/mm. A large reduction in the sensitivity for the modified electrode design are observed in case 2 and case 2-2, and the sensitivity here is reduced to 0.081 V/mm.

To further investigate the sensitivity for both electrode designs, with focuses on the influence of parameters, the sensitivity of the original electrode design and the modified

electrode design are compared on the equation point of view, as shown in equation (4-12) and (4-13) respectively. And the percentage of sensitivity of the modified electrode design compared to that of the original electrode design can be represented by equation (4-14). Hence, the reduction in sensitivity from the original electrode design to the modified electrode design can be calculated using equation (4-15).

$$\frac{dV_x}{dD_{x_{original}}} = b_{2o}/(D_x + b_{3o})^2 \quad (4-12)$$

$$\frac{dV_x}{dD_{x_{modified}}} = b_{2m}/(D_x + b_{3m})^2 \quad (4-13)$$

$$\frac{\frac{dV_x}{dD_{x_{modified}}}}{\frac{dV_x}{dD_{x_{original}}}} = \frac{b_{2m}}{b_{2o}} * \frac{\frac{1}{(D_x + b_{3m})^2}}{\frac{1}{(D_x + b_{3o})^2}} \quad (4-14)$$

$$1 - \frac{\frac{dV_x}{dD_{x_{modified}}}}{\frac{dV_x}{dD_{x_{original}}}} = 1 - \frac{b_{2m}}{b_{2o}} * \frac{\frac{1}{(D_x + b_{3m})^2}}{\frac{1}{(D_x + b_{3o})^2}} \quad (4-15)$$

With the fitted parameters for different cases and electrode designs in Table 4-9, the rate of change of the voltage value (V_x) at certain distance point (D_x) for different electrode designs could be compared, using the equation (4-14). The comparison of sensitivity for the modified electrode design to the original electrode design can be determined by product of the fraction with parameter b_2 and the fraction with parameter b_3 , as given in equation (4-14), to separately investigated and compared the influence of the added ‘gnd’ electrodes on sensitivity, from the parameters point of view, using the simulated data from Chapter 3.

Table 4-10 compares the first fractions (b_{2m}/b_{2o}) of the electrode designs with and without added gnd electrodes for case 1 and case 1-2, case 2 and case 2-2 separately. As discussed in Section 4.3.1, b_2 can be regarded as a sensitivity factor which reflects the magnitude of an intruding finger to the Rx signal. Therefore, when the parameter b_2 of the modified electrodes (b_{2m}) is bigger than that of the original electrodes (b_{2o}), the fractions will be over 100%, which indicate that, the modified electrode design will contribute to the performance of the system by increasing the sensitivity factor. Similarly, Table 4-11 presents the second fraction $(D_x + b_{3m})^{-2}/(D_x + b_{3o})^{-2}$ for both electrode designs against distance (D_x) for each case. Then, the product of these two fractions, which is also the results of simulated data for equation (4-14), are given in Table 4-12.

Table 4-10 Comparison of the sensitivity within each case: Influence of b_2

	Case 1	Case 1-2	Case 2	Case 2-2
b_{2o}	3.0776	3.0775	1.453	1.453
b_{2m}	2.2629	2.2625	0.63065	0.63019
b_{2m}/b_{2o}	73.53%	73.52%	43.40%	43.37%

Table 4-11 Comparison of the sensitivity within each case: Influence of b_3

	Case 1	Case 1-2	Case 2	Case 2-2
b_{3o}	4.4461	4.446	3.0407	3.0407
b_{3m}	4.4243	4.4238	2.7871	2.7857
D_x (mm)	$(D_x + b_{3m})^{-2}/(D_x + b_{3o})^{-2}$			
0	100.99%	101.01%	119.03%	119.15%
2	100.68%	100.69%	110.88%	110.94%
4	100.52%	100.53%	107.61%	107.66%
6	100.42%	100.43%	105.86%	105.89%
8	100.35%	100.36%	104.76%	104.78%
10	100.30%	100.31%	104.01%	104.03%
15	100.22%	100.23%	102.87%	102.89%
20	100.18%	100.18%	102.24%	102.25%
25	100.15%	100.15%	101.83%	101.84%
30	100.13%	100.13%	101.55%	101.56%

As shown in Table 4-10, the results of first fraction for case 1 and case 1-2 are 73.53% and 73.52%, while the results for case 2 and case 2-2 are 43.30% and 43.37% respectively. Since they are all less than 100%, the fraction with parameter b_2 suggests that, comparing with the original electrode design, the sensitivity of the modified electrode design will be reduced. The first fraction (b_{2m}/b_{2o}) is not dependent on D_x , while the fraction $(D_x + b_{3m})^{-2}/(D_x + b_{3o})^{-2}$ is dependent on D_x and is ranging from 119.15% to 100.13%, as shown in Table 4-11. Although slightly decreased with distance, the results of second fraction for all four case are more than 100%, which therefore, indicates a small increase in the sensitivity, by adding extra ‘gnd’ electrodes in the electrode design. In Table 4-12, the results of equation (4-14) suggests a reduced sensitivity in the modified electrode design, which is in accordance with the conclusion of Chapter 3. Comparing the results of Table 4-12 with Table 4-10 and Table 4-11, it can be indicated that, the first fractions (b_{2m}/b_{2o}) has most of the influence on the sensitivity reduction, and b_3 has a smaller influence on sensitivity than b_2 .

In Table 4-12, the results for case 1, case 1-2, case 2 and case 2-2 indicate a similar trend: the sensitivity is monotonous and decreases quickly when the distance increases. It agrees with the mechanism of the capacitive sensing [72]. Notably, in accordance with the symmetrical structure in the electrode designs, similar percentages were also observed in case 1 and case 1-2, case 2 and case 2-2. As presented in row ‘Reduction’, there will be a reduction

of 53.97% and 53.98% on average in the sensitivity for case 2 and case 2-2 respectively. These averages are slightly different from the ones mentioned in Table 3-7 section 3.5.1, where there will be a reduction of 53.54% (1-46.46%), 53.53% (1-46.47%) for case 2 and case 2-2 respectively in the sensitivity by adding extra ‘gnd’ electrodes in the modified electrode design. It is because the growth rate here is calculated using ‘derivation’ method, while the previous chapter uses the ‘average slope’ method.

Table 4-12 Comparison of the sensitivity within each case: Influence of b_2, b_3

D_x (mm)	Case 1	Case 1-2 $(b_{2m}/b_{2o}) \times [(D_x + b_{3m})^{-2}/(D_x + b_{3o})^{-2}]$	Case 2	Case 2-2
0	74.25%	74.26%	51.66%	51.68%
2	74.03%	74.03%	48.12%	48.12%
4	73.91%	73.91%	46.71%	46.69%
6	73.84%	73.83%	45.94%	45.93%
8	73.79%	73.78%	45.47%	45.45%
10	73.75%	73.74%	45.14%	45.12%
15	73.69%	73.69%	44.65%	44.62%
20	73.66%	73.65%	44.37%	44.35%
25	73.64%	73.63%	44.20%	44.17%
30	73.62%	73.61%	44.08%	44.05%
Average	73.82%	73.81%	46.03%	46.02%
Reduction (equation 4-15)	26.18%	26.19%	53.97%	53.98%

Note: For each distance point, reduction = (1-Average)*100%.

4.4.2 Further discussion on equation $D_x=f(V_1, V_2)$: Resolution of the target system

Fig. 4-10 illustrates the variation of these 196 raw data points from Comsol. Fig. 4-10 (a) presents the variation of V_1 when index finger moves, or in other words, D_1 changes. Ideally, there should be a one-to-one mapping existing between V_1 and D_1 , V_2 and D_2 . In this case, an ‘Index table’ recording this one-to-one relationship between D_x and V_x ($x=1,2$) can be constructed. And by looking up the voltage values in the ‘Index table’, the corresponding value of D_x can be simply determined. However, due to the crosstalk, there is a range of voltage signals for each D_1 value, corresponding to the varied D_2 (the motion of middle finger). For example, when V_1 is 2.5 V, D_1 could range from 6 to around 25 mm. Likewise, Fig. 4-10 (b) shows the similar relationship between D_2 and V_2 . To conclude, Fig. 4-10 indicates a significant degree of uncertainty in distance measurements due to crosstalk between finger positions, which means, it will be of poor accuracy to predict D_x by simply looking up its corresponding V_x from an index table.

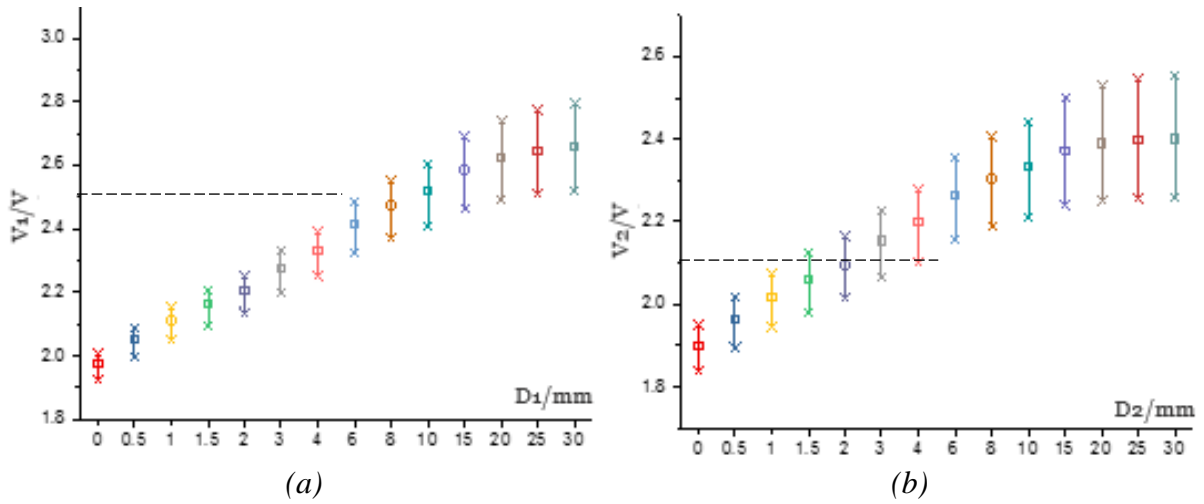
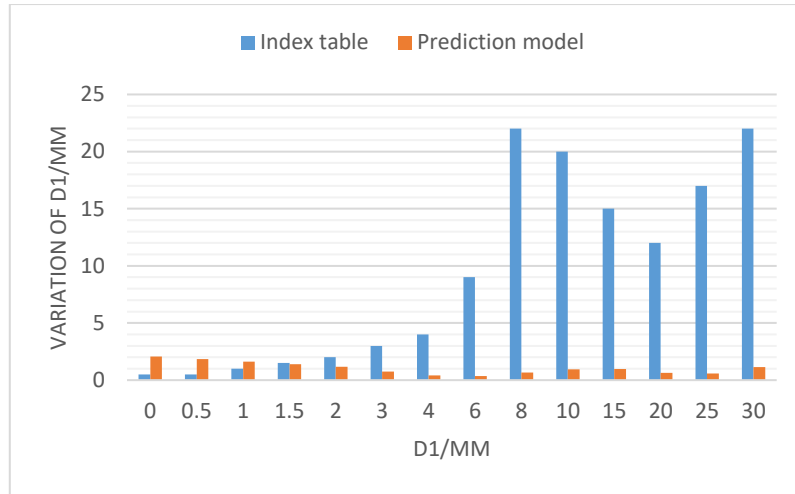


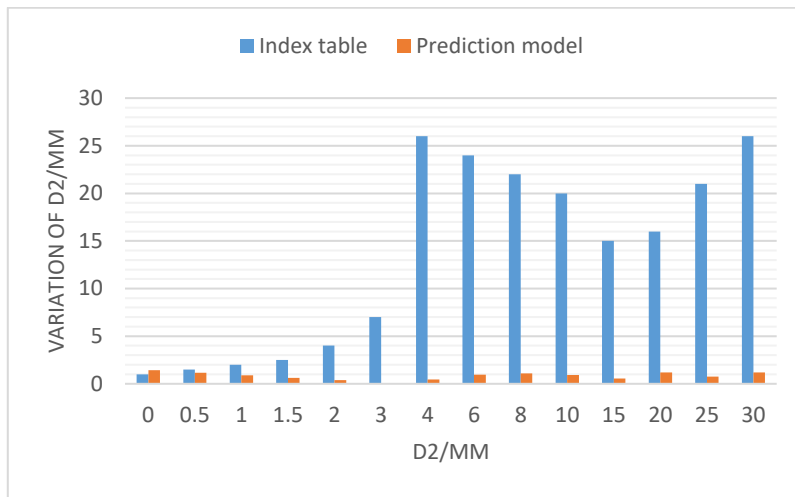
Fig. 4-10 Variation of voltage signal in raw data: (a) Variation of V_1 when D_1 is at 14 certain heights; (b) Variation of V_2 when D_2 is at 14 certain heights

To further evaluate the performance of the prediction model in combined finger motion detection, Fig. 4-11 compares the uncertainty using fitted equation $D_x=f(V_1, V_2)$ ('Prediction model' group), with the uncertainty using an index table ('Index table' group). The variation of the ' D_x ' value, namely, the uncertainty of distance was used to compare the resolution of fingers' movement sensing. From Fig. 4-11 (a), the variation of D_1 using $D_1=f(V_1, V_2)$ are kept under 2mm, while the variation of D_1 of the 'Index table' group can be up to 22mm. In Fig. 4-11 (b), the maximum variation of D_2 using prediction model (4-8) is approximately 1.4 mm while that in the 'Index table' group is 26mm. Uncertainty of prediction model is higher than the uncertainty of the 'Index table' group in very small distance (0~1.5mm). However, it is not significant compare to the whole measuring range (0~30mm), and the common measuring range (2~20mm) considering the typical finger motion ability. The detailed variation of distance using prediction model $D_x=f(V_1, V_2)$, or prediction model $D_x=f(V_x)$ are shown in Appendix L.

To conclude, the resolution of the target system can be significantly improved by using the prediction models. The average 0.94mm's resolution now indicates that targeted system is capable of detecting small movements of fingers.



(a)



(b)

Fig. 4-11 Comparing performance of prediction model $D_x=f(V_1, V_2)$ with using index table: (a) D_1 , (b) D_2 .

Note: 1) Average variation of D_1 from index table: 9.25mm; Average variation of D_1 from $D_1=f(V_1, V_2)$: 1.04mm. 2) Average variation of D_2 from index table: 13.43mm; Average variation of D_2 from $D_2=f(V_1, V_2)$: 0.83mm. 3) Average variation of D_x from index table: 11.34mm; Average variation of D_x from $D_x=f(V_1, V_2)$: 0.94mm.

4.5 Summary

In this chapter, four nonlinear equations were introduced to describe two fingers' motion in an electrical field generated by the original MGC3030 electrode layer stack-up design. The form of the equations agrees with the hypothesis based on the quasi-static electrical near field sensing theory. Additionally, the distance from finger motion and the voltage signals are shown to fit well with these prediction models. The prediction model ' $D_x=f(V_1, V_2)$ ' shows an excellent fit with uncertainty less than 1mm over a range of 30mm. It indicates that the

targeted system is capable of detecting small movements of fingers with satisfactory performance, allowing further development of the system in an experimental test.

Chapter 5 Experimental Verification Design

Previous simulated work has investigated a finite element method (FEM) simulation model based on the MGC3030 electrodes design, and proposed a mathematical relationship between the position of fingers and the voltage signals [32, 93]. However, the regression model proposed has not yet been explored in a real experimental test. Therefore, experimental verification was designed to extend the practical understanding of the prediction model on multi-finger noncontact measuring, with human subjects under laboratory conditions. Twenty-three healthy subjects (13 males and 10 females) with normal hand and finger function participated in this study. The experiment was approved by the institutional research ethics committee of the University of Southampton (ERGO/FEPS/48109).

5.1 Discussion of the FEM simulation model

Fig. 5-1 shows the schematic structure of the simulation model, where an electrical field directed from Tx electrode to GND electrode is generated and propagated three-dimensionally [72]. When fingers move towards the receptacle, they will interact with the three-dimensional electrical field and decrease the electrical field locally [72]. Therefore, the fingers' motion can be measured by the electrical field variations detected using the Rx electrodes. The signal detected by Rx electrodes under the index finger is labelled S_1 (MGC3030 Signal1), while the signal from the Rx electrode underneath the middle finger is labelled S_2 (MGC3030 Signal2). Similarly, the corresponding distances due to the movement of the index finger and the middle finger are related to D_1 and D_2 respectively.

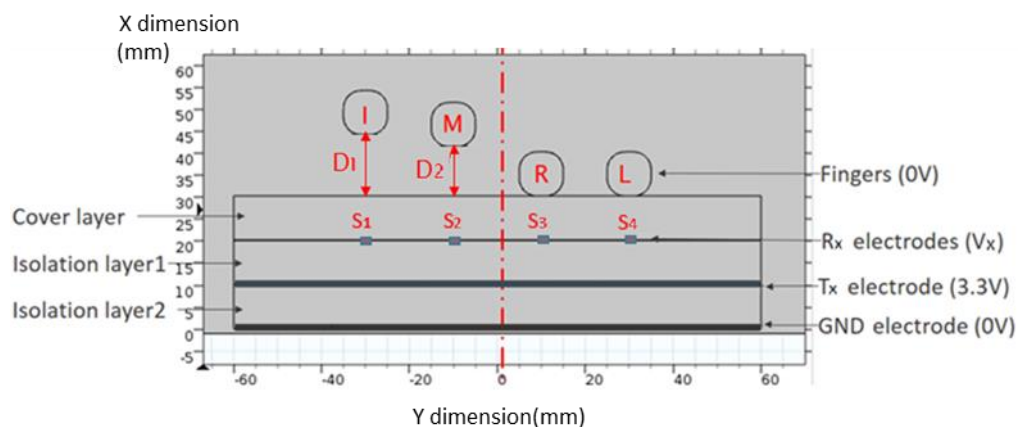


Fig. 5-1 Cross section view of the electrode design of the Comsol simulation model (Scale unit: mm)

Considering multifingered movement in the proposed electrical field under laboratory conditions, measurement of one finger will be affected by the movements of other fingers,

especially the neighbours, for two main reasons. In most cases, the signal changes are due to an electrical field leakage from the neighbouring moving finger. This is a systematic error of the MGC3030 measuring system, and is also what the term ‘crosstalk’ refers to in this thesis. When a person’s finger performs its intended movements, the real movements of other fingers may occur [38]. This unintended finger movement is called “enslaving” [94], and will also contribute to MGC3030 signal changes. Precautions were taken during the data collection and analysis steps of the experiment to prevent the unwanted movements. Particularly, a thumb can be considered completely independent during flexion-extension movements: it has the highest average individuation index which refers to the ability to move without any accompanying motion of the other fingers; and remained most stationary during instructed movements of other fingers [38, 39]. Therefore, the simulation started with only the index finger, middle finger, ring finger and little finger.

To compensate for the crosstalk due to the electrical field leakage, a nonlinear regression analysis was conducted using Matlab, as reported in Chapter 4 [32]. According to the section 4.6, the mathematical relationship between the simulated signals detected (S_1, S_2) from Rx electrodes and the corresponding distance due to fingers’ motion (D_1, D_2) were found to satisfy the following equation [32]:

$$D_x = b_3 / [(1 - b_1 * S_1) * (1 - b_2 * S_2) + b_4] \quad x=1,2 \quad (5-1)$$

where $b_1, b_2, b_3,$ and b_4 are parameters. The index finger and the middle finger have their own equation (5-1) with different fitted parameters. Since this prediction model determines the vertical moving distance of a finger with the Rx signals from both electrodes, crosstalk in two fingers’ case can be compensated. According to the simulated results [32], performance of this measuring technique can be greatly improved after using equation (5-1). The average resolution of the target system is reported to be 0.94mm [32]. It indicates that this measuring technique is capable of finger motion detection and worth investigating practically.

5.2 Experimental platform design

5.2.1 System design

Fig. 5-2 conceptualizes the experimental system to test the prediction model, which mainly includes the following units:

- MGC3030 Module: Near electric-field based sensing, using self-designed electrodes and MGC3030 chip, will be applied to the embedded device as an input sensor to allow

non-contact measurement of finger movements. Then the data read from the sensor can be processed and further calculated using a microcontroller (mbed) [1]. The controller unit of the MGC3030 motion sensor is connected to the electrodes as illustrated in Fig. 5-1, to produce high-resolution output signals corresponding to the extension and flexion of fingers.

- **Optical Sensor Module:** In order to validate the prediction model (5-1) based on the MGC3030 measuring system, an independent distance measurement to measure the distance that a finger moves away from the receptacle is required. This was accomplished using an optical sensor system based on a commercial sensor from Sharp [21], which allows a comparing technique for real-time contactless measurement. Two optical sensors are located directly above the fingertips of the index finger and the middle finger, and are fixed on a height-adjustable platform.
- **Microcontroller:** mbed development board (NXP LPC1768 ARM Cortex-M3 microcontroller) was used to perform the controlling and processing tasks for the experiment. It satisfies the current controlling requirements of the experimental system and provides sampling rate of 106 Hz. An IC with higher working frequency or larger storage capacity, such as LPC4300 series, can be selected in the future, to further improve the sampling rate and operation frequency.

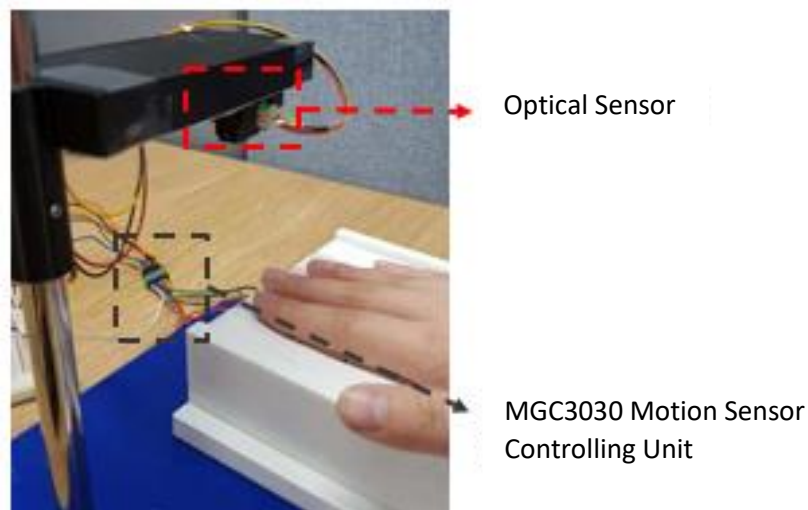


Fig. 5-2 Experimental set-up

5.2.2 Receptacle design

Fig. 5-3(a) shows the general stack-up model for the MGC3030 motion sensor. According to the MGC3030 design guide [89], Rx, Tx and GND can be made of any conductive material such as solid copper sheet or a metal mesh. The isolation between the electrodes and an optional cover layer on the top of Rx electrodes should be made of a non-conductive material. The optimum distances between Rx and Tx, Tx and GND depend on the relative permittivity of the isolation material between layers [89].

The design of the experimental hand receptacle and its electrodes has the same dimensions as the simulation model shown in Fig. 5-1 [32]. Details of the design parameters of the MGC3030 electrode stack-up are given in Table 5-1. The electrodes as well as the peripheral circuit were built in the receptacle. To help position the fingers for the best accuracy, there is a guideline on the cover layer of the receptacle.

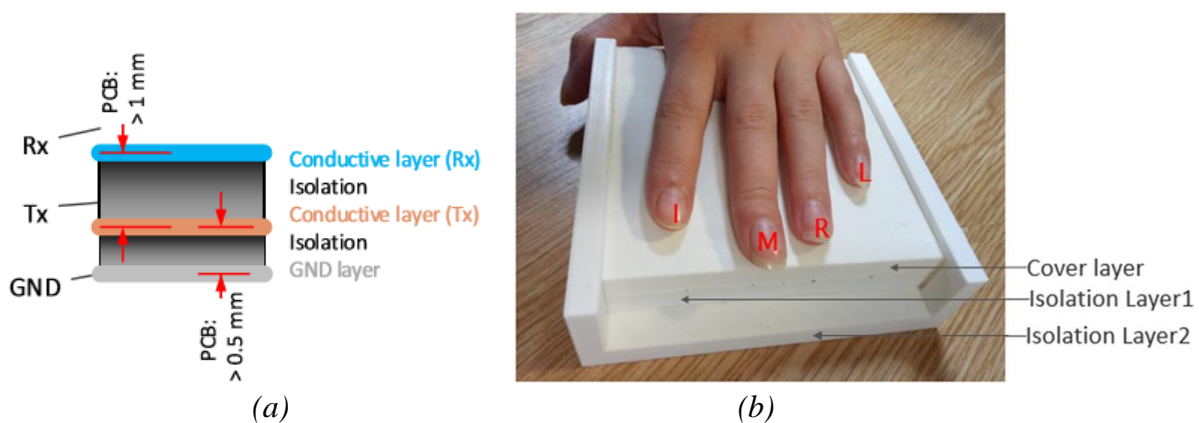


Fig. 5-3 (a) Stack-up model for MGC3030; (b) Experimental hand receptacle

Table 5-1 Design parameters of the MGC3030 electrode stack-up

Name	Material	Dimension
Rx electrode	Copper	2*50*0.2mm
Tx/GND electrode	Copper	110*100*0.2mm
Cover/isolation layers	Acrylic plastic	110*110*10mm
Spacing between the midpoint of Rx electrodes		20mm

5.3 Participants characteristics

The experiment was conducted separately for each participant and lasted approximately one hour. The basic extension and flexion of fingers was chosen as the exemplar movement. Therefore, the participants of the experiment should meet the following requirements:

- Between 18-69 years of age inclusive
- Able-bodied: physically healthy, and fit.
- Normal hand and finger function: the extension and flexion of both index & middle fingers will be required for every participant.

The exclusion criteria mainly include movement disorders or decreased ADL (activities of daily living) capability. The detailed exclusion criteria can be found in the Appendix M: Participant Questionnaire Sheet. All the twenty-three participants met the proposed requirements and finished their experiment.

The potential interpersonal influencing factors, such as gender, handedness as well as finger dimensions have also been collected during the experiment. Measuring of hand dimension consists of two main steps, as shown in Fig. 5-4:

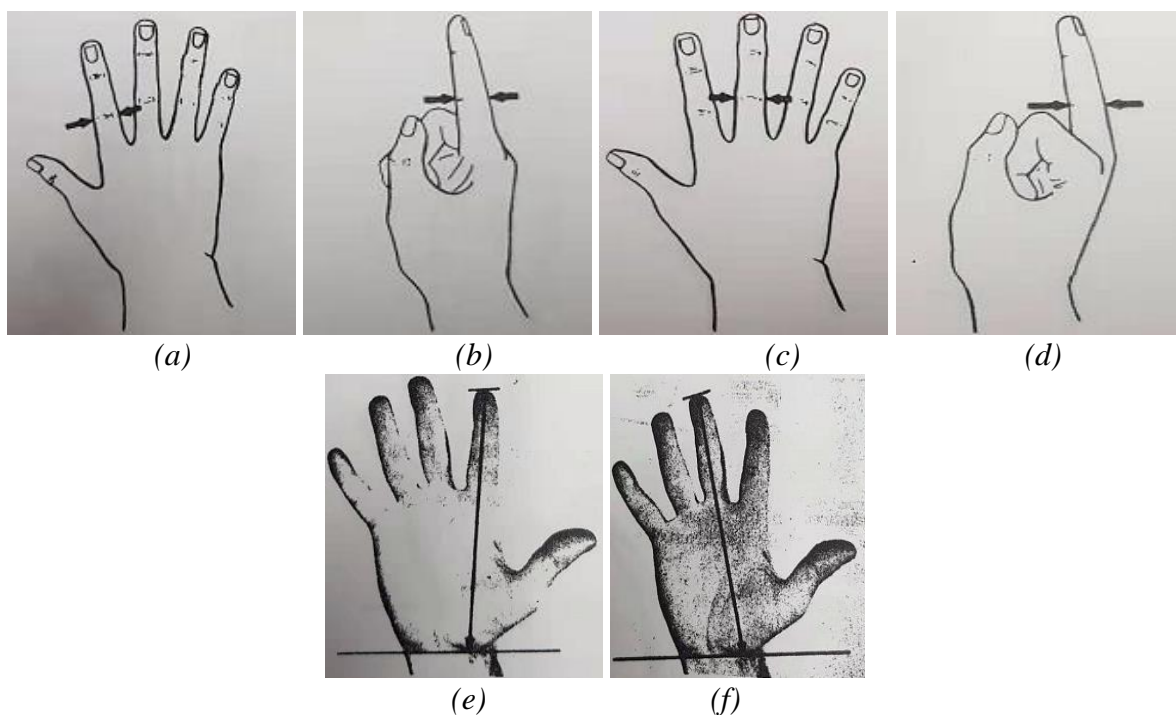


Fig. 5-4 Measurement of hand dimension: (a) the maximum breadth of the proximal interphalangeal joint of the index finger; (b) the maximum depth of the proximal interphalangeal joint of the index finger; (c) the maximum breadth of the proximal interphalangeal joint of the middle finger; (d) the maximum depth of the proximal interphalangeal joint of the middle finger; (e) the length from fingertip of the index finger to wrist crease; (f) the length from fingertip of the index finger to wrist crease.

- Subject's hand extended. Using a sliding calliper, measure the maximum breadth and maximum depth of the proximal interphalangeal joint of the index finger (Fig 5-4 (a), (b)) and the middle finger (Fig 5-4 (c), (d)).
- Subject's hand extended. With a millimetre scaled ruler, measure the distance along midpoint of the tip of the index finger (Fig. 5-4 (e)) and the middle finger (plot (f)) to the wrist crease baseline at the end of scaphoid bone.

The overall information about the participant characteristics is shown in Appendix P: Participant Characteristics. More information about the experimental process can be found in Appendix N: Participant Information Sheet and Appendix O: Participant Experiment Record.

5.4 Experiment process and data acquisition

A validation experiment has been designed to test the regression model for multi-finger noncontact measuring. For each participant, data collection consists of two parts:

- The calibration of the optical system: The optical sensors (index finger: optical sensor1; middle finger: optical sensor2) were calibrated against a millimetre scaled ruler. The purpose of the optical system was as a comparing technique for real-time contactless measurement, to measure the distance that a finger moves away from the receptacle.
- The testing of combined fingers movements, During the experiment for fingers' movement, the index finger and the middle finger were measured simultaneously with both the MGC3030 measuring system (S_x , $x=1,2$) and the optical sensor (D_x , $x=1,2$), to validate the prediction model (5-1) proposed.

Participants were seated at a table and remained still throughout the experiment. Their hand was placed on the receptacle with a horizontal posture, pronated with the fingers extended, as shown in Fig. 5-3 (b). Each finger could be extended from the flat posture but not into hyperextension. The thumb was abducted to the side of the receptacle, held stationary and had very little impact on the MGC signals detected by the Rx electrodes.

5.4.1 Calibration of the optical system

Calibration of the optical sensors was conducted for each participant. While a participant's hand was kept still on the receptacle, the platform to hold the optical sensors was adjusted up and down to vary the distance between the sensor and a fingertip. Approximately

ten distance points were measured and recorded for each participants, over a range up to 40mm. At each distance point, the optical system was sampled for 1000 times. Output samples from the optical sensor (V_o) were filtered using the ‘medfilter’ function in Matlab to remove high frequency noise. Then, an average of the 1000 sampled data (V_o) and the corresponding distance read from the ruler (D) were recorded as a distance point (D, V_o).

With the ten distance points, the polynomial distance characteristics $D=f(V_o)$ was obtained. An example fitted plot of the optical sensor for model $D = b_1 * V_o^2 + b_2 * V_o + b_3$ is given in Fig. 5-5. Here, the real distance values (red ‘□’) from the ruler, and the distance values (blue ‘*’) determined by the distance characteristics $D=f(V_o)$ from Matlab are compared. The R-squared value for the regression process of optical sensor1 (index finger) is 0.999, while for the optical sensor2 (middle finger) is 0.998. Therefore, Fig. 5-5 presents a good fit for both the optical sensor1 and optical sensor2, which is in accordance with the R-squared values from the regression process.

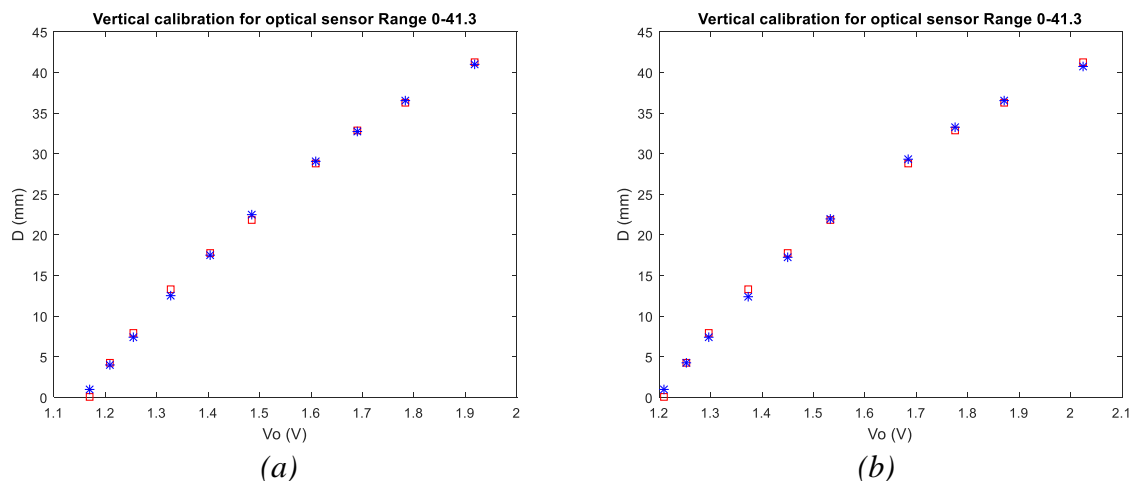


Fig. 5-5 Fitted results of optical sensor calibration from participant 20-F: (a) Optical sensor 1(R-Squared: 0.999); (b) Optical sensor 2(R-Squared: 0.998)

Table 5-2 R-squared for the optical calibration of all participants

	1-F	2-M	3-M	4-F	5-M	6-M	7-M	8-M
Opt1	0.999	0.997	0.996	0.999	0.969	0.998	0.998	0.999
Opt2	0.999	0.999	0.996	0.998	0.989	0.998	0.999	0.999
	9-M	10-M	11-M	12-M	13-F	14-M	15-F	16-F
Opt1	0.998	0.996	0.999	0.997	0.998	0.994	0.999	0.999
Opt2	0.999	0.998	0.999	0.997	0.999	0.997	0.999	0.998
	17-F	18-M	19-F	20-M	21-F	22-F	23-F	
Opt1	0.997	0.998	0.997	0.999	0.998	0.997	0.997	
Opt2	0.994	0.999	0.999	0.998	0.998	0.996	0.998	

Note: 1) Opt1: optical sensor1 for index finger; 2) Opt2: optical sensor2 for middle finger

Further to this, the R-squared for the optical calibration of all participants is presented in Table 5-2. The R^2 values for all of the 23 participants are significant and precise, which ensures a good nonlinear fit. Collectively, with the distance characteristics equation $D=f(V_o)$, the output of the optical sensors (V_o) could be used to obtain real-time distance values (D) when measuring the combined movement of fingers.

5.4.2 Testing of combined fingers movements

While testing of a combined movement of the index finger and middle finger, each participant was required to extend and flex their fingers in following order:

- The index finger extension away from the receptacle and then flexion back to the receptacle;
- The middle finger extension away from the receptacle and then flexion back to the receptacle;
- Both fingers extension away from the receptacle and then flexion back to the receptacle;
- Whole hand moved away from the receptacle;
- Hand placed back to the receptacle as required to prepare for the next combined movement.

These movements were repeated ten times for each participant. For the first three steps in this process, the palm was kept flat and still on the receptacle, while the movement of the other fingers (thumb, ring and little fingers) was avoided. As the index finger and middle finger moved, the movement was measured simultaneously with the optical system (V_{o1} , V_{o2}) and the MGC3030 measuring system (S_1 , S_2) for both fingers. Then the optical outputs (V_{o1} , V_{o2}) were applied to the distance characteristics equation $D=f(V_o)$, as illustrated in Section 5.4.1 to obtain real-time distance values (D_1 , D_2). Additionally, a median filter was applied to the distance values from both optical sensors (D_1 , D_2) for all the 23 participants with the filter width 20. Considering the sampling rates of 106 Hz, the filter width accounts for the time period of approximately 0.2 seconds. Explanations concerning the filtering issue of the optical sensors are reported in Appendix Q: Filtering Issue. Thus, the experimental results of the optical sensor (D_1 , D_2) and MGC3030 (S_1 , S_2) can be compared to verify the regression model proposed.

5.5 Discussion: Performance of the optical systems

During the experiment, the MGC3030 measuring system worked consistently well with robust outputs. However, it that the optical sensors was observed had unpredictable tracking failures. Fig. 5-6 presents an example output from both the optical sensor and the MGC3030 measuring system.

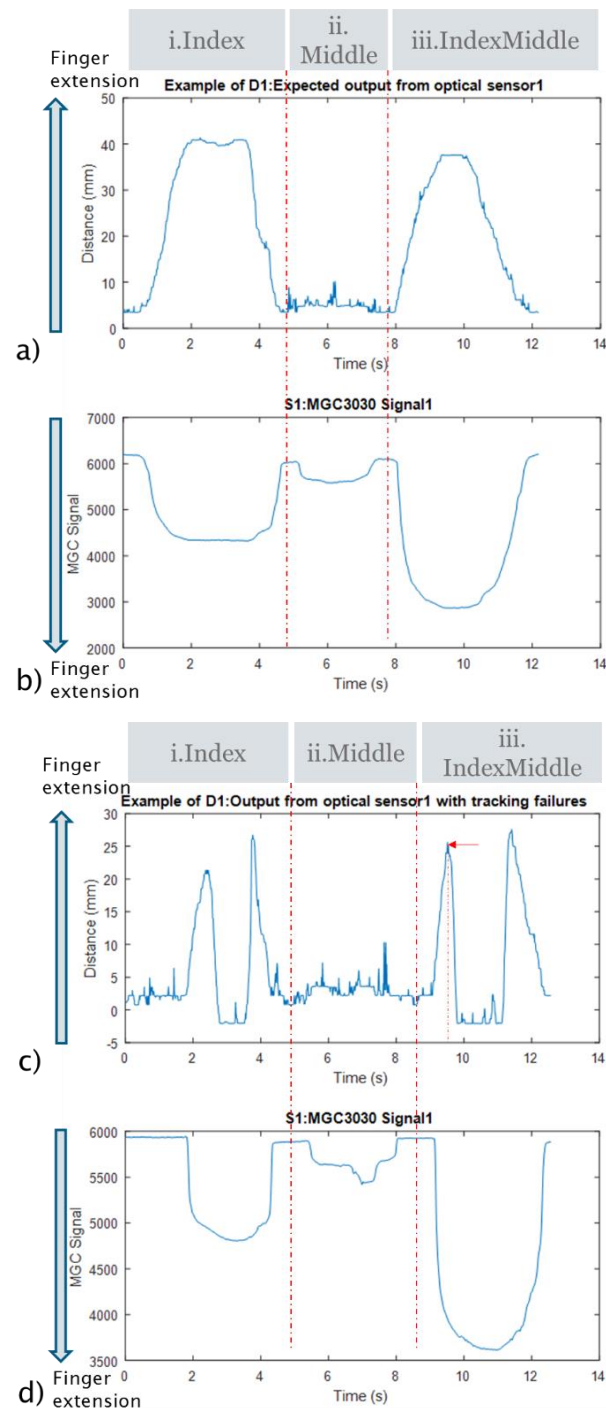


Fig. 5-6 Example outputs from experiment: a) Expected output from optical sensor, b) Output from the MGC3030 measuring system; c) Output from optical sensor with tracking failures, d) Output from the MGC3030 measuring system

For each movement, a participant was required to extend and flex their index finger twice. Therefore, the signal from the optical sensor to represent one movement of the index finger should be smooth with two peaks, as presented in Fig. 5-6 (a). Fig. 5-6 (c) presents an example output from the optical sensor with tracking failures. In plot (c), the optical sensor signal increases until it reaches about 25 mm at 9.5s, as marked in the figure. The signal should continue but instead falls down to below zero at 9.8s, as the sensor has lost track of the middle finger. Here, the distance below zero refers to the movement when the whole hand has moved away from the receptacle, which is obviously not true considering the standard movement required. Meanwhile, there are very sharp spikes observed, which indicate abnormal movements for human fingers.

For many participants in this preliminary study, these spikes and sharp signal changes in output of the optical sensors were hard to avoid. Therefore, the output from the optical sensors and MGC3030 system were reviewed at the end of each set of 10 movements. If a tracking failure was observed, the participant was asked to repeat the whole 10 movements again, until a consistent set of 10 movements for data analysis was obtained. The record for the repeated movements conducted by each participant due to a tracking failure, is presented in Fig. 5-7. Here, participant 1-F completed the experiment in 1 attempt, while participant 4-F conducted 5 attempts before a set of 10 measurements was acceptable. It suggests the alignment of the optical system is critical to obtaining high quality data from them.

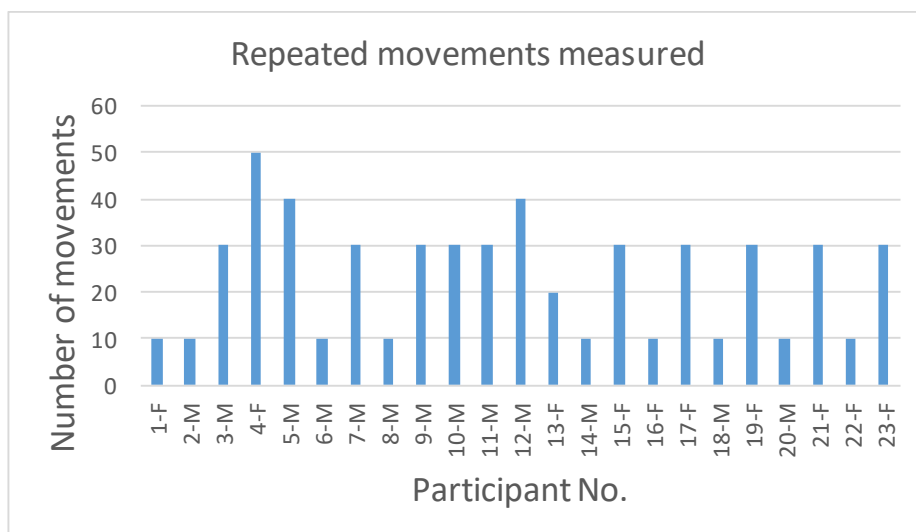


Fig. 5-7 Repeated movement conducted due to tracking failures

One possible reason is that, there were very small tremors or adductive/abductive movements when participants were extending and flexing their fingers, which resulted in a

horizontal offset. Also, the outer surface of a finger is complex and uneven. Therefore, errors are introduced and prevent the optical sensors from obtaining accurate results. Ideally, these factors should have been avoided. However, it was naturally hard for participants to control their fingers to that extent during the experiment. This would also be especially true for patients with hand impairment. A fiducial marker can effectively reduce the errors of the optical system resulting from these horizontal movements under laboratory conditions. However, it has to be well placed and attached, on each of the moving finger in every use, which requires great effort and might hinder the movement of fingers (especially for a patient). Similarly, there may be some small horizontal offset - with respect to the original position- when participants put their hand back to the receptacle to repeat the movements. This could probably be improved if calibration is applied for each movement. However, it is not ideal for the home-based provision of rehabilitation.

On the contrary, the signal detected by the MGC3030 measuring system is dominated by the closest object intruding the field lines. This refers to fingers in this application with a certain horizontal width, as presented in Fig.5-1. Therefore, one of the advantages of the reported measuring system compared to an optical system is its insensitivity to small horizontal (abduction and adduction) errors, which is in accordance with the results of the conducted experiments. Future experiments with measurements in the horizontal direction can be carried out to further investigate and quantitatively analyse the tolerance of the horizontal offset.

Another possible reason is the case that, when fingers extend, the increasing angle of incidence (AoI) could potentially affect the accuracy of the optical sensors associated with distance estimation. A positive correlation between AoI value and error magnitude was reported on short range distance measurement, based on a modern lidar sensor used in robotics (IR-ToF sensor, VL6180X) [95]. When AoI is 0° , the mean absolute error of the distance measurement is 1.5mm. Errors reached 3.6mm (static) and 11.9mm (dynamic) for AoI equal to 30° , and were 7.8mm (static) and 25.6mm (dynamic) for AoI equal to 60° . In contrast, the prediction model for the MGC3030 measuring system can be defined as the integration of the cross section simulation models, as presented in Fig. 5-1. When a finger is inclined to the horizontal plane in the experiment, it can be represented by the superposition of multiple 2D simulation models where their D_x were set to different numbers accordingly.

Collectively, although the optical system and its measuring technique have limitations for finger motion measurement for home rehabilitation, reliable data was obtained and used in

the comparisons with the MGC3030. For the optical sensor, the ‘tracking failure’ can be improved by optimizing the implementation or calibration method in future research. For example, the ‘corner cubes’ structure which is used in the lunar laser could be a potential option [96]. It features three perpendicular reflecting faces, and can help the incoming light exit in exactly the opposite direction from which it entered.

5.6 Discussion: Evaluation of the MGC3030 system

According to this preliminary study, the MGC3030 measuring system works well as a noncontact form of fingers movements in most of the 23 participants, with a measurement range of 40 mm and a sampling rate of 106 Hz. The accuracy of this system will be discussed in detail in Chapter 6. Hence, the experimental system satisfies the specifications of the MGC3030 measuring technique currently. There are some issues regarding placement, and variability due to differences between hands. Nevertheless, the application of the MGC3030 measurement system as a repeatable measurement has been demonstrated and gives confidence that such a system is an excellent candidate for application in a home-based system.

In the current experimental design, the optical system is needed as a comparing group for distance measurement. However, the optical system and its calibration steps are not necessary in the final MGC3030 measuring system. For participants with different needs for tracking improvements, the future household MGC3030 system could provide:

- a) Absolute measurement. It requires an independent measuring system, such as the optical sensor presented in this thesis, to conduct a calibration for the mathematical relationship between the distance of the finger motion (D_x) and the MGC3030 signal (S_x). After that, the MGC3030 measuring system can be used for absolute distance measurement at home. The optical sensor will only be used for a calibration procedure in the clinic and will no longer be needed in further applications.
- b) Relative measurements. It uses the generalized relationship between the distance of the finger motion (D_x) and the MGC3030 signal (S_x), and therefore, works without the requirement of the optical system or an individual calibration. A standard prediction model (5-1) will be applied to participants with the same fitted parameters (b_1 , b_2 , b_3 , and b_4). Therefore, a distance value can be obtained

with the detected MGC3030 signal only. Although this gives reduced absolute accuracy, it is suitable for relative measurements for tracking improvements.

5.7 Summary

In this chapter, the experimental verification was designed to extend the practical understanding of the prediction model on multi-finger noncontact measuring, with 23 human subjects under laboratory conditions. The experimental results of the optical sensor (D_1 , D_2) and MGC3030 (S_1 , S_2) can be compared to verify the FEM regression model proposed. It was observed from experiments that the MGC3030 measuring system worked well with robust and repeatable outputs, while the optical comparison sensors sometimes had unpredictable tracking failures.

Chapter 6 Data Analysis and Experimental Evaluation

6.1 Crosstalk

Chapter 6 analyzes the results of the validation experiment reported in Chapter 5 to evaluate the ability of the MGC3030 measuring system on measuring finger movements. Fig. 6-1 presents the experimental results from the optical system (D_1 , D_2) and the MGC3030 measuring system (S_1 , S_2) in one sample movement, which includes 3 steps: i.Index, the index finger extension and then flexion; ii.Middle, the middle finger extension and then flexion; iii.IndexMiddle, both fingers extension and then flexion. Here, optical sensor1 and optical sensor2 are placed directly above the fingertips of the guideline for the index finger (D_1) as well as the middle finger (D_2), and measure these finger movements respectively, as shown in Fig. 6-1(a).

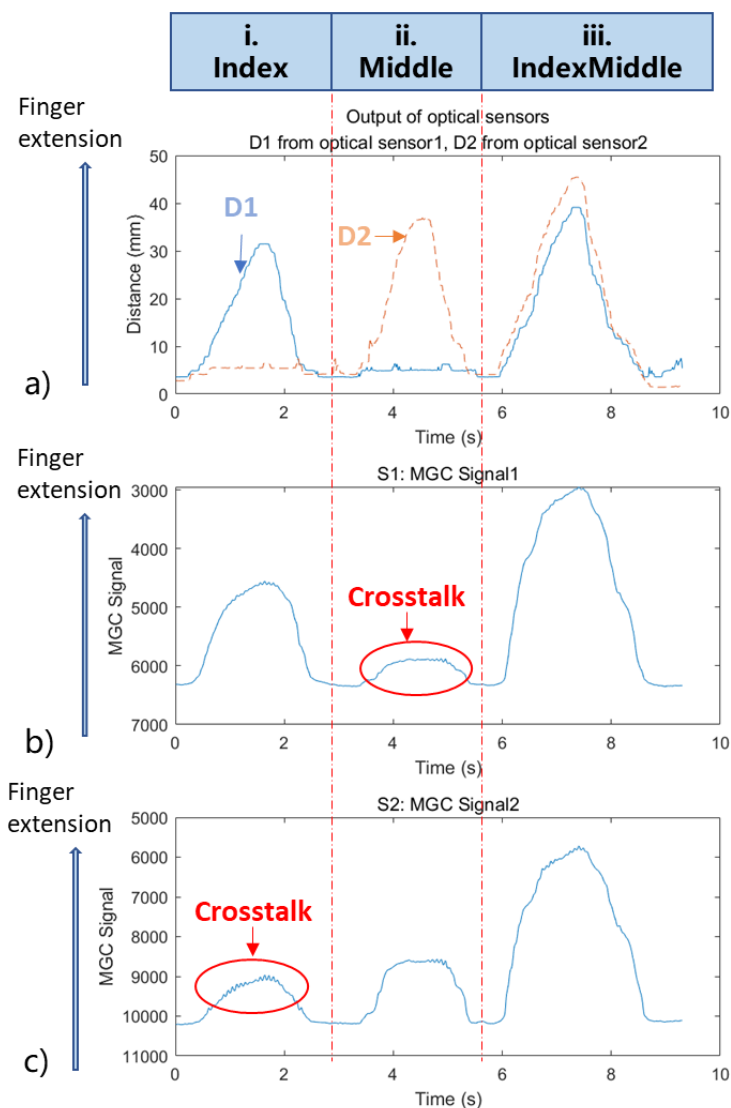


Fig. 6-1 Signal changes in one sample movement

Simultaneously, these movements are measured with the MGC3030 measuring system by signals detected from Rx electrodes under index finger and middle finger (S_1 and S_2 , as shown in Fig. 1). These MGC3030 signals are a function of the hand-Rx capacitance, Tx transmit signal and electrode capacitance [97]. When a hand is at a distance from the electrodes and has no influence, the signals are approximately zero as a baseline. A hand approaching the MGC3030 system increases the hand-Rx capacitance and causes the MGC signal to rise [97]. In this experiment, the maximum value for a person will be reached when the hand and all fingers are placed on the receptacle, while when the finger is moving up, a decreasing value will be obtained. Therefore, the MGC3030 signals have an inverse proportional function with the distances moved away from the receptacle. In Fig. 6-1(b) and Fig. 6-1(c), the y-axis direction is flipped to facilitate the reader's understanding.

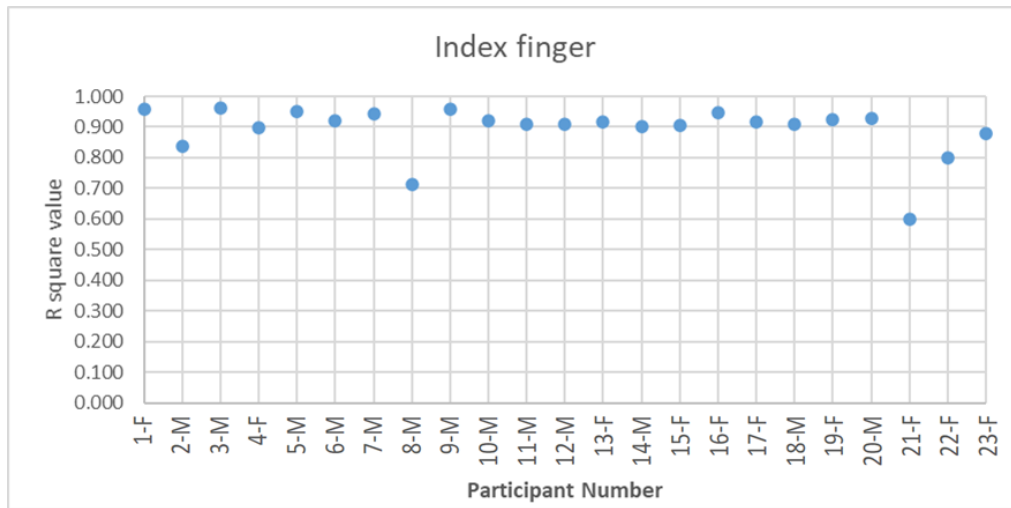
If only one finger is considered, there should be a one-to-one relationship between the position of a finger, and the MGC3030 signal from the Rx electrode under this finger [32]. However, due to the nature of electrical field, the movement of the middle finger will affect the MGC3030 Signal1 (S_1), as circled in Fig. 6-1 (b). Similarly, signal changes in S_2 are also observed in Fig.6-1 (c), due to the movement of the index finger. This phenomenon is in accordance with the FEM simulation, where crosstalk is observed especially between near neighbours [32]. In other words, it appears that the middle finger is moving when we know it is not, as shown in Fig. 6-1 (c).

6.2 Nonlinear regression

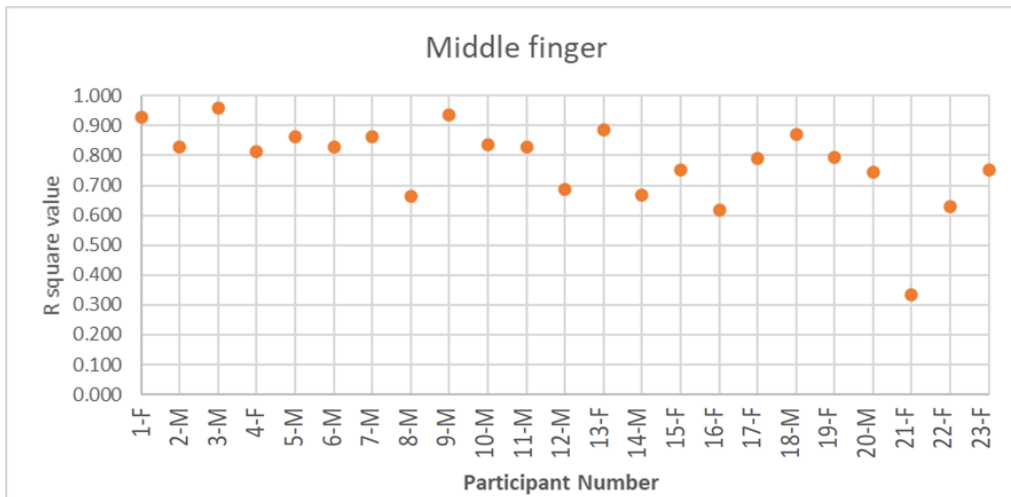
To compensate for this crosstalk, the output of the MGC3030 measuring system (S_1 , S_2) together with the simultaneous output of the optical sensors (D_1 , D_2) was fitted to the prediction model as presented in equation (5-1), using the Matlab function block 'fitlm'. This function fits the model to variables in the dataset/table, and returns the nonlinear model which presents a least-square fit of the response to the data. From the nonlinear regression, the fitted parameters b_1 , b_2 , b_3 , b_4 and the R^2 values were obtained from the Matlab output. With the fitted parameters and equation (5-1), predicted values of distance (D_{p1} , D_{p2}) can be obtained using the MGC3030 signals (S_1 , S_2).

The R^2 value is always between 0 and 1, and is a statistical measurement of how close the data are to the fitted regression line [96]. In general, the higher the R^2 , the better the model fits the data. Fig. 6-2 shows the R^2 values for the nonlinear regression analysis from the 23 participants. For each participant, the R^2 value is the arithmetical mean value of the repeated

movements. As presented in Fig. 6-2 (a), the main distribution of R^2 values for the nonlinear regression process of the index finger is 0.9~1. There are few R^2 values which fall between 0.8~0.9, and two outliers (8-M, 21-F) which fall to 0.714 and 0.600. Therefore, it can be indicated from the nonlinear regression process for the index finger that, the distance calculated from the optical sensors (D_1, D_2) and the signals detected on the Rx electrodes (S_1, S_2) fit well with the prediction model for most of the participants.



(a)



(b)

Fig. 6-2 The mean R^2 values of the nonlinear regression analysis for the experimental results of the 23 participants

Similarly, Fig. 6-2 (b) shows the arithmetical mean of the R^2 values for the experimental results from the middle finger. Here, the main distribution of R^2 values for the nonlinear regression process of the middle finger is 0.6~1, with a low value of 0.335 (21-F). The

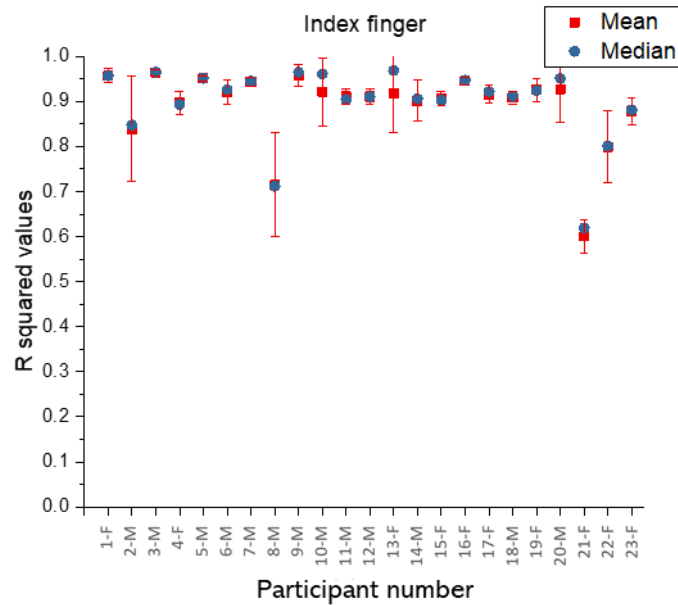
prediction model tends to have better performance for the index finger and have more individual difference the fitting of data to the middle finger. It agrees with the mechanism of the prediction model, where two fingers' movements are considered simultaneously to deal with the crosstalk caused by a neighbouring finger. Considering the hand placing on the receptacle in the experiment (as explained in Chapter 5.4), for index finger, the only neighbouring finger to deal with is the middle finger. Hence, the application of prediction model (5-1) to the experimental results of the index finger and the middle finger can nicely compensate for this crosstalk. However, the middle finger is adjacent to both the index finger and the ring finger. Therefore, for middle finger, a more comprehensive nonlinear regression analysis is required in the future, to compensate for the crosstalk due to both the movement of the index finger, as conducted in this research, and the movement of the ring finger, with a similar experiment which includes the middle finger and the ring finger. A discussion about the prediction models for three/four finger movement can be found in Section 6.4.2.

Fig. 6-3 presents the distribution of the R^2 values for the repeated movements of the 23 participants. The distribution of these R^2 values from the nonlinear regression analysis of the index finger and middle finger are presented in plot (a) and plot (b) respectively. For each participant, the mean value of R^2 values is marked with '■', while the median value is marked with '●'. The red line '-' represents the standard deviation of the R^2 values from the repeated movements for each participant. As shown in Fig. 6-3(a), the distribution of R^2 values of the index finger for participants number 1-F, 3-M, 5-M, 7-M, 11-M, 12-M, 15-F, 16-F, 17-F, and 18-M are significant and precise, which represent good repeatability and ensures a good nonlinear fit.

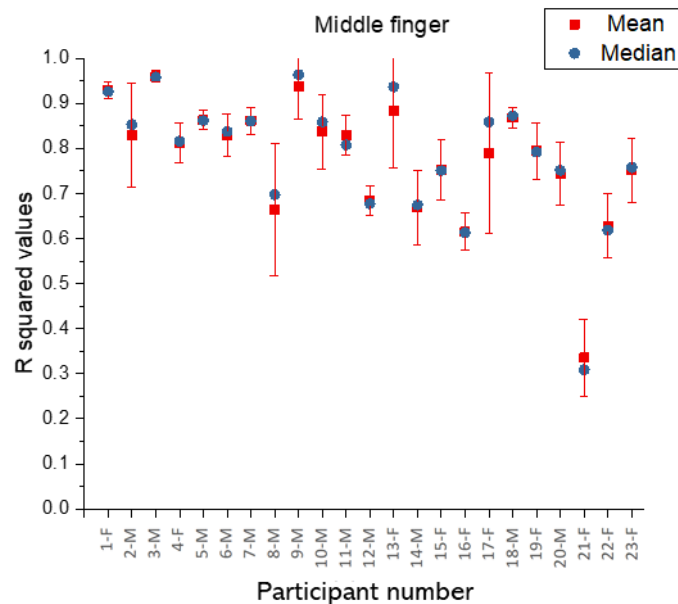
The R-squared values in Fig. 6-3(b) shows more variation in the response to the experimental data for the middle finger, and it agrees with the discussed results in Fig. 6-2. For participant 1-F and 3-M, the R-squared results indicate a good degree of fit and repeatability, between the model and the data from the middle finger. Particularly, for participant 21-F, although its mean R^2 value and median R^2 value for both fingers are outliers comparing to the other participants, the distribution of the R^2 value is of general precision and is quite repetitive.

An R^2 value does not indicate whether a regression model is adequate [98]. In some fields, it is entirely expected that a low R^2 value will be obtained. For example, a regression process that attempts to measure human movement, such as limb movements [99-101], psychology [102, 103], clinical epidemiology [104], or demographics [105], typically have

lower R^2 values [96]. It seems that humans are simply harder to predict than physical processes. However, the R^2 values could still be applied to draw important conclusions about how changes in the predictor values are associated with changes in the response value. Regardless of the R^2 value, the significant coefficients still represent the mean change in the response for one unit of change in the predictor while holding other predictors in the model constant. And this type of information can be extremely valuable.



(a)



(b)

Fig. 6-3 Standard distribution of R^2 values for the nonlinear regression analysis for the experimental results of the 23 participants

Collectively, the experimental results from repeated movements of 23 participants in this research supports the prediction model (5-1). From Fig. 6-2 and Fig. 6-3, the prediction model fits well with the experimental results of the index finger, while there is more individual difference in the fitting of the model to data from the experiments of the middle finger.

6.3 Reduced crosstalk after using the prediction model

From the nonlinear regression, the fitted parameters b_1 , b_2 , b_3 , and b_4 were obtained. With the fitted parameters and equation (5-1), predicted values of distance (D_{p1} , D_{p2}) can be obtained using the MGC3030 signals (S_1 , S_2). To better evaluate the performance of the prediction model, data analyses are focused on the steps i and ii where the index finger and middle extend and flex in turn and separately.

Fig. 6-4 compares the crosstalk before and after using the prediction model to compensate for both index finger and middle finger. Fig. 6-4 (a) shows the MGC3030 signal from Rx electrode under the index finger. In the figure, S_{1-i} refers to the signal change of MGC3030 Signal1 due to the measured movement of index finger. Since S_{1-ii} represents the signal change of MGC3030 Signal1 when the middle finger moves, it shows the largest crosstalk when measuring the movement of index finger using the MGC3030 measuring system. Accordingly, Fig. 6-4 (b) presents the predicted distance of D_1 after applying the MGC3030 signals (S_1 , S_2) to the prediction model (5-1). D_{p1-i} is the predicted distance change of the MGC3030 measuring system for index finger's movement, while D_{p1-ii} refers to the distance change due to the crosstalk resulted from the movement of middle finger. By comparing the MGC3030 signals in Fig. 6-4 a) and the predicted distance after fitting to the prediction model in Fig. 6-4 b), it was observed that the prediction model works well to compensate the crosstalk. To further evaluate the performance of prediction model on reducing crosstalk for index finger, S_{1-ii}/S_{1-i} , D_{p1-ii}/D_{p1-i} can be used to reflect the impact of crosstalk before and after applying the prediction model for comparison.

Similarly, Fig. 6-4 (c) illustrates the MGC3030 Signal2 from the Rx electrode under the middle finger, whereas Fig. 6-4 (d) shows the results after applying MGC3030 signals to the prediction model. In accordance, S_{2-i}/S_{2-ii} and D_{p2-i}/D_{p2-ii} compare the signal changes due to crosstalk before and after compensated by the prediction model when measuring the middle finger. Here, S_{2-ii} refers to the signal change when middle finger moved, while S_{2-i} represents biggest crosstalk due to the movement of index finger. D_{p2-ii} is the predicted distance change

of middle finger's movement after compensated by the prediction model (5-1), while D_{p2-i} refers to the predicted distance change from crosstalk.

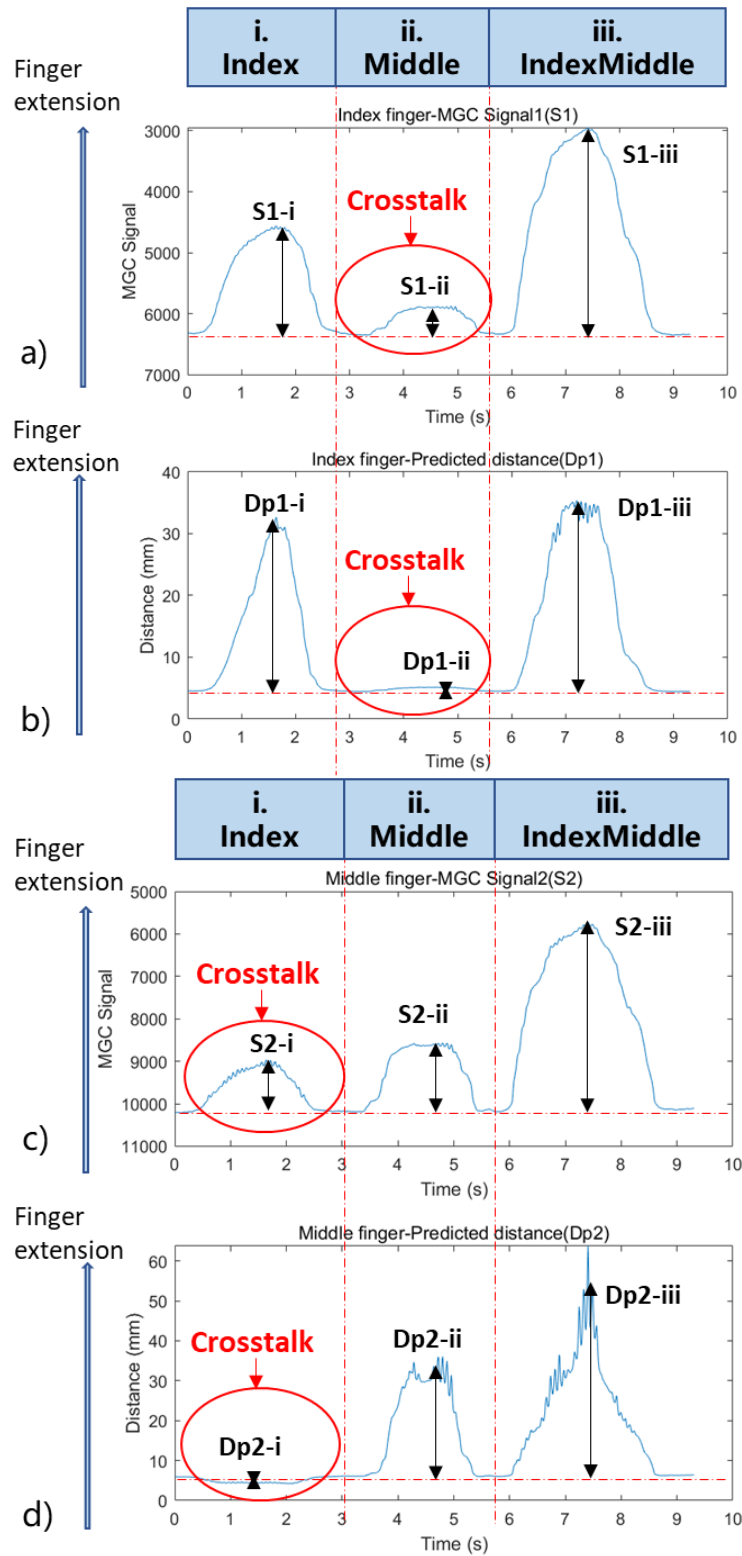


Fig. 6-4 Improvement on crosstalk after using the prediction model

Particularly, there were tiny fluctuations when the middle finger of the participant reached a large height. As shown by the burrs in Fig. 6-4 (c), fluctuations were recorded by the MGC3030 system (S_2), while the optical signal (D_2) did not act to the fluctuations, as shown in Fig. 6-1(a). These fluctuations may come from tiny physiological tremors, which are usually asymptomatic or invisible. A discussion about tremors observed from the experiment can be found in Section 6.4.4.

Since signal of the MGC3030 sensor (S_x) is inversely proportional to its distance from the human body (D_x) in the prediction model (5-1), out of sync for recording the fluctuations of the middle finger will bring in a larger distance uncertainty for the predicted distance (D_{p2}) at the far end. Therefore, as presented in Fig. 6-4(d), the same MGC signal change will represents a larger distance change at the far end (D_{p2-ii} , D_{p2-iii}). The predicted distance for index finger (D_{p1}) also fluctuated because it is a function of S_2 as well in the prediction relation (5-1) $D_x=f(S_1, S_2)$. This is especially obvious for the predicted distance for index finger at step-iii (D_{p1-iii}), when the index finger reaches its far end while the fluctuations of the middle finger also has significant impact. As show in Fig.6-4 (b), a bigger distance uncertainty was introduced in the predicted distance of the index finger (D_{p1-iii}), as a result of which, the predicted distance based on the MGC3030 signals (D_{p1}) show different distance values compared with the experimental data from the optical sensors (D_1).

To take a general view on the performance of the prediction model in measuring the combined finger motion, the impact of crosstalk before and after using the prediction model for both fingers were investigated, as shown in Table 6-1. Here, the experimental result for each participant is the average of the 10 repeated movements. The output of the optical sensors (D_1 , D_2) were analysed to evaluate the performance of the optical distance measuring system. The comparison with D_{x-ii}/D_{x-i} ($x=1,2$) for both index finger and middle finger was presented in Table 6-1. Here, D_{1-ii}/D_{1-i} refers to the impact of crosstalk on optical sensor1 when measuring the index finger, due to the movement of the middle finger. This crosstalk is not expected to affect the optical system considering the mechanism of the optical measurement. Based on the experimental results, D_{1-ii}/D_{1-i} of the 23 participants remained below 1%, with an average of 0.38%. Similarly, D_{2-ii}/D_{2-i} represents the impact of crosstalk due to the movement of the index finger, when optical sensor2 measures the middle finger. The D_{2-ii}/D_{2-i} from the output of the optical system is 0.70% on average, and most of them remain below 1%. Possible reasons of outliers here can be found in the discussion. In general, the comparison

with D_{1-ii}/ D_{1-i} and D_{2-ii}/ D_{2-i} demonstrates the good reliability of the optical sensor as a comparing system.

Table 6-1 Experimental results of twenty-three participants: The average level of crosstalk before and after using the prediction model

	Index finger			Middle finger		
	D_{1-ii}/ D_{1-i}	S_{1-ii}/ S_{1-i}	D_{p1-ii}/ D_{p1-i}	D_{2-i}/ D_{2-ii}	S_{2-i}/ S_{2-ii}	D_{p2-i}/ D_{p2-ii}
1-F	0.88%	33.22%	4.60%	0.79%	34.56%	1.27%
2-M	0.14%	32.77%	2.19%	0.66%	47.50%	3.81%
3-M	0.31%	23.92%	2.28%	0.50%	63.06%	0.15%
4-F	0.89%	23.18%	3.94%	3.31%	64.09%	0.15%
5-M	0.37%	25.27%	1.79%	0.86%	51.23%	9.79%
6-M	0.36%	38.98%	0.98%	2.80%	35.71%	1.52%
7-M	0.55%	31.09%	2.83%	0.58%	43.48%	2.63%
8-M	0.39%	24.76%	0.40%	0.22%	69.14%	1.20%
9-M	0.18%	38.93%	2.18%	0.29%	37.51%	4.01%
10-M	0.56%	15.15%	2.74%	0.24%	79.11%	4.76%
11-M	0.42%	51.50%	3.16%	0.42%	25.48%	1.09%
12-M	0.47%	11.28%	2.38%	0.10%	137.08%	4.67%
13-F	0.52%	21.71%	1.60%	0.54%	88.72%	5.72%
14-M	0.12%	22.69%	4.82%	0.19%	104.42%	4.14%
15-F	0.24%	20.51%	0.53%	0.62%	58.50%	2.31%
16-F	0.25%	10.93%	0.86%	0.03%	150.25%	1.19%
17-F	0.18%	24.81%	0.96%	0.12%	59.93%	1.33%
18-M	0.05%	25.33%	2.44%	1.00%	60.58%	1.99%
19-F	0.30%	33.06%	2.28%	0.59%	63.98%	4.54%
20-M	0.30%	25.92%	3.17%	1.31%	50.46%	4.84%
21-F	0.39%	42.77%	6.83%	0.27%	101.74%	53.19%
22-F	0.42%	14.72%	1.95%	0.26%	120.13%	13.43%
23-F	0.41%	16.95%	4.89%	0.50%	90.96%	3.12%
Mean	0.38%	26.50%	2.60%	0.70%	71.20%	5.69%

Note: 1) The first column shows the participant identification number of the 23 participants. 2) Experimental result for each participant is the arithmetical mean of ten repeated movement.

On the basis of the results from 23 participants on measuring index finger, the average level of crosstalk in MGC3030 Signal1 (S_{1-ii}/ S_{1-i}) is 26.50%, which is reduced to 2.60% after applying to the prediction model (D_{p1-ii}/ D_{p1-i}). For the middle finger, a bigger crosstalk is expected and observed, considering the anatomical structure of the hand. In this case, the average impact of crosstalk in MGC3030 Signal2 (S_{2-i}/ S_{2-ii}) is 71.20%. It indicates that, the crosstalk (S_{2-i}) and the effective signal (S_{2-ii}) in MGC3030 Signal2 have similar magnitudes, as shown in Fig. 6-4 c). Therefore, simply relating the MGC3030 signal to the distance will bring in a great variation of distance. However, after using the prediction model, the level of

uncertainty is greatly reduced, from 71.20% to 5.69% on average. In brief, the experimental results supports those of the prediction model derived from simulation [32]. Therefore, for all the tested participants, the crosstalk can be effectively compensated by applying the prediction model to MGC3030 signals.

In addition to the level of uncertainty reported above, the resolution of absolute distance measurement is also important in real use. Therefore, the mean resolutions of combined finger motion detection were also obtained from the experiment. The mean value of the distance change due to crosstalk— D_{p1-ii} and D_{p2-i} as presented in Fig. 6-4—were calculated to represent the resolution of the index finger and the middle finger respectively. Table 6-2 details the uncertainty of measurement and the whole movement range of each participants.

Table 6-2 Experimental results of twenty-three participants: The uncertainty of measurement and the movement range (mm)

Participant Number	Index finger		Middle finger	
	Uncertainty	Movement range	Uncertainty	Movement range
1-F	0.76	20.89	0.26	22.35
2-M	0.63	42.42	0.89	35.08
3-M	0.56	28.53	0.04	28.37
4-F	0.37	15.18	0.02	17.62
5-M	0.57	34.49	2.09	33.12
6-M	0.18	23.20	0.15	27.81
7-M	0.57	22.51	0.58	23.29
8-M	0.38	32.93	0.37	35.88
9-M	0.76	38.30	0.44	42.77
10-M	0.70	42.99	0.69	43.81
11-M	1.22	39.97	0.27	33.30
12-M	0.70	29.40	0.50	20.15
13-F	0.51	45.15	1.01	44.61
14-M	1.85	39.06	1.11	35.86
15-F	0.10	20.57	0.14	22.41
16-F	0.29	33.67	0.22	32.52
17-F	0.31	33.80	0.26	36.57
18-M	0.39	23.02	0.39	29.45
19-F	1.05	46.97	1.50	44.52
20-M	0.54	22.66	0.44	24.40
21-F	1.49	33.36	7.65	32.68
22-F	0.49	33.29	1.43	34.68
23-F	0.45	13.42	0.23	12.94
Mean	0.65	31.12	0.90	31.05

Note: 1) Unit of uncertainties and movement ranges: mm. 2) Experimental result for each participant is the mean value of ten repeated movement.

The last row of Table 6-2 shows the mean uncertainty and movement range of both index and middle finger based on the results of 23 subjects. With interpersonal difference considered, the mean uncertainties of measurement using the prediction model are 0.65mm and 0.90mm, which are 2.08% and 2.89% of the mean movement range, for index finger and middle finger respectively.

It can be observed from the experimental results presented in Fig.6-2, Fig.6-3, Table 6-1 and Table 6-2 that, participant 21-F is always an outlier among the 23 participants, while participant 8-M has general performance except for R^2 value of the index finger. Therefore, it is worthwhile to further explore the experimental outputs and data characteristics of participant 21-F. Fig.6-5 compares the output of the MGC3030 measuring system for one sample movement from participant 21-F with the output from participant 13-F. During the experiment, the index finger of both participants shares a similar movement range, as shown in Fig.6-5 (a) and Fig.6-5 (c). However, the MGC signal in plot (b) ranges from 5300 to 6100, while in plot (d), the signal change is between 3000 and 6300. The output from participant 21-F tends to be more concentrated and has little change in accordance with finger motion.

The other 9 repeated movements of participant 21-F present similar behaviour as Fig.6-5. Moreover, since this extreme case was noticed during the experimental process, the participant 21-F was asked and agreed to repeat another 10 sample movements for both her right hand and left hand, where similar characteristics remain in the out from MGC3030 measuring system all the time. Details of the output from these repeated movements can be found in Appendix R: Experimental Results for Extreme Case 21-F. Therefore, this research records the experimental results for participants 21-F as an abnormal but typical case for the application of MGC 3030 measuring system. In the future, it will be worthwhile investigating the physical difference of this person compared to other subjects. Such experiment might involve the skin conductivity and could be performed with the hand covered with a thin layer of conductive gel.

Collectively, the prediction model greatly reduces the crosstalk on measuring the combined finger motion, and performs well with the MGC3030 measuring system. The mean resolutions suggest that the MGC3030 measuring system is capable of measuring the small movements of fingers.

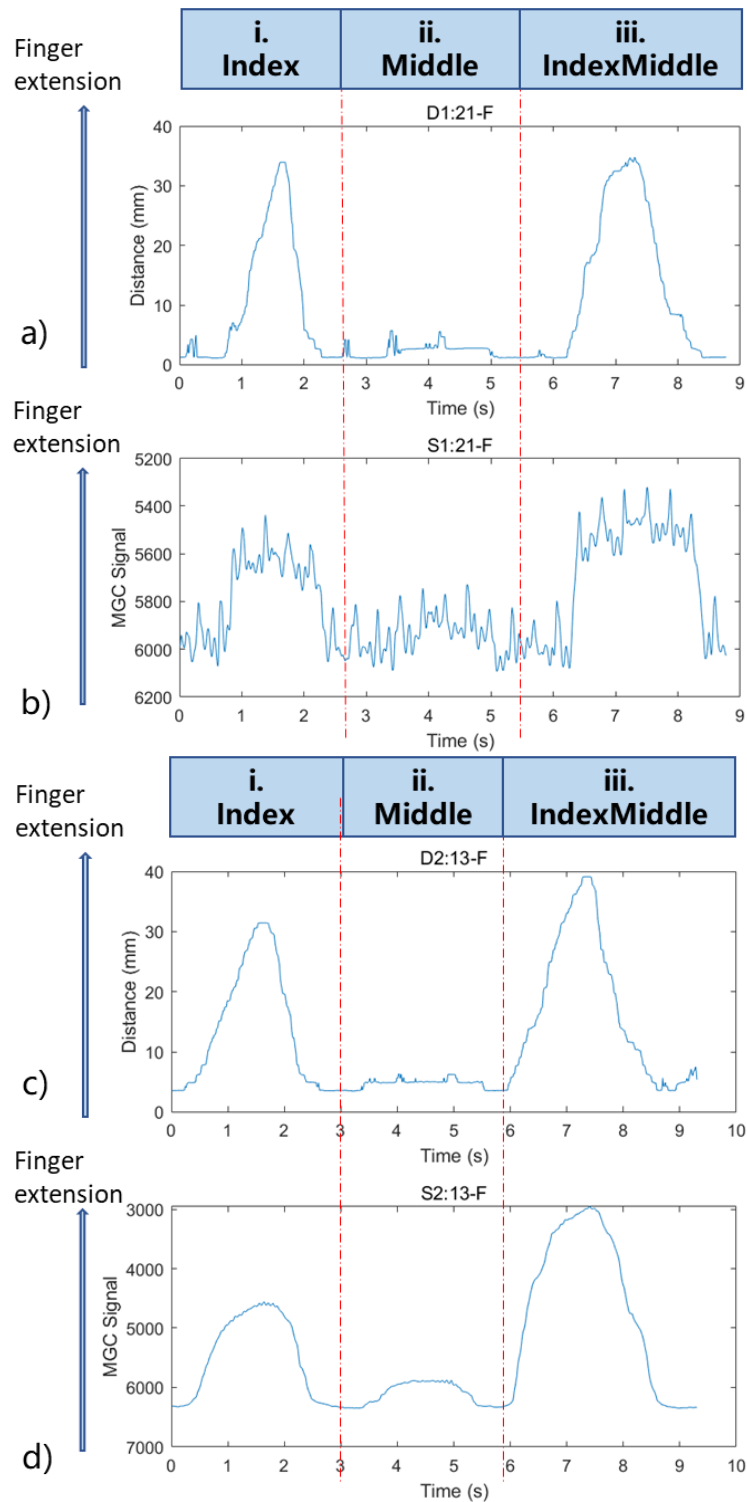


Fig. 6-5. Example outputs from experiment: a) D_1 : Output from optical sensor1 for 21-F, b) S_1 : Output from the MGC3030 measuring system for 21-F; c) D_2 : Output from optical sensor1 for 13-F, d) S_2 : Example of normal output: Output from the MGC3030 measuring system for 13-F

6.4 Discussion:

6.4.1 Evaluation of the validation results and the MGC3030 system

This study conducted initial physical trials with twenty-three healthy subjects to validate a noncontact easy-to-use approach for finger displacement measurement. With the experimental results, the vertical moving distance (D_1 , D_2) and the detected signals using the MGC3030 measuring system (S_1 , S_2) fit well with the prediction model in the nonlinear regression process in Matlab. From experimental results in Table 6-1 and Table 6-2, the prediction model can greatly reduce the resolution uncertainty, and therefore improve the performance of the MGC3030 measuring system on the contactless finger movement measurement in a multi-finger case. Using the prediction model, the mean uncertainty of index finger is 0.65mm for maximum movement range across the participants from 13.42mm to 46.97mm, while the uncertainty for middle finger is 0.90mm, with the movement range from 12.94mm to 44.61mm. This aligns with the resolution of the prediction model in FEM simulation, which is 0.94mm over a range of 30mm [32].

In rehabilitation training, patients have to work harder than normal to complete some simple functional exercises. Successful attempts of stroke therapy should provide quantifiable progress or functional benefits, to motivate the patients throughout repetitive training sessions [3]. Without visible progress or feedback, they might lose interest and give up easily. The validation results of preliminary study demonstrate the ability of the MGC3030 system on measuring tiny movements of the fingers with average resolution less 1mm. Therefore, the device allows the patient to track probably the unobvious progress easily, to motivate their rehabilitation exercises. It can be even more helpful if the records are accessible for the health experts as well.

In addition, the MGC3030 measuring system can work without a great overhead in signal processing. For each participant, once the personalized fitted parameters (b_1 , b_2 , b_3 , b_4) of the prediction model is obtained from calibration steps as reported in this thesis, this individualized model can be download to the MGC3030 measuring device for home-based rehabilitation usage. Unlike Electromyography (EMG) [56] or vision based systems [35], it can be realized with a low cost MCU, such as the microcontroller used in this research (NXP LPC1768). Together with the low-cost feature of the MGC3030 chip (4 GBP), the system provides the possibility to be realized in an inexpensive and portable equipment. In the future, the option of not having individual calibration, but to have a standard calibration that doesn't

require personalization, will also be investigated. Although this gives reduced absolute accuracy, it may be suitable for relative measurements for tracking improvements. Coupled with the contactless measurement function, the MGC3030 measuring system requires no additional effort such as set-up and wearing attachments, and is particularly user-friendly for patients for independent home-based use.

6.4.2 Discussion of the prediction models for three/four finger movement

Based on the distribution of the R^2 values reported in Fig. 6-2 and Fig. 6-3 as well as the experimental results given in Table 6-1 and 6-2, the prediction model has better performance for the index finger and has more individual difference the fitting of data to the middle finger. For middle finger, a more comprehensive nonlinear regression analysis is required, to compensate for the crosstalk due to both the movement of the index finger and the ring finger. In other words, the equation for the middle finger should consider the movement of the index finger, middle finger and ring finger simultaneously, which indicates a three-finger model $D_x=f(S_1, S_2, S_3)$.

i. The three-finger model $D_x=f(S_1, S_2, S_3)$

As stated in Section 6.1, there is an inverse proportional function between with the distances moved away from the receptacle (D_x) and the MGC3030 signal (S_x). Considering the structure of the prediction model (5-1), the three-finger model for the middle finger $D_2=f(S_1, S_2, S_3)$ should consider the movement of the index finger, middle finger and ring finger. Therefore, the optimised equation should include these components: $(1 - b_1 * S_1)^{-1}$, $(1 - b_2 * S_2)^{-1}$, $(1 - b_3 * S_3)^{-1}$. Therefore, hypothesis for the three-finger model for the middle finger $D_2=f(S_1, S_2, S_3)$ could be:

$$D_2 = a_1 * f(S_1, S_2) + a_2 * f(S_2, S_3)$$

$$= \frac{b_3}{[(1 - b_1 * S_1) * (1 - b_2 * S_2) + b_4]} + \frac{b_7}{[(1 - b_5 * S_2) * (1 - b_6 * S_3) + b_8]}$$

Or,

$$D_2 = \frac{b_3}{[(1 - b_1 * S_1) * (1 - b_2 * S_2) * (1 - b_5 * S_2) + b_4]}$$

Additionally, the machine learning approach is also potential way for investigating the three-finger model $D_x=f(S_1, S_2, S_3)$. For example, a neural network can be trained using the experimental data. Then, comparison could be made between the non-linear model $D_x=f(S_1,$

S2, S3) and the neural network using the same experimental data. Machine learning algorithms build a model based on training data to make predictions or decisions without being explicitly programmed to do so. However, when the prediction model is obtained mindlessly from the experimental data, it is easy to ignore the underlying mechanism between the input and output data. Therefore, in this research, the experimental data will be applied to a machine learning system as well, as a supplement to current regression models.

ii. The four-finger model $D_x=f(S_1, S_2, S_3, S_4)$

The formula in three-finger case can prompt the structure of the formula in four-finger case. In addition, it is observed from both the simulation as well as the experiment that, the movement of the non-adjacent finger has very little effect on the MGC signal of a moving finger. Therefore, the three-finger model $D_x=f(S_1, S_2, S_3)$ could be good enough for the measurement of the multi-finger measurement application, as a convenient option.

6.4.3 Potential- uses of electric field sensing in broader applications: Enslaving

Humans rarely move one finger alone when performing functional tasks in daily routine [38]. When a finger performs its intended movements, the unintended finger movement of other fingers is called “enslaving” [38, 94]. The study of “enslaving” could be helpful in clinical diagnosis and in supporting research into independent finger movement. Therefore, it is of interest to both clinicians and control engineers [38, 106].

Although the unintended finger movement of the human hand is avoided in this experiment, the MGC3030 measuring system also provides the possibility to detect and record these movements. The MGC3030 measuring system is capable of measuring real-time finger movements for all the four fingers simultaneously. Therefore, the movements of the other two fingers could also be calculated in a similar way as reported in this thesis, by applying signals detected from Rx electrodes (S_3, S_4) to the prediction model (5-1). Therefore, from the amplitude and the speed of signal changes, it has the potential to detect unwanted finger movements and hand position changes.

6.4.4 Potential- uses of electric field sensing in broader applications: Tremor

In order to assess and treat tremor-based diseases, precise frequency and amplitude measurement for tremors will be helpful for adjusting medication levels [24]. The experimental system can capture data at 106 samples per second. This dynamic response is high enough to allow for a contactless study of tremor in fingers, up to a frequency of about 20Hz. Fig. 6-6

presents an example output from the experiment where noticeable tremors were not only observed by the naked eye, but also recorded by the MGC3030 measuring system. Fig. 6-6 (a) and (b) are example output of one sample movement from the optical sensor1 and from the Rx electrodes under index finger respectively. Plot (c) and plot (d) intercept and detail the MGC3030 signal presented in plot (b). Plot (c) shows the tremors recorded when the index finger moved only, and highlights the 9 cycles which were recorded between 1.4s and 2.4s. Therefore, the frequency of the tremor detected here is approximately 9 Hz, which, as previously mentioned, may indicate a central neurogenic component of physiological tremor. Physiologic tremor is a tremor or trembling of a limb or other body part which occurs in normal individuals. Therefore, this is an expected result in consideration of the fact that all the 23 participants in this experiment are required to have normal hand and finger functions, without any movement disorders or decreased ADL capability. Tremors in plot (d) were recorded when the index finger and middle finger moved together. Similarly, between 7.6s and 8.6s, there are 11 cycles highlighted, which represents a frequency of approximately 11Hz and tends to reveal a physiological tremor as well.

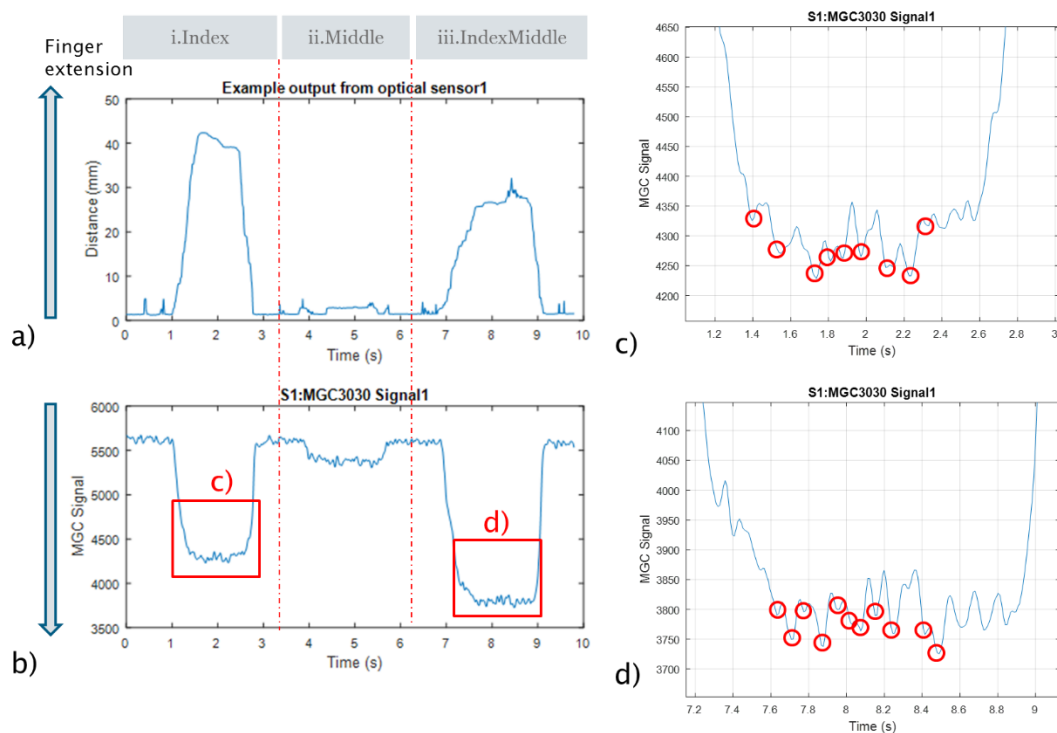


Fig.6-6. Example outputs from 14-M: a) D_1 : Output from optical sensor1, b) S_1 : Output from the MGC3030 measuring system; c) S_1 : Tremor recorded when index finger moves, d) Tremor recorded when both index and middle finger move

Collectively, Fig. 6-6 presents a simply application of the MGC3030 measuring system on tremor detection. The frequency of tremor was easily obtained from the MGC3030 signal. As a movement measuring system with resolution less than 1mm, the proposed system could also be used for precise amplitude measurement. It will be helpful for the tremor-based diseases treatment at home and worth further investigation in the future.

6.5 Summary

The validation results of preliminary study demonstrate the ability of the proposed system on measuring the movements of fingers. The prediction model greatly compensates the crosstalk, and therefore performs well on measuring the combined fingers' motion. The mean resolution of the targeted system are 0.65mm and 0.90mm, which are 2.08% and 2.89% of the full-scale range, for the index finger and the middle finger respectively.

The MGC3030 measuring system can be realized in an inexpensive and portable device. The combination of the noncontact measuring feature and the lack of complicated set-up (no physical connection of electronics to the person), makes it particularly attractive as the basis of an easy-to-use home-based independent rehabilitation system. Moreover, it provides the potential for broader applications of finger movement measurement, concerning the record and assessment of the enslaving and tremor.

Chapter 7 Conclusion and Future Work

7.1 Conclusion

This research targets the technology for the home-based hand rehabilitation, addressing the ease of use to promote motivation of practice. To guide this research forward, research questions were proposed at the beginning of the thesis. The main body of the thesis investigates the contactless measurement technique of the MGC3030 measuring system by answering these questions:

- What are the key requirements for an easy-to-use finger displacement sensor for the home-based hand rehabilitation, and what is the current state of the art?

The literature review for the home-based medical equipment in both the market and academic application indicates that, a good home-based rehabilitation device is closely related to the ease of setting and use. Towards this target, the contactless form of finger movement measurement is preferred, and realized using the MGC3030 motion sensor. Based on the quasi-static electrical near field sensing, the targeted system can be used without any sensing elements attached. Together with the low-cost feature of the MGC3030 chip (4 GBP), the system provides the possibility to be realized in an inexpensive and portable equipment.

- What techniques offer the best performance and what level of solution can it give?

A FEM simulation for the MGC3030 electrodes in Comsol Multiphysics was conducted, where the electrical field variation due to a moving finger can be produced and analysed, to measure the extension and flexion of fingers in a contactless form. In this simulation model, a ‘crosstalk’ is observed due to an electrical field leakage from a neighbouring moving finger.

To optimize the performance of the targeted system by reducing this crosstalk, the electrode designs with and without ‘gnd’ electrodes placed in between the Rx electrodes, were compared. In general, added ‘gnd’ electrodes can reduce the ‘crosstalk’, but at the cost of reducing the sensitivity. Therefore, approaches for further exploring the ‘crosstalk’ issue is required.

Based on a nonlinear regression in Matlab for the original simulation model without added ‘gnd’ electrodes, four nonlinear equations were introduced, to describe the mathematic relationships between the fingers’ motion (D_1 , D_2) and the voltage signals (V_1 , V_2) of the Rx

electrodes. These equations agree with the quasi-static electrical near field sensing theory, and fit well with the simulated data. The prediction model ' $D_x=f(V_1, V_2)$ ' shows an excellent fit with uncertainty of 0.94mm over a range of 30mm. Collectively, the nonlinear regression results suggest further development of the system in an experimental test.

- How well does the developed technique perform on human subjects?

The experimental verification was designed to extend the practical understanding of the prediction model and the MGC3030 measuring system on human subjects. An optical system was applied in this study as a comparing technique for real-time contactless measurement of fingers. Twenty-three healthy subjects (13 males and 10 females) with normal hand and finger function participated in the experiment.

During the experiment, the prediction model works well with the MGC3030 measuring system in most of the participants, while the optical sensors and its measuring technique have limitations when dealing with horizontal offsets and increasing angles. However, reliable data was obtained and used in the comparisons with the MGC3030.

The output of the MGC3030 measuring system (S_1, S_2) together with the simultaneous output of the optical sensors (D_1, D_2) was fitted to the prediction model ' $D_x=f(S_1, S_2)$ '. The validation results demonstrate the performance of the proposed system on human subjects, and supports the ability of the prediction model on dealing with the crosstalk when measuring the combined fingers' motion. The mean resolution of the targeted system are 0.65mm and 0.90mm, which account for 2.08% and 2.89% of the full-scale range, for the index finger and the middle finger respectively. Moreover, the experimental system can capture data at 106 samples per second. This dynamic response provides the potential for a contactless study of enslaving and tremor (up to a frequency of about 20Hz) in fingers.

To conclude, the results reported in this thesis show that, the contactless measurement technique of the MGC3030 measuring system is capable of measuring the small movements of fingers, with excellent technical parameters. With the combination of the noncontact measuring feature, the lack of complicated set-up, and the low-cost feature, this system is user friendly as the basis of a home-based independent rehabilitation system.

7.2 Suggestions for future work

The designed system provides a basic framework for conveniently tracking the extension and flexion movements of fingers using MGC3030 motion sensor. Targeting a rehabilitation device for post-stroke patients, the feature ease of use has been demonstrated as once calibrated to the user, the user merely has to place their hand upon the device to use it, without extra donning or setting efforts. The proposed system could be improved in future as follows.

- Future work can further improve the ease of use by providing necessary guidance and feedback to the user [1]. For example, a LED can be used to allowing intuitive visual feedback of progress, as the light changed relative to finger distance moved. An LCD can be included to provide guidance information for use and present the results of multi-finger distance measurement. The device could also provide the option to communicate via USB to a host PC, allowing more comprehensive analysis and visualization of performance.
- This thesis reports the performance of the designed system with the prediction model for movements of two fingers. In the future, an investigation can be conducted for all the fingers, based on the two neighbouring fingers' problem as addressed in this thesis. A discussion about the prediction models for three/four finger movement can be found in Section 6.4.2.
- A personalized receptacle design is proposed in section 7.3 for future research, to improve the ease of use and increase the accuracy of the motion tracking function. The receptacle could be customized for each user at different recovery stages, to follow the shape of patient's hand and make it easier for them to use the device. Additionally, the palm and the fingers could be placed snugly on the three-dimensional model of a hand, to avoid the horizontal offset.
- The potential interpersonal influencing factors, such as gender, handedness as well as finger dimensions have also been collected during the experiment. In the future, a detailed study of the effect of these interpersonal differences on the parameters of the prediction model can be investigated. It will be helpful for obtaining a standard prediction model, which can be applied to a group of participants with the same fitted

parameters (b_1 , b_2 , b_3 , and b_4), and therefore, can work without the requirement of an individual calibration.

- From the results presented in Section 5.5, the MGC3030 measuring system has tolerance for the small horizontal (abduction and adduction) errors. Future experiments with measurements in the horizontal direction can be carried out to further investigate and quantitatively evaluate the tolerance of MGC3030 measuring system for the horizontal offset.

7.3 A personalized receptacle design

The rehabilitation progresses can effectively exercise and strengthen the reduced muscle tone of the impaired hand. As the finger extension-flexion rehabilitation progresses, the closed hand of patient after a stroke may gradually open, which may lead to a change in the shape of the hand. A personalized receptacle design, which matches the shape of the impaired hand, is proposed for future research. It fits the specific patient's hand at certain recovery level, and thereby improves the recovery outcome of hand rehabilitation. In addition, the horizontal offset could be avoided with the palm and the fingers placed snugly on the receptacle. This receptacle design consists of three parts:

- Hand modelling to match the outer shape with patient's hand without hindering the movement of fingers;
- Electrodes layer stack-up design to cut the receptacle into layers with inner grooves and holes to meet the requirements of MGC3030;
- Design for assembly to fit the layers together and reserve space for periphery circuits.

7.3.1 Hand modelling

A scanned hand model was download from the internet, as an example for hand modelling, as show in Fig. 7-1(b). This is a 3D object type of file and can be edit in Solidworks. Starting with a solid cuboid and a scanned hand model represented in Fig. 7-1(a) and (b) respectively, a subtraction of the hand model was created using the indent feature of Solidworks, as shown in Fig. 7-1(c). Then, this subtracted part was carefully modified, as is shown in Fig. 7-1(d), to make sure that all the four fingers and the thumb could move freely in an extension and flexion motion.

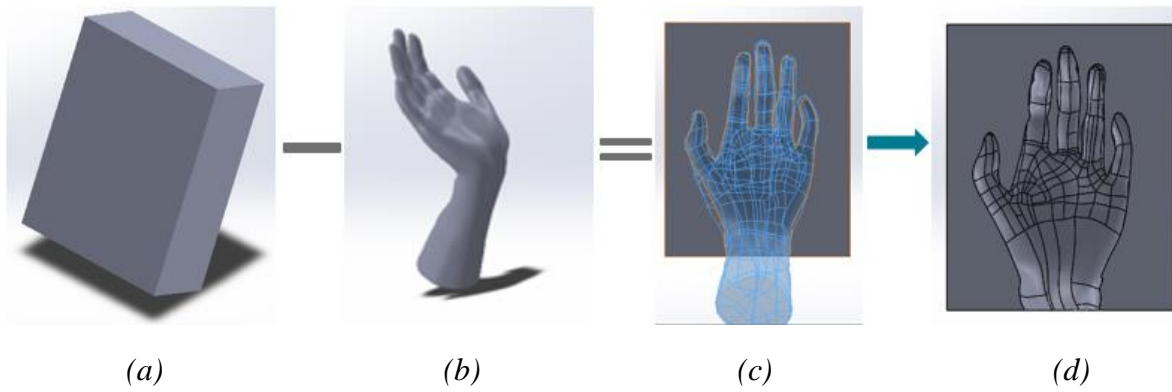


Fig. 7-1 Hand Modelling in Solidworks

7.3.2 Electrodes layer stack-up design

The subtracted part was cut into curved layers with the features of the hand reflected in the profile of the original receptacle for better detecting accuracy. Here, the profile of four fingers and a thumb was simulated by curvilinear lines offsetting from the outline of the receptacle, as shown in Fig. 7-2 (a). After adding guidelines to cover the whole region and connect the curved lines together, a closed loop was produced. Based on this loop, a surface that contains the information of each finger could then be created, shown as plot (b). By copying and moving the surface to certain places, the original receptacle could be divided into separated parts, each with accurate height and the same features of hand, shown in Fig. 7-2 (c).

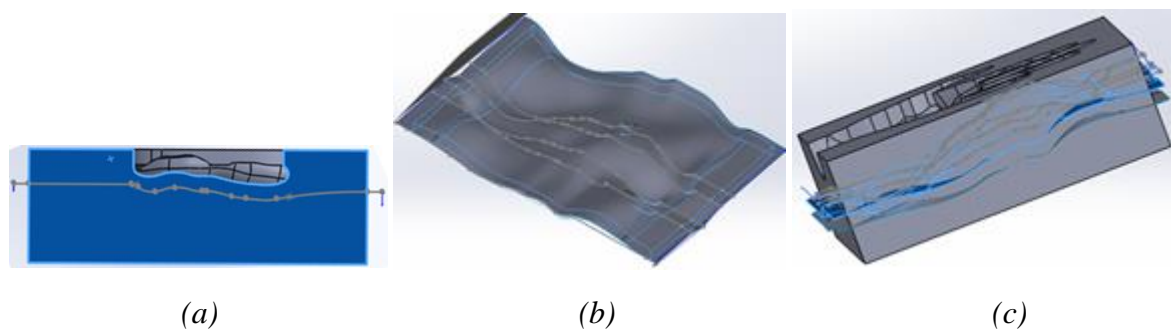


Fig. 7-2 Stack-up design

The receptacle was finally cut into four parts considering the structure of the electrode stack mentioned in Fig. 7-3. The idea is that the person under using the system can place their impaired hand on the top layer comfortably and extend and flex their fingers freely. Between the top layer and isolation layer1, five Rx electrodes are placed underneath four fingers and a thumb, to track their motion. The Tx electrode and the GND electrode are placed between isolation layer1 and isolation layer2, isolation layer2 and bottom layer respectively.

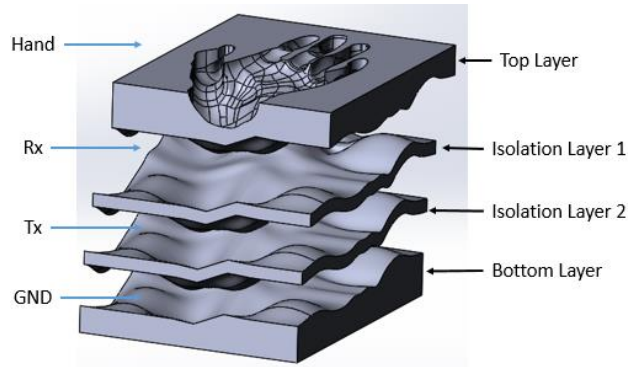
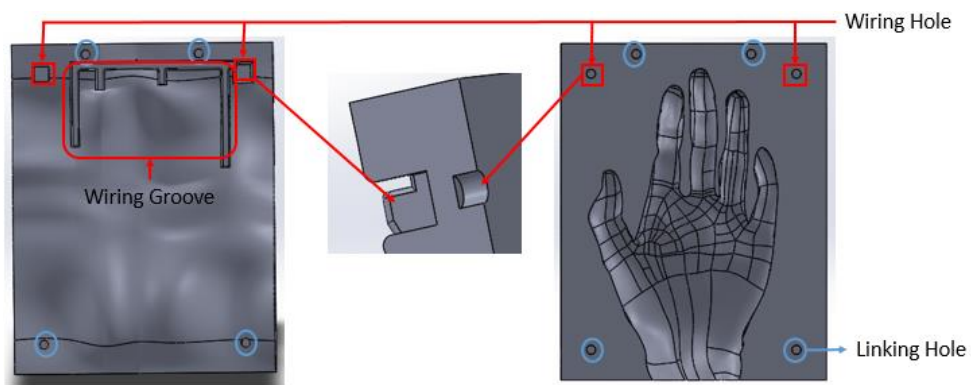


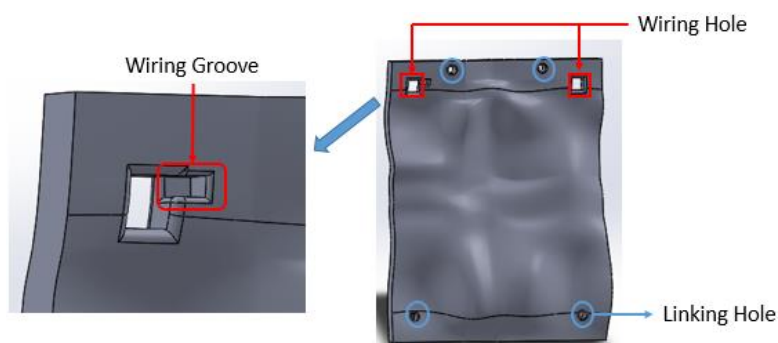
Fig. 7-3 Stack-up design in Solidworks

7.3.3 The design for assembly

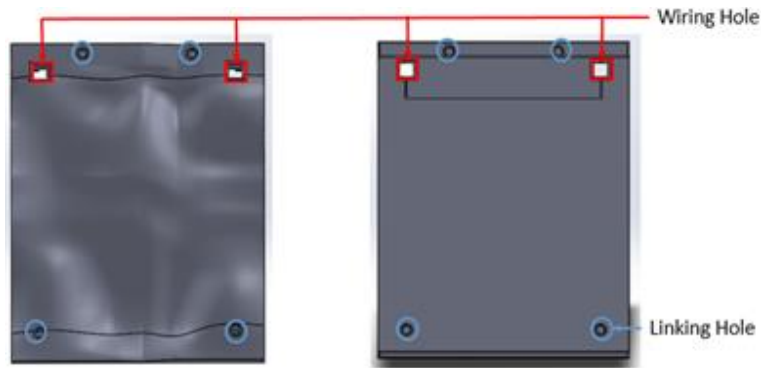
The design for the assembly was added for manufacture and integration. As highlighted in Fig. 7-4, linking columns and holes together with thread structure would be utilized to connect the four layers together and to avoid the offset between layers. Wiring grooves and holes would then be added as the reserved space for the electrical connection.



(a)



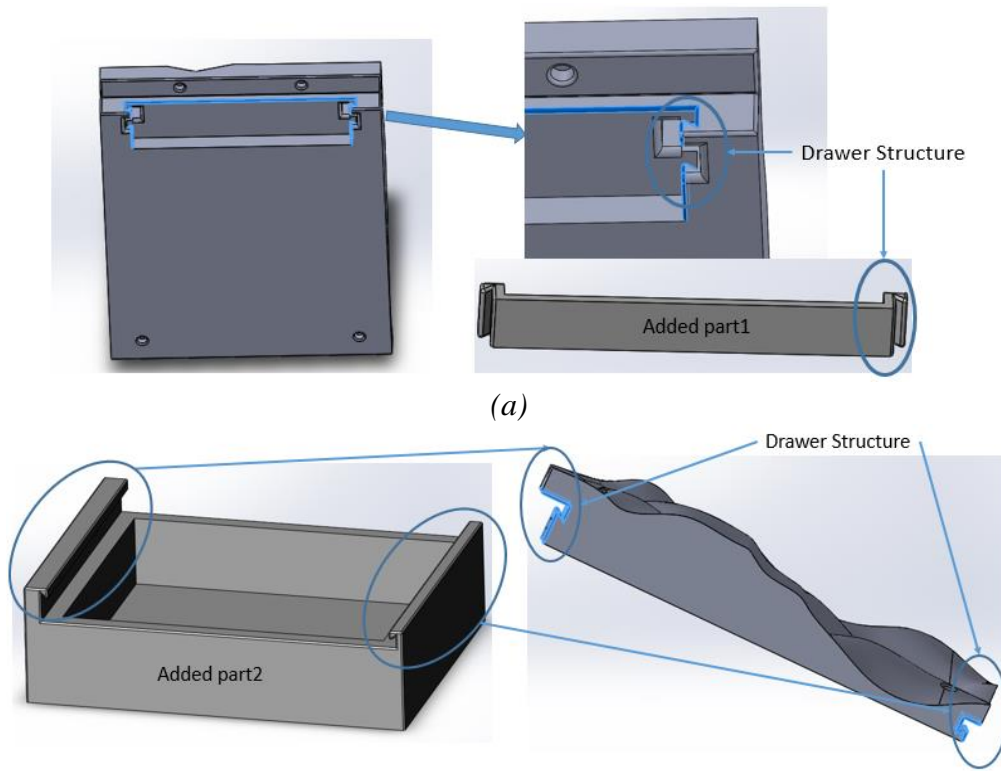
(b)



(c)

Fig. 7-4 Design for assembly: (a) Top layer, (b) Isolation layer1&2, (c) Bottom layer

Apart from the main parts, there are other auxiliary parts. Fig. 7-5 shows two drawer panels (Added part 1& Added part 2) that can be inserted to the bottom part of the receptacle. A drawer structure was used to fit the receptacle with added parts for hardware integration. The added part1 in Fig. 7-5(a) is intended to place the MGC3030 Microchip within the receptacle, so the electrodes feeding lines can be short for less noise/interference, and be hidden in the receptacle for better stability. Also, it helps to keep the area underneath the Rx electrodes clear of feeding line traces to avoid crosstalk [89]. Another added part is presented in Fig. 7-5(b), which is adjustable and flexible for periphery circuit design later on. It can also keep the electrodes and feeding lines away from ground, analogue or digital sources of the system.



(a)

(b)

Fig. 7-5 Added parts: (a) Drawer panel, (b) Bottom added for periphery circuits

7.3.4 3D printing

Prior to manufacture, the four main parts were cut into quarters for better 3D printing quality. The design of assembling uses a boss and concave pit structure, which is marked with red squares in Fig. 7-6. Here only the upper left quarter of each layer was printed as an example. The assembling quartered model of the receptacle is shown in Fig. 7-7.

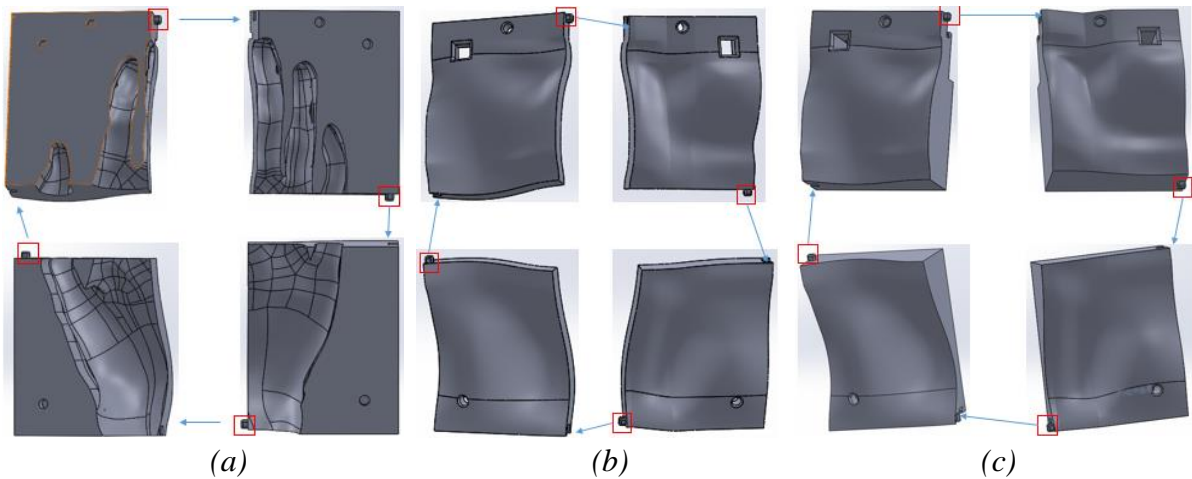


Fig. 7-6 3D printing design: (a) Receptacle-Top, (b) Receptacle-Isolation layer1&2, (c) Receptacle-Bottom

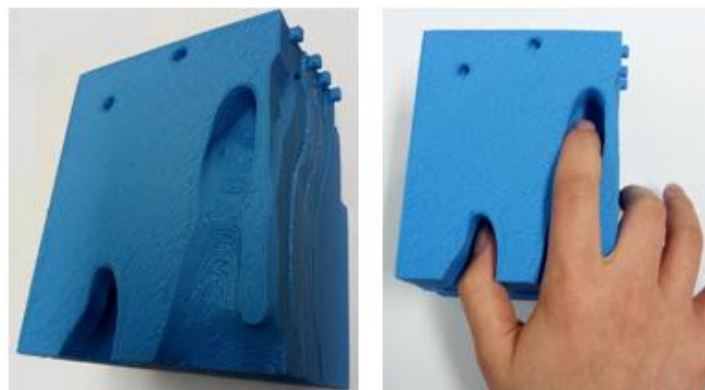


Fig. 7-7 3D printing model: Quartered receptacle

Appendix A: Detailed Settings of Comsol Simulation Model

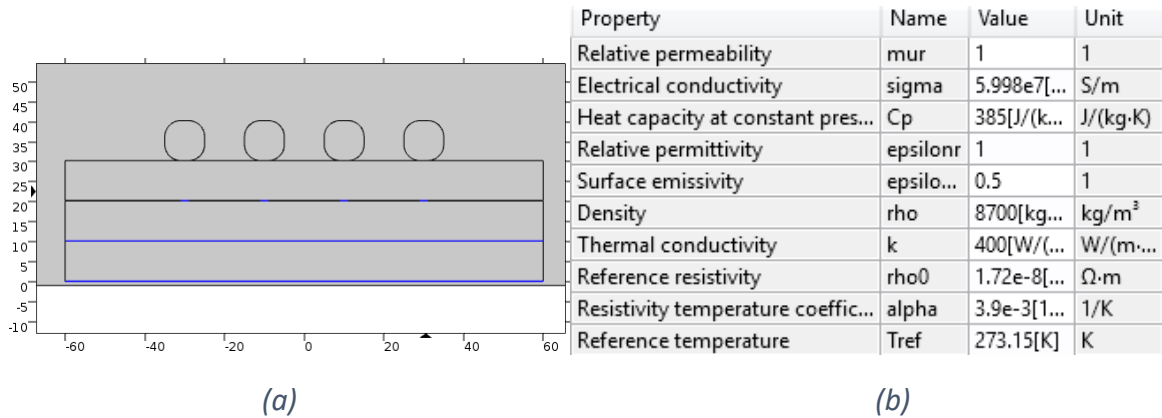


Fig. A-1 Basic settings of Copper in simulation model: (a) Geometry, (b) Detailed material setting

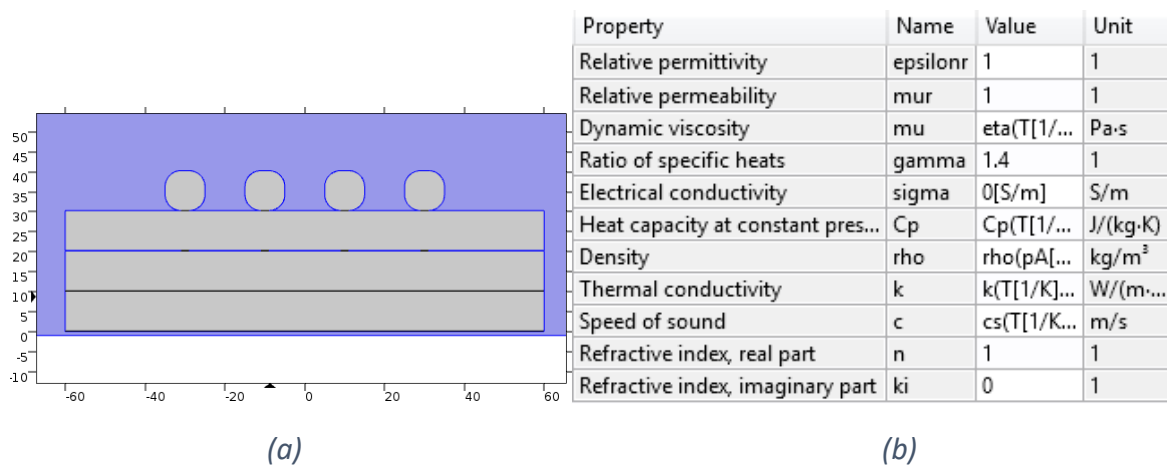


Fig. A-2 Basic settings of Air in simulation model:(a) Geometry, (b) Detailed material settings

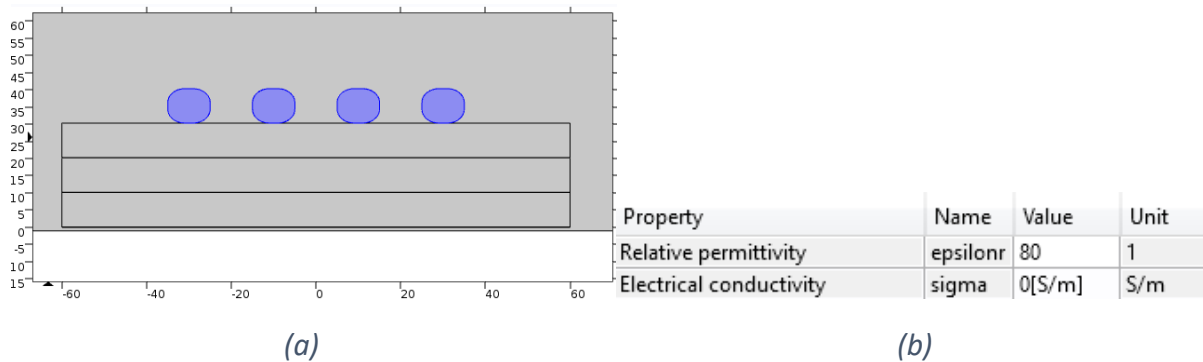


Fig. A-3 Basic settings of Water in simulation model: (a) Geometry, (b) Detailed material settings

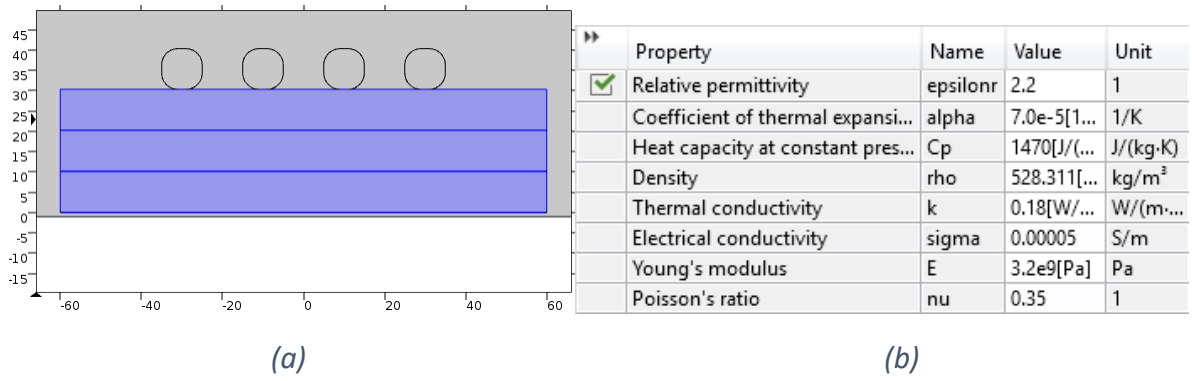


Fig. A-4 Basic settings of Acrylic in simulation model: (a) Geometry, (b) Detailed material settings

Appendix B: Finger Movements Discussion

To explore different combinations of index finger (I), middle finger (M), ring finger (R) and little finger (L), possible cases are discussed as follows:

A. One finger moves:

Cases when pick one finger from four include:

$$C_4^1 = 4$$

$$\{X|I, M, R, L\}$$

B. Two fingers move:

Cases when pick two fingers from four include:

$$C_4^2 = 6$$

Table B-1 Finger combinations when two finger moves

	I	M	R	L
I		IM	IR	IL
M	ML		MR	ML
R	RI	RM		RL
L	LI	LM	LR	

$$\{X|IM,IR,IL,MR,ML,RL\}$$

C. Three fingers move:

Cases when pick three fingers from four:

$$C_4^3 = 4$$

$$\{X|IMR, IML, IRL, MRL\}$$

D. Four fingers move:

Cases when pick four fingers from four:

$$C_4^4 = 1$$

$$\{X|IMRL\}$$

Therefore, there is one case only (Case 9: IMRL) if all four fingers move together.

Appendix C: Distance and Corresponding Voltage Values for Original Electrodes Design

Table C-1 Case 1: Index(I) finger moves

Distance (mm)	V ₁ (V)	Sensitivity-V ₁ (V/mm)	V ₂ (V)	V ₃ (V)	V ₄ (V)
0	1.92663		1.83788	1.83788	1.92663
2	2.13640	0.10489	1.87362	1.84017	1.92677
4	2.24931	0.05645	1.89447	1.84151	1.92684
6	2.32195	0.03632	1.90848	1.84241	1.92688
8	2.37217	0.02511	1.91840	1.84305	1.92691
10	2.40833	0.01808	1.92565	1.84352	1.92693
15	2.46376	0.01109	1.93682	1.84425	1.92697
20	2.49327	0.00590	1.94273	1.84464	1.92698
25	2.51061	0.00347	1.94616	1.84488	1.92699
30	2.52163	0.00220	1.94830	1.84504	1.92701
average		0.02928			

Table C-2 Case 1-2: Little(L) finger moves

Distance (mm)	V ₁ (V)	V ₂ (V)	V ₃ (V)	V ₄ (V)	Sensitivity- V ₄ (V/mm)
0	1.92663	1.83788	1.83788	1.92663	
2	1.92677	1.84017	1.87362	2.13640	0.10489
4	1.92685	1.84152	1.89447	2.24932	0.05646
6	1.92689	1.84242	1.90848	2.32196	0.03632
8	1.92692	1.84306	1.91841	2.37217	0.02511
10	1.92694	1.84352	1.92565	2.40833	0.01808
15	1.92696	1.84425	1.93682	2.46376	0.01108
20	1.92698	1.84465	1.94273	2.49327	0.00590
25	1.92699	1.84488	1.94615	2.51061	0.00347
30	1.92702	1.84504	1.94831	2.52163	0.00220
average					0.02928

Table C-3 Case 2: Middle(M) finger moves

Distance (mm)	V ₁ (V)	V ₂ (V)	Sensitivity-V ₂ (V/mm)	V ₃ (V)	V ₄ (V)
0	1.92663	1.83788		1.83788	1.92663
2	1.95838	2.01354	0.08783	1.86931	1.92865
4	1.97601	2.10229	0.04438	1.88677	1.92978
6	1.98718	2.15526	0.02649	1.89784	1.93050
8	1.99455	2.18877	0.01675	1.90515	1.93097
10	1.99949	2.21058	0.01091	1.91005	1.93128

15	2.00602	2.23859	0.00560	1.91653	1.93169
20	2.00875	2.24994	0.00227	1.91923	1.93185
25	2.01009	2.25528	0.00107	1.92051	1.93194
30	2.01086	2.25820	0.00058	1.92122	1.93199
Average			0.02176		

Table C-4 Case 2-2: Ring(R) finger moves

Distance (mm)	V ₁ (V)	V ₂ (V)	V ₃ (V)	Sensitivity- V ₃ (V/mm)	V ₄ (V)
0	1.92663	1.83788	1.83788		1.92663
2	1.92866	1.86931	2.01354	0.08783	1.95838
4	1.92978	1.88677	2.10229	0.04438	1.97601
6	1.93050	1.89784	2.15526	0.02649	1.98718
8	1.93097	1.90515	2.18877	0.01675	1.99455
10	1.93128	1.91005	2.21058	0.01091	1.99949
15	1.93169	1.91653	2.23859	0.00560	2.00602
20	1.93186	1.91923	2.24994	0.00227	2.00875
25	1.93194	1.92052	2.25528	0.00107	2.01008
30	1.93199	1.92122	2.25820	0.00058	2.01085
Average				0.02176	

Table C-5 Case 3: Index & Middle(IM) fingers move

Distance (mm)	V ₁ (V)	Sensitivity- V ₁ (V/mm)	V ₂ (V)	Sensitivity- V ₂ (V/mm)	V ₃ (V)	V ₄ (V)
0	1.92663		1.83788		1.83788	1.92663
2	2.17922	0.12630	2.06070	0.11141	1.87305	1.92888
4	2.32854	0.07466	2.18956	0.06443	1.89456	1.93026
6	2.43225	0.05185	2.27682	0.04363	1.90951	1.93122
8	2.50909	0.03842	2.33975	0.03146	1.92041	1.93192
10	2.56814	0.02953	2.38685	0.02355	1.92860	1.93244
15	2.66794	0.01996	2.46351	0.01533	1.94188	1.93330
20	2.72834	0.01208	2.50804	0.00891	1.94954	1.93381
25	2.76744	0.00782	2.53620	0.00563	1.95439	1.93417
30	2.79404	0.00532	2.55510	0.00378	1.95767	1.93445
average		0.04066		0.03424		

Table C-6 Case 3-2: Ring & Little(RL) finger moves

Distance (mm)	V ₁ (V)	V ₂ (V)	V ₃ (V)	Sensitivity- V ₃ (V/mm)	V ₄ (V)	Sensitivity- V ₄ (V/mm)
0	1.92663	1.83788	1.83788		1.92663	
2	1.92890	1.87320	2.06073	0.11143	2.17923	0.12630
4	1.93029	1.89472	2.18961	0.06444	2.32855	0.07466

6	1.93124	1.90967	2.27687	0.04363	2.43226	0.05185
8	1.93194	1.92058	2.33980	0.03147	2.50910	0.03842
10	1.93246	1.92877	2.38690	0.02355	2.56815	0.02953
15	1.93332	1.94205	2.46357	0.01533	2.66796	0.01996
20	1.93384	1.94972	2.50810	0.00891	2.72836	0.01208
25	1.93419	1.95457	2.53626	0.00563	2.76745	0.00782
30	1.93447	1.95785	2.55516	0.00378	2.79405	0.00532
average				0.03424		0.04066

Table C-7 Case 4: Index & Ring(IR) fingers move

Distance (mm)	V ₁ (V)	Sensitivity-V ₁ (V/mm)	V ₂ (V)	V ₃ (V)	Sensitivity-V ₃ (V/mm)	V ₄ (V)
0	1.92663		1.83788	1.83788		1.92663
2	2.13884	0.10610	1.90523	2.01627	0.08920	1.95859
4	2.25347	0.05731	1.94380	2.10701	0.04537	1.97640
6	2.32733	0.03693	1.96912	2.16144	0.02722	1.98771
8	2.37843	0.02555	1.98655	2.19604	0.01730	1.99520
10	2.41521	0.01839	1.99884	2.21866	0.01131	2.00022
15	2.47154	0.01126	2.01672	2.24794	0.00586	2.00690
20	2.50153	0.00600	2.02547	2.26005	0.00242	2.00973
25	2.51923	0.00354	2.03033	2.26598	0.00119	2.01116
30	2.53059	0.00227	2.03335	2.26947	0.00070	2.01203
average		0.02971			0.02228	

Table C-8 Case 4-2: Middle & Little(ML) finger moves

Distance (mm)	V ₁ (V)	V ₂ (V)	Sensitivity-V ₂ (V/mm)	V ₃ (V)	V ₄ (V)	Sensitivity-V ₄ (V/mm)
0	1.92663	1.83788		1.83788	1.92663	
2	1.95860	2.01628	0.08920	1.90523	2.13885	0.10611
4	1.97641	2.10701	0.04536	1.94380	2.25347	0.05731
6	1.98772	2.16144	0.02722	1.96912	2.32733	0.03693
8	1.99520	2.19604	0.01730	1.98655	2.37843	0.02555
10	2.00023	2.21867	0.01131	1.99884	2.41522	0.01839
15	2.00690	2.24794	0.00586	2.01672	2.47154	0.01126
20	2.00973	2.26005	0.00242	2.02547	2.50153	0.00600
25	2.01116	2.26599	0.00119	2.03033	2.51923	0.00354
30	2.01203	2.26947	0.00070	2.03335	2.53059	0.00227
average			0.02228			0.02971

Table C-9 Case 5: Index & Little(IL) fingers move

Distance (mm)	V ₁ (V)	Sensitivity-V ₁ (V/mm)	V ₂ (V)	V ₃ (V)	V ₄ (V)	Sensitivity-V ₄ (V/mm)
0	1.92663		1.83788	1.83788	1.92663	
2	2.13656	0.10497	1.87591	1.87591	2.13656	0.10497
4	2.24959	0.05651	1.89811	1.89811	2.24959	0.05651
6	2.32232	0.03636	1.91304	1.91304	2.32232	0.03636
8	2.37258	0.02513	1.92361	1.92361	2.37258	0.02513
10	2.40879	0.01810	1.93133	1.93133	2.40879	0.01810
15	2.46427	0.01110	1.94322	1.94322	2.46427	0.01110
20	2.49381	0.00591	1.94953	1.94953	2.49381	0.00591
25	2.51119	0.00348	1.95320	1.95320	2.51119	0.00348
30	2.52228	0.00222	1.95552	1.95552	2.52228	0.00222
average		0.02931				0.02931

Table C-10 Case 6: Middle & Ring(MR) fingers move

Distance (mm)	V ₁ (V)	V ₂ (V)	Sensitivity-V ₂ (V/mm)	V ₃ (V)	Sensitivity-V ₃ (V/mm)	V ₄ (V)
0	1.92663	1.83788		1.83788		1.92663
2	1.96179	2.05534	0.10873	2.05534	0.10873	1.96179
4	1.98296	2.17872	0.06169	2.17872	0.06169	1.98296
6	1.99745	2.26048	0.04088	2.26048	0.04088	1.99744
8	2.00781	2.31790	0.02871	2.31790	0.02871	2.00781
10	2.01541	2.35956	0.02083	2.35956	0.02083	2.01541
15	2.02717	2.42337	0.01276	2.42336	0.01276	2.02716
20	2.03343	2.45681	0.00669	2.45681	0.00669	2.03342
25	2.03711	2.47598	0.00383	2.47598	0.00383	2.03711
30	2.03949	2.48787	0.00238	2.48787	0.00238	2.03948
average			0.03183		0.03183	

Table C-11 Case 7: Index & Middle & Ring(IMR) fingers move

Distance (mm)	V ₁ (V)	Sensitivity - V ₁ (V/mm)	V ₂ (V)	Sensitivity - V ₂ (V/mm)	V ₃ (V)	Sensitivity - V ₃ (V/mm)	V ₄ (V)
0	1.92663		1.83788		1.83788		1.92663
2	2.18339	0.12838	2.10292	0.13252	2.05995	0.11104	1.96213
4	2.33814	0.07737	2.26768	0.08238	2.18941	0.06473	1.98386
6	2.44773	0.05480	2.38566	0.05899	2.27779	0.04419	1.99902
8	2.53058	0.04142	2.47499	0.04467	2.34202	0.03212	2.01014
10	2.59558	0.03250	2.54485	0.03493	2.39048	0.02423	2.01852

15	2.70944	0.02277	2.66583	0.02420	2.47048	0.01600	2.03229
20	2.78218	0.01455	2.74153	0.01514	2.51823	0.00955	2.04047
25	2.83170	0.00990	2.79206	0.01011	2.54946	0.00625	2.04588
30	2.86692	0.00704	2.82744	0.00708	2.57124	0.00436	2.04977
average		0.04319		0.04556		0.03472	

Table C-12 Case 7-2: Middle & Ring & Little(MRL) finger moves

Distance (mm)	V ₁ (V)	V ₂ (V)	Sensitivity - V ₂ (V/mm)	V ₃ (V)	Sensitivity - V ₃ (V/mm)	V ₄ (V)	Sensitivity - V ₄ (V/mm)
0	1.92663	1.83788		1.83788		1.92663	
2	1.96213	2.05995	0.11104	2.10293	0.13252	2.18339	0.12838
4	1.98386	2.18941	0.06473	2.26768	0.08238	2.33814	0.07737
6	1.99902	2.27779	0.04419	2.38566	0.05899	2.44773	0.05480
8	2.01014	2.34202	0.03212	2.47499	0.04467	2.53058	0.04142
10	2.01853	2.39048	0.02423	2.54485	0.03493	2.59558	0.03250
15	2.03229	2.47048	0.01600	2.66583	0.02420	2.70944	0.02277
20	2.04047	2.51823	0.00955	2.74153	0.01514	2.78218	0.01455
25	2.04589	2.54946	0.00625	2.79206	0.01011	2.83170	0.00990
30	2.04977	2.57124	0.00436	2.82744	0.00708	2.86692	0.00704
average			0.03472		0.04556		0.04319

Table C-13 Case 8: Index & Middle & Little(IML)/Index & Ring & Little(IRL) fingers move

Distance (mm)	V ₁ (V)	Sensitivity - V ₁ (V/mm)	V ₂ (V)	Sensitivity - V ₂ (V/mm)	V ₃ (V)	V ₄ (V)	Sensitivity - V ₄ (V/mm)
0	1.92663		1.83788		1.83788	1.92663	
2	2.17947	0.12642	2.06344	0.11278	1.90898	2.13912	0.10624
4	2.32907	0.07480	2.19432	0.06544	1.95162	2.25410	0.05749
6	2.43304	0.05198	2.28309	0.04439	1.98085	2.32834	0.03712
8	2.51012	0.03854	2.34717	0.03204	2.00191	2.37980	0.02573
10	2.56936	0.02962	2.39512	0.02398	2.01752	2.41692	0.01856
15	2.66955	0.02004	2.47319	0.01561	2.04228	2.47399	0.01141
20	2.73023	0.01214	2.51858	0.00908	2.05607	2.50461	0.00612
25	2.76962	0.00788	2.54743	0.00577	2.06458	2.52291	0.00366
30	2.79660	0.00540	2.56704	0.00392	2.07029	2.53491	0.00240
average		0.04076		0.03478			0.02986

Table C-14 Case 8-2: Index & Ring & Little(IRL) finger moves

Distance (mm)	V ₁ (V)	Sensitivity - V ₁ (V/mm)	V ₂ (V)	V ₃ (V)	Sensitivity - V ₃ (V/mm)	V ₄ (V)	Sensitivity - V ₄ (V/mm)
---------------	--------------------	-------------------------------------	--------------------	--------------------	-------------------------------------	--------------------	-------------------------------------

0	1.92663		1.83788	1.83788		1.92663	
2	2.13913	0.10625	1.90913	2.06348	0.11280	2.17948	0.12643
4	2.25412	0.05749	1.95178	2.19437	0.06544	2.32908	0.07480
6	2.32836	0.03712	1.98102	2.28314	0.04439	2.43305	0.05198
8	2.37982	0.02573	2.00209	2.34722	0.03204	2.51012	0.03854
10	2.41695	0.01857	2.01771	2.39519	0.02398	2.56938	0.02963
15	2.47402	0.01141	2.04246	2.47325	0.01561	2.66956	0.02004
20	2.50464	0.00612	2.05626	2.51864	0.00908	2.73024	0.01214
25	2.52295	0.00366	2.06478	2.54750	0.00577	2.76964	0.00788
30	2.53494	0.00240	2.07048	2.56711	0.00392	2.79661	0.00540
average		0.02986			0.03478		0.04076

Table C-15 Case 9: Index & Middle & Ring & Little(IMRL) fingers move

Distance (mm)	V ₁ (V)	Sensitivity-V ₁ (V/mm)	V ₂ (V)	Sensitivity-V ₂ (V/mm)	V ₃ (V)	Sensitivity-V ₃ (V/mm)	V ₄ (V)	Sensitivity-V ₄ (V/mm)
0	1.92663		1.83788		1.83788		1.92663	
2	2.18383	0.12860	2.10757	0.13484	2.10757	0.13484	2.18382	0.12860
4	2.33940	0.07779	2.27849	0.08546	2.27849	0.08546	2.33940	0.07779
6	2.45012	0.05536	2.40329	0.06240	2.40329	0.06240	2.45012	0.05536
8	2.53431	0.04209	2.49972	0.04821	2.49972	0.04821	2.53431	0.04209
10	2.60083	0.03326	2.57675	0.03852	2.57675	0.03852	2.60083	0.03326
15	2.71906	0.02365	2.71530	0.02771	2.71530	0.02771	2.71906	0.02365
20	2.79670	0.01553	2.80725	0.01839	2.80725	0.01839	2.79670	0.01553
25	2.85136	0.01093	2.87220	0.01299	2.87220	0.01299	2.85136	0.01093
30	2.89172	0.00807	2.92009	0.00958	2.92009	0.00958	2.89172	0.00807
average		0.04392		0.04868		0.04868		0.04392

Appendix D: Distance and Corresponding Voltage Values for Modified Electrodes Design

Table D-1 Case 1: Index(I) finger moves

Distance (mm)	V ₁ (V)	Sensitivity-V ₁ (V/mm)	V ₂ (V)	V ₃ (V)	V ₄ (V)
0	1.67836		1.36984	1.36981	1.67834
2	1.83532	0.07848	1.38515	1.37032	1.67835
4	1.91827	0.04147	1.39427	1.37064	1.67835
6	1.97132	0.02653	1.40049	1.37085	1.67835
8	2.00800	0.01834	1.40499	1.37097	1.67833
10	2.03446	0.01323	1.40831	1.37110	1.67832
15	2.07550	0.00821	1.41357	1.37126	1.67831
20	2.09773	0.00444	1.41642	1.37136	1.67830
25	2.11101	0.00266	1.41811	1.37143	1.67830
30	2.11954	0.00171	1.41917	1.37148	1.67831
average		0.02167			

Table D-2 Case 1-2: Little(L) finger moves

Distance (mm)	V ₁ (V)	V ₂ (V)	V ₃ (V)	V ₄ (V)	Sensitivity- V ₄ (V/mm)
0	1.67836	1.36984	1.36981	1.67834	
2	1.67836	1.37034	1.38511	1.83530	0.07848
4	1.67838	1.37066	1.39423	1.91826	0.04148
6	1.67836	1.37085	1.40046	1.97129	0.02652
8	1.67836	1.37100	1.40494	2.00795	0.01833
10	1.67835	1.37112	1.40827	2.03445	0.01325
15	1.67834	1.37130	1.41353	2.07548	0.00821
20	1.67833	1.37140	1.41638	2.09771	0.00444
25	1.67833	1.37148	1.41808	2.11096	0.00265
30	1.67835	1.37153	1.41916	2.11949	0.00171
average					0.02167

Table D-3 Case 2: Middle(M) finger moves

Distance (mm)	V ₁ (V)	V ₂ (V)	Sensitivity-V ₂ (V/mm)	V ₃ (V)	V ₄ (V)
0	1.67836	1.36984		1.36981	1.67834
2	1.68901	1.45823	0.04419	1.37991	1.67867
4	1.69482	1.50045	0.02111	1.38547	1.67886
6	1.69849	1.52482	0.01219	1.38897	1.67900
8	1.70089	1.53993	0.00755	1.39127	1.67905
10	1.70250	1.54967	0.00487	1.39283	1.67909

15	1.70463	1.56206	0.00248	1.39489	1.67915
20	1.70553	1.56714	0.00102	1.39577	1.67916
25	1.70599	1.56963	0.00050	1.39619	1.67914
30	1.70627	1.57106	0.00029	1.39644	1.67914
Average			0.01047		

Table D-4 Case 2-2: Ring(R) finger moves

Distance (mm)	V ₁ (V)	V ₂ (V)	V ₃ (V)	Sensitivity- V ₃ (V/mm)	V ₄ (V)
0	1.67836	1.36984	1.36981		1.67834
2	1.67869	1.37996	1.45821	0.04420	1.68900
4	1.67889	1.38549	1.50041	0.02110	1.69479
6	1.67901	1.38901	1.52479	0.01219	1.69845
8	1.67908	1.39131	1.53989	0.00755	1.70086
10	1.67913	1.39287	1.54963	0.00487	1.70249
15	1.67917	1.39491	1.56199	0.00247	1.70460
20	1.67918	1.39579	1.56707	0.00102	1.70549
25	1.67918	1.39625	1.56957	0.00050	1.70595
30	1.67918	1.39650	1.57100	0.00029	1.70623
Average				0.01046	

Table D-5 Case 3: Index & Middle(IM) fingers move

Distance (mm)	V ₁ (V)	Sensitivity- V ₁ (V/mm)	V ₂ (V)	Sensitivity- V ₂ (V/mm)	V ₃ (V)	V ₄ (V)
0	1.67836		1.36984		1.36981	1.67834
2	1.85017	0.08591	1.47835	0.05425	1.38082	1.67871
4	1.94610	0.04796	1.53766	0.02966	1.38735	1.67892
6	2.01053	0.03221	1.57671	0.01953	1.39187	1.67906
8	2.05726	0.02337	1.60451	0.01390	1.39517	1.67918
10	2.09272	0.01773	1.62528	0.01038	1.39765	1.67925
15	2.15206	0.01187	1.65938	0.00682	1.40174	1.67937
20	2.18786	0.00716	1.67970	0.00406	1.40419	1.67945
25	2.21113	0.00466	1.69291	0.00264	1.40581	1.67951
30	2.22709	0.00319	1.70199	0.00182	1.40694	1.67958
average		0.02601		0.01590		

Table D-6 Case 3-2: Ring & Little(RL) finger moves

Distance (mm)	V ₁ (V)	V ₂ (V)	V ₃ (V)	Sensitivity- V ₃ (V/mm)	V ₄ (V)	Sensitivity- V ₄ (V/mm)
0	1.67836	1.36984	1.36981		1.67834	
2	1.67872	1.38090	1.47832	0.05426	1.85014	0.08590

4	1.67895	1.38747	1.53764	0.02966	1.94607	0.04797
6	1.67909	1.39199	1.57667	0.01951	2.01047	0.03220
8	1.67919	1.39527	1.60450	0.01391	2.05723	0.02338
10	1.67926	1.39776	1.62526	0.01038	2.09267	0.01772
15	1.67939	1.40186	1.65938	0.00683	2.15202	0.01187
20	1.67947	1.40432	1.67971	0.00406	2.18782	0.00716
25	1.67953	1.40593	1.69291	0.00264	2.21109	0.00465
30	1.67960	1.40706	1.70199	0.00182	2.22705	0.00319
average				0.01590		0.02600

Table D-7 Case 4: Index & Ring (IR) fingers move

Distance (mm)	V ₁ (V)	Sensitivity-V ₁ (V/mm)	V ₂ (V)	V ₃ (V)	Sensitivity-V ₃ (V/mm)	V ₄ (V)
0	1.67836		1.36984	1.36981		1.67834
2	1.83572	0.07868	1.39527	1.45879	0.04449	1.68899
4	1.91901	0.04164	1.40999	1.50147	0.02134	1.69483
6	1.97221	0.02660	1.41973	1.52618	0.01236	1.69850
8	2.00906	0.01843	1.42659	1.54159	0.00770	1.70095
10	2.03568	0.01331	1.43149	1.55145	0.00493	1.70254
15	2.07685	0.00823	1.43884	1.56415	0.00254	1.70468
20	2.09916	0.00446	1.44260	1.56944	0.00106	1.70559
25	2.11249	0.00267	1.44476	1.57215	0.00054	1.70610
30	2.12111	0.00172	1.44614	1.57384	0.00034	1.70643
average		0.02175			0.01059	

Table D-8 Case 4-2: Middle & Little(ML) finger moves

Distance (mm)	V ₁ (V)	V ₂ (V)	Sensitivity-V ₂ (V/mm)	V ₃ (V)	V ₄ (V)	Sensitivity-V ₄ (V/mm)
0	1.67836	1.36984		1.36981	1.67834	
2	1.68903	1.45885	0.04450	1.39527	1.83575	0.07870
4	1.69486	1.50152	0.02133	1.40997	1.91899	0.04162
6	1.69854	1.52622	0.01235	1.41969	1.97221	0.02661
8	1.70096	1.54160	0.00769	1.42656	2.00905	0.01842
10	1.70258	1.55153	0.00496	1.43148	2.03567	0.01331
15	1.70471	1.56418	0.00253	1.43882	2.07681	0.00823
20	1.70562	1.56947	0.00106	1.44257	2.09911	0.00446
25	1.70611	1.57219	0.00054	1.44475	2.11245	0.00267
30	1.70644	1.57388	0.00034	1.44612	2.12107	0.00172
average			0.01059			0.02175

Table D-9 Case 5: Index & Little(IL) fingers move

Distance (mm)	V ₁ (V)	Sensitivity-V ₁ (V/mm)	V ₂ (V)	V ₃ (V)	V ₄ (V)	Sensitivity-V ₄ (V/mm)
0	1.67836		1.36984	1.36981	1.67834	
2	1.83534	0.07849	1.38565	1.38564	1.83532	0.07849
4	1.91831	0.04149	1.39509	1.39504	1.91827	0.04147
6	1.97134	0.02651	1.40151	1.40149	1.97133	0.02653
8	2.00800	0.01833	1.40616	1.40614	2.00796	0.01832
10	2.03450	0.01325	1.40963	1.40958	2.03446	0.01325
15	2.07548	0.00820	1.41504	1.41502	2.07550	0.00821
20	2.09769	0.00444	1.41799	1.41797	2.09771	0.00444
25	2.11098	0.00266	1.41974	1.41969	2.11095	0.00265
30	2.11954	0.00171	1.42086	1.42081	2.11951	0.00171
average		0.02168				0.02167

Table D-10 Case 6: Middle & Ring(MR) fingers move

Distance (mm)	V ₁ (V)	V ₂ (V)	Sensitivity-V ₂ (V/mm)	V ₃ (V)	Sensitivity-V ₃ (V/mm)	V ₄ (V)
0	1.67836	1.36984		1.36981		1.67834
2	1.68966	1.47177	0.05096	1.47172	0.05095	1.68963
4	1.69617	1.52510	0.02666	1.52508	0.02668	1.69616
6	1.70049	1.55872	0.01681	1.55870	0.01681	1.70048
8	1.70354	1.58155	0.01141	1.58154	0.01142	1.70354
10	1.70574	1.59776	0.00810	1.59774	0.00810	1.70574
15	1.70910	1.62210	0.00487	1.62206	0.00486	1.70908
20	1.71087	1.63474	0.00253	1.63470	0.00253	1.71085
25	1.71194	1.64206	0.00146	1.64203	0.00146	1.71193
30	1.71268	1.64672	0.00093	1.64669	0.00093	1.71266
average			0.01375		0.01375	

Table D-11 Case 7: Index & Middle & Ring(IMR) fingers move

Distance (mm)	V ₁ (V)	Sensitivity - V ₁ (V/mm)	V ₂ (V)	Sensitivity - V ₂ (V/mm)	V ₃ (V)	Sensitivity - V ₃ (V/mm)	V ₄ (V)
0	1.67836		1.36984		1.36981		1.67834
2	1.85098	0.08631	1.49197	0.06106	1.47284	0.05151	1.68964
4	1.94802	0.04852	1.56263	0.03533	1.52772	0.02744	1.69624
6	2.01368	0.03283	1.61129	0.02433	1.56312	0.01770	1.70070
8	2.06180	0.02406	1.64732	0.01802	1.58781	0.01234	1.70386
10	2.09868	0.01844	1.67522	0.01395	1.60597	0.00908	1.70620
15	2.16165	0.01259	1.72335	0.00963	1.63529	0.00587	1.70997
20	2.20097	0.00786	1.75372	0.00607	1.65273	0.00349	1.71220

25	2.22746	0.00530	1.77430	0.00412	1.66436	0.00233	1.71373
30	2.24622	0.00375	1.78895	0.00293	1.67270	0.00167	1.71489
average		0.02663		0.01949		0.01460	

Table D-12 Case 7-2: Middle & Ring & Little(MRL) finger moves

Distance (mm)	V ₁ (V)	V ₂ (V)	Sensitivity - V ₂ (V/mm)	V ₃ (V)	Sensitivity - V ₃ (V/mm)	V ₄ (V)	Sensitivity - V ₄ (V/mm)
0	1.67836	1.36984		1.36981		1.67834	
2	1.68968	1.47288	0.05152	1.49192	0.06105	1.85095	0.08630
4	1.69627	1.52775	0.02743	1.56257	0.03533	1.94798	0.04851
6	1.70073	1.56316	0.01771	1.61126	0.02434	2.01369	0.03286
8	1.70388	1.58785	0.01235	1.64729	0.01801	2.06177	0.02404
10	1.70623	1.60605	0.00910	1.67521	0.01396	2.09863	0.01843
15	1.71000	1.63537	0.00586	1.72334	0.00963	2.16161	0.01260
20	1.71223	1.65281	0.00349	1.75371	0.00607	2.20093	0.00786
25	1.71376	1.66443	0.00233	1.77430	0.00412	2.22741	0.00530
30	1.71492	1.67278	0.00167	1.78895	0.00293	2.24618	0.00375
average			0.01461		0.01949		0.02663

Table D-13 Case 8: Index & Middle & Little(IML)/Index & Ring & Little(IRL) fingers move

Distance (mm)	V ₁ (V)	Sensitivity - V ₁ (V/mm)	V ₂ (V)	Sensitivity - V ₂ (V/mm)	V ₃ (V)	V ₄ (V)	Sensitivity - V ₄ (V/mm)
0	1.67836		1.36984		1.36981	1.67834	
2	1.85021	0.08593	1.47898	0.05457	1.39615	1.83577	0.07871
4	1.94616	0.04797	1.53875	0.02989	1.41186	1.91905	0.04164
6	2.01059	0.03221	1.57812	0.01968	1.42263	1.97234	0.02665
8	2.05738	0.02340	1.60622	0.01405	1.43047	2.00921	0.01844
10	2.09287	0.01775	1.62718	0.01048	1.43631	2.03588	0.01333
15	2.15226	0.01188	1.66160	0.00688	1.44570	2.07718	0.00826
20	2.18811	0.00717	1.68215	0.00411	1.45105	2.09963	0.00449
25	2.21147	0.00467	1.69557	0.00268	1.45438	2.11314	0.00270
30	2.22759	0.00322	1.70496	0.00188	1.45667	2.12202	0.00178
average		0.02602		0.01602			0.02178

Table D-14 Case 8-2: Index & Ring & Little(IRL) finger moves

Distance (mm)	V ₁ (V)	Sensitivity - V ₁ (V/mm)	V ₂ (V)	V ₃ (V)	Sensitivity - V ₃ (V/mm)	V ₄ (V)	Sensitivity - V ₄ (V/mm)
0	1.67836		1.36984	1.36981		1.67834	
2	1.83579	0.07872	1.39625	1.47891	0.05455	1.85018	0.08592

4	1.91905	0.04163	1.41195	1.53870	0.02989	1.94611	0.04797
6	1.97239	0.02667	1.42277	1.57809	0.01970	2.01058	0.03223
8	2.00925	0.01843	1.43057	1.60619	0.01405	2.05737	0.02340
10	2.03591	0.01333	1.43642	1.62716	0.01048	2.09287	0.01775
15	2.07722	0.00826	1.44581	1.66155	0.00688	2.15221	0.01187
20	2.09967	0.00449	1.45116	1.68210	0.00411	2.18807	0.00717
25	2.11319	0.00270	1.45451	1.69559	0.00270	2.21147	0.00468
30	2.12206	0.00178	1.45679	1.70497	0.00188	2.22759	0.00322
average		0.02178			0.01603		0.02602

Table D-15 Case 9: Index & Middle & Ring & Little(IMRL) fingers move

Distance (mm)	V ₁ (V)	Sensitivity- V ₁ (V/mm)	V ₂ (V)	Sensitivity- V ₂ (V/mm)	V ₃ (V)	Sensitivity- V ₃ (V/mm)	V ₄ (V)	Sensitivity- V ₄ (V/mm)
0	1.67836		1.36984		1.36981		1.67834	
2	1.85103	0.08634	1.49308	0.06162	1.49307	0.06163	1.85102	0.08634
4	1.94819	0.04858	1.56530	0.03611	1.56524	0.03609	1.94815	0.04857
6	2.01408	0.03295	1.61574	0.02522	1.61571	0.02524	2.01404	0.03294
8	2.06244	0.02418	1.65371	0.01899	1.65366	0.01897	2.06238	0.02417
10	2.09962	0.01859	1.68363	0.01496	1.68357	0.01496	2.09955	0.01859
15	2.16359	0.01279	1.73701	0.01068	1.73695	0.01068	2.16352	0.01279
20	2.20425	0.00813	1.77258	0.00712	1.77252	0.00712	2.20418	0.00813
25	2.23232	0.00561	1.79803	0.00509	1.79797	0.00509	2.23225	0.00561
30	2.25283	0.00410	1.81706	0.00380	1.81699	0.00380	2.25276	0.00410
average		0.02681		0.02040		0.02040		0.02681

Appendix E: Comparison of Two Electrode Designs within Each Case

Table E-1 Comparison within case1

Distance (mm)	Sensitivity- V_1		
	Without gnd (V/mm)	With gnd (V/mm)	Percentage
0			
2	0.10489	0.07848	74.824%
4	0.05646	0.04147	73.462%
6	0.03632	0.02653	73.037%
8	0.02511	0.01834	73.032%
10	0.01808	0.01323	73.178%
15	0.01109	0.00821	74.039%
20	0.00590	0.00444	75.297%
25	0.00347	0.00266	76.615%
30	0.00220	0.00171	77.394%
average	0.02928	0.02167	74.542%

Table E-2 Comparison within case 1-2

Distance (mm)	Sensitivity- V_4		
	Without gnd (V/mm)	With gnd (V/mm)	Percentage
0			
2	0.10489	0.07848	74.827%
4	0.05646	0.04148	73.461%
6	0.03632	0.02652	73.009%
8	0.02511	0.01833	73.000%
10	0.01808	0.01325	73.298%

15	0.01109	0.00821	74.028%
20	0.00590	0.00445	75.288%
25	0.00347	0.00265	76.464%
30	0.00220	0.00171	77.405%
average	0.02928	0.02167	74.531%

Table E-3 Comparison within case 2

Distance (mm)	Sensitivity- V_2		
	Without gnd (V/mm)	With gnd (V/mm)	Percentage
0			
2	0.08783	0.04419	50.313%
4	0.04438	0.02111	47.573%
6	0.02649	0.01219	46.013%
8	0.01675	0.00755	45.093%
10	0.01091	0.00487	44.669%
15	0.00560	0.00248	44.224%
20	0.00227	0.00102	44.782%
25	0.00107	0.00050	46.629%
30	0.00058	0.00029	48.885%
average	0.02176	0.01047	46.465%

Table E-4 Comparison within case 2-2

Distance (mm)	Sensitivity- V_3		
	Without gnd (V/mm)	With gnd (V/mm)	Percentage
0			

2	0.08783	0.04420	50.325%
4	0.04438	0.02110	47.544%
6	0.02649	0.01219	46.024%
8	0.01675	0.00755	45.087%
10	0.01091	0.00487	44.632%
15	0.00560	0.00247	44.135%
20	0.00227	0.00102	44.782%
25	0.00107	0.00050	46.816%
30	0.00058	0.00029	48.885%
average	0.02176	0.01046	46.470%

Table E-5 Comparison within case 3

Distance (mm)	Sensitivity- V_1			Sensitivity- V_2		
	Without gnd (V/mm)	With gnd (V/mm)	Percentage	Without gnd (V/mm)	With gnd (V/mm)	Percentage
0						
2	0.12630	0.08591	68.019%	0.11141	0.05425	48.696%
4	0.07466	0.04796	64.242%	0.06443	0.02966	46.028%
6	0.05185	0.03222	62.126%	0.04363	0.01953	44.756%
8	0.03842	0.02337	60.822%	0.03146	0.01390	44.182%
10	0.02953	0.01773	60.054%	0.02355	0.01038	44.083%
15	0.01996	0.01187	59.449%	0.01533	0.00682	44.486%
20	0.01208	0.00716	59.272%	0.00891	0.00407	45.643%
25	0.00782	0.00466	59.534%	0.00563	0.00264	46.919%
30	0.00532	0.00319	59.981%	0.00378	0.00182	48.042%
average	0.04066	0.02601	61.500%	0.03424	0.01590	45.871%

Table E-6 Comparison within case 3-2

Distance (mm)	Sensitivity- V_3			Sensitivity- V_4		
	Without gnd (V/mm)	With gnd (V/mm)	Percentage	Without gnd (V/mm)	With gnd (V/mm)	Percentage
0						
2	0.11143	0.05426	48.691%	0.12630	0.08590	68.011%
4	0.06444	0.02966	46.031%	0.07466	0.04797	64.249%
6	0.04363	0.01951	44.726%	0.05185	0.03220	62.091%
8	0.03147	0.01391	44.219%	0.03842	0.02338	60.854%
10	0.02355	0.01038	44.064%	0.02953	0.01773	60.032%
15	0.01533	0.00683	44.509%	0.01996	0.01187	59.461%
20	0.00891	0.00407	45.638%	0.01208	0.00716	59.272%
25	0.00563	0.00264	46.909%	0.00782	0.00466	59.534%
30	0.00378	0.00182	48.042%	0.00532	0.00319	59.970%
average	0.03424	0.01590	45.870%	0.04066	0.02600	61.497%

Table E-7 Comparison within case 4

Distance (mm)	Sensitivity- V_1			Sensitivity- V_3		
	Without gnd (V/mm)	With gnd (V/mm)	Percentage	Without gnd (V/mm)	With gnd (V/mm)	Percentage
0						
2	0.10610	0.07868	74.155%	0.08920	0.04449	49.877%
4	0.05731	0.04164	72.659%	0.04537	0.02134	47.043%
6	0.03694	0.02660	72.021%	0.02722	0.01236	45.393%
8	0.02555	0.01843	72.132%	0.01730	0.00770	44.540%
10	0.01839	0.01331	72.354%	0.01131	0.00493	43.578%
15	0.01127	0.00823	73.094%	0.00586	0.00254	43.374%

20	0.00600	0.00446	74.358%	0.00242	0.00106	43.701%
25	0.00354	0.00267	75.339%	0.00119	0.00054	45.746%
30	0.00227	0.00172	75.880%	0.00070	0.00034	48.494%
average	0.02971	0.02175	73.555%	0.02228	0.01059	45.749%

Table E-8 Comparison within case 4-2

Distance (mm)	Sensitivity- V_2			Sensitivity- V_4		
	Without gnd (V/mm)	With gnd (V/mm)	Percentage	Without gnd (V/mm)	With gnd (V/mm)	Percentage
0						
2	0.08920	0.04450	49.892%	0.10611	0.07870	74.172%
4	0.04537	0.02133	47.025%	0.05731	0.04162	72.620%
6	0.02722	0.01235	45.380%	0.03693	0.02661	72.055%
8	0.01730	0.00769	44.464%	0.02555	0.01842	72.093%
10	0.01132	0.00496	43.853%	0.01840	0.01331	72.367%
15	0.00586	0.00253	43.211%	0.01126	0.00823	73.047%
20	0.00242	0.00106	43.701%	0.00600	0.00446	74.358%
25	0.00119	0.00055	45.914%	0.00354	0.00267	75.374%
30	0.00070	0.00034	48.494%	0.00227	0.00172	75.880%
average	0.02228	0.01059	45.770%	0.02971	0.02175	73.552%

Table E-9 Comparison within case 5

Distance (mm)	Sensitivity- V_1			Sensitivity- V_4		
	Without gnd (V/mm)	With gnd (V/mm)	Percentage	Without gnd (V/mm)	With gnd (V/mm)	Percentage
0						
2	0.10497	0.07849	74.774%	0.10497	0.07849	74.777%

4	0.05652	0.04149	73.412%	0.05651	0.04147	73.382%
6	0.03636	0.02651	72.912%	0.03636	0.02653	72.959%
8	0.02513	0.01833	72.928%	0.02513	0.01832	72.887%
10	0.01810	0.01325	73.218%	0.01810	0.01325	73.191%
15	0.01110	0.00820	73.855%	0.01110	0.00821	73.964%
20	0.00591	0.00444	75.173%	0.00591	0.00444	75.173%
25	0.00348	0.00266	76.438%	0.00348	0.00265	76.180%
30	0.00222	0.00171	77.197%	0.00222	0.00171	77.187%
average	0.02931	0.02168	74.434%	0.02931	0.02167	74.411%

Table E-10 Comparison within case 6

Distance (mm)	Sensitivity- V_2			Sensitivity- V_3		
	Without gnd (V/mm)	With gnd (V/mm)	Percentage	Without gnd (V/mm)	With gnd (V/mm)	Percentage
0						
2	0.10873	0.05097	46.874%	0.10873	0.05095	46.863%
4	0.06169	0.02667	43.222%	0.06169	0.02668	43.245%
6	0.04088	0.01681	41.123%	0.04088	0.01681	41.124%
8	0.02871	0.01142	39.757%	0.02871	0.01142	39.771%
10	0.02083	0.00810	38.907%	0.02083	0.00810	38.907%
15	0.01276	0.00487	38.147%	0.01276	0.00486	38.116%
20	0.00669	0.00253	37.799%	0.00669	0.00253	37.799%
25	0.00384	0.00146	38.149%	0.00384	0.00147	38.201%
30	0.00238	0.00093	39.235%	0.00238	0.00093	39.235%
average	0.03183	0.01375	40.357%	0.03183	0.01375	40.362%

Table E-11 Comparison within case 7

Distance (mm)	Sensitivity- V ₁			Sensitivity- V ₂			Sensitivity- V ₃		
	Without gnd (V/mm)	With gnd (V/mm)	Percentage	Without gnd (V/mm)	With gnd (V/mm)	Percentage	Without gnd (V/mm)	With gnd (V/mm)	Percentage
0									
2	0.12838	0.08631	67.228%	0.13252	0.06106	46.077%	0.11104	0.05152	46.395%
4	0.07737	0.04852	62.709%	0.08238	0.03533	42.891%	0.06473	0.02744	42.389%
6	0.05480	0.03283	59.912%	0.05899	0.02433	41.242%	0.04419	0.01770	40.059%
8	0.04142	0.02406	58.085%	0.04467	0.01802	40.332%	0.03212	0.01235	38.436%
10	0.03250	0.01844	56.739%	0.03493	0.01395	39.930%	0.02423	0.00908	37.475%
15	0.02277	0.01259	55.305%	0.02420	0.00963	39.783%	0.01600	0.00587	36.654%
20	0.01455	0.00787	54.066%	0.01514	0.00607	40.124%	0.00955	0.00349	36.517%
25	0.00990	0.00530	53.489%	0.01011	0.00412	40.738%	0.00625	0.00233	37.224%
30	0.00705	0.00375	53.272%	0.00708	0.00293	41.408%	0.00436	0.00167	38.283%
average	0.04319	0.02663	57.867%	0.04556	0.01949	41.392%	0.03472	0.01460	39.270%

Table E-12 Comparison within case 7-2

Distance (mm)	Sensitivity- V ₂			Sensitivity- V ₃			Sensitivity- V ₄		
	Without gnd (V/mm)	With gnd (V/mm)	Percentage	Without gnd (V/mm)	With gnd (V/mm)	Percentage	Without gnd (V/mm)	With gnd (V/mm)	Percentage
0									
2	0.11104	0.05152	46.398%	0.13252	0.06106	46.072%	0.12838	0.08630	67.224%
4	0.06473	0.02744	42.386%	0.08238	0.03533	42.884%	0.07737	0.04851	62.701%
6	0.04419	0.01771	40.066%	0.05899	0.02434	41.268%	0.05480	0.03286	59.964%
8	0.03212	0.01235	38.435%	0.04467	0.01801	40.326%	0.04142	0.02404	58.026%
10	0.02423	0.00910	37.559%	0.03493	0.01396	39.969%	0.03250	0.01843	56.713%
15	0.01600	0.00586	36.648%	0.02420	0.00963	39.783%	0.02277	0.01260	55.309%

20	0.00955	0.00349	36.513%	0.01514	0.00607	40.122%	0.01455	0.00787	54.062%
25	0.00625	0.00233	37.218%	0.01011	0.00412	40.734%	0.00990	0.00530	53.479%
30	0.00436	0.00167	38.315%	0.00708	0.00293	41.408%	0.00704	0.00375	53.279%
average	0.03472	0.01461	39.282%	0.04556	0.01949	41.396%	0.04319	0.02663	57.862%

Table E-13 Comparison within case 8

Distance (mm)	Sensitivity- V_1			Sensitivity- V_2			Sensitivity- V_4		
	Without gnd (V/mm)	With gnd (V/mm)	Percentage	Without gnd (V/mm)	With gnd (V/mm)	Percentage	Without gnd (V/mm)	With gnd (V/mm)	Percentage
0									
2	0.12642	0.08593	67.968%	0.11278	0.05457	48.382%	0.10625	0.07871	74.087%
4	0.07480	0.04797	64.135%	0.06544	0.02989	45.669%	0.05749	0.04164	72.426%
6	0.05198	0.03222	61.971%	0.04439	0.01968	44.348%	0.03712	0.02665	71.787%
8	0.03854	0.02340	60.710%	0.03204	0.01405	43.868%	0.02573	0.01844	71.660%
10	0.02962	0.01775	59.901%	0.02398	0.01048	43.701%	0.01856	0.01333	71.817%
15	0.02004	0.01188	59.275%	0.01561	0.00688	44.091%	0.01142	0.00826	72.370%
20	0.01214	0.00717	59.089%	0.00908	0.00411	45.268%	0.00612	0.00449	73.318%
25	0.00788	0.00467	59.292%	0.00577	0.00268	46.500%	0.00366	0.00270	73.825%
30	0.00540	0.00322	59.748%	0.00392	0.00188	47.884%	0.00240	0.00178	74.000%
average	0.04076	0.02602	61.343%	0.03478	0.01602	45.523%	0.02986	0.02178	72.810%

Table E-14 Comparison within case 8-2

Distance (mm)	Sensitivity- V_1			Sensitivity- V_3			Sensitivity- V_4		
	Without gnd (V/mm)	With gnd (V/mm)	Percentage	Without gnd (V/mm)	With gnd (V/mm)	Percentage	Without gnd (V/mm)	With gnd (V/mm)	Percentage
0									
2	0.10625	0.07872	74.085%	0.11280	0.05455	48.360%	0.12643	0.08592	67.960%

4	0.05750	0.04163	72.403%	0.06544	0.02989	45.679%	0.07480	0.04797	64.127%
6	0.03712	0.02667	71.851%	0.04439	0.01970	44.373%	0.05199	0.03223	62.006%
8	0.02573	0.01843	71.631%	0.03204	0.01405	43.857%	0.03854	0.02340	60.709%
10	0.01857	0.01333	71.802%	0.02398	0.01048	43.704%	0.02963	0.01775	59.899%
15	0.01141	0.00826	72.367%	0.01561	0.00688	44.069%	0.02004	0.01187	59.243%
20	0.00612	0.00449	73.318%	0.00908	0.00411	45.263%	0.01214	0.00717	59.084%
25	0.00366	0.00270	73.860%	0.00577	0.00270	46.726%	0.00788	0.00468	59.411%
30	0.00240	0.00178	74.031%	0.00392	0.00188	47.858%	0.00540	0.00322	59.729%
average	0.02986	0.02178	72.816%	0.03478	0.01603	45.543%	0.04076	0.02602	61.352%

Table E-15 Comparison within case 9

Distance (mm)	Sensitivity- V_1			Sensitivity- V_2			Sensitivity- V_3			Sensitivity- V_4		
	Without gnd (V/mm)	With gnd (V/mm)	Percentage	Without gnd (V/mm)	With gnd (V/mm)	Percentage	Without gnd (V/mm)	With gnd (V/mm)	Percentage	Without gnd (V/mm)	With gnd (V/mm)	Percentage
0												
2	0.12860	0.08634	67.135%	0.13484	0.06162	45.697%	0.13484	0.06163	45.703%	0.12860	0.08634	67.140%
4	0.07779	0.04858	62.448%	0.08546	0.03611	42.253%	0.08546	0.03609	42.227%	0.07779	0.04857	62.433%
6	0.05536	0.03295	59.513%	0.06240	0.02522	40.415%	0.06240	0.02524	40.444%	0.05536	0.03294	59.509%
8	0.04209	0.02418	57.444%	0.04821	0.01899	39.383%	0.04822	0.01897	39.351%	0.04209	0.02417	57.416%
10	0.03326	0.01859	55.895%	0.03852	0.01496	38.830%	0.03852	0.01496	38.830%	0.03326	0.01859	55.892%
15	0.02365	0.01280	54.111%	0.02771	0.01068	38.526%	0.02771	0.01068	38.523%	0.02365	0.01279	54.106%
20	0.01553	0.00813	52.360%	0.01839	0.00712	38.694%	0.01839	0.00712	38.694%	0.01553	0.00813	52.360%
25	0.01093	0.00561	51.354%	0.01299	0.00509	39.181%	0.01299	0.00509	39.181%	0.01093	0.00561	51.354%
30	0.00807	0.00410	50.824%	0.00958	0.00381	39.731%	0.00958	0.00380	39.720%	0.00807	0.00410	50.824%
average	0.04392	0.02681	56.787%	0.04868	0.02040	40.301%	0.04868	0.02040	40.297%	0.04392	0.02681	56.781%

Appendix F: Variation of Voltage Signal due to the Neighbouring Fingers

Table F-1 Variation of V_1 due to the movement of middle finger in original electrode design

V_1 (V)		D-middle (mm)										Variation of V_1	
		0	2	4	6	8	10	15	20	25	30	Δ (V)	average (V)
D-index (mm)	0	1.92663	1.95838	1.97601	1.98718	1.99455	1.99949	2.00602	2.00875	2.01009	2.01086	0.08423	1.98780
	2	2.13640	2.17922	2.20363	2.21941	2.22997	2.23711	2.24655	2.25041	2.25222	2.25323	0.11682	2.22082
	4	2.24931	2.29939	2.32854	2.34777	2.36085	2.36980	2.38170	2.38650	2.38867	2.38983	0.14052	2.35024
	6	2.32195	2.37729	2.41014	2.43225	2.44759	2.45824	2.47263	2.47843	2.48095	2.48225	0.16030	2.43617
	8	2.37217	2.43140	2.46716	2.49171	2.50909	2.52141	2.53843	2.54535	2.54832	2.54978	0.17761	2.49748
	10	2.40833	2.47045	2.50848	2.53504	2.55424	2.56814	2.58792	2.59616	2.59966	2.60131	0.19298	2.54297
	15	2.46376	2.53010	2.57162	2.60160	2.62418	2.64135	2.66794	2.68024	2.68564	2.68807	0.22431	2.61545
	20	2.49327	2.56144	2.60451	2.63613	2.66053	2.67970	2.71158	2.72834	2.73648	2.74024	0.24697	2.65522
	25	2.51061	2.57953	2.62320	2.65549	2.68071	2.70085	2.73587	2.75622	2.76744	2.77315	0.26254	2.67831
	30	2.52163	2.59084	2.63470	2.66721	2.69273	2.71328	2.74981	2.77237	2.78612	2.79404	0.27241	2.69227
Average											0.18787	2.46767	

Table F-2 Variation of V_2 due to the movement of index finger in original electrode design

V_2 (V)		D-index (mm)										Variation of V_2	
		0	2	4	6	8	10	15	20	25	30	Δ (V)	average (V)

D-middle (mm)	0	1.83788	1.87362	1.89447	1.90848	1.91840	1.92565	1.93682	1.94273	1.94616	1.94830	0.11042	1.91325
	2	2.01354	2.06070	2.08883	2.10804	2.12180	2.13188	2.14739	2.15546	2.16004	2.16286	0.14932	2.11506
	4	2.10229	2.15658	2.18956	2.21245	2.22903	2.24130	2.26020	2.26995	2.27538	2.27866	0.17636	2.22154
	6	2.15526	2.21447	2.25103	2.27682	2.29580	2.30999	2.33208	2.34344	2.34967	2.35335	0.19809	2.28819
	8	2.18877	2.25141	2.29063	2.31874	2.33975	2.35569	2.38091	2.39395	2.40101	2.40511	0.21634	2.33260
	10	2.21058	2.27558	2.31673	2.34663	2.36934	2.38685	2.41511	2.42993	2.43790	2.44246	0.23188	2.36311
	15	2.23859	2.30659	2.35034	2.38290	2.40838	2.42870	2.46351	2.48303	2.49371	2.49965	0.26106	2.40554
	20	2.24994	2.31895	2.36358	2.39714	2.42380	2.44551	2.48441	2.50804	2.52179	2.52954	0.27960	2.42427
	25	2.25528	2.32460	2.36947	2.40333	2.43040	2.45263	2.49347	2.51974	2.53620	2.54603	0.29074	2.43311
	30	2.25820	2.32760	2.37251	2.40643	2.43360	2.45601	2.49759	2.52516	2.54340	2.55510	0.29690	2.43756
Average												0.22107	2.29342

Table F-3 Variation of V_2 due to the movement of ring finger in original electrode design

V_2 (V)		D-ring (mm)										Variation of V_2	
		0	2	4	6	8	10	15	20	25	30	Δ (V)	average (V)
D-middle (mm)	0	1.83788	1.86931	1.88677	1.89784	1.90515	1.91005	1.91653	1.91923	1.92052	1.92122	0.08334	1.89845
	2	2.01354	2.05534	2.07916	2.09457	2.10489	2.11188	2.12113	2.12493	2.12670	2.12763	0.11409	2.09598
	4	2.10229	2.15061	2.17872	2.19726	2.20987	2.21851	2.23005	2.23474	2.23686	2.23797	0.13568	2.19969
	6	2.15526	2.20812	2.23943	2.26048	2.27506	2.28522	2.29898	2.30458	2.30707	2.30834	0.15307	2.26425

	8	2.18877	2.24480	2.27851	2.30159	2.31790	2.32946	2.34549	2.35209	2.35498	2.35642	0.16765	2.30700
	10	2.21058	2.26882	2.30428	2.32895	2.34672	2.35956	2.37785	2.38556	2.38893	2.39056	0.17998	2.33618
	15	2.23859	2.29967	2.33753	2.36459	2.38477	2.40000	2.42337	2.43420	2.43906	2.44134	0.20275	2.37631
	20	2.24994	2.31201	2.35072	2.37872	2.39997	2.41638	2.44306	2.45681	2.46354	2.46677	0.21683	2.39379
	25	2.25528	2.31768	2.35666	2.38496	2.40659	2.42349	2.45176	2.46748	2.47598	2.48039	0.22511	2.40203
	30	2.25820	2.32070	2.35975	2.38813	2.40988	2.42694	2.45587	2.47259	2.48232	2.48787	0.22967	2.40622
Average												0.17082	2.26799

Table F-4 Variation of V_1 due to the movement of middle finger in modified electrode design

V_1 (V)		D-middle (mm)										Variation of V_1	
		0	2	4	6	8	10	15	20	25	30	Δ (V)	average (V)
D-index (mm)	0	1.67836	1.68901	1.69482	1.69849	1.70089	1.70250	1.70463	1.70553	1.70599	1.70627	0.02791	1.69865
	2	1.83532	1.85017	1.85854	1.86391	1.86752	1.86995	1.87315	1.87447	1.87510	1.87547	0.04015	1.86436
	4	1.91827	1.93593	1.94610	1.95281	1.95737	1.96050	1.96465	1.96633	1.96710	1.96752	0.04925	1.95366
	6	1.97132	1.99101	2.00265	2.01053	2.01596	2.01978	2.02494	2.02702	2.02793	2.02841	0.05709	2.01196
	8	2.00800	2.02922	2.04208	2.05093	2.05726	2.06178	2.06805	2.07060	2.07170	2.07225	0.06425	2.05319
	10	2.03446	2.05688	2.07068	2.08039	2.08751	2.09272	2.10020	2.10333	2.10465	2.10529	0.07082	2.08361
	15	2.07550	2.09958	2.11484	2.12605	2.13471	2.14142	2.15206	2.15706	2.15926	2.16025	0.08475	2.13207
	20	2.09773	2.12245	2.13831	2.15023	2.15973	2.16740	2.18065	2.18786	2.19140	2.19305	0.09533	2.15888

	25	2.11101	2.13589	2.15191	2.16407	2.17392	2.18206	2.19689	2.20598	2.21113	2.21379	0.10278	2.17466
	30	2.11954	2.14441	2.16041	2.17260	2.18254	2.19084	2.20643	2.21670	2.22323	2.22709	0.10755	2.18438
Average												0.06999	2.03154

Table F-5 Variation of V_2 due to the movement of index finger in modified electrode design

V_2 (V)		D-index (mm)										Variation of V_2	
		0	2	4	6	8	10	15	20	25	30	Δ (V)	average (V)
D-middle (mm)	0	1.36984	1.38515	1.39427	1.40049	1.40499	1.40831	1.41357	1.41642	1.41811	1.41917	0.04933	1.40303
	2	1.45823	1.47835	1.49059	1.49904	1.50525	1.50988	1.51717	1.52107	1.52333	1.52474	0.06651	1.50276
	4	1.50045	1.52345	1.53766	1.54771	1.55516	1.56075	1.56960	1.57431	1.57698	1.57862	0.07817	1.55247
	6	1.52482	1.54978	1.56546	1.57671	1.58514	1.59158	1.60189	1.60737	1.61043	1.61228	0.08745	1.58255
	8	1.53993	1.56625	1.58294	1.59519	1.60451	1.61173	1.62347	1.62974	1.63322	1.63528	0.09535	1.60223
	10	1.54967	1.57688	1.59434	1.60733	1.61738	1.62528	1.63840	1.64553	1.64947	1.65175	0.10208	1.61560
	15	1.56206	1.59040	1.60887	1.62294	1.63416	1.64329	1.65938	1.66874	1.67400	1.67699	0.11493	1.63408
	20	1.56714	1.59582	1.61461	1.62906	1.64077	1.65049	1.66842	1.67970	1.68645	1.69034	0.12320	1.64228
	25	1.56963	1.59838	1.61723	1.63178	1.64364	1.65358	1.67236	1.68486	1.69291	1.69782	0.12819	1.64622
	30	1.57106	1.59980	1.61864	1.63320	1.64509	1.65508	1.67418	1.68728	1.69618	1.70199	0.13093	1.64825
Average												0.09761	1.58295

Table F-6 Variation of V_2 due to the movement of ring finger in modified electrode design

V_2 (V)		D-ring (mm)										Variation of V_2	
		0	2	4	6	8	10	15	20	25	30	Δ (V)	average (V)
D-middle (mm)	0	1.36984	1.37996	1.38549	1.38901	1.39131	1.39287	1.39491	1.39579	1.39625	1.39650	0.02666	1.38919
	2	1.45823	1.47177	1.47938	1.48429	1.48759	1.48983	1.49282	1.49407	1.49468	1.49502	0.03679	1.48477
	4	1.50045	1.51608	1.52510	1.53101	1.53504	1.53782	1.54157	1.54312	1.54385	1.54425	0.04380	1.53183
	6	1.52482	1.54191	1.55195	1.55872	1.56336	1.56664	1.57115	1.57301	1.57388	1.57433	0.04951	1.55998
	8	1.53993	1.55805	1.56884	1.57630	1.58155	1.58531	1.59059	1.59279	1.59380	1.59432	0.05439	1.57815
	10	1.54967	1.56847	1.57983	1.58781	1.59356	1.59776	1.60382	1.60642	1.60759	1.60818	0.05851	1.59031
	15	1.56206	1.58171	1.59389	1.60265	1.60922	1.61425	1.62210	1.62581	1.62752	1.62836	0.06630	1.60676
	20	1.56714	1.58707	1.59950	1.60855	1.61550	1.62095	1.62998	1.63474	1.63714	1.63833	0.07119	1.61389
	25	1.56963	1.58963	1.60214	1.61128	1.61832	1.62393	1.63352	1.63900	1.64206	1.64370	0.07406	1.61732
	30	1.57106	1.59106	1.60357	1.61273	1.61980	1.62546	1.63527	1.64113	1.64464	1.64672	0.07566	1.61914
Average												0.05569	1.55913

Appendix G Data from COMSOL Simulation

Table G-1 Raw data of X-Y Map

V ₁	V ₂	D-index																												
		V ₃	0	0.5	1	1.5	2	3	4	6	8	10	15	20	25	30														
D- mid dle	0		1.926 628	1.837 881	1.996 114	1.849 288	2.051 489	1.858 687	2.097 38	1.866 679	2.136 402	1.873 62	2.199 753	1.885 174	2.249 311	1.894 466	2.321 951	1.908 476	2.372 167	1.918 404	2.408 331	1.925 651	2.463 76	1.936 824	2.493 269	1.942 725	2.510 612	1.946 155	2.521 627	1.948 303
			1.837 882	1.926 626	1.838 612	1.926 671	1.839 213	1.926 706	1.839 726	1.926 738	1.840 174	1.926 769	1.840 914	1.926 806	1.841 512	1.926 838	1.842 413	1.926 884	1.843 054	1.926 914	1.843 522	1.926 934	1.844 253	1.926 967	1.844 642	1.926 975	1.844 881	1.926 994	1.845 039	1.927 011
	0.5		1.936 931	1.897 153	2.007 477	1.909 649	2.063 772	1.919 978	2.110 439	1.928 773	2.150 159	1.936 424	2.214 726	1.949 196	2.265 293	1.959 489	2.339 518	1.975 057	2.390 88	1.986 117	2.427 883	1.994 197	2.484 529	2.006 637	2.514 58	2.013 187	2.532 154	2.016 966	2.543 276	2.019 327
			1.848 073	1.927 289	1.848 889	1.927 332	1.849 606	1.927 375	1.850 217	1.927 412	1.850 751	1.927 444	1.851 642	1.927 496	1.852 361	1.927 535	1.853 455	1.927 599	1.854 23	1.927 634	1.854 798	1.927 66	1.855 678	1.927 695	1.856 15	1.927 715	1.856 432	1.927 733	1.856 616	1.927 753
	1		1.945 303	1.943 686	2.016 739	1.957 111	2.073 79	1.968 222	2.121 121	1.977 696	2.161 432	1.985 949	2.227 026	1.999 757	2.278 455	2.010 912	2.354 047	2.027 832	2.406 41	2.039 874	2.444 15	2.048 684	2.501 872	2.062 237	2.532 387	2.069 344	2.550 156	2.073 423	2.561 355	2.075 956
			1.856 359	1.927 818	1.857 299	1.927 874	1.858 12	1.927 925	1.858 82	1.927 967	1.859 431	1.928 004	1.860 455	1.928 064	1.861 286	1.928 111	1.862 554	1.928 19	1.863 452	1.928 228	1.864 113	1.928 26	1.865 135	1.928 305	1.865 677	1.928 328	1.865 999	1.928 348	1.866 206	1.928 371
	1.5		1.952 348	1.981 702	2.024 538	1.995 92	2.082 241	2.007 707	2.130 146	2.017 775	2.170 974	2.026 555	2.237 466	2.041 274	2.289 655	2.053 19	2.366 453	2.071 309	2.419 732	2.084 247	2.458 151	2.093 724	2.516 857	2.108 282	2.547 797	2.115 89	2.565 739	2.120 236	2.576 996	2.122 917
			1.863 332	1.928 274	1.864 377	1.928 331	1.865 288	1.928 388	1.866 07	1.928 436	1.866 75	1.928 477	1.867 898	1.928 546	1.868 828	1.928 599	1.870 252	1.928 679	1.871 271	1.928 735	1.872 023	1.928 779	1.873 173	1.928 825	1.873 782	1.928 852	1.874 143	1.928 88	1.874 367	1.928 896
	2		1.958 384	2.013 54	2.031 248	2.028 465	2.089 524	2.040 853	2.137 935	2.051 442	2.179 22	2.060 696	2.246 512	2.076 226	2.299 389	2.088 833	2.377 289	2.108 042	2.431 405	2.121 8	2.470 448	2.131 885	2.530 096	2.147 39	2.561 435	2.155 46	2.579 53	2.160 044	2.590 845	2.162 864
			1.869 311	1.928 654	1.870 458	1.928 727	1.871 456	1.928 79	1.872 307	1.928 839	1.873 055	1.928 884	1.874 313	1.928 96	1.875 341	1.929 024	1.876 907	1.929 11	1.878 038	1.929 172	1.878 868	1.929 215	1.880 149	1.929 276	1.880 82	1.929 306	1.881 211	1.929 329	1.881 458	1.929 352
	3		1.968 271	2.064 081	2.042 252	2.080 191	2.101 497	2.093 596	2.150 771	2.105 087	2.192 838	2.115 149	2.261 511	2.132 092	2.315 578	2.145 902	2.395 451	2.167 069	2.451 096	2.182 314	2.491 31	2.193 529	2.552 738	2.210 786	2.584 85	2.219 716	2.603 242	2.224 737	2.614 65	2.227 798
			1.879 102	1.929 287	1.880 421	1.929 368	1.881 565	1.929 441	1.882 55	1.929 502	1.883 413	1.929 554	1.884 873	1.929 643	1.886 069	1.929 716	1.887 911	1.929 823	1.889 245	1.929 896	1.890 231	1.929 951	1.891 752	1.930 026	1.892 544	1.930 063	1.892 996	1.930 088	1.893 278	1.930 113
	4		1.976 014	2.102 293	2.050 902	2.119 372	2.110 933	2.133 609	2.160 913	2.145 842	2.203 627	2.156 577	2.273 457	2.174 715	2.328 541	2.189 562	2.410 136	2.212 445	2.467 164	2.229 035	2.508 476	2.241 3	2.571 622	2.260 202	2.604 508	2.269 949	2.623 2	2.275 378	2.634 702	2.278 656
			1.886 771	1.929 781	1.888 244	1.929 88	1.889 509	1.929 953	1.890 606	1.930 021	1.891 571	1.930 082	1.893 208	1.930 183	1.894 556	1.930 264	1.896 647	1.930 389	1.898 172	1.930 476	1.899 311	1.930 545	1.901 061	1.930 629	1.901 969	1.930 672	1.902 481	1.930 699	1.902 796	1.930 724
	6		1.987 185	2.155 264	2.063 422	2.173 798	2.124 646	2.189 311	2.175 704	2.202 687	2.219 412	2.214 469	2.291 054	2.234 5	2.347 773	2.251 031	2.432 248	2.276 821	2.491 714	2.295 797	2.535 044	2.309 985	2.601 603	2.332 08	2.636 131	2.343 439	2.655 493	2.349 666	2.667 215	2.353 352

		1.897 844	1.930 497	1.899 546	1.930 603	1.901 022	1.930 698	1.902 301	1.930 777	1.903 43	1.930 848	1.905 365	1.930 97	1.906 972	1.931 07	1.909 506	1.931 222	1.911 387	1.931 334	1.912 803	1.931 414	1.915 024	1.931 536	1.916 171	1.931 593	1.916 802	1.931 624	1.917 181	1.931 65
		1.994 551	2.188 769	2.071 709	2.208 299	2.133 755	2.224 693	2.185 564	2.238 873	2.229 974	2.251 406	2.302 918	2.272 818	2.360 852	2.290 625	2.447 586	2.318 736	2.509 088	2.339 747	2.554 239	2.355 69	2.624 181	2.380 911	2.660 533	2.393 947	2.680 709	2.401 015	2.692 73	2.405 113
	8	1.905 151	1.930 966	1.907 026	1.931 084	1.908 652	1.931 188	1.910 066	1.931 278	1.911 324	1.931 357	1.913 488	1.931 494	1.915 306	1.931 609	1.918 215	1.931 793	1.920 412	1.931 918	1.922 1	1.932 019	1.924 799	1.932 173	1.926 202	1.932 244	1.926 967	1.932 287	1.927 411	1.932 309
		1.999 489	2.210 582	2.077 277	2.230 791	2.139 886	2.247 788	2.192 214	2.262 522	2.237 113	2.275 579	2.310 983	2.297 979	2.369 798	2.316 727	2.458 235	2.346 631	2.521 408	2.369 344	2.568 141	2.386 845	2.641 351	2.415 107	2.679 703	2.429 926	2.700 855	2.437 903	2.713 281	2.442 459
	1 0	1.910 053	1.931 279	1.912 05	1.931 405	1.913 786	1.931 517	1.915 299	1.931 614	1.916 65	1.931 7	1.918 986	1.931 847	1.920 967	1.931 973	1.924 175	1.932 173	1.926 658	1.932 326	1.928 599	1.932 443	1.931 782	1.932 628	1.933 466	1.932 72	1.934 376	1.932 765	1.934 896	1.932 793
		2.006 02	2.238 589	2.084 639	2.259 655	2.147 99	2.277 417	2.201 003	2.292 861	2.246 554	2.306 593	2.321 668	2.330 3	2.381 704	2.350 341	2.472 631	2.382 895	2.538 433	2.408 376	2.587 925	2.428 701	2.667 944	2.463 509	2.711 583	2.483 025	2.735 867	2.493 706	2.749 806	2.499 646
	1 5	1.916 535	1.931 687	1.918 695	1.931 825	1.920 577	1.931 946	1.922 224	1.932 053	1.923 701	1.932 147	1.926 281	1.932 314	1.928 497	1.932 457	1.932 182	1.932 692	1.935 152	1.932 879	1.937 583	1.933 033	1.941 875	1.933 297	1.944 342	1.933 444	1.945 699	1.933 517	1.946 453	1.933 556
		2.008 754	2.249 944	2.087 703	2.271 306	2.151 341	2.289 322	2.204 617	2.304 996	2.250 415	2.318 951	2.326 001	2.343 092	2.386 504	2.363 58	2.478 426	2.397 138	2.545 352	2.423 798	2.596 159	2.445 506	2.680 245	2.484 412	2.728 343	2.508 042	2.756 225	2.521 788	2.772 372	2.529 545
	2 0	1.919 231	1.931 855	1.921 453	1.932 002	1.923 384	1.932 126	1.925 073	1.932 233	1.926 594	1.932 331	1.929 257	1.932 504	1.931 559	1.932 654	1.935 438	1.932 911	1.938 624	1.933 111	1.941 312	1.933 285	1.946 348	1.933 61	1.949 54	1.933 812	1.951 428	1.933 926	1.952 496	1.933 986
		2.010 087	2.255 284	2.089 18	2.276 745	2.152 942	2.294 84	2.206 327	2.310 584	2.252 223	2.324 6	2.327 993	2.348 859	2.388 671	2.369 473	2.480 954	2.403 327	2.548 321	2.430 397	2.599 657	2.452 633	2.685 636	2.493 469	2.736 478	2.519 736	2.767 437	2.536 195	2.786 121	2.546 028
	2 5	1.920 514	1.931 937	1.922 753	1.932 083	1.924 701	1.932 209	1.926 406	1.932 321	1.927 938	1.932 421	1.930 622	1.932 595	1.932 948	1.932 749	1.936 877	1.933 005	1.940 144	1.933 218	1.942 933	1.933 404	1.948 334	1.933 764	1.952 014	1.934 01	1.954 392	1.934 169	1.955 826	1.934 26
		2.010 857	2.258 199	2.090 026	2.279 692	2.153 848	2.297 81	2.207 285	2.313 569	2.253 226	2.327 597	2.329 074	2.351 875	2.389 831	2.372 514	2.482 247	2.406 426	2.549 775	2.433 603	2.601 313	2.456 009	2.688 067	2.497 592	2.740 244	2.525 16	2.773 15	2.543 402	2.794 04	2.555 096
	3 0	1.921 222	1.931 991	1.923 467	1.932 138	1.925 418	1.932 265	1.927 126	1.932 376	1.928 659	1.932 476	1.931 344	1.932 654	1.933 678	1.932 814	1.937 61	1.933 064	1.940 896	1.933 283	1.943 715	1.933 471	1.949 258	1.933 849	1.953 186	1.934 125	1.955 897	1.934 319	1.957 672	1.934 446

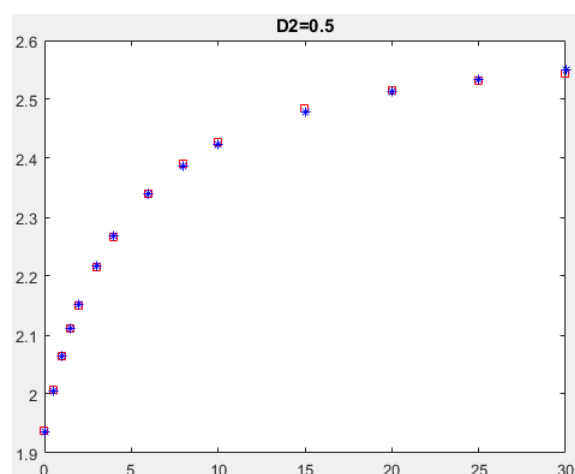
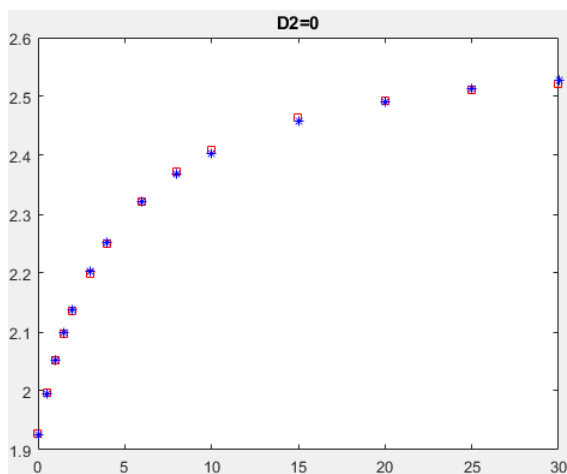
Appendix H: Nonlinear Fitting Results for Equation $V_1=f(D_1)$

Table H-1 Parameters of nonlinear curve fitting equation $V_1=f(D_1)$

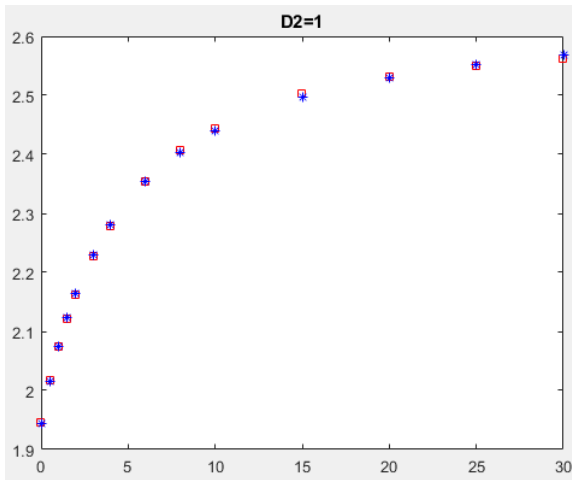
D_2	Parameters in $V_1=f(D_1)$				
	b_1	b_2	b_3	Root Mean Squared Error	R-Squared
0	2.6185	3.1156	4.4941	0.00352	1
0.5	2.6427	3.1901	4.5105	0.00373	1
1	2.663	3.256	4.5265	0.00392	1
1.5	2.6807	3.317	4.5432	0.0041	1
2	2.6964	3.3746	4.5607	0.00426	1
3	2.7239	3.4852	4.6001	0.00455	1
4	2.7474	3.5931	4.6453	0.00479	1
6	2.7866	3.8092	4.753	0.00512	1
8	2.8185	4.0284	4.8793	0.00527	1
10	2.845	4.2478	5.0174	0.00524	1
15	2.8938	4.759	5.3651	0.00465	1
20	2.9243	5.1586	5.6512	0.00383	1
25	2.9421	5.4224	5.844	0.00326	1
30	2.9517	5.5719	5.954	0.00305	1
Average	2.781043	4.023493	4.953171	0.004235	1

Start1= [$b_1=2.2$, $b_2=2.5$, $b_3=2$];

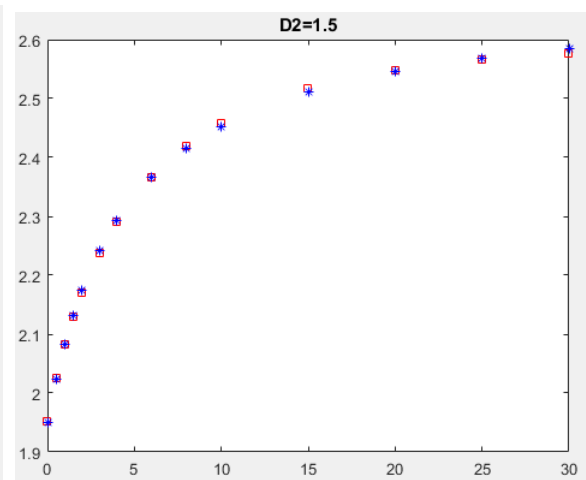
Number of observations: 14, Error degrees of freedom: 11.



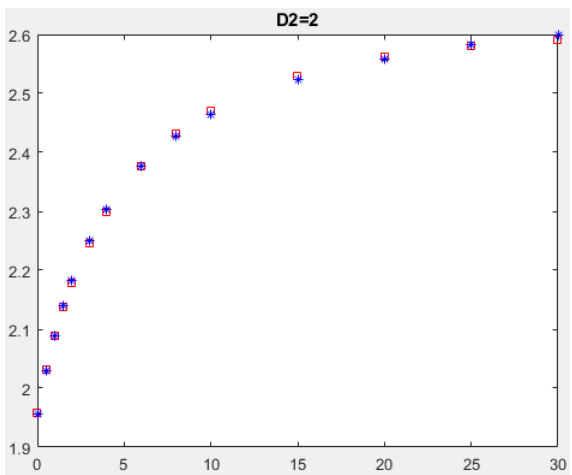
(a) When D_2 is fixed to 0mm



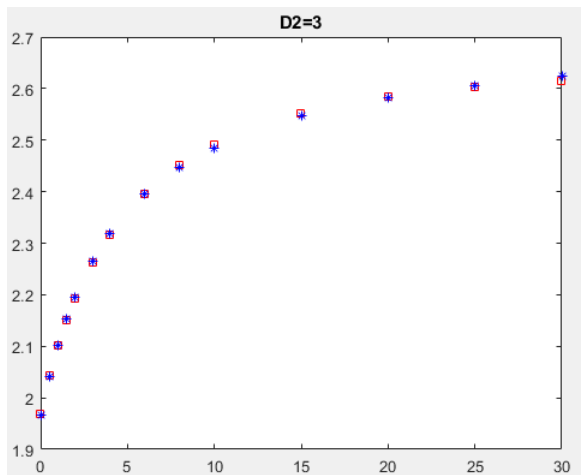
(b) When D_2 is fixed to 0.5mm



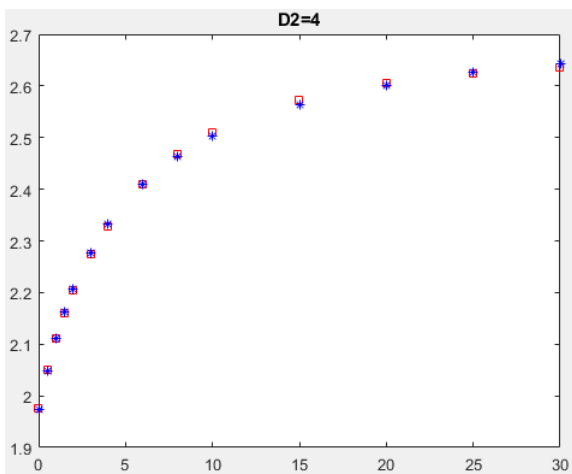
(c) When D_2 is fixed to 1mm



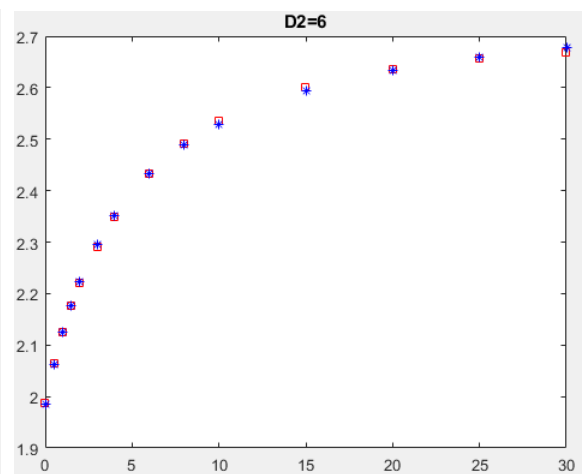
(d) When D_2 is fixed to 1.5mm



(e) When D_2 is fixed to 2mm

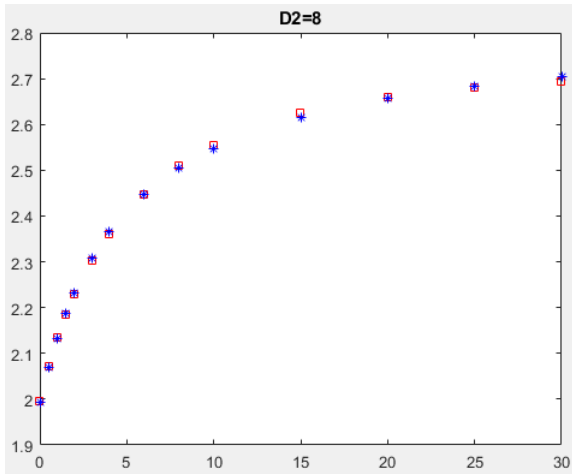


(f) When D_2 is fixed to 3mm

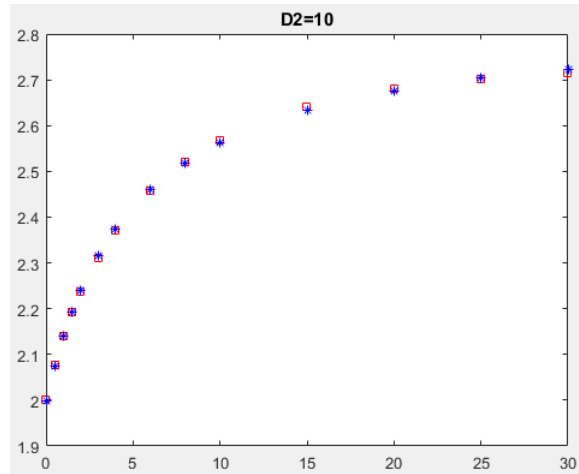


(g) When D_2 is fixed to 4mm

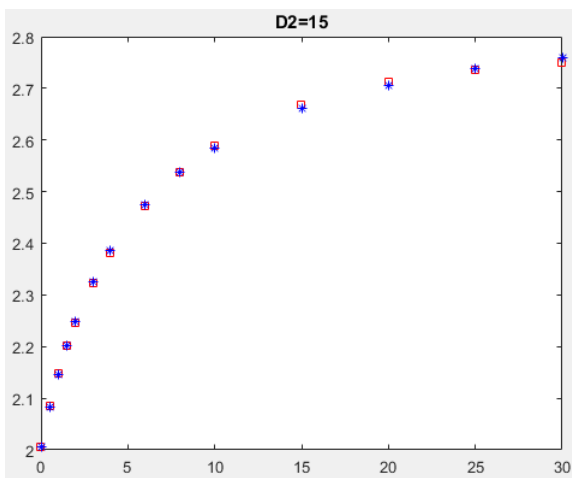
(h) When D_2 is fixed to 6mm



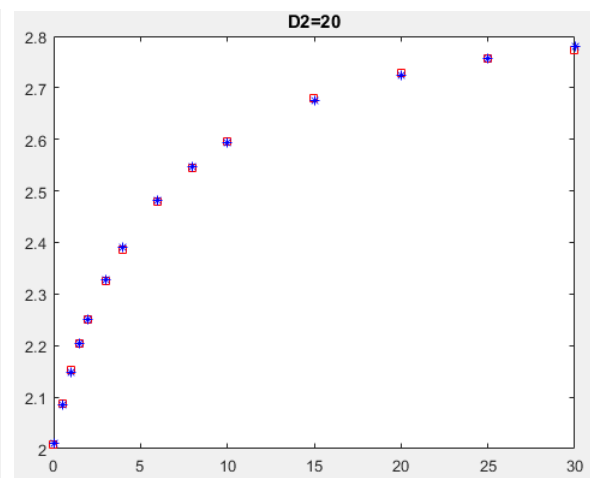
(i) When D_2 is fixed to 8mm



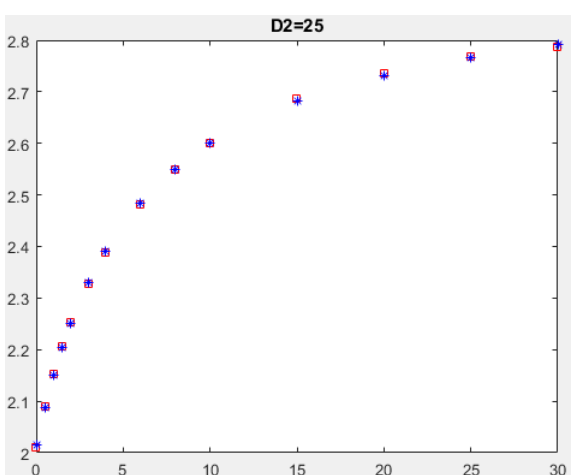
(j) When D_2 is fixed to 10mm



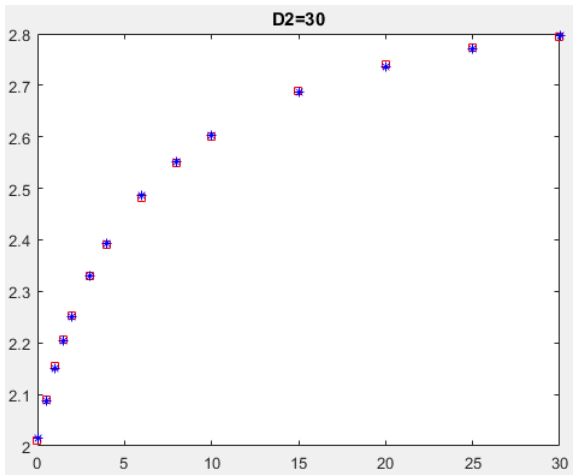
(k) When D_2 is fixed to 15mm



(l) When D_2 is fixed to 20mm



(m) When D_2 is fixed to 25mm



(n) When D_2 is fixed to 30mm

Fig. H-1 Fitted curves for $V_1=f(D_1)$

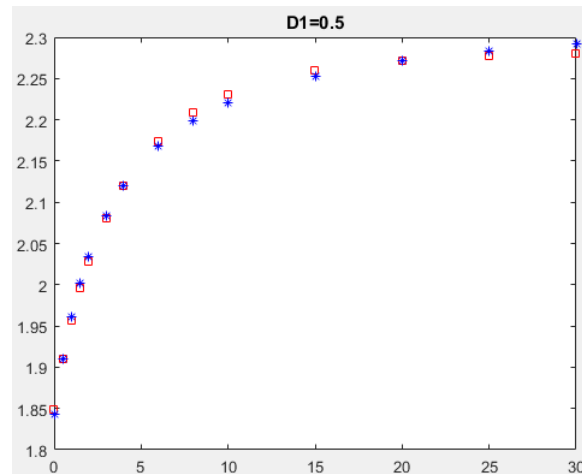
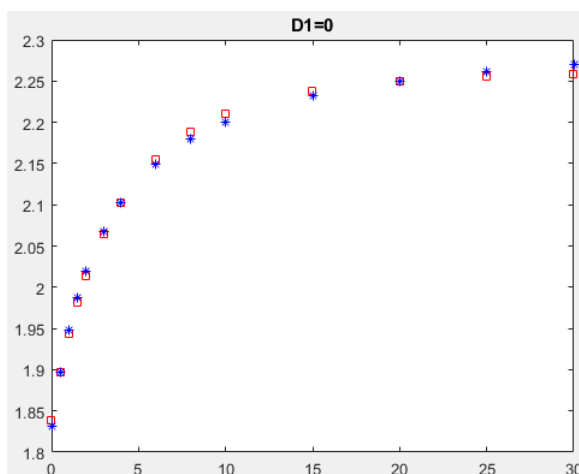
Appendix I: Nonlinear Fitting Results for Equation $V_2=f(D_2)$

Table I-1 Parameters of nonlinear curve fitting equation $V_2=f(D_2)$

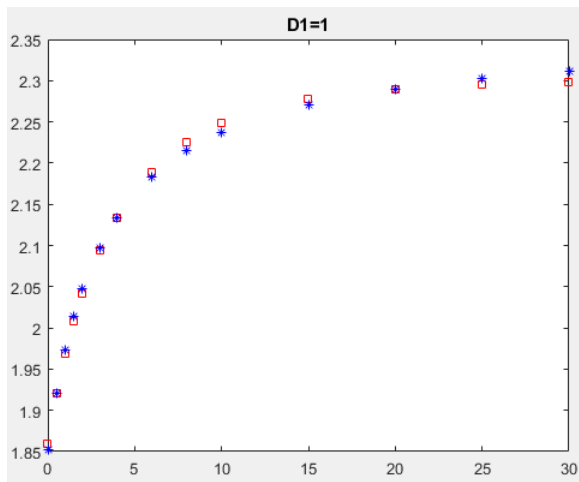
D ₁	V ₂ =f(D ₂)				
	b ₁	b ₂	b ₃	Root Mean Squared Error	R-Squared
0	2.3165	1.5321	3.1579	0.0075	0.998
0.5	2.3398	1.5812	3.1793	0.00775	0.998
1	2.3596	1.6247	3.199	0.00796	0.998
1.5	2.3769	1.6648	3.2181	0.00816	0.998
2	2.3924	1.7027	3.2372	0.00834	0.998
3	2.4193	1.7746	3.2766	0.00864	0.998
4	2.4425	1.8439	3.3189	0.00889	0.998
6	2.4811	1.9805	3.4129	0.0092	0.998
8	2.5126	2.1171	3.5181	0.00929	0.998
10	2.5391	2.2534	3.6308	0.00918	0.998
15	2.589	2.5776	3.9174	0.00827	0.998
20	2.622	2.8485	4.1674	0.00689	0.998
25	2.6432	3.0469	4.3531	0.00552	0.999
30	2.6562	3.1751	4.4732	0.00447	1
Average	2.477871	2.123079	3.575707	0.007861429	0.9982143

Start2=[sb₁₁=2.2, sb₁₂=4.0, sb₁₃=5.0];

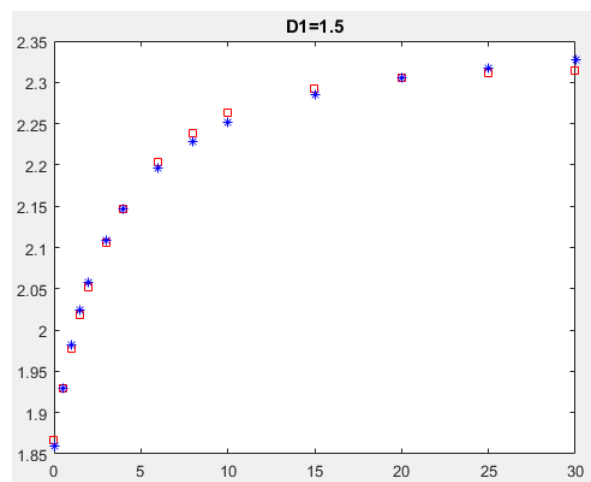
Number of observations: 14, Error degrees of freedom: 11.



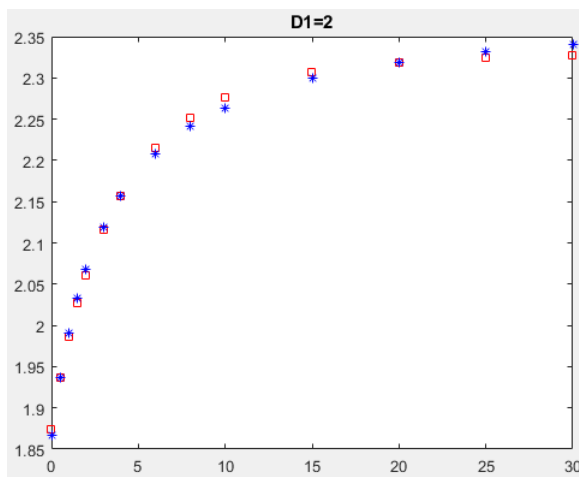
(a) When D_1 is fixed to 0mm



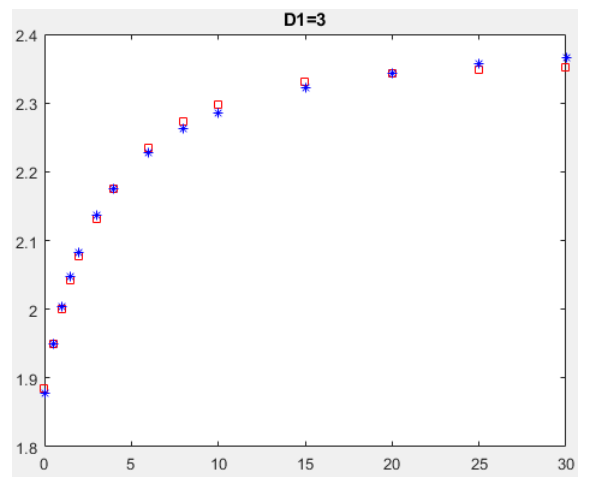
(b) When D_1 is fixed to 0.5mm



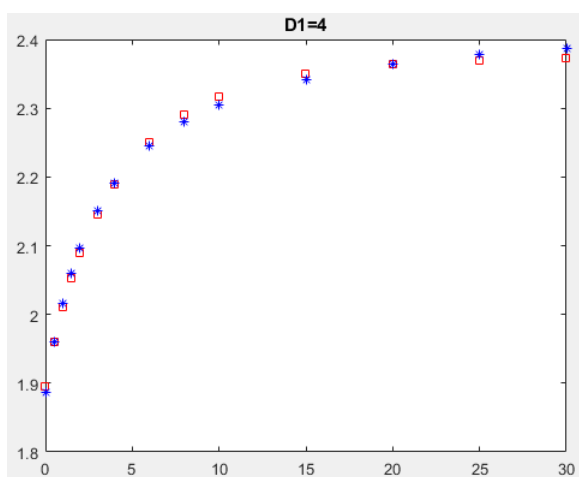
(c) When D_1 is fixed to 1mm



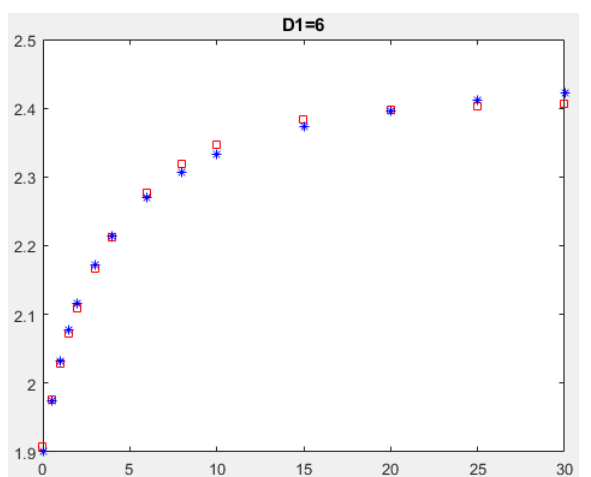
(d) When D_1 is fixed to 1.5mm



(e) When D_1 is fixed to 2mm



(f) When D_1 is fixed to 3mm

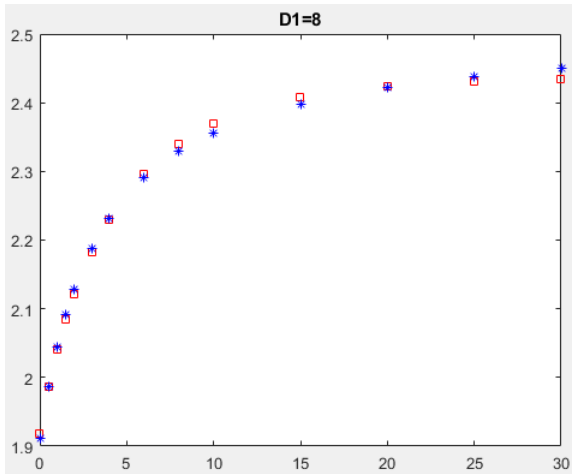


(g) When D_1 is fixed to 4mm

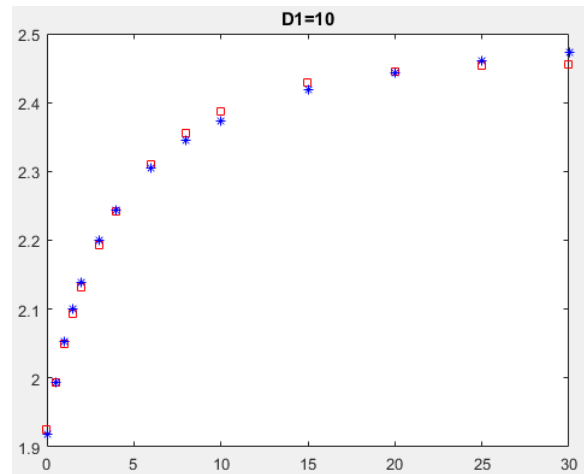


(h) When D_1 is fixed to 6mm

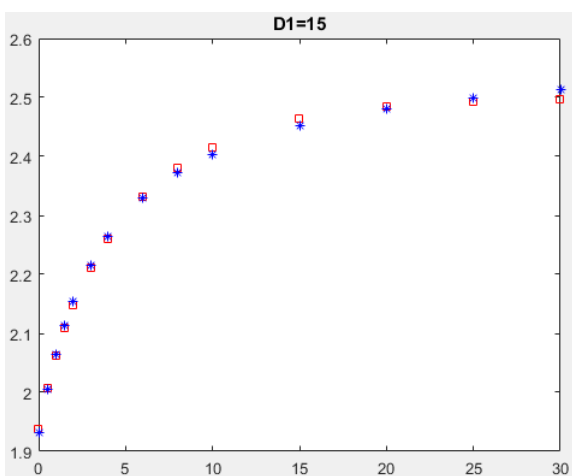




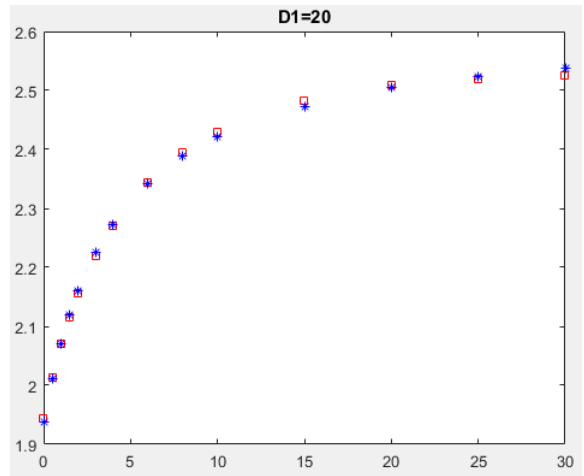
(i) When D_1 is fixed to 8mm



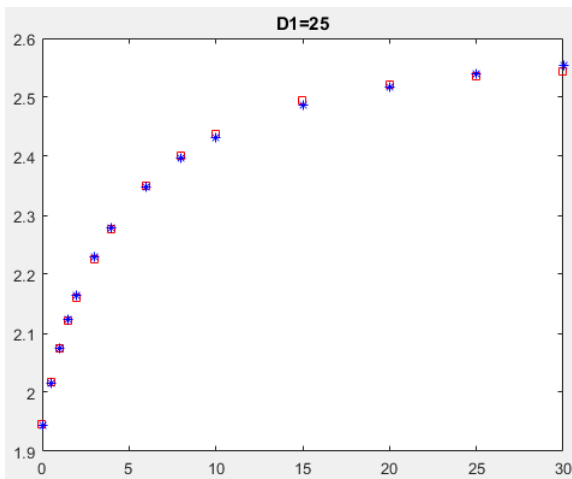
(j) When D_1 is fixed to 10mm



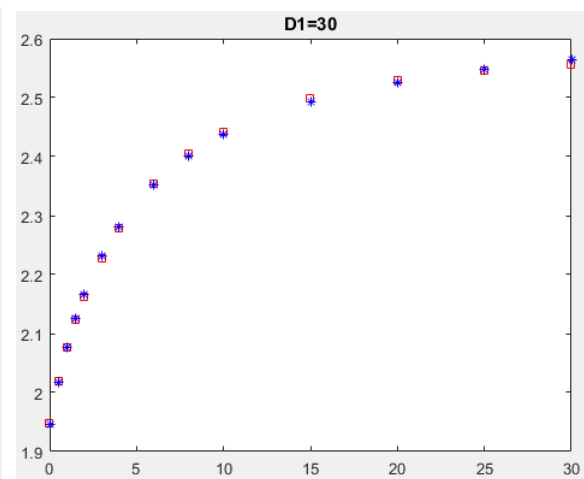
(k) When D_1 is fixed to 15mm



(l) When D_1 is fixed to 20mm



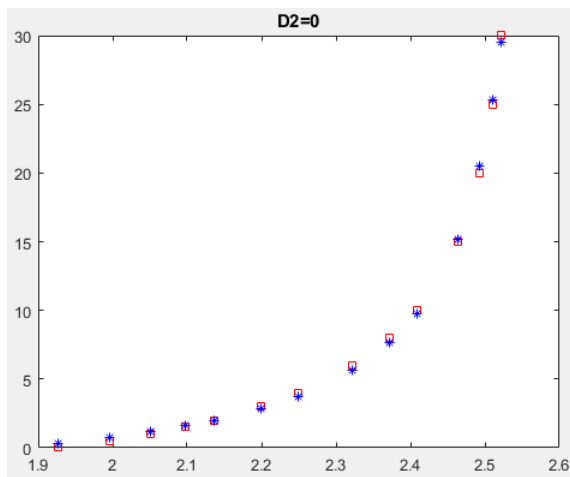
(m) When D_1 is fixed to 25mm



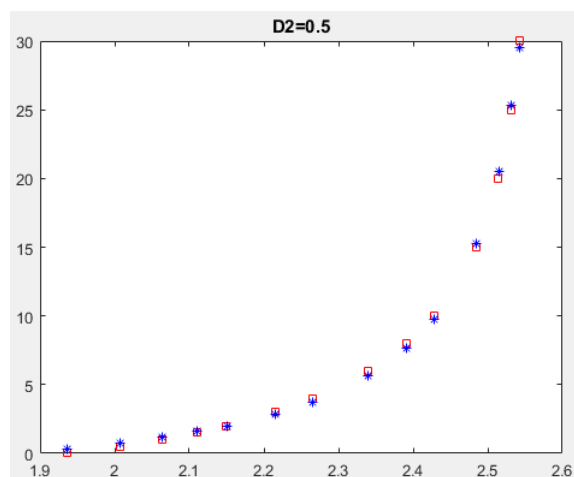
(n) When D_1 is fixed to 30mm

Fig. I-1 Fitted curves for $V_2=f(D_2)$

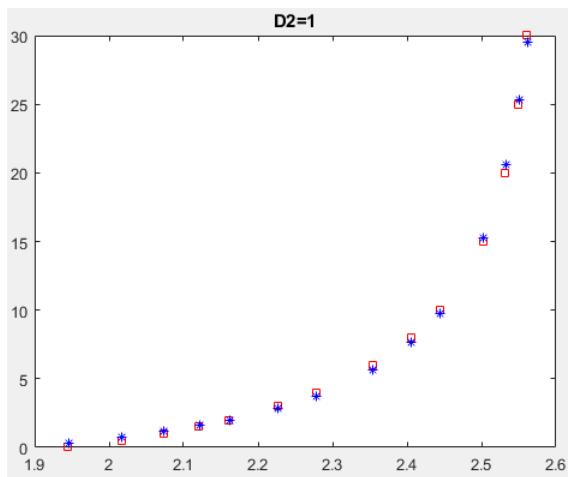
Appendix J: Nonlinear Fitting Results for Equation $D_1=f(V_1)$



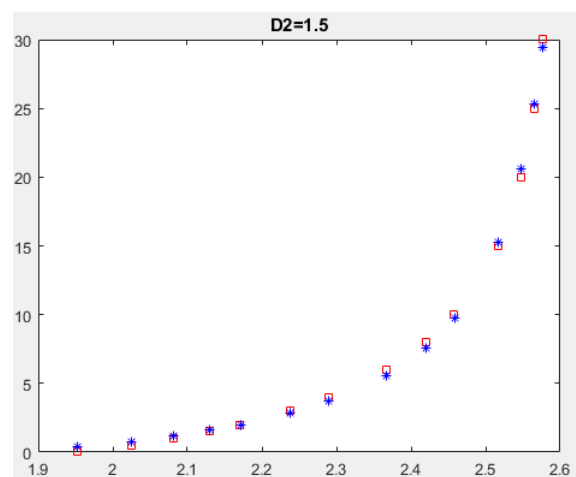
(a) When D_2 is fixed to 0mm



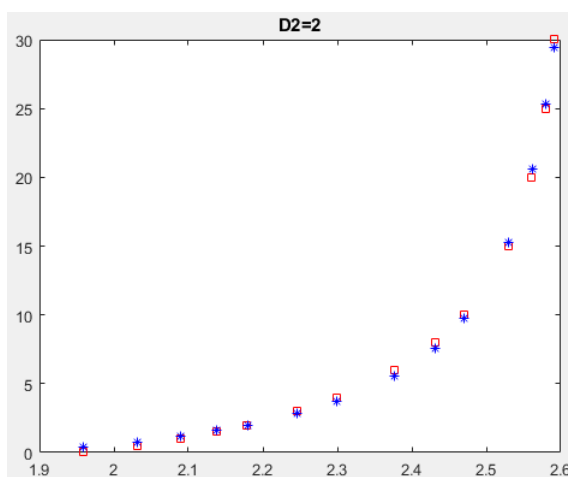
(b) When D_2 is fixed to 0.5mm



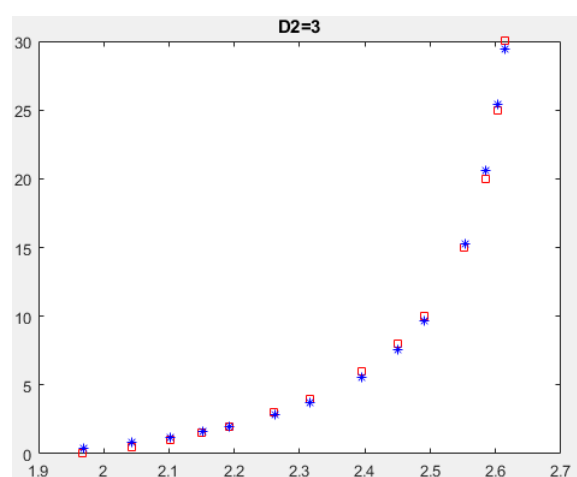
(c) When D_2 is fixed to 1mm



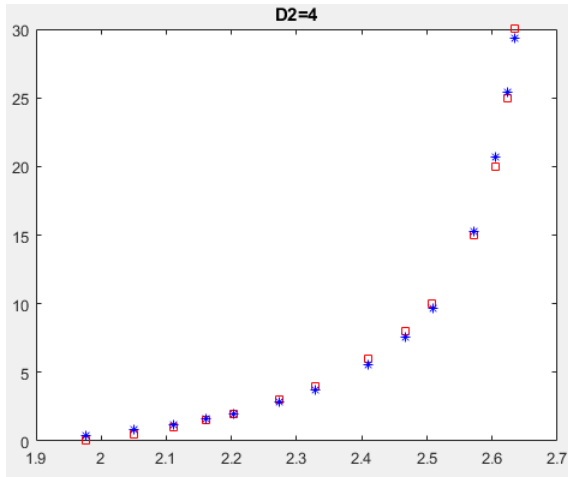
(d) When D_2 is fixed to 1.5mm



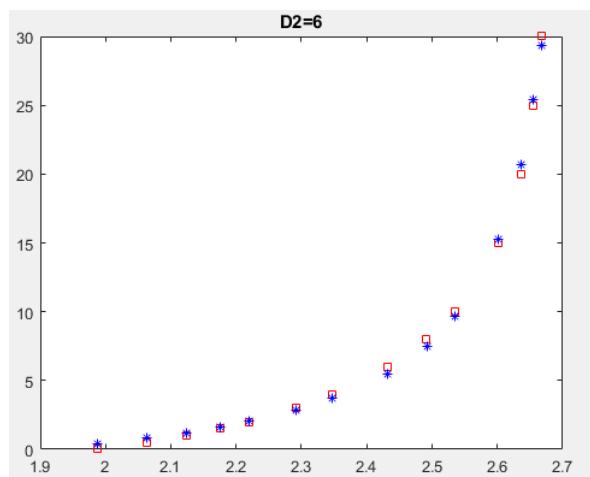
(e) When D_2 is fixed to 2mm



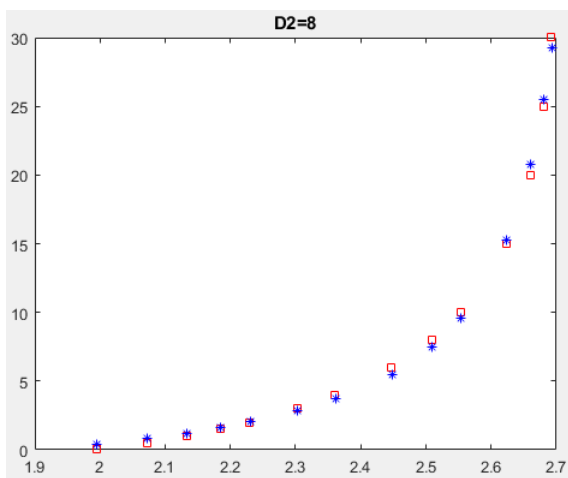
(f) When D_2 is fixed to 3mm



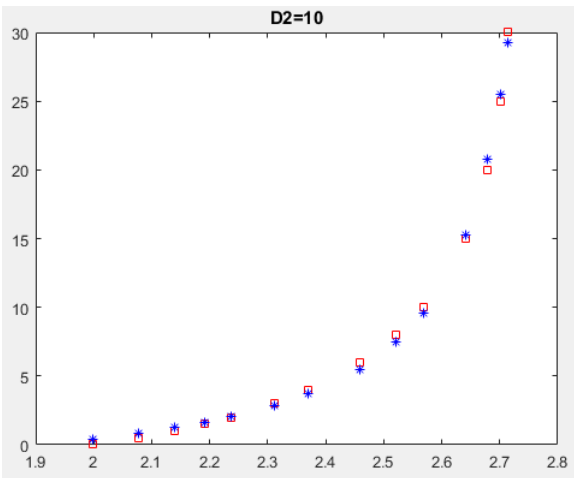
(g) When D_2 is fixed to 4mm



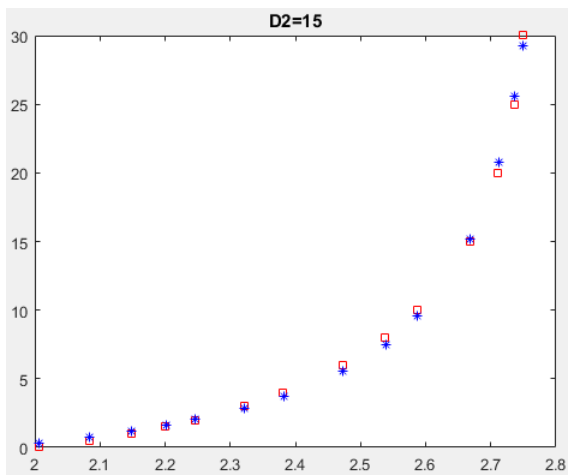
(h) When D_2 is fixed to 6mm



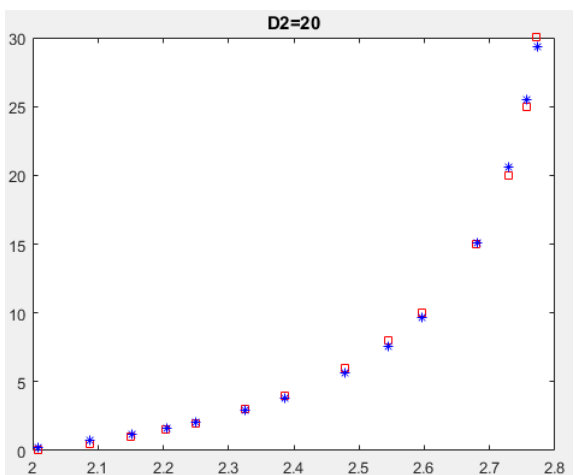
(i) When D_2 is fixed to 8mm



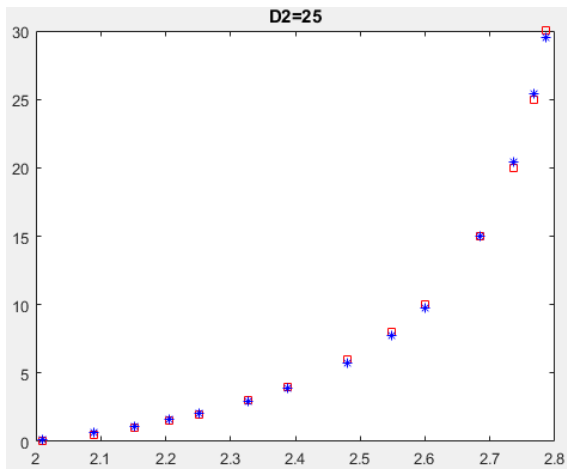
(j) When D_2 is fixed to 10mm



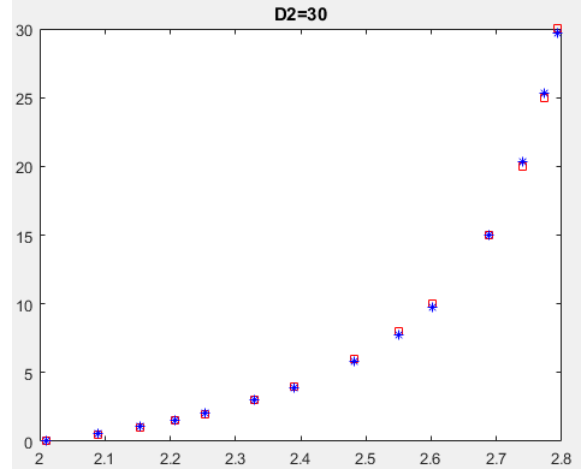
(k) When D_2 is fixed to 15mm



(l) When D_2 is fixed to 20mm



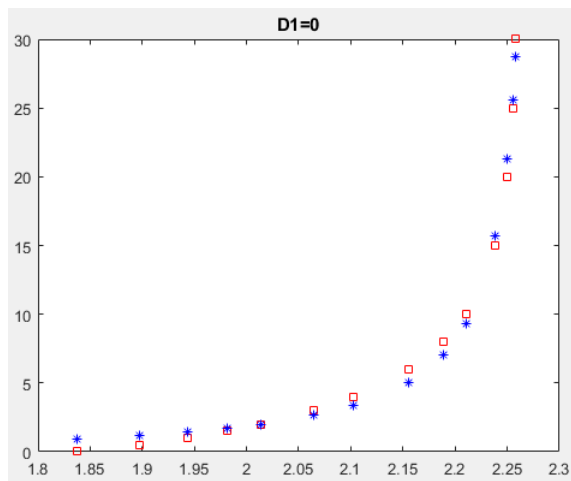
(m) When D_2 is fixed to 25mm



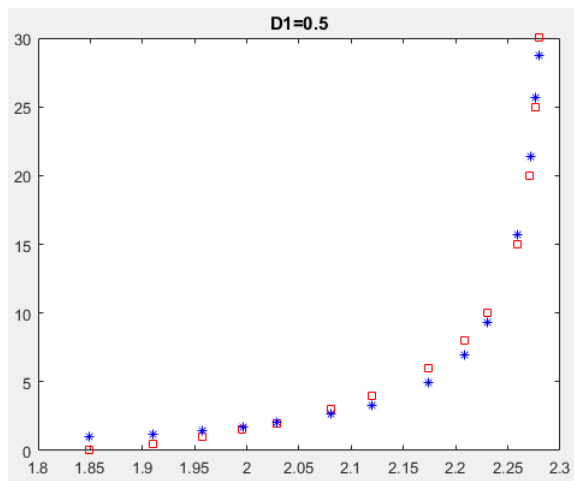
(n) When D_2 is fixed to 30mm

Fig. J-1 Fitted curves for $V_1=f(D_1)$

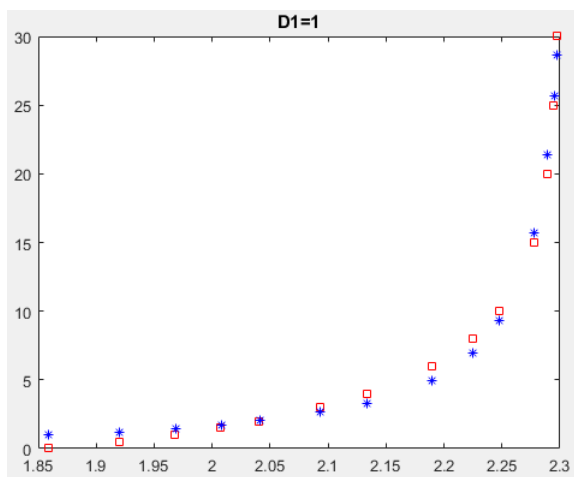
Appendix K: Nonlinear Fitting Results for Equation $D_2=f(V_2)$



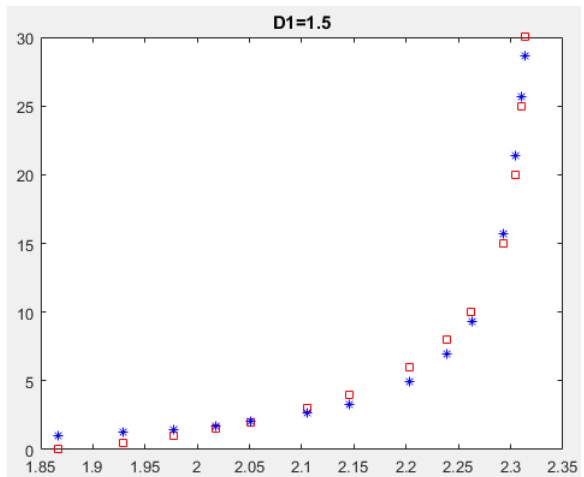
(a) When D_1 is fixed to 0mm



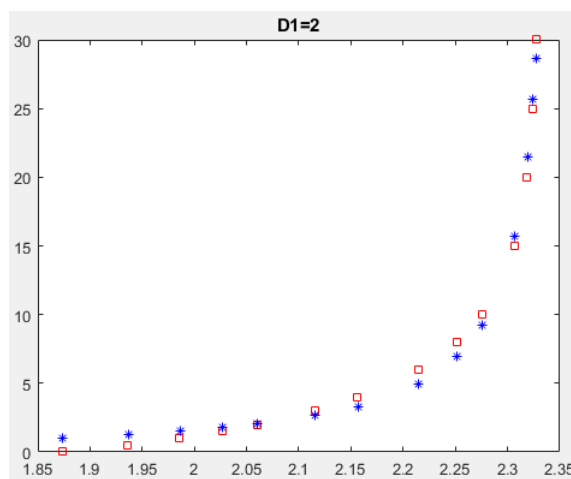
(b) When D_1 is fixed to 0.5mm



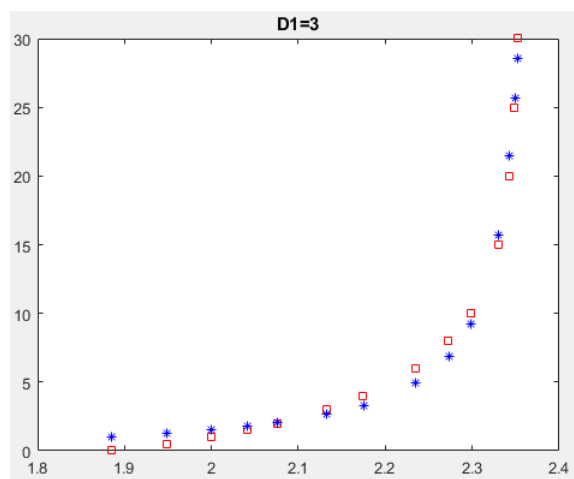
(c) When D_1 is fixed to 1mm



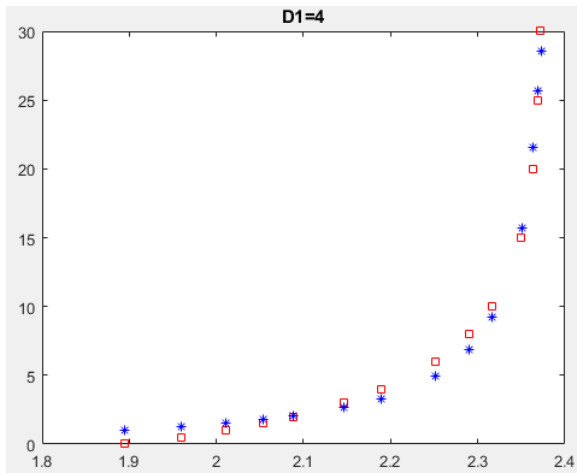
(d) When D_1 is fixed to 1.5mm



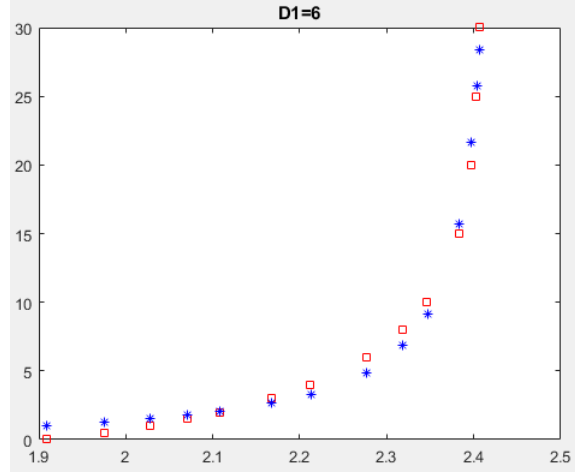
(e) When D_1 is fixed to 2mm



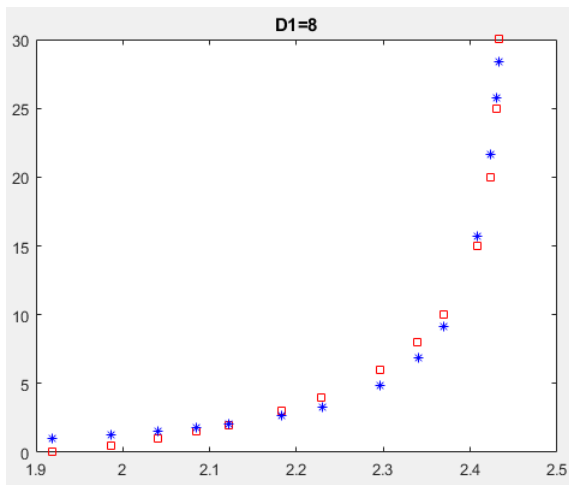
(f) When D_1 is fixed to 3mm



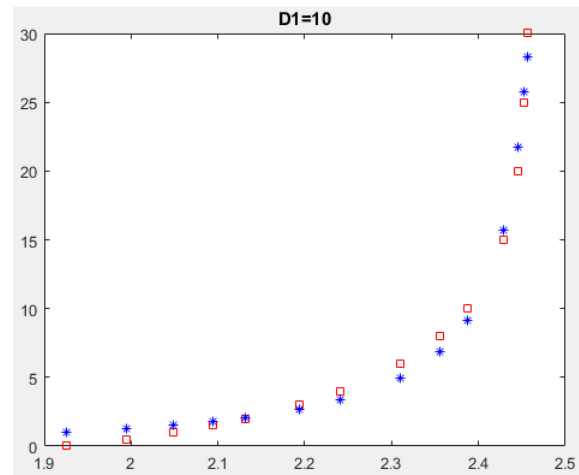
(g) When D_1 is fixed to 4mm



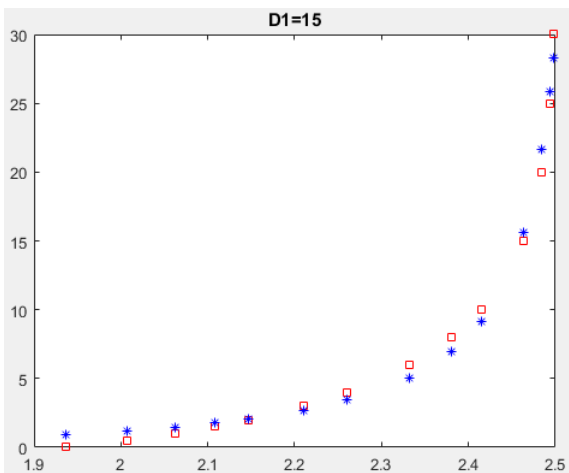
(h) When D_1 is fixed to 6mm



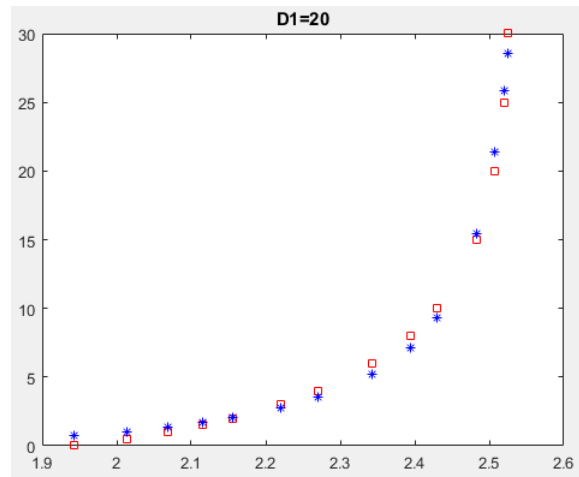
(i) When D_1 is fixed to 8mm



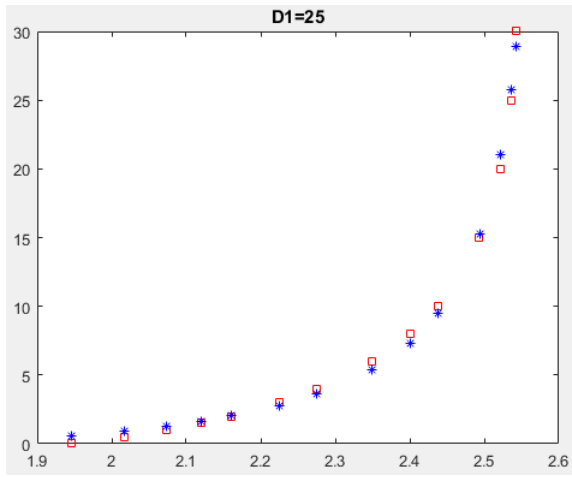
(j) When D_1 is fixed to 10mm



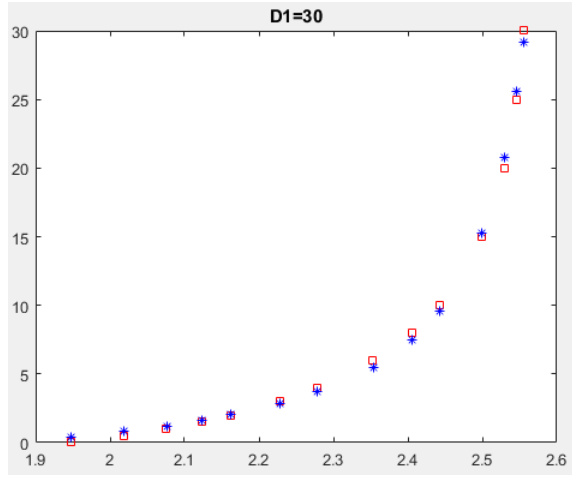
(k) When D_1 is fixed to 15mm



(l) When D_1 is fixed to 20mm



(m) When D_1 is fixed to 25mm



(n) When D_1 is fixed to 30mm

Fig. K-1 Fitted curves for $D_2=f(V_2)$

Appendix L: Improvement of Accuracy using the Prediction Models

Table L-1 Variation of D_1 using raw data to detect index finger's movement

V_1		D-index													
		0	0.5	1	1.5	2	3	4	6	8	10	15	20	25	30
D-middle	0	1.926 628	1.996 114	2.051 489	2.097 38	2.136 402	2.199 753	2.249 311	2.321 951	2.372 167	2.408 331	2.463 76	2.493 269	2.510 612	2.521 627
	0.5	1.936 931	2.007 477	2.063 772	2.110 439	2.150 159	2.214 726	2.265 293	2.339 518	2.390 88	2.427 883	2.484 529	2.514 58	2.532 154	2.543 276
	1	1.945 303	2.016 739	2.073 79	2.121 121	2.161 432	2.227 026	2.278 455	2.354 047	2.406 41	2.444 15	2.501 872	2.532 387	2.550 156	2.561 355
	1.5	1.952 348	2.024 538	2.082 241	2.130 146	2.170 974	2.237 466	2.289 655	2.366 453	2.419 732	2.458 151	2.516 857	2.547 797	2.565 739	2.576 996
	2	1.958 384	2.031 248	2.089 524	2.137 935	2.179 22	2.246 512	2.299 389	2.377 289	2.431 405	2.470 448	2.530 096	2.561 435	2.579 53	2.590 845
	3	1.968 271	2.042 252	2.101 497	2.150 771	2.192 838	2.261 511	2.315 578	2.395 451	2.451 096	2.491 31	2.552 738	2.584 85	2.603 242	2.614 65
	4	1.976 014	2.050 902	2.110 933	2.160 913	2.203 627	2.273 457	2.328 541	2.410 136	2.467 164	2.508 476	2.571 622	2.604 508	2.623 2	2.634 702
	6	1.987 185	2.063 422	2.124 646	2.175 704	2.219 412	2.291 054	2.347 773	2.432 248	2.491 714	2.535 044	2.601 603	2.636 131	2.655 493	2.667 215
	8	1.994 551	2.071 709	2.133 755	2.185 564	2.229 974	2.302 918	2.360 852	2.447 586	2.509 088	2.554 239	2.624 181	2.660 533	2.680 709	2.692 73

	10	1.999 489	2.077 277	2.139 886	2.192 214	2.237 113	2.310 983	2.369 798	2.458 235	2.521 408	2.568 141	2.641 351	2.679 703	2.700 855	2.713 281
	15	2.006 02	2.084 639	2.147 99	2.201 003	2.246 554	2.321 668	2.381 704	2.472 631	2.538 433	2.587 925	2.667 944	2.711 583	2.735 867	2.749 806
	20	2.008 754	2.087 703	2.151 341	2.204 617	2.250 415	2.326 001	2.386 504	2.478 426	2.545 352	2.596 159	2.680 245	2.728 343	2.756 225	2.772 372
	25	2.010 087	2.089 18	2.152 942	2.206 327	2.252 223	2.327 993	2.388 671	2.480 954	2.548 321	2.599 657	2.685 636	2.736 478	2.767 437	2.786 121
	30	2.010 857	2.090 026	2.153 848	2.207 285	2.253 226	2.329 074	2.389 831	2.482 247	2.549 775	2.601 313	2.688 067	2.740 244	2.773 15	2.794 04
Difference values			0.069 486	0.055 375	0.045 892	0.039 021	0.063 352	0.049 558	0.072 64	0.050 216	0.036 164	0.055 429	0.029 51	0.017 342	0.011 016
Difference values		0.084 228	0.093 912	0.102 359	0.109 904	0.116 825	0.129 32	0.140 519	0.160 295	0.177 608	0.192 982	0.224 307	0.246 974	0.262 539	0.272 413
Difference distance		1	1	2	2.5	4	5	6	14	37	60	95	110	120	125
Percentage of difference distance			2	2	1.666 667	2	1.666 667	1.5	2.333 333	4.625	6	6.333 333	5.5	4.8	4.166 667

Note: 1) The difference value is the real voltage difference when middle finger is fixed to zero. 2) Difference voltage values of each index distance, resulted from middle finger, will decide the wrong distance value. 3) To compare the wrong distance decided by both Index finger and Middle finger with the real distance of index finger, we get the difference distance. 4) The values of index distance more than 30 are predicted to increase in the same trend of the last data point.

Table L-2 Variation of D_2 using raw data to detect middle finger's movement

V_2		I-index														Difference values	Difference values	Difference distance	Percentage of difference distance
		0	0.5	1	1.5	2	3	4	6	8	10	15	20	25	30				
D-middle	0	1.837881	1.849288	1.858687	1.866679	1.87362	1.885174	1.894466	1.908476	1.918404	1.925651	1.936824	1.942725	1.946155	1.948303		0.110421706	1.5	
	0.5	1.897153	1.909649	1.919978	1.928773	1.936424	1.949196	1.959489	1.975057	1.986117	1.994197	2.006637	2.013187	2.016966	2.019327	0.059272065	0.122173483	2.5	5
	1	1.943686	1.957111	1.968222	1.977696	1.985949	1.999757	2.010912	2.027832	2.039874	2.048684	2.062237	2.069344	2.073423	2.075956	0.046532528	0.132270613	3	3
	1.5	1.981702	1.99592	2.007707	2.017775	2.026555	2.041274	2.05319	2.071309	2.084247	2.093724	2.108282	2.11589	2.120236	2.122917	0.038015985	0.141215627	4.5	3
	2	2.01354	2.028465	2.040853	2.051442	2.060696	2.076226	2.088833	2.108042	2.1218	2.131885	2.14739	2.15546	2.160044	2.162864	0.031838499	0.149323825	6	3
	3	2.064081	2.080191	2.093596	2.105087	2.115149	2.132092	2.145902	2.167069	2.182314	2.193529	2.210786	2.219716	2.224737	2.227798	0.050540242	0.163717405	12	4
	4	2.102293	2.119372	2.133609	2.145842	2.156577	2.174715	2.189562	2.212445	2.229035	2.2413	2.260202	2.269949	2.275378	2.278656	0.038212575	0.176362617	66	16.5

	6	2.15 5264	2.17 3798	2.18 9311	2.20 2687	2.21 4469	2.23 45	2.25 1031	2.27 6821	2.29 5797	2.30 9985	2.33 208	2.34 3439	2.34 9666	2.35 3352	0.05297 1024	0.19808 7976	189	31.5
	8	2.18 8769	2.20 8299	2.22 4693	2.23 8873	2.25 1406	2.27 2818	2.29 0625	2.31 8736	2.33 9747	2.35 569	2.38 0911	2.39 3947	2.40 1015	2.40 5113	0.03350 4345	0.21634 4896	277	34.625
	10	2.21 0582	2.23 0791	2.24 7788	2.26 2522	2.27 5579	2.29 7979	2.31 6727	2.34 6631	2.36 9344	2.38 6845	2.41 5107	2.42 9926	2.43 7903	2.44 2459	0.02181 3954	0.23187 6178	340	34
	15	2.23 8589	2.25 9655	2.27 7417	2.29 2861	2.30 6593	2.33 03	2.35 0341	2.38 2895	2.40 8376	2.42 8701	2.46 3509	2.48 3025	2.49 3706	2.49 9646	0.02800 629	0.26105 7269	430	28.666 66667
	20	2.24 9944	2.27 1306	2.28 9322	2.30 4996	2.31 8951	2.34 3092	2.36 358	2.39 7138	2.42 3798	2.44 5506	2.48 4412	2.50 8042	2.52 1788	2.52 9545	0.01135 5261	0.27960 0554	480	24
	25	2.25 5284	2.27 6745	2.29 484	2.31 0584	2.32 46	2.34 8859	2.36 9473	2.40 3327	2.43 0397	2.45 2633	2.49 3469	2.51 9736	2.53 6195	2.54 6028	0.00534 0251	0.29074 3805	500	20
	30	2.25 8199	2.27 9692	2.29 781	2.31 3569	2.32 7597	2.35 1875	2.37 2514	2.40 6426	2.43 3603	2.45 6009	2.49 7592	2.52 516	2.54 3402	2.55 5096	0.00291 4721	0.29689 6595	500	16.666 66667

Note: 1) The difference value is the real voltage difference when index finger is fixed to zero. 2) Difference voltage values of each middle distance, resulted from index finger, will decide the wrong distance value. 3) To compare the wrong distance decided by both Index finger and Middle finger with the real distance of Middle finger, we get the difference distance. 4) Then, the percentage of difference distance compared with real distance of middle finger is calculated. 5) The values of middle distance more than 30 are predicted to increase in the same trend of the last data point.

Table L-3 Variation of D_1 using prediction model $D_1=f(V_1, V_2)$ to detect movement of index finger

		0	0.5	1	1.5	2	3	4	6	8	10	15	20	25	30
D_2	0	1.8052 16	1.5431 02	1.2795 7	1.0186 15	0.7626 76	0.2713 45	0.1868 38	0.9891 48	1.6281 13	2.1013 59	2.6076 05	2.3095 59	1.4198 09	0.1204 9

0.5	1.8570 58	1.6036 01	1.3489 87	1.0971 03	0.8506 67	0.3798 64	0.0556 52	0.8050 04	1.3803 54	1.7787 4	2.055	1.4864 09	0.3184 18	1.2449 57
1	1.8990 33	1.6525 2	1.4049 28	1.1602 5	0.9212 66	0.4663 25	0.0480 97	0.6619 11	1.1916 11	1.5386 43	1.6739 07	0.9793 91	0.2584 22	1.8059 25
1.5	1.9341 86	1.6933 76	1.4515 42	1.2127 37	0.9797 96	0.5375 68	0.1329 58	0.5470 39	1.0428 71	1.3536 87	1.4050 05	0.6728 3	0.5136 96	1.8917 18
2	1.9641 74	1.7282 29	1.4912 3	1.2573 16	1.0293 8	0.5975 48	0.2039 92	0.4523 23	0.9227 75	1.2083 03	1.2121 03	0.4953 73	0.5714 08	1.7100 54
3	2.0129 11	1.7846 97	1.5553 77	1.3291 81	1.1090 52	0.6932 07	0.3161 48	0.3057 19	0.7415 45	0.9955 72	0.9672 89	0.3577 08	0.3973 77	1.0027 44
4	2.0506 9	1.8283 95	1.6048 65	1.3844 27	1.1700 76	0.7658 59	0.4005 08	0.1981 05	0.6123 63	0.8492 45	0.8273 96	0.3528 32	0.0924 56	0.2165 75
6	2.1044 55	1.8904 21	1.6749 43	1.4623 97	1.2558 36	0.8669 86	0.5166 57	0.0535 64	0.4436 66	0.6644 91	0.6746 43	0.4201 14	0.4409 92	1.0054 92
8	2.1393 56	1.9305 99	1.7202	1.5125 75	1.3107 95	0.9311 56	0.5895 66	0.0352 15	0.3423 48	0.5544 24	0.5759 71	0.4304 42	0.7043 9	1.6530 26
10	2.1624 82	1.9571 76	1.7500 59	1.5455 78	1.3468 22	0.9729 15	0.6365 78	0.0912 17	0.2786 35	0.4841 34	0.4924 47	0.3622 17	0.7284 67	1.8581 31
15	2.1926 92	1.9917 76	1.7887 6	1.5881 44	1.3930 45	1.0258 15	0.6953 46	0.1593 71	0.2029 9	0.3993 22	0.3377 71	0.0373 56	0.2286 49	1.3067 22
20	2.2051 87	2.0059 85	1.8045 17	1.6053 13	1.4114 97	1.0464 65	0.7176 7	0.1836 65	0.1784 44	0.3736 52	0.2692 34	0.2329 02	0.4277 77	0.2390 48

	25	2.2112 09	2.0127 83	1.8120 11	1.6134 13	1.4201 21	1.0558 99	0.7275 88	0.1933 95	0.1698 05	0.3667 74	0.2514 76	0.3610 95	0.8800 82	0.7140 29
	30	2.2146 33	2.0166 5	1.8162 57	1.6179 89	1.4249 83	1.0611 74	0.7331 69	0.1986 42	0.1657 08	0.3644 53	0.2502 57	0.4040 63	1.1029 49	1.3364 44
	Average	2.0538 06	1.8313 79	1.6073 75	1.3860 74	1.1704 29	0.7622 95	0.4257 69	0.3481 65	0.6643 74	0.9309 14	0.9714 36	0.6358 78	0.5774 92	1.1503 83

Table L-4 Variation of D_2 using prediction model $D_2=f(V_1, V_2)$ to detect movement of middle finger

		D ₁														
		0	0.5	1	1.5	2	3	4	6	8	10	15	20	25	30	Average
D ₂	0	1.3299 68	1.3494 2	1.3647 68	1.3773 08	1.3877 99	1.4044 18	1.4169 96	1.4345 54	1.4458 8	1.4534 92	1.4639 24	1.4686 05	1.4710 02	1.4723 38	1.4171 77
	0.5	1.0443	1.0671 6	1.0850 95	1.0996 21	1.1116 68	1.1305 37	1.1445 72	1.1637 06	1.1756 1	1.1832 88	1.1930 42	1.1968 69	1.1985 26	1.1993 16	1.1423 79
	1	0.7658 51	0.7924 01	0.8130 42	0.8295 91	0.8431 95	0.8642 27	0.8795 79	0.8999 23	0.9119 72	0.9193 34	0.9276 13	0.9300 11	0.9305 69	0.9305 36	0.8741 32
	1.5	0.4984 23	0.5289 11	0.5524 16	0.5711 04	0.5862 82	0.6094 38	0.6259 61	0.6471 05	0.6589 21	0.6655 68	0.6714 59	0.6718	0.6708 49	0.6696 96	0.6162 81
	2	0.2444 94	0.2793 55	0.3059 65	0.3268 68	0.3437 16	0.3689 2	0.3865 16	0.4080 36	0.4191 39	0.4245 55	0.4271 17	0.4246 91	0.4217 17	0.4191 55	0.3714 46

3	0.2153 79	0.1704 28	0.1367 69	0.1108 77	0.0905 28	0.0612 17	0.0419 59	0.0209 02	0.0127 87	0.0113 51	0.0189 59	0.0294 14	0.0380 83	0.0446 37	0.0716 64
4	0.6026 24	0.5451 24	0.5030 1	0.4713 41	0.4470 97	0.4136 39	0.3932 45	0.3745 92	0.3717 65	0.3765 96	0.3998 64	0.4223 42	0.4394 22	0.4518 01	0.4437 47
6	1.1321 52	1.0397 94	0.9745 69	0.9279	0.8942 4	0.8521 07	0.8312 46	0.8233 06	0.8383 14	0.8637 34	0.9372 29	0.9990 76	1.0436 59	1.0748 83	0.9451 58
8	1.3222 67	1.1774 97	1.0787 62	1.0112 37	0.9650 77	0.9134 66	0.8942 38	0.9038 46	0.9446 88	0.9993 39	1.1486 67	1.2741 61	1.3642 24	1.4270 01	1.1017 48
10	1.2088 73	0.9903 53	0.8457 74	0.7510 32	0.6895 7	0.6283 64	0.6130 64	0.6444 25	0.7121 53	0.7974 45	1.0354 48	1.2471 72	1.4038 69	1.5130 49	0.9343 28
15	0.2597 96	0.2226 47	0.5198 38	0.6940 41	0.7889 55	0.8478 94	0.8269 56	0.7282 06	0.6313 6	0.5373 02	0.2313 48	0.1676 06	0.5399 56	0.8256 52	0.5586 83
20	0.2672 13	1.0366 15	1.4715 58	1.6861 1	1.7668 82	1.7234 68	1.5859 94	1.3422 67	1.2389 28	1.2407	1.3203 3	1.1468 14	0.7420 42	0.3078 86	1.2054 86
25	0.4154 81	0.5761 34	1.0843 21	1.2817 56	1.2913 61	1.0530 49	0.7272 69	0.2334 17	0.0567 21	0.1166 48	0.6844 13	1.1260 38	1.1230 88	0.7997 44	0.7549 6
30	2.1985 23	1.0578 37	0.5259 5	0.3867 62	0.4723 94	0.9382 95	1.4697 3	2.2502 33	2.5570 75	2.5164 64	1.6825 06	0.7063 13	0.1213 92	0.0295 01	1.2080 7

Table L-5 Variation of D_1 using prediction model $D_1=f(V_1)$ to detect movement of index finger

NO.1 $D_2=0\text{mm}$	NO.2 $D_2=0.5\text{mm}$	NO.3 $D_2=1\text{mm}$	NO.4 $D_2=1.5\text{mm}$	NO.5 $D_2=2\text{mm}$	NO.6 $D_2=3\text{mm}$	NO.7 $D_2=4\text{mm}$
-----------------------	-------------------------	-----------------------	-------------------------	-----------------------	-----------------------	-----------------------

D ₁	D _{1p}	Varition of D ₁	D _{1p}	Varition of D ₁	D _{1p}	Varition of D ₁	D _{1p}	Varition of D ₁	D _{1p}	Varition of D ₁	D _{1p}	Varition of D ₁	D _{1p}	Varition of D ₁
0	0.316801	0.316801109	0.329147	0.329146826	0.34054	0.340540067	0.351185	0.351185485	0.36085	0.360850233	0.378102	0.378101866	0.392278	0.392277977
0.5	0.743849	0.243848633	0.752868	0.252867937	0.761322	0.26132183	0.769284	0.26928371	0.776661	0.276660743	0.790049	0.290049178	0.801482	0.301481786
1	1.162091	0.162091392	1.16814	0.168140255	1.173796	0.173796371	1.179219	0.179218909	1.184339	0.184339481	1.193919	0.19391877	1.202472	0.202471784
1.5	1.578988	0.078988055	1.581989	0.081989479	1.584988	0.084988011	1.587979	0.087978609	1.5909	0.090899868	1.59672	0.096719756	1.602318	0.102318302
2	1.998844	0.001155894	1.999042	0.000958369	1.999499	0.000501193	2.000164	0.000163552	2.000971	0.000971239	2.003079	0.003078605	2.005688	0.005687724
3	2.856225	0.143775172	2.851561	0.148439353	2.847444	0.152556302	2.843848	0.156151933	2.840686	0.159314449	2.835654	0.164345678	2.832272	0.167728093
4	3.74484	0.255160041	3.736128	0.263871989	3.72819	0.271809659	3.72092	0.2790797	3.7144	0.285599755	3.702854	0.297145778	3.693749	0.306251362
6	5.626342	0.37365789	5.612906	0.387094492	5.6002	0.399799734	5.587828	0.412171594	5.576506	0.423493859	5.555619	0.444380793	5.537399	0.462600748
8	7.638276	0.361724107	7.624365	0.37563486	7.61096	0.389039518	7.597915	0.402084985	7.585492	0.414507516	7.561678	0.438321609	7.539635	0.460364861
10	9.751175	0.248825333	9.741077	0.25892337	9.731054	0.268945834	9.721351	0.278648542	9.711265	0.288735105	9.691644	0.308356486	9.672683	0.327316713

15	15.21861	0.218605467	15.22665	0.226654608	15.23429	0.234289833	15.24125	0.241254206	15.24805	0.248046912	15.25959	0.259592909	15.26862	0.268619364
20	20.51667	0.516666381	20.53704	0.537042029	20.55621	0.556212981	20.57467	0.574665123	20.59305	0.59304995	20.62804	0.628035745	20.66111	0.661109082
25	25.32204	0.322039128	25.33238	0.332376585	25.34311	0.343106825	25.35422	0.354221011	25.36353	0.363529961	25.38373	0.383727518	25.40362	0.403615884
30	29.52526	0.474737848	29.50671	0.493291581	29.4884	0.511600176	29.47017	0.529830697	29.4533	0.546699831	29.41932	0.580675414	29.38668	0.613320814
D ₁	NO.8		NO.9		NO.10		NO.11		NO.12		NO.13		NO.14	
	D _{1p}	Varition of D ₁	D _{1p}	Varition of D ₁	D _{1p}	Varition of D ₁	D _{1p}	Varition of D ₁	D _{1p}	Varition of D ₁	D _{1p}	Varition of D ₁	D _{1p}	Varition of D ₁
0	0.411073	0.411072913	0.416535	0.41653453	0.40872	0.408719553	0.340685	0.340684621	0.237226	0.237226173	0.139551	0.139551012	0.069748	0.069748244
0.5	0.817935	0.317934853	0.825144	0.325144479	0.822802	0.322801967	0.780507	0.280506533	0.709929	0.209928956	0.641508	0.141508487	0.592083	0.09208267
1	1.216055	0.216055442	1.224065	0.224065301	1.225927	0.225927349	1.205405	0.205404655	1.163528	0.163527846	1.120897	0.120897373	1.089458	0.089458407
1.5	1.612544	0.112543931	1.620549	0.120549319	1.62556	0.125560478	1.623598	0.123598301	1.607125	0.107125315	1.587554	0.087554188	1.572269	0.072268985
2	2.012147	0.012146551	2.01943	0.019430353	2.026668	0.026668497	2.040488	0.040487641	2.04661	0.046609945	2.047814	0.047813917	2.047166	0.047165652
3	2.830364	0.169636465	2.834434	0.16556581	2.843714	0.156285524	2.881559	0.118440758	2.925365	0.074635334	2.962104	0.037896356	2.986722	0.013278004

4	3.6829 01	0.317099 129	3.6819 46	0.318054 164	3.6904 19	0.309581 246	3.7430 8	0.256919 503	3.8151 86	0.184813 98	3.8800 4	0.119960 415	3.9252 05	0.074795 084
6	5.5100 79	0.489920 874	5.4964 3	0.503570 261	5.4967 62	0.503238 197	5.5541 23	0.445877 308	5.6559 4	0.344059 75	5.7553 3	0.244669 81	5.8272 49	0.172750 61
8	7.5025	0.497500 091	7.4768 44	0.523155 933	7.4653 7	0.534629 893	7.5001 8	0.499820 164	7.5964 93	0.403507 209	7.7021 72	0.297827 578	7.7823 75	0.217624 662
10	9.6362 74	0.363725 814	9.6056 9	0.394310 429	9.5839 85	0.416015 256	9.5802	0.419800 14	9.6405 69	0.359430 592	9.7244 52	0.275548 478	9.7944 87	0.205513 457
15	15.279 38	0.279379 509	15.278 61	0.278610 054	15.265 84	0.265835 79	15.191 05	0.191053 91	15.100 47	0.100470 117	15.042 08	0.042081 076	15.018 65	0.018648 274
20	20.720 09	0.720085 721	20.765 78	0.765783 501	20.794 43	0.794433 478	20.771 39	0.771392 752	20.629 14	0.629137 457	20.450 22	0.450222 799	20.313 43	0.313425 096
25	25.442 14	0.442139 391	25.478 08	0.478083 598	25.508 57	0.508569 646	25.552 79	0.552788 207	25.528 1	0.528103 892	25.436 52	0.436516 625	25.325 32	0.325322 309
30	29.326 52	0.673475 876	29.276 46	0.723544 348	29.241 23	0.758766 609	29.234 94	0.765058 719	29.344 32	0.655682 716	29.509 76	0.490242 811	29.655 84	0.344157 813

Table L-6 Variation of D_2 using prediction model $D_2=f(V_2)$ to detect movement of middle finger

D ₂	NO.1 D1=0mm		NO.2 D1=0.5mm		NO.3 D1=1mm		NO.4 D1=1.5mm		NO.5 D1=2mm		NO.6 D1=3mm		NO.7 D1=4mm	
	D _{2p}	Varition of D ₂	D _{2p}	Varition of D ₂	D _{2p}	Varition of D ₂	D _{2p}	Varition of D ₂	D _{2p}	Varition of D ₂	D _{2p}	Varition of D ₂	D _{2p}	Varition of D ₂

0	0.9540 12	0.954012 424	0.9654 77	0.965477 124	0.9762 15	0.976215 225	0.9863 06	0.986306 41	0.9956 03	0.995602 615	1.0114 28	1.011428 184	1.0230 38	1.023037 771
0. 5	1.2030 69	0.703069 054	1.2127 05	0.712705 33	1.2218 08	0.721807 577	1.2304 15	0.730415 004	1.2384 26	0.738425 891	1.2523 66	0.752365 773	1.2630 61	0.763061 013
1	1.4596 18	0.459617 542	1.4673 84	0.467384 482	1.4747 34	0.474733 969	1.4817 3	0.481730 044	1.4883 27	0.488327 489	1.5000 97	0.500096 856	1.5095 74	0.509573 765
1. 5	1.7280 85	0.228085 018	1.7337 98	0.233797 603	1.7392 57	0.239256 744	1.7445 49	0.244549 408	1.7495 94	0.249594 363	1.7589 3	0.258930 269	1.7668 71	0.266870 916
2	2.0112 8	0.011279 854	2.0149 08	0.014908 199	2.0183 85	0.018384 872	2.0218 08	0.021808 149	2.0252 26	0.025226 14	2.0318 11	0.031811 048	2.0379 62	0.037962 432
3	2.6302 14	0.369786 211	2.6293 1	0.370689 505	2.6285 38	0.371462 056	2.6280 28	0.371971 99	2.6278 13	0.372187 379	2.6282 28	0.371771 63	2.6298 72	0.370128 059
4	3.3283 96	0.671603 673	3.3228 91	0.677109 462	3.3176 22	0.682378 431	3.3129 1	0.687089 833	3.3087 85	0.691215 413	3.3023 43	0.697657 169	3.2985 92	0.701407 909
6	4.9887 32	1.011267 672	4.9747 39	1.025260 537	4.9614 41	1.038558 935	4.9488 7	1.051129 905	4.9370 94	1.062905 651	4.9166 91	1.083308 672	4.9008 27	1.099173 148
8	7.0056 91	0.994308 652	6.9869 08	1.013092 426	6.9688 98	1.031102 428	6.9515 71	1.048429 457	6.9350 3	1.064970 179	6.9047 67	1.095233 012	6.8792 52	1.120747 596
1 0	9.3261 66	0.673833 66	9.3088 83	0.691116 611	9.2922 01	0.707799 085	9.2757 93	0.724206 607	9.2598 99	0.740101 248	9.2295 09	0.770490 672	9.2022 11	0.797789 263
1 5	15.67	0.669998 776	15.678 9	0.678896 491	15.688 19	0.688189 127	15.697 26	0.697264 733	15.705 42	0.705419 138	15.720 07	0.720073 907	15.731 48	0.731481 64

20	21.33281	1.332808736	21.36043	1.36042762	21.38751	1.387512573	21.41359	1.413592494	21.44015	1.440152892	21.49083	1.49083316	21.53741	1.53741038
25	25.61767	0.617667754	25.62879	0.628788915	25.63884	0.638837092	25.65025	0.650253179	25.65979	0.659792761	25.68011	0.68011128	25.698	0.698003933
30	28.74426	1.255738912	28.7149	1.285098668	28.68635	1.313648354	28.6569	1.343100402	28.62883	1.371167259	28.57281	1.427188931	28.52184	1.478155594
D ₂	NO.8 D ₂ =6mm		NO.9 D ₂ =8mm		NO.10 D ₂ =10mm		NO.11 D ₂ =15mm		NO.12 D ₂ =20mm		NO.13 D ₂ =25mm		NO.14 D ₂ =30mm	
	D _{2p}	Varition of D ₂	D _{2p}	Varition of D ₂	D _{2p}	Varition of D ₂	D _{2p}	Varition of D ₂	D _{2p}	Varition of D ₂	D _{2p}	Varition of D ₂	D _{2p}	Varition of D ₂
0	1.033756	1.033755589	1.025534	1.02553418	0.999689	0.999688522	0.874642	0.874642106	0.708584	0.708584372	0.551068	0.551067588	0.429698	0.429698227
0.5	1.274833	0.774832605	1.271678	0.771678046	1.254518	0.754517727	1.163332	0.663332369	1.039325	0.539325251	0.921374	0.421373657	0.830642	0.330642453
1	1.521684	0.521683923	1.522722	0.522721861	1.513306	0.513306456	1.453243	0.453243317	1.368166	0.368166273	1.286827	0.286827039	1.224309	0.224309475
1.5	1.778596	0.278596074	1.783134	0.283133647	1.780683	0.280682573	1.749483	0.24948327	1.700923	0.20092319	1.65393	0.153929754	1.617775	0.117775204
2	2.048615	0.048614649	2.055898	0.055897637	2.059572	0.059571933	2.055263	0.055263153	2.041081	0.041080541	2.026371	0.026370532	2.015065	0.015064547
3	2.636541	0.363459464	2.647108	0.352891882	2.660753	0.339247326	2.703955	0.296044657	2.75222	0.247780331	2.796414	0.203586182	2.830288	0.169712135
4	3.298794	0.701206281	3.309649	0.690350797	3.330008	0.669991969	3.411408	0.588591975	3.512868	0.487131697	3.607807	0.392193032	3.680685	0.319314865

6	4.8828 38	1.117161 903	4.8856 98	1.114302 313	4.9080 86	1.091914 332	5.0325 22	0.967478 113	5.2055 29	0.794470 916	5.3722 68	0.627732 361	5.5015 58	0.498442 268
8	6.8425 84	1.157416 202	6.8292 15	1.170784 752	6.8397 18	1.160281 932	6.9545 97	1.045403 493	7.1405 3	0.859469 7	7.3299 45	0.670055 025	7.4806 08	0.519392 287
1 0	9.1562 63	0.843736 609	9.1285 18	0.871482 14	9.1193 06	0.880693 65	9.1753 47	0.824653 163	9.3085 59	0.691440 718	9.4631 5	0.536850 219	9.5957 91	0.404208 53
1 5	15.742 97	0.742970 025	15.739 3	0.739303 272	15.716 94	0.716939 603	15.589 91	0.589911 347	15.420 83	0.420834 946	15.292 91	0.292909 217	15.228 32	0.228319 056
2 0	21.622 27	1.622266 417	21.679 94	1.679944 431	21.711 45	1.711453 653	21.644 08	1.644081 399	21.388 56	1.388561 026	21.060 73	1.060732 375	20.789 19	0.789192 048
2 5	25.735 91	0.735909 425	25.770 71	0.770713 122	25.801 35	0.801348 887	25.857 59	0.857593 105	25.852 89	0.852890 983	25.755 47	0.755468 802	25.598 8	0.598795 126
3 0	28.424 35	1.575648 091	28.350 89	1.649114 086	28.304 62	1.695379 902	28.334 62	1.665378 54	28.559 93	1.440073 069	28.881 74	1.118261 951	29.177 27	0.822726 006

Appendix M: Participant Questionnaire Sheet

Participant Questionnaire Sheet:

Study Title: [A measurement system for hand rehabilitation](#)

Researcher: [Nan HU](#) **Ethics Number:** [48109](#)

Please fill in the following questionnaire to determine your eligibility for this experiment. If yes to any of the following questions please give details.

1. Are you aged 18-69 inclusive? Yes / No

2. Do you have a known hand impairment? Yes / No

3. Have you ever had any recent pain, infections, surgery or bleeding from either of hand? Yes / No

4. Do you experience any hand injuries or disease (such as arthritis, peripheral nerve disease, central nervous system injury, brachial plexus injury or any other disease in either your hand or your finger)? Yes / No

5. Do you suffer from congenital dysplasia in either your hand or your finger? Yes / No

Participant Information Sheet

Study Title: [A measurement system for hand rehabilitation](#)

Researcher: [NAN HU](#)

ERGO number: [48109](#)

You are being invited to take part in the above research study. To help you decide whether you would like to take part or not, it is important that you understand why the research is being done and what it will involve. Please read the information below carefully and ask questions if anything is not clear or you would like more information before you decide to take part in this research. You may like to discuss it with others but it is up to you to decide whether or not to take part. If you are happy to participate you will be asked to sign a consent form.

What is the research about?

This research is for a PhD program on a measurement system for hand rehabilitation. It investigates contactless finger displacement measurement based on electrical near field sensing. A notable advantage of this adoption is the non-contact form of measuring without complicated setting-up and donning steps. Previous work has investigated the feasibility of using electrical near field sensing, and proposed a mathematic relationship between the fingers' motion and the signals detected. Therefore, the rationale for conducting this study is to verify the regression model proposed.

Why have I been asked to participate?

You have been chosen for this experiment, as you are student or staff from the University of Southampton and between the age of 18 and 69 years inclusive, with normal hand and finger function.

What will happen to me if I take part?

1. You will be asked to fill in a questionnaire assessing eligibility for participation.
2. The information of your gender and handedness will be collected. Measuring of your hand dimension will be conducted following steps below:
 - While your hand extended, the maximum breadth and maximum depth of your proximal interphalangeal joint of digit 2 and digit 3 will be measured with the sliding calliper.
 - While your hand extended, the distance along midpoint of the tip of digit 2 and digit 3 to your wrist crease baseline at the end of scaphoid bone will be measured with a ruler.
3. For testing, you are required to sit and relax, and try to refrain from moving unless need

- be. Tissues will be provided before the experiment to ensure your hand clean and dry.
4. Experimental tests of your right hand will be conducted. You are required to place you right hand on the receptacle with a horizontal posture with respect to the guidance line. If at any point during the test you wish to stop, you have the right to do so.
 - Calibration of an optical sensor will be conducted first. During this process, you are required to keep you right hand on the receptacle without any unnecessary movement, while the platform to hold the optical sensor will be adjusted to get varied distance. The calibration process will take approximately 10 minutes.
 - Breaks of 5 minutes will then be given. Tissues will be provided if you find your hand sweating.
 - Testing of combined movement of index finger and middle finger of your right hand will then be conducted, while the movement of the other fingers (ring & little finger) should be avoid. Each finger can be extended from the flat posture but not into hyperextension. You will be asked to move the index & middle fingers up and down for three consecutive times, take your hand away from the receptacle, and then place your hand back to the receptacle as required. You will be required to repeat the described movements for 10 times.
 5. Breaks of 5 minutes will then be given. Tissues will be provided if required.
 6. Similar to step 4, experimental tests of your left hand will be conducted. You are required to place you left hand on the receptacle with a horizontal posture with respect to the guidance line.
 - Calibration of an optical sensor will be conducted first. While the platform to hold the optical sensor adjusted to get varied distance, you are required to keep you left hand on the receptacle without any unnecessary movement.
 - Breaks of 5 minutes will then be given. Tissues will be provided if you find your hand sweating.
 - Testing of combined movement of index finger and middle finger of your left hand will then be conducted, while the movement of the ring & little finger should be avoid. Each finger can be extended from the flat posture but not into hyperextension. You will be asked to move the index & middle fingers up and down for three consecutive times, take your hand away from the receptacle, and then place your hand back to the receptacle as required. You will be required to repeat the described movements for 10 times.
 7. In total, the entire appointment will last approximately 1 hour.

Are there any benefits in my taking part?

Taking part in this study will help to expand knowledge regarding contactless finger displacement sensing as a measurement system for hand rehabilitation.

Are there any risks involved?

There could be some minimal risks. However, these risks have been assessed and correct precautions have been put in place to reduce these risks by adhering to safety procedures. First-aiders will stand by during the whole process to help ensure the safety and health of the participants.

We are willing to help if you have any distressed feeling either during or following this study. If at any point during the test you wish to stop, you have the right to do so.

What data will be collected?

As part of this study, email address and a signed consent form will be collected; the consent form will be digitised and the hard copy version shredded. Other than that, measurements as described in the section 'What will happen to me if I take part?' above as well as your gender and handedness will be collected.

Your information will not be released or viewed by anyone other than researchers involved in this project. All the information you give will be saved in a password-protected file on a University of Southampton network. The information will only be used for the purpose of this study. All data will be destroyed on completion of my degree.

All responses are treated as confidential, and in no case will responses from individual participants be identified. All data will be pooled and published in aggregate form only, where the data would appear only as a string of numbers, so your responses will remain totally anonymous.

Will my participation be confidential?

Your participation and the information we collect about you during the course of the research will be kept strictly confidential.

Only members of the research team and responsible members of the University of Southampton may be given access to data about you for monitoring purposes and/or to carry out an audit of the study to ensure that the research is complying with applicable regulations. Individuals from regulatory authorities (people who check that we are carrying out the study correctly) may require access to your data. All of these people have a duty to keep your information, as a research participant, strictly confidential.

Data Protection Privacy Notice

The University of Southampton conducts research to the highest standards of research integrity. As a publicly-funded organisation, the University has to ensure that it is in the public interest when we use personally-identifiable information about people who have agreed to take part in research. This means that when you agree to take part in a research study, we will use information about you in the ways needed, and for the purposes specified, to conduct and complete the research project. Under data protection law, 'Personal data' means any information that relates to and is capable of identifying a living individual. The University's data protection policy governing the use of personal data by the University can be found on its website (<https://www.southampton.ac.uk/legalservices/what-we-do/data-protection-and-foi.page>).

This Participant Information Sheet tells you what data will be collected for this project and whether this includes any personal data. Please ask the research team if you have any questions or are unclear what data is being collected about you.

Our privacy notice for research participants provides more information on how the University of Southampton collects and uses your personal data when you take part in one of our research projects and can be found at <http://www.southampton.ac.uk/assets/sharepoint/intranet/Is/Public/Research%20and%20Integrity%20Privacy%20Notice/Privacy%20Notice%20for%20Research%20Participants.pdf>

Any personal data we collect in this study will be used only for the purposes of carrying out our research and will be handled according to the University's policies in line with data protection law. If any personal data is used from which you can be identified directly, it will not be disclosed to anyone else without your consent unless the University of Southampton is required by law to disclose it.

Data protection law requires us to have a valid legal reason ('lawful basis') to process and use your Personal data. The lawful basis for processing personal information in this research study is for the performance of a task carried out in the public interest. Personal data collected for research will not be used for any other purpose.

For the purposes of data protection law, the University of Southampton is the 'Data Controller' for this study, which means that we are responsible for looking after your information and using it properly. The University of Southampton will keep identifiable information about you for **until successful completion of my degree** after the study has finished after which time any link between you and your information will be removed.

To safeguard your rights, we will use the minimum personal data necessary to achieve our research study objectives. Your data protection rights – such as to access, change, or transfer such information - may be limited, however, in order for the research output to be reliable and accurate. The University will not do anything with your personal data that you would not reasonably expect.

If you have any questions about how your personal data is used, or wish to exercise any of your rights, please consult the University's data protection webpage (<https://www.southampton.ac.uk/legalservices/what-we-do/data-protection-and-foi.page>) where you can make a request using our online form. If you need further assistance, please contact the University's Data Protection Officer (data.protection@soton.ac.uk).

Do I have to take part?

No, it is entirely up to you to decide whether or not to take part. If you decide you want to take part, you will need to sign a consent form to show you have agreed to take part.

If at any time you decide you do not wish to continue, please just let the researcher know.

What happens if I change my mind?

You have the right to change your mind and withdraw at any time without giving a reason and without your participant rights (*or routine care if a patient*) being affected.

Your participation is voluntary and you may withdraw consent at any time without your legal rights being affected and without the need for justification.

If you withdraw from the study, we will keep the information about you that we have already obtained for the purposes of achieving the objectives of the study only.

What will happen to the results of the research?

Your personal details will remain strictly confidential. Research findings made available in any reports or publications will not include information that can directly identify you without your specific consent.

All the information you give will be saved in a password-protected file on University of Southampton network. The information can only be accessed by me and the supervision team, and will only be used for the purpose of this study. All data will be destroyed on completion of my degree.

The results of this study might be published as a conference / journal paper, and will be reported in my PhD thesis. The results will remain strictly confidential and will not be directly identifiable from any report or publication. Results will be aggregated across all participants; no single participant will be identified. You can receive a copy of the results if you would like.

Where can I get more information?

Should you require any additional information, please contact Nan HU (nh1u16@soton.ac.uk).

What happens if there is a problem?

If you have a concern about any aspect of this study, you should speak to the researchers who will do their best to answer your questions.

If you remain unhappy or have a complaint about any aspect of this study, please contact the University of Southampton Research Integrity and Governance Manager (023 8059 5058, rgoinfo@soton.ac.uk).

We are always willing to help if there is a problem. Please contact Nan HU (nh1u16@soton.ac.uk).

Thank you.

Thank you for taking the time to read the information sheet and considering taking part in the research.

Appendix O: Participant Experiment Record

Name of the participant: _____ Participant identification number: _____



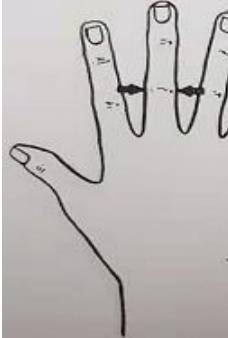

Data/time: _____ / _____ Gender: Male Female Note: _____

Pre-experiment Checklist:



- Documents:**
 - Participant Information Sheet
 - Consent Form
 - Participant Questionnaire Sheet
 - Participant Experiment Record
 - Pen
- Measuring tools:**
 - Calliper
 - Ruler
 - Tissue
 - Band aid
- Experiment setting**
 - Measuring system set-up
 - Function of measuring system checked in advance
 - Staff on the ground/desk cleaned
 - Participant's folder built

During the experiment:

2. Provide the participant with a participant information sheet.
3. A consent form provided. The participant give written consent before testing can commence.
4. A questionnaire administered assessing medical history and eligibility for participation.
5. Grouping information collected: Email address: _____
 Gender: Male Female Handedness: Right Left
6. Tissues provided.
7. Measuring of hand dimension conducted:
 - Subject's hand extended. With the sliding calliper, measure the maximum breadth and maximum depth of the proximal interphalangeal joint of digit 2 (plot (a),(b)) and digit 3 (plot (c),(d)).

Proximal interphalangeal joint (mm)				
	Index		Middle	
				
R				
L				

- Subject's hand extended. With the ruler, measure the distance along midpoint of the tip of digit 2 and digit 3 to the wrist crease baseline at the end of scaphoid bone.

Length: finger tip to wrist crease (mm)	
	Middle
	
R	

L		
---	--	--

8. Tissues will be provided.
9. Participant seated and asked to remain still throughout testing.
10. Experimental tests of right hand:
 - **Researcher to illustrate the position of hand:** Right hand of the participant should adopt a horizontal posture on the receptacle, and position the fingers with respect to the guidance line on the receptacle.
 - **Researcher to prompt participant to keep their right hand on the receptacle** during the calibration of the distance measuring system. The platform to hold the optical sensor will be adjusted to get varied distance.

R1.1	R1.2	R1.3	R1.4	R1.5	R1.6	R1.7	R1.8	R1.9	R1.10

- Breaks of 5 minutes will be given to the participant **while their right hand kept on the receptacle.**
- The distance and the corresponding voltage output of the optical sensor will be saved.
- Researcher to explain the combined movement of index finger and middle finger of the right hand, **while the movement of the other fingers (ring & little finger) should be avoided.** Index & middle finger can be **extended from the flat posture but not into hyperextension.** Participant will be asked to **move their index & middle fingers up and down slowly for three consecutive times, move their hand away from the receptacle, then place their hand back to the receptacle as required.** The described movements should **repeat for 10 times.**

R2.0	R2.1	R2.2	R2.3	R2.4	R2.5	R2.6	R2.7	R2.8	R2.9	R2.10

11. Breaks of 5 minutes will be given to the participant.
12. MGC3030 output will be saved.
13. Tissues will be provided if the participant has a sweat hand.
14. Experimental tests of left hand:

- **Researcher to illustrate the position of hand:** right hand should adopt a horizontal posture on the receptacle with respect to the guidance line.
- **Researcher to prompt participant to keep their left hand on the receptacle** during the calibration of the distance measuring system. The platform to hold the optical sensor will be adjusted to get varied distance.

L1.1	L1.2	L1.3	L1.4	L1.5	L1.6	L1.7	L1.8	L1.9	L1.10

- Breaks of 5 minutes will be given to the participant **while their left hand kept on the receptacle.**
- The distance and the corresponding voltage output of the optical sensor will be saved.
- Researcher to explain the combined movement of index finger and middle finger of the right hand, **while the movement of the other fingers (ring & little finger) should be avoided.** Index & middle finger can be **extended from the flat posture but not into hyperextension.** Participant will be asked to **move their index & middle fingers up and down slowly for three consecutive times, move their hand away from the receptacle, then place their hand back to the receptacle as required.** The described movements should **repeat for 10 times.**

L2.0	L2.1	L2.2	L2.3	L2.4	L2.5	L2.6	L2.7	L2.8	L2.9	L2.10

15. MGC3030 output will be saved.

16. Pre-processing the experimental outputs. Participants have the option of being debriefed on the experimental results.

Post – experiment data analysing

Right Hand				Left Hand			
Optical sensor calibration							
No.	opt1	opt2	Note	No.	opt1	opt2	Note
1				1			
2				2			
3				3			
4				4			
5				5			
6				6			
7				7			
8				8			
9				9			
10				10			
Type in 'V= D ₁ ', 'V= D ₂ '				Type in 'V= D ₁ ', 'V= D ₂ '			
Plot & Result 1 & 2		Matlab 1 & 2		Plot & Result 1 & 2		Matlab 1 & 2	
Note							
Sample movements							
No.	Range	Index	Middle	No.	Range	Index	Middle
1				1			
2				2			
3				3			
4				4			
5				5			
6				6			
7				7			
8				8			
9				9			
10				10			
Note:							

Signature

Appendix P: Participant Characteristics

Table P-1 General information of participants

Participant Identification Number	Gender	Handedness
1-F	F	R
2-M	M	R
3-M	M	R
4-F	F	R
5-M	M	R
6-M	M	R
7-M	M	R
8-M	M	L
9-M	M	R
10-M	M	R
11-M	M	R
12-M	M	R
13-F	F	R
14-M	M	R
15-F	F	R
16-F	F	R
17-F	F	R
18-M	M	R
19-F	F	R
20-M	M	R
21-F	F	R
22-F	F	R
23-F	F	R

Table P-2 Measurement of hand dimension1: Proximal interphalangeal joint (mm)

Participant Identification Number	Right Hand				Left Hand			
	Index Finger		Middle finger		Index Finger		Middle finger	
	Width	Depth	Width	Depth	Width	Depth	Width	Depth
1-F	16.5	14.85	17.19	14.98	15.94	14.41	16.94	15.33
2-M	17.75	15.74	19.15	17.36	18.05	15.64	18.71	17.11
3-M	18.13	15.8	18.27	16.14	18.2	15.97	18.47	16.39
4-F	17.35	15.05	16.99	15.51	16.48	14.54	16.06	14.56
5-M	19.29	17.59	18.09	17.31	19.59	17.13	18.51	16.78
6-M	18.9	17.29	18.66	17.1	18.08	16.45	18.34	17.04
7-M	17.94	15.87	18.47	17.23	17.47	16.02	17.41	16.26
8-M	18.74	15.73	18.9	15.84	18.61	15.9	18.21	15.91
9-M	20.2	20.25	20.88	18.72	20	19.43	19.65	18.74
10-M	19.99	18.99	19.28	16.78	19.25	18.01	19.18	16.93
11-M	22.13	18.8	21.69	19.25	22.11	19.43	21.08	20.01
12-M	18.28	16.03	18.1	17.3	18.53	15.66	17.85	16.98
13-F	17.63	15.3	17.66	14.76	16.83	14.86	17.89	14.99
14-M	19.5	17.99	20	17.75	18.95	16.65	19.12	18.4
15-F	15.95	15.09	15.86	15.37	15.16	14.05	15.5	14.87
16-F	16.26	15.44	16.3	15.24	16.64	15.03	15.96	14.97
17-F	17.61	14.76	17.58	15.34	17.24	15.17	17.56	14.94
18-M	18.28	16.5	18.84	17.02	17.76	16.16	17.5	16.56
19-F	16.78	16.36	17.34	15.91	16.59	14.92	17.07	15.25
20-M	18.2	17.32	19.67	18.73	17.96	16.74	18.16	17.11
21-F	17.76	14.38	18.47	16.07	16.36	14.35	17.65	15.23
22-F	17.09	16.11	18.2	16.4	16.71	15.41	16.71	16.46
23-F	17.26	15.7	18.37	16	17.52	16.28	18.19	16.17

Table P-3 Measurement of hand dimension2: Proximal interphalangeal joint (mm)

Participant Identification Number	Right Hand		Left Hand	
	Index	Middle	Index	Middle
1-F	164	177	165	177
2-M	163	175	163	175
3-M	178	187	183	192
4-F	169	176.5	172	182.5
5-M	178	184.5	180	185.5
6-M	166.5	178	166.5	182
7-M	172	183	172	184
8-M	178	190.5	178.5	188
9-M	197	207.5	193	207
10-M	192.5	203.5	195	206
11-M	209	225	208.5	224
12-M	180	187.5	182	190.5
13-F	161	167	164	174
14-M	182	195	181.5	196.5
15-F	159	165	157	164.5
16-F	177.5	183.5	176	182.5
17-F	163.5	168	162	167
18-M	182.5	193	184.5	194.5
19-F	163.5	176.5	164	178.5
20-M	175	184	175	183
21-F	161.5	173	165	172
22-F	163.5	176	165	175
23-F	173.5	181.5	173	183

Appendix Q: Filtering Issue

Based on the output distance characteristics of the optical sensor, signal change due to the distance change rather smoothly and slowly [21], as shown in Fig. Q-1. However, the signals of both optical sensors from experiment are contaminated with very tall, narrow “spikes” occurring at random intervals and with random amplitudes, but with widths of only one or a few points, as presented in Chapter 5.5.

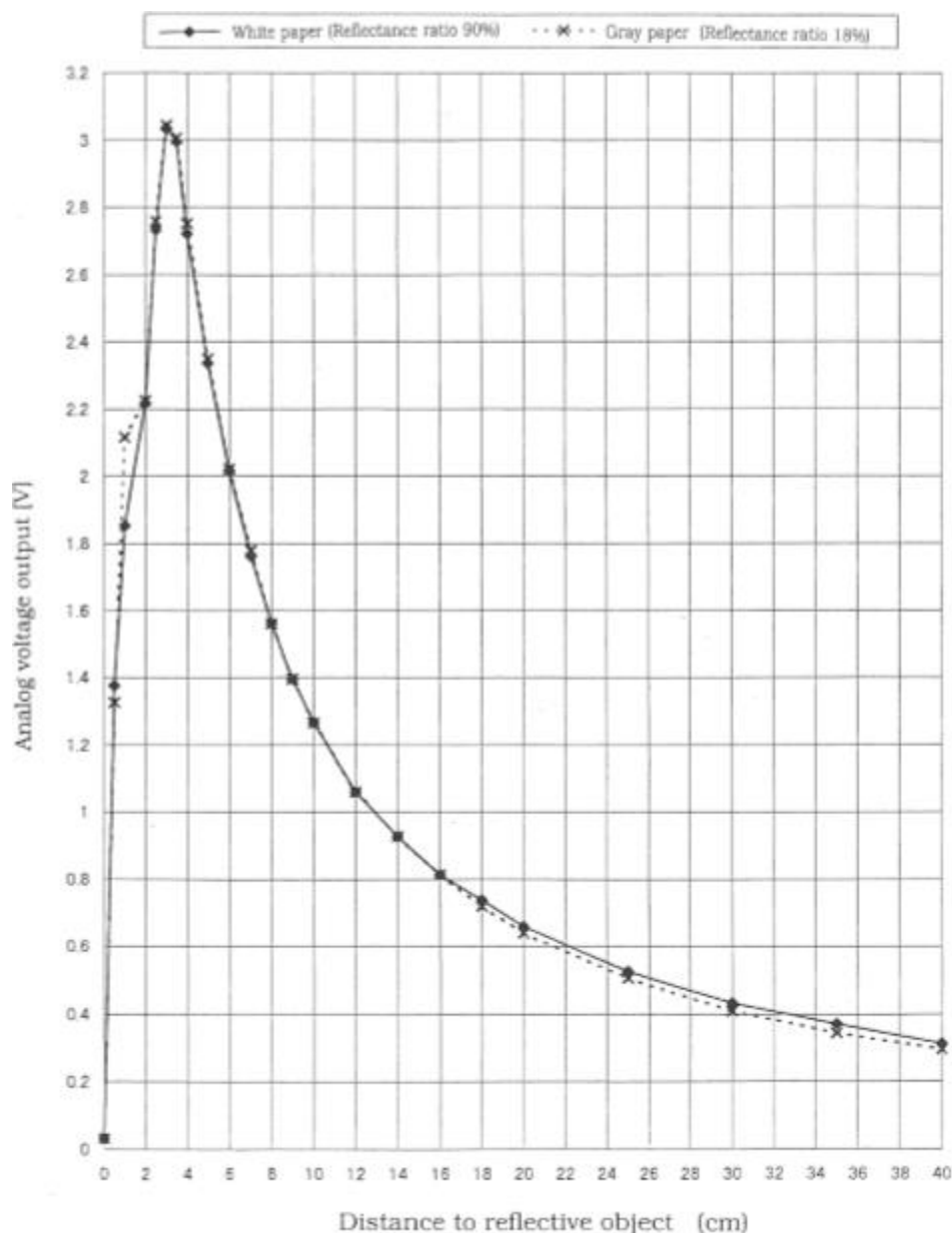


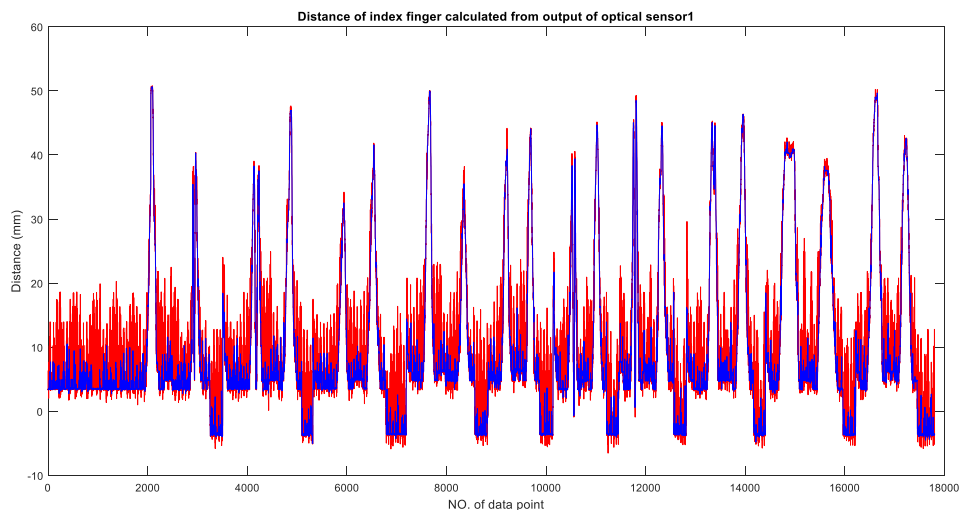
Fig.Q-1 Output distance characteristics of the optical sensor

This type of interference is difficult to eliminate using smoothing methods which replaces a point in the signal with the average of adjacent points, without distorting the signal [107]. However, a “median” filter, which replaces each point with the median of adjacent

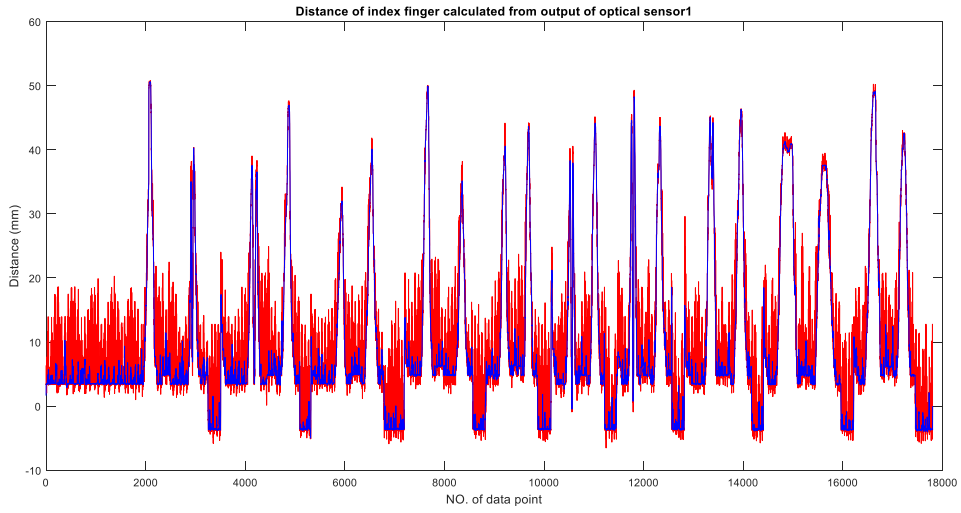
points, can effectively eliminate narrow spikes, with little change in the signal, if the width of the spikes is only one or a few points and equal to or less than m . Therefore, the true signals will not be much distorted while the “spikes” will be reduced. Consequently, the filtered signal allows more accurate signal characteristics processing and analysing, including peak position, peak amplitude, width, etc.

For peak-type signals, the critical factor is the smooth ratio, which is the ratio between the smooth width and the number of points in the half-width of the peak [107]. In general, increasing the smoothing ratio improves the signal-to-noise ratio but causes a reduction in amplitude and an increase in the bandwidth of the peak. As smooth width increases, the smoothing ratio increases, noise is reduced quickly at first, then more slowly, and the peak height is also reduced, slowly at first, then more quickly, as shown in Fig. Q-2. The best smooth ratio depends on the purpose of the peak measurement. If the ultimate objective of the measurement is to measure the peak height or width, then smooth ratios below 0.2 should be used [107].

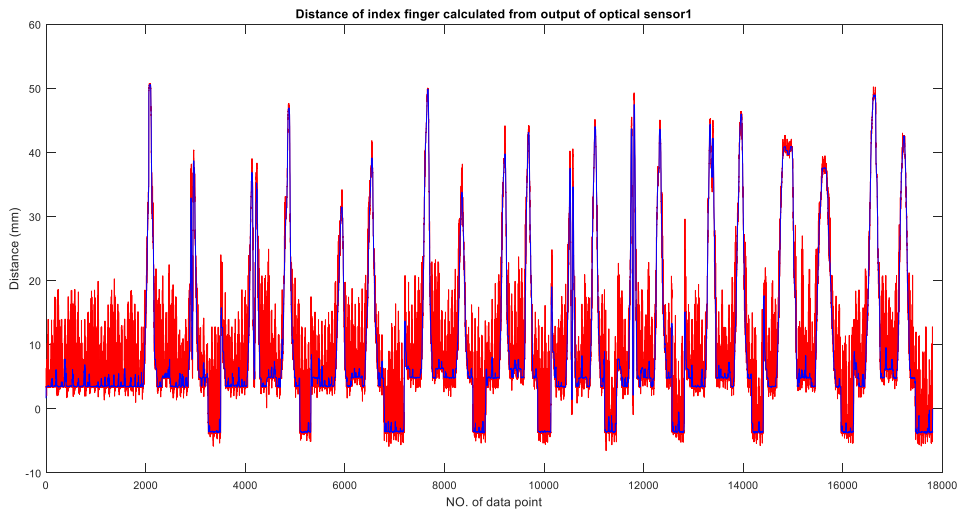
Particularly, the maximum improvement depends on the number of points in the peak: the more points in the peak, the greater smooth widths can be employed without peak height reduction, and the greater the noise reduction. Considering the mechanism of the median filter, for a signal with n points in the peak, the maximum filter width should be less than $2n$. If not, the peak height will be lost.



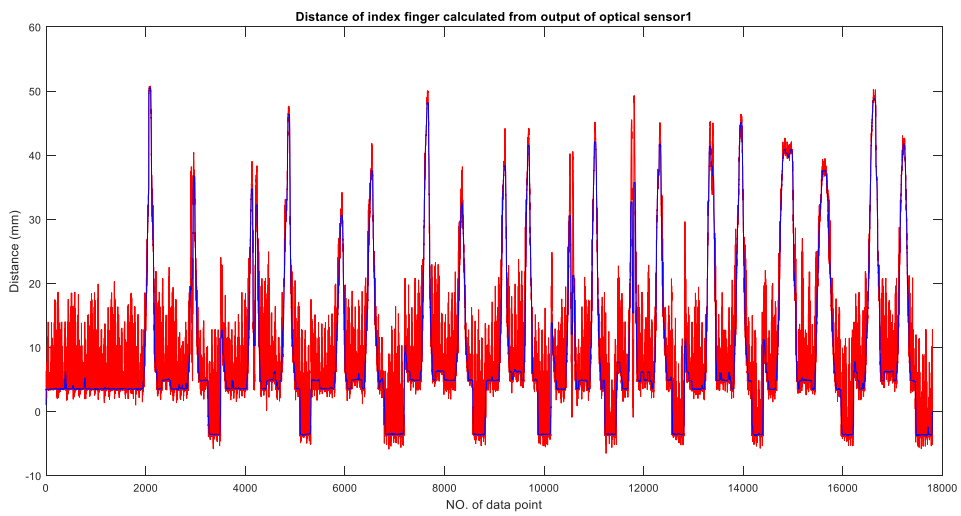
(a) Smooth width = 5



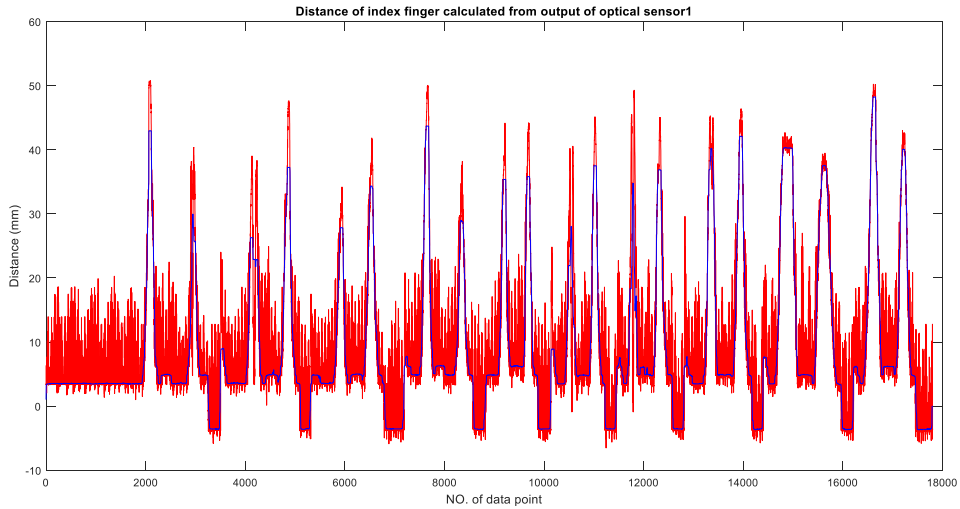
(b) Smooth width = 10



(c) Smooth width = 20



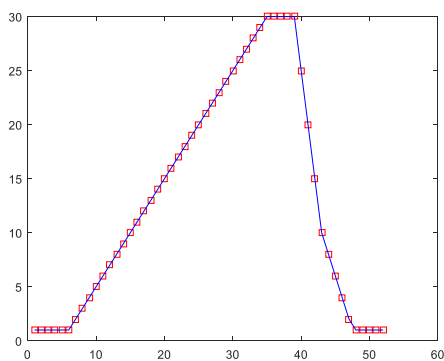
(d) Smooth width = 50



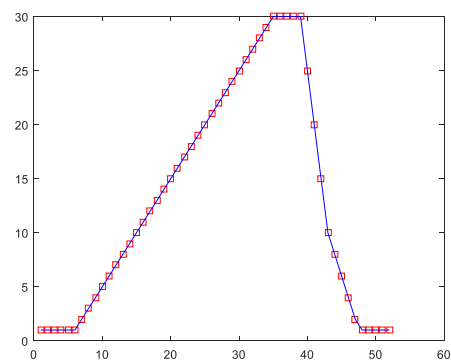
(e) Smooth width = 100

Fig. Q-2 Measured distance from optical sensor1 (- before filtered, - after filtered by median filter)

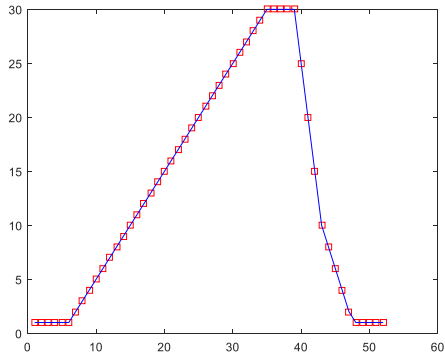
Fig. Q-3 shows the simplest case where the signal to analyse is $\{x| 1, 1, 1, 1, 1, 1, 2, 3, 4, 5, 6, 7, 8, 9, 10, 11, 12, 13, 14, 15, 16, 17, 18, 19, 20, 21, 22, 23, 24, 25, 26, 27, 28, 29, \underline{30}, \underline{30}, \underline{30}, \underline{30}, 25, 20, 15, 10, 8, 6, 4, 2, 1, 1, 1, 1, 1\}$. Here, the peak height is 30 and there are 5 points in the peak ($n=5$). The red squares '□' show the original signal, while the blue lines '-' in Fig. Q-3 (a),(b),(c),(d) shows the signal after filtered by median filter with filter width 3, 5, 9, 10. It can be indicated from the plots that the filtered signal '-' in Fig. Q-3 (d) start to lose the peak height, where the filter width reaches 10 ($2n$), and the maximum filtered width here is 9 ($2n-1$) points. The form of the equation between the number of points in the peak and the maximum filter width can be slightly different in the case of even numbers.



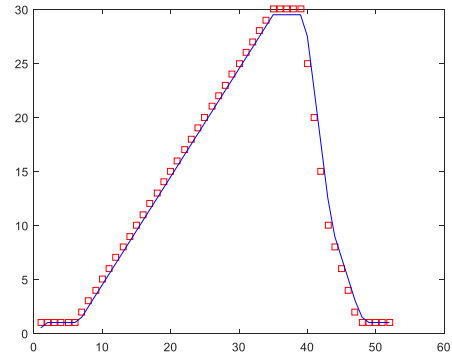
(a)



(b)



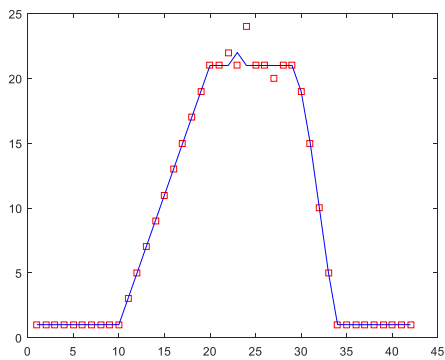
(c)



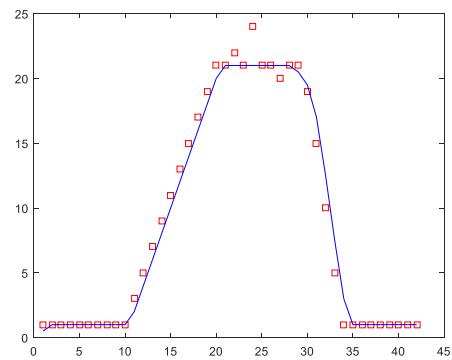
(d)

Fig. Q-3 Example set1 with different filtering width

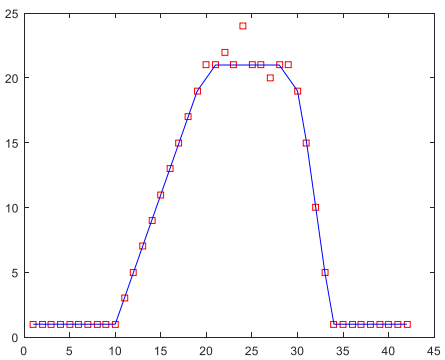
However, in the real situation, there tend to be noise in the signal and that is the case to apply filtering technique. Therefore, another set $\{x| 1, 1, 1, 1, 1, 1, 1, 1, 1, 1, 1, 3, 5, 7, 9, 11, 13, 15, 17, 19, \underline{21, 21, 22, 21, 24, 21, 21, 20, 21, 21}, 19, 15, 10, 5, 1, 1, 1, 1, 1, 1, 1, 1, 1\}$ is taken as an example. Here, the peak height is 21 and the number of points in the peak is 10 ($n=10$). Similarly, the red squares '□' show the original signal, while the blue lines '-' in Fig. Q-4 (a),(b),(c),(d) shows the signal after filtered by median filter with filter width 3, 10, 17, 20.



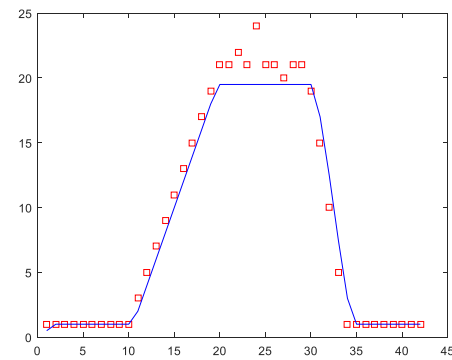
(a)



(b)



(c)



(d)

Fig. Q-4 Example set2 with different filtering width

The filtered signal ‘-’ in Fig. Q-4 (d) with filtered width 20 (2n) starts to lose the peak height, and the maximum filtered width here is 17 (2n-3) points. Collectively, the filter width of a median filter should be somewhere less than 2 times of the number of points in the peak, if not, the peak height will be lost. The messier the signal in the peak, the smaller the filter width should be.

It is very important, however, to apply exactly the same signal processing steps to the standard signals as to the sample signals, otherwise a large systematic error will result. For the output of the optical sensors, there are a group of messy signals with different number of points in the peak $\{n_1, n_2, n_3, n_4 \dots\}X$. Therefore, the filter width is depend on the smallest number $\{n_{\min}|n_1, n_2, n_3, n_4 \dots\}$. From the experimental result of both optical sensors, the n_{\min} is 10 points. Fig. Q-5 shows the movement with the smallest number of points in the peak (13F-5). The blue line ‘-’ show the original signal, while the blue lines ‘-’ in Fig. Q-5 (a),(b),(c),(d) shows the signal after filtered by median filter with filter width 10, 20, 30, 40.

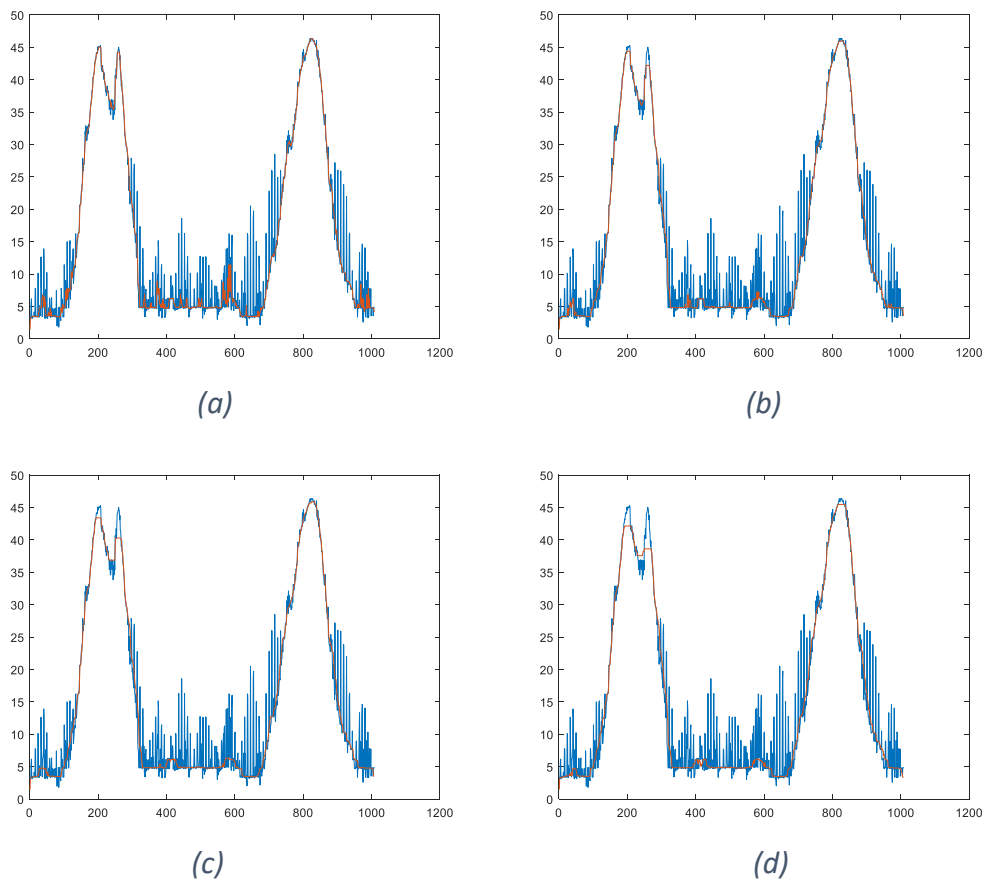
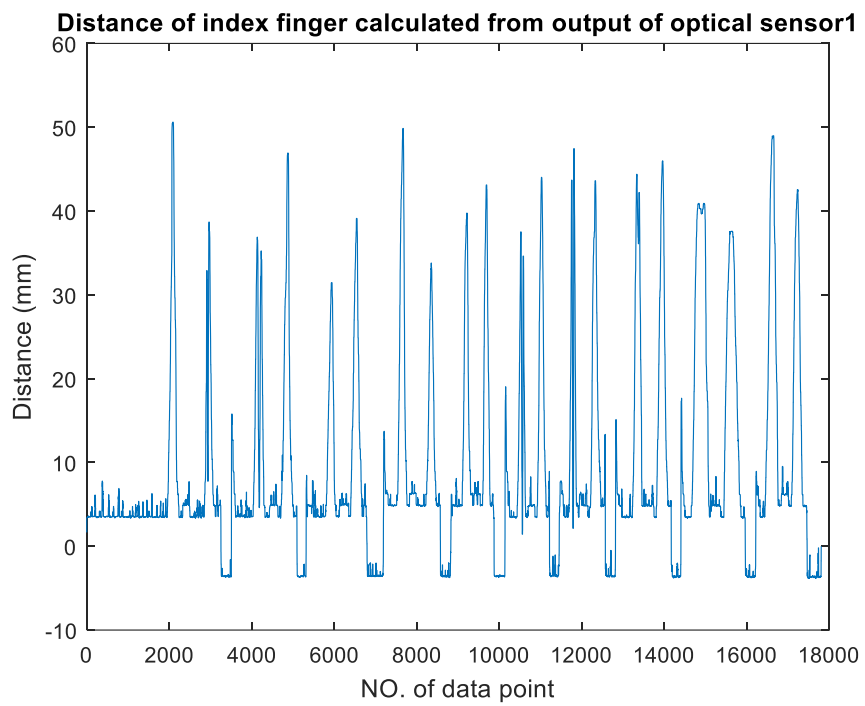


Fig. Q-5 Output of the optical sensors with different filtering width

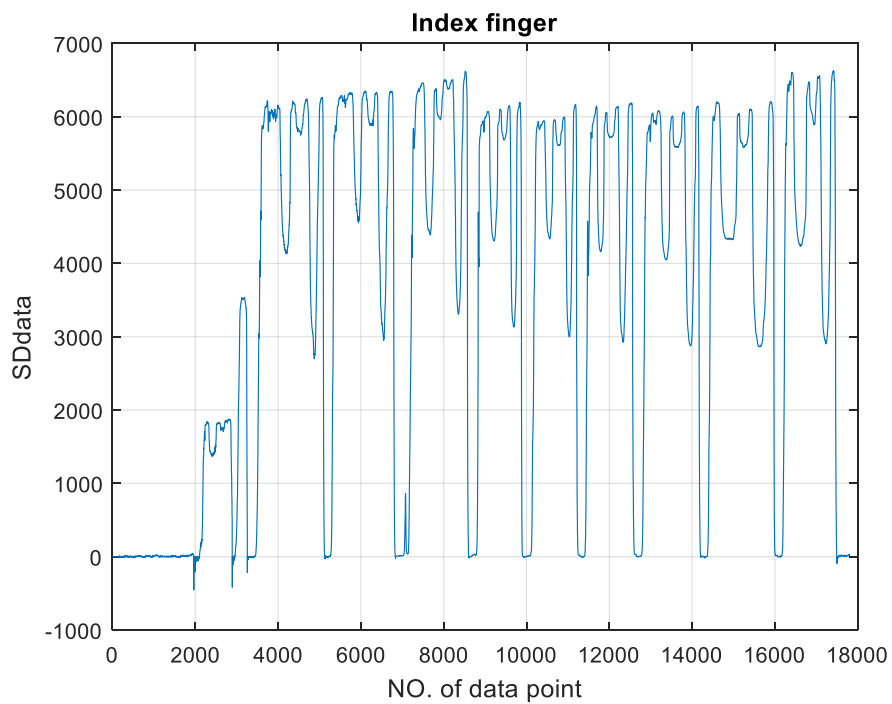
It can be observed from the plots that, the median filter with width of 20 points can effectively eliminates the 'spikes' in the signal while nicely maintain the peak height. This filtering technique supports the '2n' hypothesis proposed in the exemplar sets, and was applied to the experimental results of the optical sensors for all the participants for pre-processing purpose.

In conclusion, to deal with the 'spikes' noise observed in the optical outputs, a 'median' filter was selected to improve the signal processing and analysing performance. The median filter was applied to the output of both optical sensors for all the 23 participants with the filter width 20. Considering the sampling rates of 106 Hz, the filter width accounts for the time period of approximately 0.2 seconds, which well satisfies the requirement of the peak height measurement for finger movement in this research.

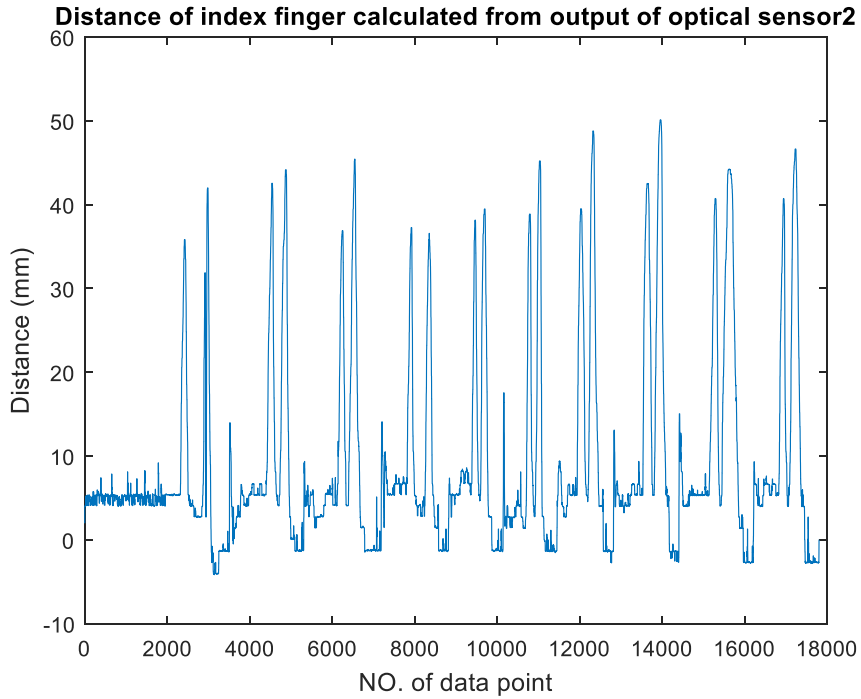
Appendix R: Experimental Results for Extreme Case 21-F



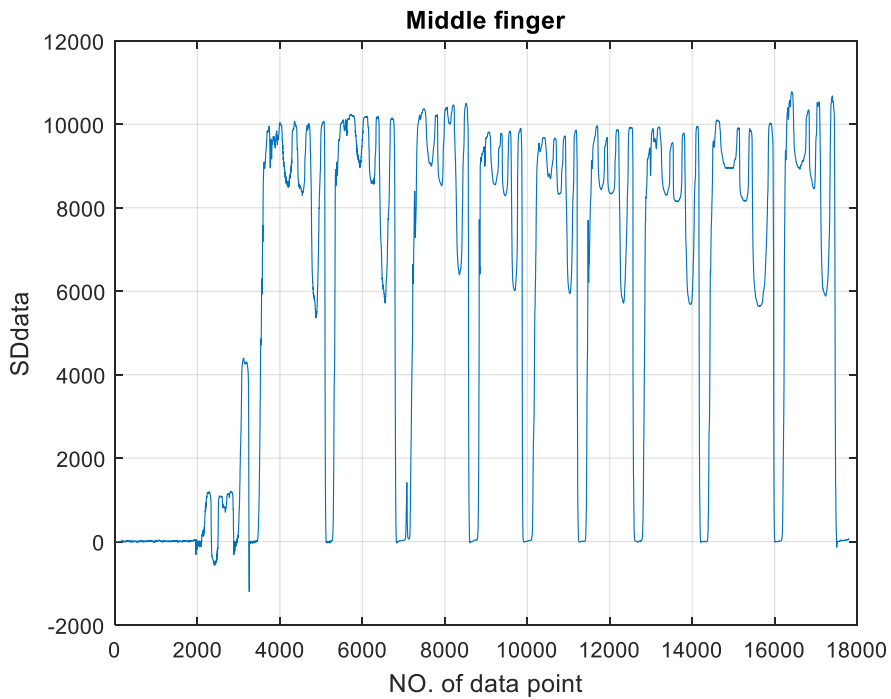
(a)



(b)

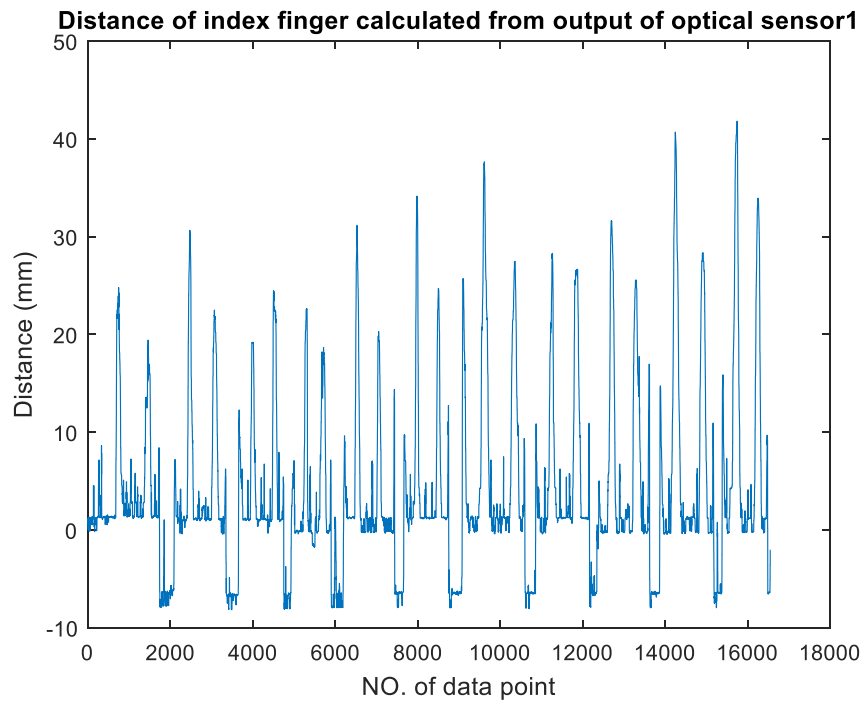


(c)

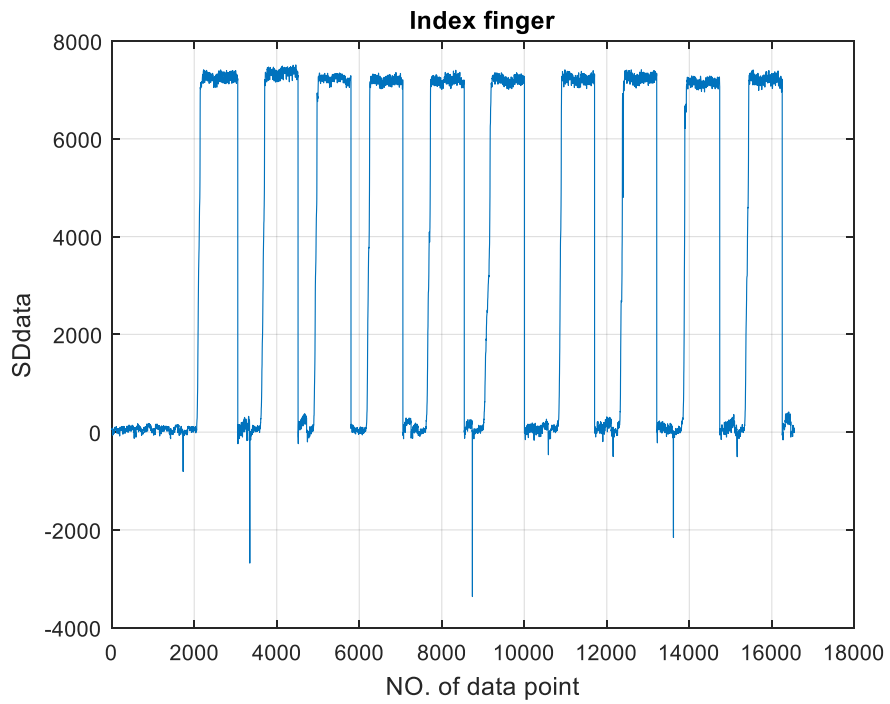


(d)

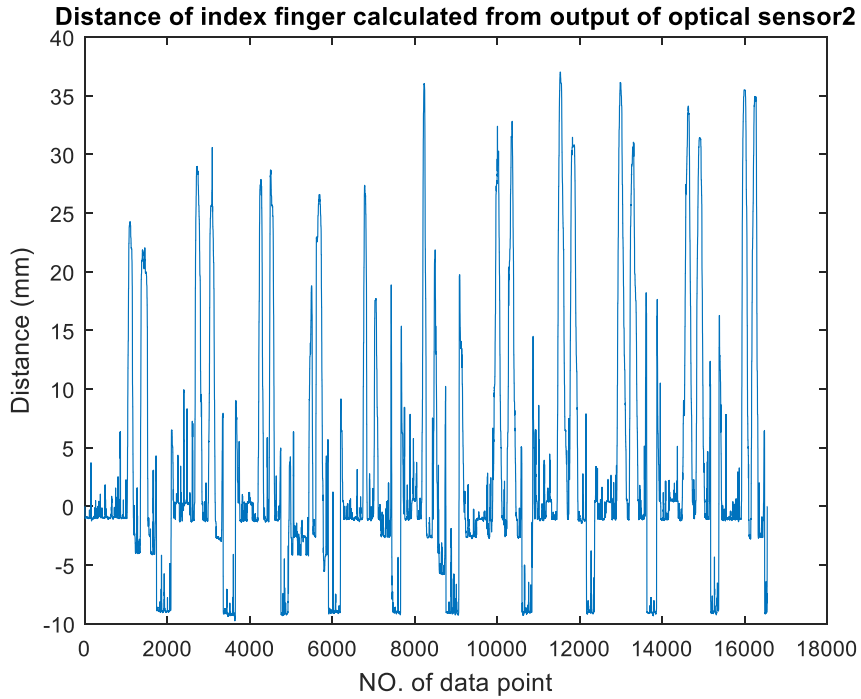
Fig. R-1 Example output from experiment for participant 13-F to compare with: a) Output from optical sensor1 (D_1); b) Output from the MGC3030 measuring system for the index finger (S_1); c) Output from optical sensor2 (D_2); d) Output from the MGC3030 measuring system for the middle finger (S_2)



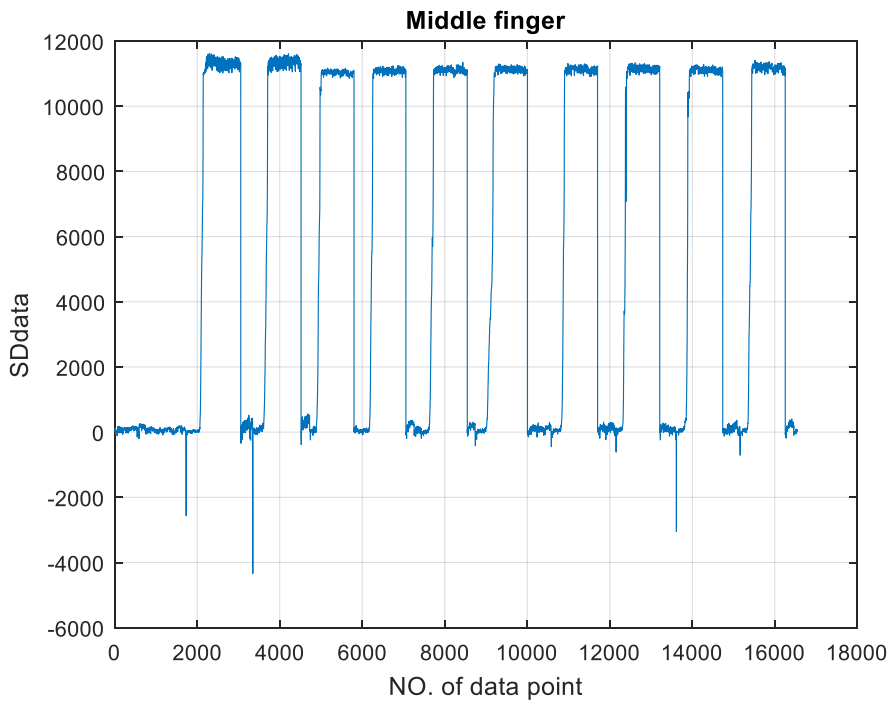
(a)



(b)

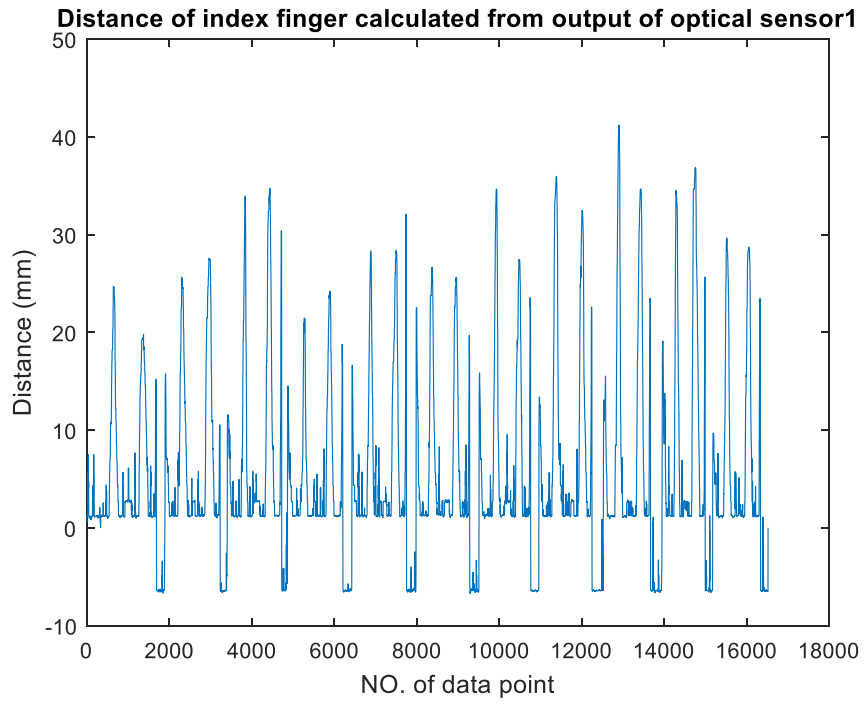


(c)

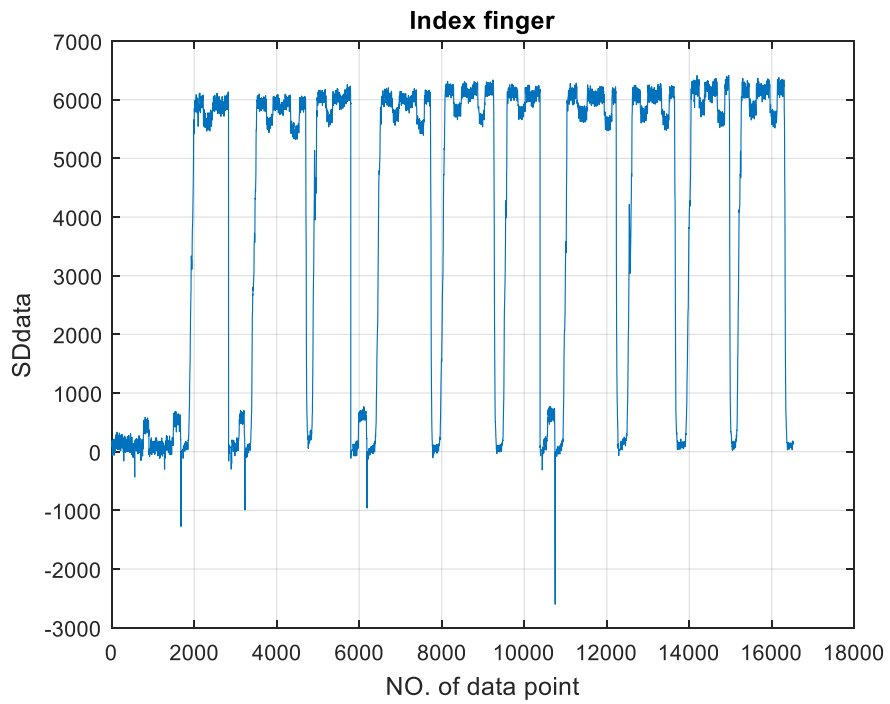


(d)

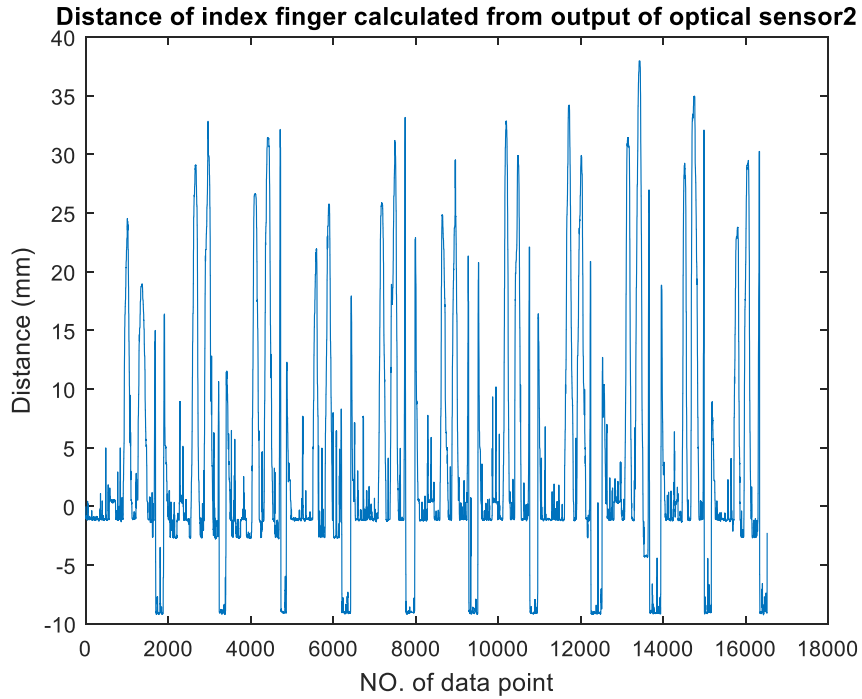
Fig. R-2 Example output1 from experiment for participant 21-F (Right hand): a) Output from optical sensor1 (D_1); b) Output from the MGC3030 measuring system for the index finger (S_1); c) Output from optical sensor2 (D_2); d) Output from the MGC3030 measuring system for the middle finger (S_2)



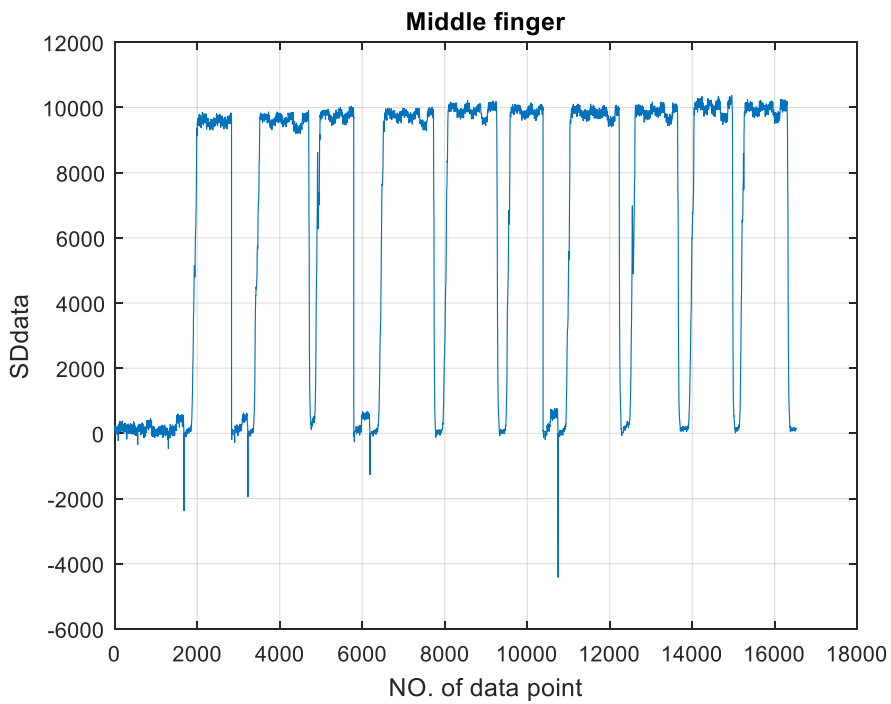
(a)



(b)

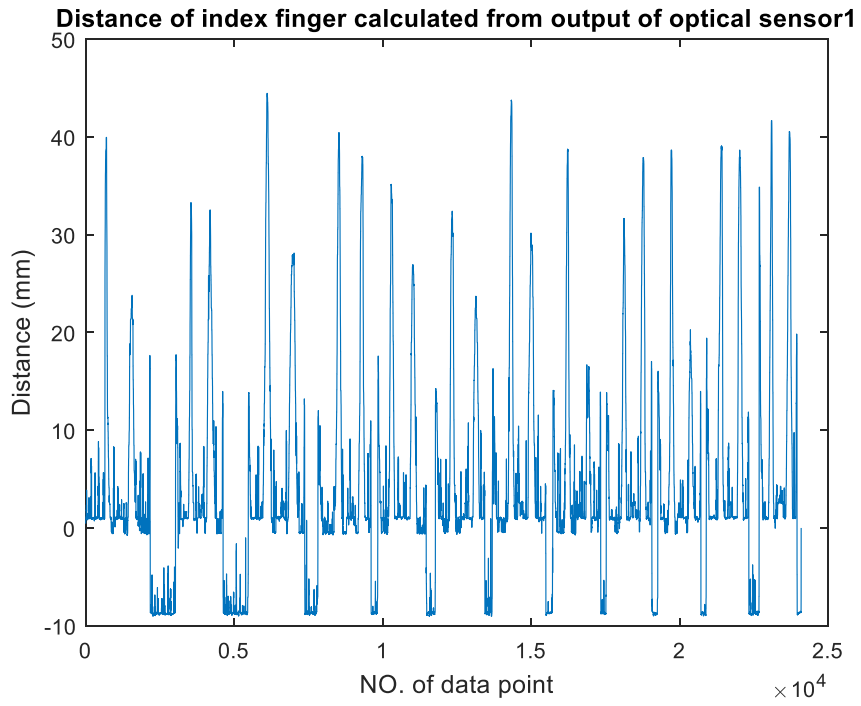


(c)

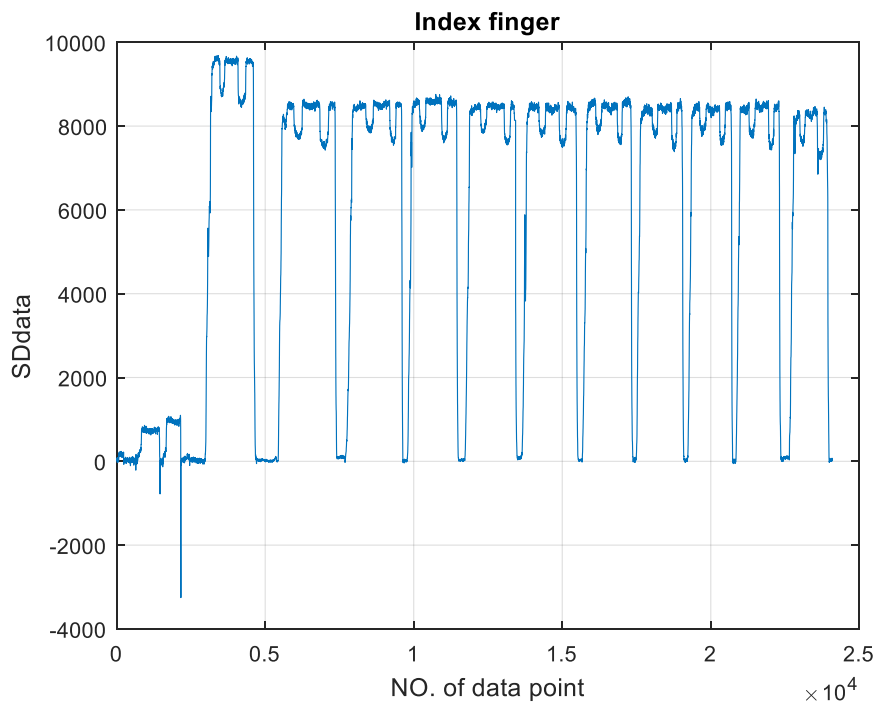


(d)

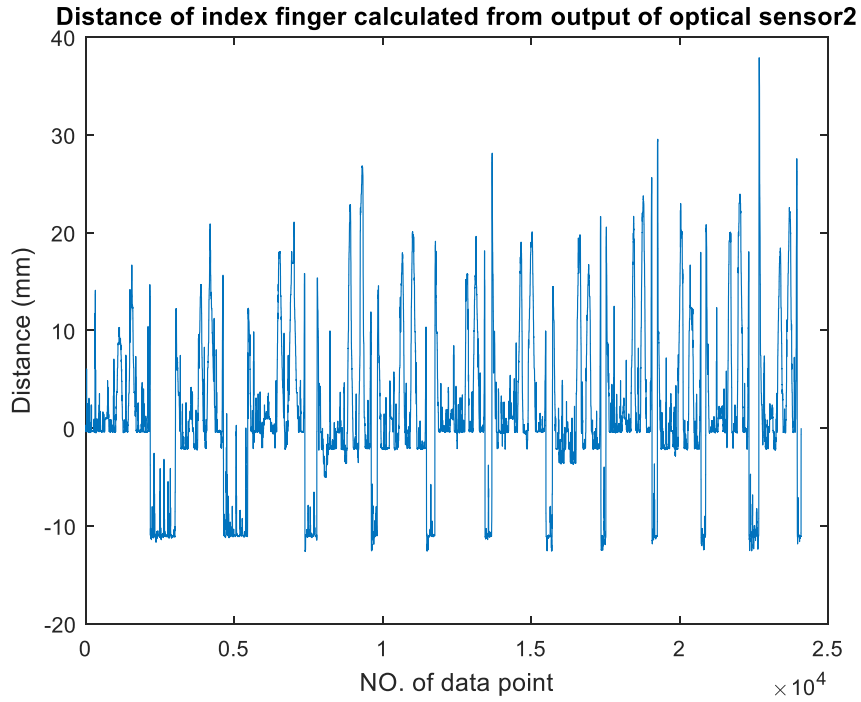
Fig. R-3 Example output2 from experiment for participant 21-F (Right hand, raw data for Fig.6-5): a) Output from optical sensor1 (D_1); b) Output from the MGC3030 measuring system for the index finger (S_1); c) Output from optical sensor2 (D_2); d) Output from the MGC3030 measuring system for the middle finger (S_2)



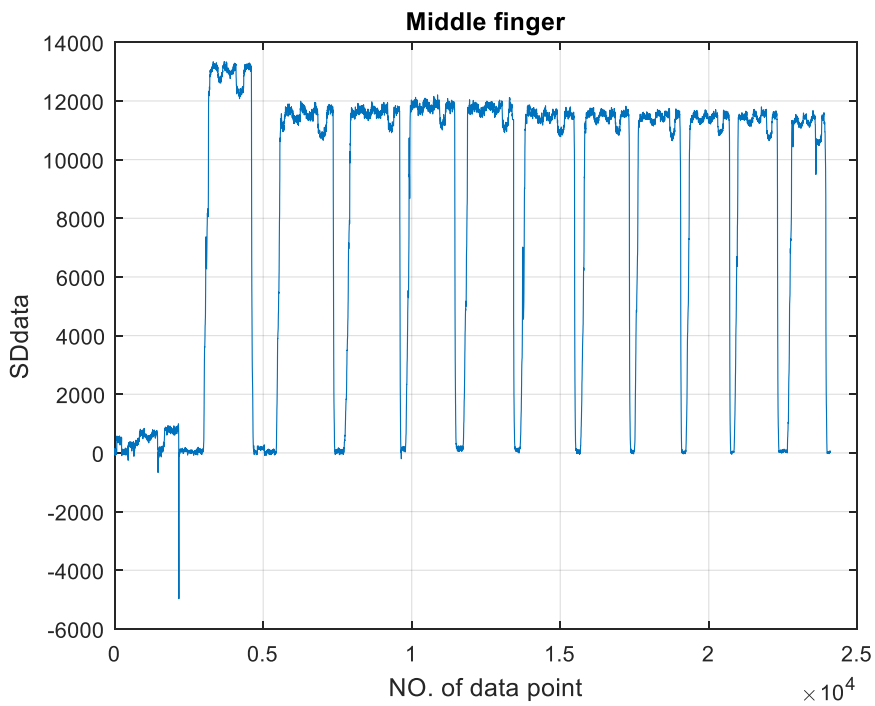
(a)



(b)



(c)



(d)

Fig. R-4 Example output3 from experiment for participant 21-F (Left hand): a) Output from optical sensor1 (D_1); b) Output from the MGC3030 measuring system for the index finger (S_1); c) Output from optical sensor2 (D_2); d) Output from the MGC3030 measuring system for the middle finger (S_2)

List of References

1. Harris, N.R. and D. Sthapit. *Towards a personalised rehabilitation system for post stroke treatment*. in *2016 IEEE Sensors Applications Symposium (SAS)*. 2016. IEEE.
2. O'Sullivan, S., *Stroke In: O'Sullivan SB and Schmitz TJ*. Physical Rehabilitation. FA Davis, Philadelphia, PA, 2007: p. 706-776.
3. Lum, P., et al., *Robotic devices for movement therapy after stroke: current status and challenges to clinical acceptance*. Topics in stroke rehabilitation, 2002. **8**(4): p. 40-53.
4. Hatem, S.M., et al., *Rehabilitation of motor function after stroke: a multiple systematic review focused on techniques to stimulate upper extremity recovery*. Frontiers in human neuroscience, 2016. **10**: p. 442.
5. Hughes, A.-M., et al., *Translation of evidence-based Assistive Technologies into stroke rehabilitation: users' perceptions of the barriers and opportunities*. BMC Health Services Research, 2014. **14**(1): p. 124.
6. Anderson, C., et al., *Home or hospital for stroke rehabilitation? Results of a randomized controlled trial*. Stroke, 2000. **31**(5): p. 1024-1031.
7. Osuagwu, B.A., et al., *Home-based rehabilitation using a soft robotic hand glove device leads to improvement in hand function in people with chronic spinal cord injury: a pilot study*. Journal of neuroengineering and rehabilitation, 2020. **17**(1): p. 1-15.
8. Tanabe, H., M. Ikuta, and Y. Morita, *Validation of the efficiency of a robotic rehabilitation training system for recovery of severe plegic hand motor function after a stroke*. IEEE Int Conf Rehabil Robot, 2017. **2017**: p. 579-584.
9. Lee, J., et al., *A multichannel-near-infrared-spectroscopy-triggered robotic hand rehabilitation system for stroke patients*. IEEE Int Conf Rehabil Robot, 2017. **2017**: p. 158-163.
10. Vanoglio, F., et al., *Feasibility and efficacy of a robotic device for hand rehabilitation in hemiplegic stroke patients: a randomized pilot controlled study*. Clin Rehabil, 2017. **31**(3): p. 351-360.
11. Kim, D.H., S.W. Lee, and H.S. Park, *Feedback control of biomimetic exotendon device for hand rehabilitation in stroke*. Conf Proc IEEE Eng Med Biol Soc, 2014. **2014**: p. 3618-21.
12. Ang, K.K., et al., *Brain-computer interface-based robotic end effector system for wrist and hand rehabilitation: results of a three-armed randomized controlled trial for chronic stroke*. Front Neuroeng, 2014. **7**: p. 30.
13. Park, W., et al., *A rehabilitation device to improve the hand grasp function of stroke patients using a patient-driven approach*. IEEE Int Conf Rehabil Robot, 2013. **2013**: p. 6650482.
14. Lee, S.W., K.A. Landers, and H.S. Park, *Biomimetic hand exotendon device (BiomHED) for functional hand rehabilitation in stroke*. IEEE Int Conf Rehabil Robot, 2013. **2013**: p. 6650388.
15. Haraguchi, M. and J. Furusho, *Passive-type rehabilitation system for upper limbs which can display the exact resistance force in the orientation opposite to hand motion*. IEEE Int Conf Rehabil Robot, 2013. **2013**: p. 6650360.
16. Mousavi Hondori, H., et al., *A Spatial Augmented Reality rehab system for post-stroke hand rehabilitation*. Stud Health Technol Inform, 2013. **184**: p. 279-85.
17. Ho, N.S., et al., *An EMG-driven exoskeleton hand robotic training device on chronic stroke subjects: task training system for stroke rehabilitation*. IEEE Int Conf Rehabil Robot, 2011. **2011**: p. 5975340.
18. Brokaw, E.B., R.J. Holley, and P.S. Lum, *Hand spring operated movement enhancer (HandSOME) device for hand rehabilitation after stroke*. Conf Proc IEEE Eng Med Biol Soc, 2010. **2010**: p. 5867-70.
19. Saka, Ö., A. McGuire, and C. Wolfe, *Cost of stroke in the United Kingdom*. Age and ageing, 2009. **38**(1): p. 27-32.

20. Timmermans, A.A., et al., *Arm and hand skills: training preferences after stroke*. Disabil Rehabil, 2009. **31**(16): p. 1344-52.
21. *GP2Y0A41SK0F Distance Measuring Sensor Data Sheet*. Available from: http://www.farnell.com/datasheets/2364614.pdf?_ga=2.67804183.76592176.1576531166-1810837110.1564135961.
22. Bhatia, K.P., et al., *Consensus Statement on the classification of tremors. from the task force on tremor of the International Parkinson and Movement Disorder Society*. Movement Disorders, 2018. **33**(1): p. 75-87.
23. Deuschl, G., et al., *Consensus statement of the movement disorder society on tremor*. Movement Disorders, 1998. **13**(S3): p. 2-23.
24. Alper, M.A., D. Morris, and L. Tran. *Remote detection and measurement of limb tremors*. in *2018 5th International Conference on Electrical and Electronic Engineering (ICEEE)*. 2018. IEEE.
25. Raza, C. and R. Anjum, *Parkinson's disease: Mechanisms, translational models and management strategies*. Life sciences, 2019. **226**: p. 77-90.
26. Zhu, R. and Z. Zhou, *A real-time articulated human motion tracking using tri-axis inertial/magnetic sensors package*. IEEE Transactions on Neural systems and rehabilitation engineering, 2004. **12**(2): p. 295-302.
27. Dai, H., P. Zhang, and T.C. Lueth, *Quantitative assessment of parkinsonian tremor based on an inertial measurement unit*. Sensors, 2015. **15**(10): p. 25055-25071.
28. Pavone, E., *Joint Range of Motion and Muscle Length Testing*. Physical Therapy, 2003. **83**(3): p. 302.
29. Cleveland, D., *Diagrams for showing limitation of movements through joints, as used by the Board of Pensions Commissioners for Canada*. Canadian Medical Association Journal, 1918. **8**(12): p. 1070-1076.
30. Kuo, L.-C., et al., *Functional workspace for precision manipulation between thumb and fingers in normal hands*. Journal of electromyography and kinesiology, 2009. **19**(5): p. 829-839.
31. Pham, T.H., et al., *Quantification of the finger functional range via explicit descriptions of reachable subspaces*. IEEE Transactions on Instrumentation and Measurement, 2016. **65**(6): p. 1412-1422.
32. Hu, N., P.H. Chappell, and N.R. Harris, *Finger Displacement Sensing: FEM Simulation and Model Prediction of a Three-Layer Electrode Design*, in *IEEE Transactions on Instrumentation and Measurement*. 2018. p. 1432-1440.
33. Borghetti, M., E. Sardini, and M. Serpelloni, *Sensorized glove for measuring hand finger flexion for rehabilitation purposes*. IEEE Transactions on Instrumentation and Measurement, 2013. **62**(12): p. 3308-3314.
34. Herrera-Luna, I., et al., *Sensor Fusion Used in Applications for Hand Rehabilitation: A Systematic Review*. IEEE Sensors Journal, 2019. **19**(10): p. 3581-3592.
35. Zhu, X. and K.F. Li. *Real-Time Motion Capture: An Overview*. in *2016 10th International Conference on Complex, Intelligent, and Software Intensive Systems (CISIS)*. 2016.
36. Bain, G., et al., *The functional range of motion of the finger joints*. Journal of Hand Surgery (European Volume), 2015. **40**(4): p. 406-411.
37. Boian, R., et al., *Virtual reality-based post-stroke hand rehabilitation*. Studies in health technology and informatics, 2002: p. 64-70.
38. Häger-Ross, C. and M.H. Schieber, *Quantifying the independence of human finger movements: comparisons of digits, hands, and movement frequencies*. Journal of Neuroscience, 2000. **20**(22): p. 8542-8550.

39. Lang, C.E. and M.H. Schieber, *Human finger independence: limitations due to passive mechanical coupling versus active neuromuscular control*. Journal of neurophysiology, 2004. **92**(5): p. 2802-2810.
40. Friedman, N., et al., *Retraining and assessing hand movement after stroke using the MusicGlove: comparison with conventional hand therapy and isometric grip training*. Journal of neuroengineering and rehabilitation, 2014. **11**(1): p. 76.
41. Friedman, N., et al. *MusicGlove: Motivating and quantifying hand movement rehabilitation by using functional grips to play music*. in *Engineering in Medicine and Biology Society, EMBC, 2011 Annual International Conference of the IEEE*. 2011. IEEE.
42. Chiu, Y.H., et al., *Fuzzy logic-based mobile computing system for hand rehabilitation after neurological injury*. Technol Health Care, 2017.
43. Hoffman, H., et al., *Rehabilitation of hand function after spinal cord injury using a novel handgrip device: a pilot study*. J Neuroeng Rehabil, 2017. **14**(1): p. 22.
44. Choi, K.S. and K.H. Lo, *A hand rehabilitation system with force feedback for children with cerebral palsy: two case studies*. Disabil Rehabil, 2011. **33**(17-18): p. 1704-14.
45. Radder, B., et al., *Home rehabilitation supported by a wearable soft-robotic device for improving hand function in older adults: A pilot randomized controlled trial*. PloS one, 2019. **14**(8).
46. Haghshenas-Jaryani, M., C. Pande, and B.M. Wijesundara. *Soft Robotic Bilateral Hand Rehabilitation System for Fine Motor Learning*. in *2019 IEEE 16th International Conference on Rehabilitation Robotics (ICORR)*. 2019. IEEE.
47. Webster, A., et al., *The co-design of hand rehabilitation exercises for multiple sclerosis using hand tracking system*, in *Biomedical Visualisation*. 2019, Springer. p. 83-96.
48. Haghshenas-Jaryani, M., et al., *A pilot study on the design and validation of a hybrid exoskeleton robotic device for hand rehabilitation*. Journal of Hand Therapy, 2020.
49. Ottensmeyer, M.P., et al., *Functional MRI in Conjunction with a Novel MRI-compatible Hand-induced Robotic Device to Evaluate Rehabilitation of Individuals Recovering from Hand Grip Deficits*. JoVE (Journal of Visualized Experiments), 2019(153): p. e59420.
50. Pani, D., et al., *A Device for Local or Remote Monitoring of Hand Rehabilitation Sessions for Rheumatic Patients*. IEEE J Transl Eng Health Med, 2014. **2**: p. 2100111.
51. Kim, J.Y., et al., *Development and evaluation of a method to measure wrist range of motion on paretic hand rehabilitation device*. IEEE Int Conf Rehabil Robot, 2017. **2017**: p. 1337-1342.
52. Placidi, G., et al., *Measurements by a LEAP-based virtual glove for the hand rehabilitation*. Sensors, 2018. **18**(3): p. 834.
53. Ates, S., C.J. Haarman, and A.H. Stienen, *SCRIPT passive orthosis: design of interactive hand and wrist exoskeleton for rehabilitation at home after stroke*. Autonomous Robots, 2017. **41**(3): p. 711-723.
54. Ma, Z., P. Ben-Tzvi, and J. Danoff, *Hand Rehabilitation Learning System With an Exoskeleton Robotic Glove*. IEEE Trans Neural Syst Rehabil Eng, 2016. **24**(12): p. 1323-1332.
55. Reaz, M., M. Hussain, and F. Mohd-Yasin, *Techniques of EMG signal analysis: detection, processing, classification and applications*. Biological procedures online, 2006. **8**(1): p. 11-35.
56. Zaheer, F., S.H. Roy, and C.J. De Luca, *Preferred sensor sites for surface EMG signal decomposition*. Physiological measurement, 2012. **33**(2): p. 195-206.
57. Sonkusare, J.S., et al. *A Review on Hand Gesture Recognition System*. in *2015 International Conference on Computing Communication Control and Automation*. 2015.
58. Janaki, V.M.S., S. Babu, and S.S. Sreekanth. *Real time recognition of 3D gestures in mobile devices*. in *2013 IEEE Recent Advances in Intelligent Computational Systems (RAICS)*. 2013.
59. Zhang, Z., *Microsoft Kinect Sensor and Its Effect*. IEEE MultiMedia, 2012. **19**(2): p. 4-10.
60. Ren, Z., et al., *Robust Part-Based Hand Gesture Recognition Using Kinect Sensor*. IEEE Transactions on Multimedia, 2013. **15**(5): p. 1110-1120.

61. Zhou, H. and H. Hu, *Human motion tracking for rehabilitation—A survey*. Biomedical signal processing and control, 2008. **3**(1): p. 1-18.
62. Covarrubias, M., M. Bordegoni, and U. Cugini, *Force sensitive handles and capacitive touch sensor for driving a flexible haptic-based immersive system*. Sensors, 2013. **13**(10): p. 13487-13508.
63. Ramezani Akhmareh, A., et al., *A Tagless Indoor Localization System Based on Capacitive Sensing Technology*. Sensors, 2016. **16**(9): p. 1448.
64. Rashid, A. and O. Hasan, *Wearable technologies for hand joints monitoring for rehabilitation: A survey*. Microelectronics Journal, 2019. **88**: p. 173-183.
65. O'Reilly, M., et al., *Wearable inertial sensor systems for lower limb exercise detection and evaluation: a systematic review*. Sports Medicine, 2018. **48**(5): p. 1221-1246.
66. *3D Guidance driveBAY™*. Available from: <http://www.nexgenergo.com/ergonomics/ascension9.html>.
67. Clark, R.A., et al., *Validity of the Microsoft Kinect for assessment of postural control*. Gait & posture, 2012. **36**(3): p. 372-377.
68. Yeung, L., et al., *Evaluation of the Microsoft Kinect as a clinical assessment tool of body sway*. Gait & posture, 2014. **40**(4): p. 532-538.
69. Blumrosen, G., et al., *Noncontact tremor characterization using low-power wideband radar technology*. IEEE transactions on biomedical engineering, 2011. **59**(3): p. 674-686.
70. Krupicka, R., et al., *Motion capture system for finger movement measurement in Parkinson disease*. Radioengineering, 2014. **23**(2): p. 659-664.
71. Dardas, N.H. and N.D. Georganas, *Real-time hand gesture detection and recognition using bag-of-features and support vector machine techniques*. IEEE Transactions on Instrumentation and Measurement, 2011. **60**(11): p. 3592-3607.
72. *MGC3030/3130 3D Tracking and Gesture Controller Data Sheet*. Available from: <http://ww1.microchip.com/downloads/en/DeviceDoc/40001667C.pdf>.
73. Sciberras, J., *Interactive gesture controller for a motorised wheelchair*. 2015, Murdoch University.
74. Filippeschi, A., et al., *Survey of motion tracking methods based on inertial sensors: A focus on upper limb human motion*. Sensors, 2017. **17**(6): p. 1257.
75. Fuentes del Toro, S., et al., *Validation of a low-cost electromyography (EMG) system via a commercial and accurate EMG device: Pilot study*. Sensors, 2019. **19**(23): p. 5214.
76. Gohel, V. and N. Mehendale, *Review on electromyography signal acquisition and processing*. Biophysical Reviews, 2020: p. 1-7.
77. Huang, Y., et al., *Translation of robot-assisted rehabilitation to clinical service: a comparison of the rehabilitation effectiveness of EMG-driven robot hand assisted upper limb training in practical clinical service and in clinical trial with laboratory configuration for chronic stroke*. Biomedical engineering online, 2018. **17**(1): p. 1-17.
78. Mousavi Hondori, H. and M. Khademi, *A review on technical and clinical impact of microsoft kinect on physical therapy and rehabilitation*. Journal of medical engineering, 2014. **2014**.
79. Postolache, G., et al. *Wrist and hand rehabilitation software platform based on leap motion controller*. in *3rd International Conference on Sensors Engineering and Electronics Instrumentation Advances, SEIA'2017*. 2017. International Frequency Sensor Association.
80. Guzsvinecz, T., V. Szucs, and C. Sik-Lanyi, *Suitability of the Kinect sensor and Leap Motion controller—A literature review*. Sensors, 2019. **19**(5): p. 1072.
81. Taylor, J. and K. Curran, *Using leapmotion and gamification to facilitate and encourage rehabilitation for hand injuries: leap motion for rehabilitation*. Handbook of Research on Holistic Perspectives in Gamification for Clinical Practice, 2015: p. 183-192.
82. Gieser, S.N., A. Boisselle, and F. Makedon. *Real-time static gesture recognition for upper extremity rehabilitation using the leap motion*. in *International Conference on Digital Human*

- Modeling and Applications in Health, Safety, Ergonomics and Risk Management*. 2015. Springer.
83. Iosa, M., et al., *Leap motion controlled videogame-based therapy for rehabilitation of elderly patients with subacute stroke: a feasibility pilot study*. *Topics in stroke rehabilitation*, 2015. **22**(4): p. 306-316.
 84. Khademi, M., et al. *Free-hand interaction with leap motion controller for stroke rehabilitation*. in *Proceedings of the extended abstracts of the 32nd annual ACM conference on Human factors in computing systems*. 2014. ACM.
 85. *Confocal Displacement Sensor: CL-3000 Series*
Available from: http://gts-adriatic.rs/wp-content/uploads/2018/12/AS_100320_CL-3000_C_611I32_US_1108-1.pdf.
 86. *DM160226 - MGC3030 - Woodstar Development Kit*. Available from: <https://www.microchipdirect.com/dev-tools/DM160226?productLoaded=true&allDevTools=true>.
 87. Montanaro, L., et al., *A touchless human-machine interface for the control of an elevator*.
 88. Hu, N., P. Chappell, and N. Harris, *Finger displacement sensing: FEM simulation and modelling of a customizable three-layer electrode design*, in *2018 IEEE International Instrumentation & Measurement Technology Conference*. 2018: Houston, Texas, USA.
 89. *GestIC Design Guide*. Available from: <http://www.microchip.com/downloads/en/DeviceDoc/40001721A.pdf>.
 90. *Fit nonlinear regression model - MATLAB fitnlm - MathWorks Switzerland*. Available from: <https://ch.mathworks.com/help/stats/fitnlm.html>.
 91. *Nonlinear Regression - MATLAB & Simulink - MathWorks Switzerland*. Available from: https://ch.mathworks.com/help/stats/nonlinear-regression-1.html#responsive_offcanvas.
 92. Devore, J.L., *Probability and Statistics for Engineering and the Sciences*. 2011: Cengage learning.
 93. Hu, N., P.H. Chappell, and N.R. Harris. *Finger displacement sensing: FEM simulation and modelling of a customizable three-layer electrode design*. in *2018 IEEE International Instrumentation and Measurement Technology Conference (I2MTC)*. 2018. IEEE.
 94. Aoyama, T., et al., *Neural mechanism of selective finger movement independent of synergistic movement*. *Experimental brain research*, 2019. **237**(12): p. 3485-3492.
 95. Bertuletti, S., et al., *Static and dynamic accuracy of an innovative miniaturized wearable platform for short range distance measurements for human movement applications*. *Sensors*, 2017. **17**(7): p. 1492.
 96. Crease, R.P., *How high the moon*. *Physics World*, 2019. **32**(7): p. 26-32.
 97. *MGC3030/3130 GestIC® Library Interface Description User's Guide*.
 98. *Regression Analysis: How Do I Interpret R-squared and Assess the Goodness-of-Fit? ;* Available from: <https://blog.minitab.com/blog/adventures-in-statistics-2/regression-analysis-how-do-i-interpret-r-squared-and-assess-the-goodness-of-fit>.
 99. Krishna, S., K. Vinay, and K. Raja. *Efficient meg signal decoding of direction in wrist movement using curve fitting (emdc)*. in *2011 International Conference on Image Information Processing*. 2011. IEEE.
 100. Roby-Brami, A., et al., *Hand orientation for grasping and arm joint rotation patterns in healthy subjects and hemiparetic stroke patients*. *Brain research*, 2003. **969**(1-2): p. 217-229.
 101. Pérez-González, A., M. Vergara, and J.L. Sancho-Bru, *Stiffness map of the grasping contact areas of the human hand*. *Journal of biomechanics*, 2013. **46**(15): p. 2644-2650.
 102. Einolf, C.J., *Empathic concern and prosocial behaviors: A test of experimental results using survey data*. *Social Science Research*, 2008. **37**(4): p. 1267-1279.
 103. Leonard, L.N. and R. Haines, *Computer-mediated group influence on ethical behavior*. *Computers in human behavior*, 2007. **23**(5): p. 2302-2320.

104. MacDermid, J.C., et al., *Patient versus injury factors as predictors of pain and disability six months after a distal radius fracture*. Journal of Clinical Epidemiology, 2002. **55**(9): p. 849-854.
105. Miguel-Hurtado, O., et al., *Comparing machine learning classifiers and linear/logistic regression to explore the relationship between Hand dimensions and demographic characteristics*. PloS one, 2016. **11**(11).
106. van Beek, N., et al., *Activity patterns of extrinsic finger flexors and extensors during movements of instructed and non-instructed fingers*. Journal of Electromyography and Kinesiology, 2018. **38**: p. 187-196.
107. Tom O'Haver , P.E. *A Pragmatic* Introduction to Signal Processing with Applications in Scientific Measurement*. July 12, 2020.; Available from:
<https://terpconnect.umd.edu/~toh/spectrum/Smoothing.html>